A ^{2}H AND ^{31}P NMR INVESTIGATION OF ORDER AND DYNAMICS OF LIPIDS IN HUMAN VERY LOW DENSITY LIPOPROTEINS AND MODEL MEMBRANES

by

RAVINDER SINGH CHANA

B.Sc.(Hons)., UNIVERSITY OF ESSEX, ENGLAND, 1980

M.Sc., UNIVERSITY OF ESSEX, ENGLAND, 1982

THESIS SUBMITTED IN PARTIAL FULFILLMENT OF

THE REQUIREMENTS FOR THE DEGREE OF

DOCTOR OF PHILOSOPHY

in the Department

of

CHEMISTRY

SIMON FRASER UNIVERSITY

JULY 1989

APPROVAL

Name: RAVINDER SINGH CHANA

Degree: DOCTOR OF PHILOSOPHY

Title of thesis: A ^{2}H AND ^{31}P NMR INVESTIGATION OF ORDER AND DYNAMICS OF LIPIDS IN HUMAN VERY LOW DENSITY LIPOPROTEINS AND MODEL MEMBRANES

Examining Committee:

Chairman: Dr. P.W. Percival

Dr. R.J. Cushley
Senior Supervisor

Dr. A.S. Tracey

Dr. N.M. Bhakthan
Department of Kinesiology

Dr. M.J. Poznansky
External Examiner
Department of Physiology
University of Alberta

Date Approved: July 5th, 1989

PARTIAL COPYRIGHT LICENSE

I hereby grant to Simon Fraser University the right to lend my thesis, project or extended essay (the title of which is shown below) to users of the Simon Fraser University Library, and to make partial or single copies only for such users or in response to a request from the library of any other university, or other educational institution, on its own behalf or for one of its users. I further agree that permission for multiple copying of this work for scholarly purposes may be granted by me or the Dean of Graduate Studies. It is understood that copying or publication of this work for financial gain shall not be allowed without my written permission.

Title of Thesis/Project/Extended Essay

A ^{2}H and ^{31}P NMR investigation of Order and dynamics of lipids in Human Very Low Density Lipoproteins and Model Membranes.

Author: _____

(signature)

Ravinder Singh Chana.

(name)

8th Aug 1989

(date)

ABSTRACT

The organization of phospholipid (PC) acyl chains in the surface monolayer of human very low density lipoprotein (VLDL) has been determined from the ^2H NMR order parameters, S_{CD}. Selectively deuterated phospholipids and selectively deuterated palmitic acids were incorporated into VLDL, the former using a partially purified phosphatidylcholine transfer protein. Both probes indicate the presence of two significantly different domains of PC acyl chain order. At 25°C, the average S_{CD} value of the low order domain for chain positions C2-16 was 0.014 (phospholipids), and 0.015 (C4-16, palmitic acids). For the high order domain the S_{CD} value was 0.25 at C11,12 and 0.035 (palmitic acid), and 0.029 (phospholipid), for the terminal methyl group (C16). At 40°C, the S_{CD} values of the low order domain remain unchanged while those for the high order domain decreased *e.g.* S_{CD} = 0.11 for C11,12.

A model study, on microemulsions composed of selectively deuterated phospholipids incorporated into egg PC and triolein (TO) surprisingly also indicated two significantly different domains of PC acyl chain order. At 25°C, S_{CD} of the high order domain was ≃32% lower (C11,12, phospholipid) than the corresponding position in VLDL, while that of the low order domain remained unchanged. Possible reasons for the different organization in the surface phospholipids of VLDL and egg PC/TO microemulsions compared to other lipoproteins and membranes are discussed.

Lateral diffusion coefficients D_t of phospholipids in VLDL and egg PC/TO microemulsions were determined from the viscosity-dependence of ^{31}P NMR linewidths. At 25°C, D_t values of (9.1±1.0) X 10^{-9} cm²/s, and (2.5±0.4)

X 10^{-8} cm^2/s were obtained for VLDL and egg PC/TO microemulsions, respectively. The value of D_t in VLDL is approximately three times slower than in egg PC/TO microemulsions and phospholipid bilayers.

The residual chemical shift anisotropy, $\Delta\sigma$, of phospholipids in VLDL at 25°C was 47±1 and 46±0.5 ppm measured by viscosity- and field-dependence of the ^{31}P NMR linewidths, respectively. These values are similar to phospholipid bilayers ($\Delta\sigma \simeq 45$ ppm). At 25°C, the viscosity-dependence study of egg PC/TO microemulsion yielded a $\Delta\sigma$ value of 28±1 ppm, indicating that the motions and/or the headgroup orientation of phospholipids are different in VLDL than in microemulsions.

The ^2H NMR spectra of selectively deuterated cholesterol and cholesteryl palmitate in multilamellar dispersions of dipalmitoylphosphatidylcholine were obtained at 45°C. From the quadrupolar splittings, and the atomic coordinates of cholesteryl laurate, the orientational axis of the respective molecules was calculated. From the orientation of the steroid and the carbon-deuterium bond order parameters, S_{CD}, the molecular order parameters, S_{mol}, of the steroid moiety of cholesteryl palmitate and cholesterol were found to be $\simeq 0.47$ and $\simeq 0.63$, respectively. This indicates that the time averaged fluctuations of the rigid steroid about the axis of motional averaging is greater for cholesteryl ester than for cholesterol in membranes.

ACKNOWLEDGEMENTS

I would like to thank my supervisor Dr. R. J. Cushley for his guidance, encouragement and support throughout the course of this research project. I also wish to thank Dr. K. N. Slessor and Dr. A. S. Tracey for their time and work as members of my supervisory committee.

Part of this work, viz. the organization of cholesteryl esters in membranes, reported in section VI was performed in collaboration with Dr. I. C. P. Smith of Division of Biological Sciences, National Research Council, Ottawa, and Dr. E. J. Dufourc of Centre de Paul Pascal, Domaine Universitaire. I would like to thank them for providing us with deuterated cholesterols and for performing the calculations and preparing Figure 54.

I am indebted to past and present members of the research group for their assistance and advice and many helpful discussions. Dr. S. R. Wassall, Dr. W. D. Treleaven, Dr. Y. I. Parmar, Dr. J. L. Thewalt, Dr. D. B. Fenske and Mrs. Junshi Yue.

I would like to extend my appreciation to my family and parents for their support, now and in the past. Finally, I wish to thank my wife, Jasbir, for her support and patience during the latter stages of this work.

DEDICATION

To my parents

and

to my late grandparents

TABLE OF CONTENTS

LIST OF TABLES

LIST OF FIGURES

LIST OF ABBREVIATIONS

VLDL, very low density lipoprotein; LDL, low density lipoprotein; HDL, high density lipoprotein; ^{2}H NMR, deuterium nuclear magnetic resonance; ^{31}P NMR, phosphorus-31 nuclear magnetic resonance; DSC, differential scanning calorimetry; ESR, electron spin resonance; EFG, electric field gradient; CSA, chemical shift anisotropy; EM, electron microscopy; QELS, quasi-elastic light scattering; SDS, sodium dodecyl sulfate; PAGE, polyacrylamide gel electrophoresis; PMSF, phenylmethylsulfonyl fluoride; DIFP, diisopropylfluorophosphate; PC, phosphatidylcholine; egg PC, egg phosphatidylcholine; DPPC, dipalmitoylphosphatidylcholine; PL, phospholipid; SPM, sphingomyelin; TO, triolein; TC, total cholesterol; CE, cholesteryl ester; TG, triglyceride; Pr, protein; CP, cholesteryl palmitate; CL, cholesteryl linoelate; CDI, 1,1'-carbonyldiimidazole; DDW, deuterium depleted water; EDTA, ethylenediaminetetraacetic acid; LCAT, lecithin:cholesterol acyl transferase; BSA, bovine serum albumin; DPH, 1,6-diphenyl-1,3,5-hexatriene.

CHAPTER I

INTRODUCTION

Part 1. VLDL

Plasma lipoproteins are macromolecular complexes of lipids and proteins. Their primary function is to transport non-polar lipids of dietary or endogenous origin to the tissues where they may be utilized for oxidative metabolism, storage, steroid hormone biosynthesis or maintenance of membrane and cellular function (Dolphin, 1985). Under fasting conditions plasma lipoproteins are isolated sequentially according to their density into four major groups (Small, 1981), chylomicron (CM, <0.95 g/mL), very low density lipoprotein (VLDL, <1.006 g/mL), low density lipoproteins (LDL, 1.019-1.063 g/mL), and high density lipoproteins (HDL_2, 1.063-1.125 g/mL; HDL_3, 1.125-1.21 g/mL). Other properties which uniquely characterise the lipoprotein groups are the electrophoretic mobility, molecular weight, size, lipid and protein composition. Table 1 summarizes the average chemical composition and physical properties of human lipoproteins.

Shen *et al.* (1977) have proposed that lipoproteins share common structural features based on chemical composition. In their model, lipoproteins are envisaged as spherical complexes having a central core of non-polar lipids, triglyceride and cholesteryl ester, which are stabilized by a surface monolayer of amphipathic lipids, phospholipids, free cholesterol, and apoproteins. The hydrophobic ends of the phospholipids and free cholesterol are orientated towards the centre of the particle while their polar ends face the aqueous phase with the apoproteins localized at

Table 1: Chemical composition and physical properties of human lipoproteins[a]

	CM	VLDL	LDL	HDL_2	HDL_3
	Weight % of total lipoprotein				
Protein	2	8	21	46	61
Phospholipid	4	18	24	28	20
Cholesteryl Ester	3	12	42	19	14
Cholesterol	1	7	9	4	2
Triglyceride	90	55	5	3	2
Mobility	origin	pre-β	β	α	α
Diameter (nm)	>70	25-70	22-24	7-10	4-7
MW X 10^6	10^3-10^4	5-27	3.95	0.22	0.16
Density (g/mL)	<0.95	1.006	1.019-1.063	1.063-1.125	1.125-1.21

[a] Table adapted from Scanu *et al.* (1982) and Dolphin (1985).

the lipid/water interface. Recent studies, however, have shown that small amounts of cholesteryl esters and triglycerides are also present in the surface monolayer of lipoproteins and microemulsions (Miller and Small, 1982; Miller and Small, 1983a; 1983b).

Lipoprotein metabolism

Chylomicrons, the largest and the least dense particles, are synthesized in the intestine following ingestion of dietary fat. These paticles are rich in triglycerides and contain apo A-I, A-II, A-IV, and apo B-48. The newly synthesised (nascent) chylomicrons are released into the

lymph from where they enter the plasma. En route to the plasma they acquire free cholesterol and apo Cs and E, and loose apo A-IV and phospholipids (Atkinson and Small, 1986). In the plasma, the triglyceride core is depleted by the hydrolytic action of lipoprotein lipase and, as a result, small particles (40-100 nm) are generated which have reduced triglyceride content. These particles are referred to as core remnants. During the process of hydrolysis, the excess surface phospholipids, free cholesterol, apo As and Cs are transferred to the HDL fraction. The core remnants, rich in free cholesterol and containing apo E and some apo C, A, and B-48, are cleared rapidly from the plasma by the liver through a receptor-mediated mechanism, a process in which both B-E receptors and chylomicron receptor are involved (Brown and Goldstein, 1983; Mahley and Innerarity, 1983).

VLDL particles are synthesised in the endoplasmic reticulum and golgi apparatus in the liver (Alexander *et al.*, 1976; Higgins and Hutson, 1984; Higgins, 1988) and are involved in transporting endogenous triglyceride and cholesterol. The nascent particles are rich in triglyceride and contain apo B-100, E and some C. From the space of Disse, en route to the plasma, the particles begin to aquire apo C-II, C-III and E from the HDL fraction. This process is completed in the plasma where the HDL levels are high. Once in the plasma, a number of physical changes ensue. The particles begin to acquire cholesteryl esters by exchanging triglycerides with the HDL particles. This process is mediated by lipid transfer proteins present in the plasma (Barter and Lally, 1979; Hopkins and Barter, 1979; Zilversmit, 1984; Tall, 1986). VLDL particles are catabolized by endothelial-bound extrahepatic lipoprotein lipase such that the core triglycerides are

hydrolysed to diacylglycerol, monoacylglycerol and fatty acids (Cryer, 1981; Homash and Homash, 1983; Breckenridge, 1985). Lipoprotein lipase may also hydrolyse the phospholipids at the surface (Fielding, 1978). Apo C-II is a cofactor for lipoprotein lipase and its presence initiates the hydrolysis of lipoprotein triacylglycerols. The role of hepatic lipase in the metabolism of VLDL remains speculative (Breckenridge, 1985). During the lipolytic process, VLDL undergoes a number of structural changes, such as depletion of triglyceride in the core, reduction of particle size, loss of phospholipids, apo C and apo E to the HDL fraction, increase in cholesterol/triglyceride ratio and increase in particle density (Mjos *et al.*, 1975; Eisenberg and Schurr, 1976). The resulting VLDL remnant, also referred as the intermediate density lipoprotein (IDL), can have a number of metabolic pathways. IDL may either be removed rapidly from the circulation by the liver or metabolized further to low density lipoprotein (LDL) in the plasma (Havel, 1984). During the conversion to LDL most of the triglycerides (more than 98%) are hydrolysed, most of the surface coating, phospholipids (≃75%) and unesterified cholesterol (≃85%), and all of the apoprotein (apo C's and E) with the exception of apo B-100 are deleted from the lipoprotein surface (Eisenberg, 1980). Of all the lipoproteins, LDL appears to be the only one that results from such an interconversion.

LDL particles are isolated in a density range of 1.019-1.063 g/mL, having a diameter of 22-24 nm. The LDL core is predominantly cholesteryl ester with some triglyceride, possesses apo B-100 and shows β electrophoretic mobility. LDL is involved in transporting cholesterol to peripheral tissues. The cellular uptake of LDL is mediated by the apo B,E

receptors located on cell membranes (Goldstein and Brown, 1977; Brown and Goldstein, 1983; Mahley and Innerarity, 1983). High levels of LDL in the plasma have been correlated with atherosclerosis and its accumulation in the atheroma is well established (Hoff *et al.*, 1978; Hoff and Gaubatz, 1982).

Another class of cholesterol-rich lipoprotein which has also been linked with accelerated atherosclerosis (Mahley, 1979; Mahley, 1985) occurs in humans with type III hyperlipoproteinemia (Mahley *et al.*, 1979; Quin *et al.*, 1985; Mahley *et al.*, 1980) and in animals maintained on a high cholesterol diet (Mahley and Angelin, 1984; Fainaru *et al.*, 1980). These lipoproteins are isolated in the same density range as normal VLDL, and are referred to as β-VLDL. Unlike VLDL which are triglyceride-rich, β-VLDL are cholesteryl ester-rich and exhibit delayed clearance from the plasma.

High density lipoproteins (HDL) are synthesized by the liver and intestine. Two types of nascent HDL particles are secreted by the liver into plasma, they are spherical (≃8.0 nm) and discoidal in shape (Atkinson and Small, 1986). The discoidal particles contain cholesterol and phospholipid molecules which are surrounded by apo A-1 (Tall and Small, 1980). A space filling model has suggested that amphipathic helical regions of the apoproteins bind with the phospholipids through hydrophobic and hydrophilic interactions (Segrest, 1974). In the plasma, the cholesterol at the surface is converted to cholesteryl ester by the action of lecithin:cholesterol acyl transferase (LCAT), activated by apo A-I, and the hydrophobic cholesteryl ester molecules move into the core of the particle and produce HDL_3-like particles (Atkinson and Small, 1986). The two major forms of HDL particles are HDL_2 and HDL_3. High concentrations of HDL in

the plasma have been correlated with reduced risk of atherosclerosis (Miller and Miller, 1975). The exact mechanism by which cholesterol is removed from the peripheral tissues is not known, however a proposed mechanism suggests that HDLs apo A-I containing come into contact with cells and acquire cholesterol which is then subsequently esterified by LCAT and trapped in the core. The accumulation of cholesteryl ester leads to the enlargement of HDL_3, loss of apo A-I and acquisition of apo E. The resulting HDL_2-like particles are then removed from the circulation by the hepatic apo E receptors (Dolphin, 1985). The cholesteryl esters in HDL_2 may also be transferred to either chylomicrons or VLDL particles by the lipid transfer proteins present in the plasma. Hence, HDL is also involved in lipid transport.

From the above discussion, it is evident that lipoproteins are continuously undergoing structural changes in the plasma due to a number of enzymes, transfer proteins and receptor recognitions events. These changes are believed to take place at the surface where the components of the monolayer can be utilized. The surface bound apoproteins have been shown to be responsible for a number of physiological functions (LaRosa *et al.*, 1970, Fielding *et al.*, 1972; Brown and Goldstein, 1977; Brown and Goldstein, 1983; Mahley and Innerarity, 1983). Several studies have suggested that physical properties of lipoproteins and their lipids may play an important role in their regulation. The degree of fluidity of the core lipids is influenced by dietary intake (Pagnan *et al.*, 1977; Mahley and Innerarity, 1983, Hui *et al.*, 1984) and has been suggested to alter and affect the surface properties of lipoproteins. For instance, the interactions of lipoprotein lipase with the surface components may become

impeded and thereby result in delayed clearance of β-VLDL from plasma (Chait *et al.*, 1978). It has also been shown that LDL containing saturated fatty acids caused a decrease in the fractional catabolic rate of apoprotein B (Thompson and Siguurdson, 1974). The hydrolytic activity of lipoprotein lipase, LCAT and phospholipase A has been shown to depend upon the physical state of their substrate lipids (Zilversmit, 1968; Verger *et al.*, 1973; Soutar *et al.*, 1975). A recent study reports that selective delipidation of surface phospholipids in LDL particles by phospholipase A_2 altered the expression of epitopes of apo B-100 and effected the interaction of lipoprotein with cells (Kleinman *et al.*, 1988). Association of apoproteins obtained from VLDL and HDL with lipids has been shown to depend upon the liquid crystalline state of the lipids (Morrisett *et al.*, 1975; Pownall *et al.*, 1974; Pownall *et al.*, 1977). The activity of phospholipid transfer proteins is influenced by the surface charge and membrane fluidity (DiCorleto *et al.*, 1977; Kasper and Helmkamp, 1981; Bozzato and Tinker, 1982). Evidence suggests that the organization and physical state of lipids in the surface monolayer of VLDL is of considerable importance during the lipoprotein conversion to IDL and LDL (lipoprotein linked with atherosclerosis).

No comprehensive investigations of the organization and dynamics of phospholipid in the surface of VLDL have been performed. In view of this, we decided to investigate the outer monolayer structure of VLDL using ^{2}H NMR and ^{31}P NMR spectroscopy. ^{2}H NMR spectroscopy was used to determine the orientational order and mobility of phospholipid acyl chains from selectively deuterated phosphatidylcholine and selectively deuterated palmitic acid incorporated into human VLDL. In addition, ^{31}P NMR

spectroscopy was used to measure the lateral diffusion coefficient D_t and the residual chemical shift anisotropy $\Delta\sigma$ of the phosphate segment of phospholipid molecules in the surface of VLDL. In addition, both techniques were used to study egg PC/TO microemulsions, model structures of VLDL.

Structure of VLDL

VLDL particles isolated at density 1.006 g/mL are heterogenous in size, diameter ranging 25-70 nm, and show pre-β mobility. They contains approximately 90% lipid and 10% protein by weight, with triglycerides being the major lipid component (Table 1). Triglyceride fatty acids are predominantly oleate (35.2%) followed by palmitate (24.7%) and stearate (22.5%). The cholesteryl esters are predominantly oleate (34.6%) followed by linoleate (26.0%) and palmitate (22.8%), while the phospholipids are predominantly palmitate (36.4%) and approximately equal amounts of linoleate (16.1%), oleate (13.2%), and stearate (18.7%) (Scanu and Kruski, 1975). The major phospholipids are PC (59.7%) followed by SPM (14.5%) and PE (4.6%) (Scanu *et al.*, 1982). The current structural model based upon the chemical composition, enzymatic and physical data suggests the spherical VLDL particles consist of a hydrophobic core triglycerides and cholesteryl esters, surrounded by an amphiphilic surface monolayer composed of apoproteins, phospholipids and cholesterol. As mentioned earlier, some cholesteryl esters and triglycerides are also expected to reside in the surface monolayer. A pictorial model of VLDL structure is represented in Figure 1.

Figure 1: Structural model of very low density lipoprotein. Figure from Morrisett *et al.*, 1977a.

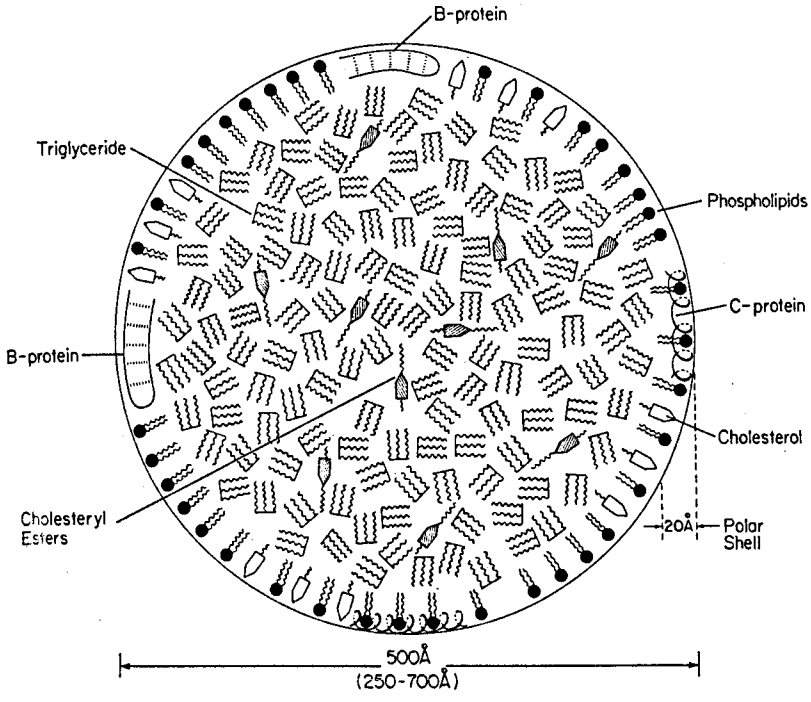

Surface monolayer

Studies with five different phospholipases have shown that 3-10% of the phospholipids, depending on the type of the phospholipid, were inaccessible to hydrolysis and have been suggested to be associated with the apoproteins (Reman *et al.*, 1978). The hydrolytic activity of phospholipase C and sphingomyelinase towards the polar groups of phospholipids was observed to be higher then the two phospholipases A_2 employed. The data from that study was correlated with a previous study of Demel *et al*, (1975) who had examined the enzyme activity on the monolayers

of lecithin and mixtures of lecithin/sphingomyelin as a function of surface pressure. The substrate accessibility in the VLDL surface was observed to correspond closely to the phospholipid monolayer at a surface pressure of 15 dynes/cm at the water-air interface. Reman *et al.* (1978) have shown that VLDL particles of diameter 38.6 nm have approximately 77% of their surface covered by polar lipids based on surface area occupied by phospholipids and cholesterol at this surface pressure.

The unesterified cholesterol is approximately 7% by weight of VLDL particles and is believed to be localized in the surface. The exact amount of free cholesterol in the surface monolayer is not known. Eisenberg and Olivecrona (1979) based on the phase diagram of free cholesterol, cholesteryl ester and phospholipids have shown that particles of molecular weights 56.3 X 10^6 and 8.2 X 10^6 Daltons have $\simeq$67% and $\simeq$82% of free cholesterol, respectively, located in the phospholipid-protein monolayer while the remainder was solubilized in the triglyceride core. The fluorescence quenching studies of cholestatrienol indicate that at least 81% of the fluorescence probe is located in the surface monolayer (Schroeder *et al.*, 1979b). This amount of free cholesterol corresponds to approximately 40 mol % with respect to phospholipids. By way of contrast, as much as 50 mol % of cholesterol can be incorporated in phospholipid bilayers (Ladbrooke *et al.*, 1968).

VLDL contains three major types of apoproteins, apo B-100, apo C (CI, CII and CIII), and apo E. The concentration of apo C and apo E in the particles relies on the density of the particles (Eisenberg, 1979) and as the density of the particle increases the concentration of apo C and apo E decreases in relation to apo B-100. The decline of apo C content with

decreasing size and increasing particle density is rapid compared to the decline of apo E (Kane *et al.*, 1975; Eisenberg, 1979).

Two major forms of apo B are apo B-100 and apo B-48. Apo B-100 is synthesized in the liver (Glickman *et al.*, 1986) and associates with LDL and VLDL while apo B-48 is synthesized in the intestine (Glickman *et al.*, 1986) and is associated with chylomicrons. Apo B-100 is the largest and the most abundant apoprotein having a MW of 549,000 whereas apo B-48 has a MW of 264,000. Recently, a complete sequence of cDNA coding of apo B-100 has shown that the apoprotein is a single polypeptide chain containing 4536 amino acid residues (Chen *et al.*, 1986; Knott *et al.*, 1986). The primary sequence has two forms of internal repeats: an amphipathic helical region and a hydrophobic proline-rich domain (Li *et al.*, 1988). The secondary structure at the hydrophobic regions are believed to form amphipathic β-strands and β-turns which are suggested to participate in the lipid binding (Osterman *et al.*, 1984). Osterman *et al.* (1984) have reported that synthetic amphipathic β-strand peptides were able to organize lipids into LDL-type particles and, further, were able to bind tightly with plasma LDL, suggesting that both the amphipathic α-helical region and amphipathic β-strand region in apo B-100 may be involved in lipid binding.

The three forms of apo C are apo C-I, C-II, and C-III, which together, comprise approximately 40-60% of the apoproteins (Scanu *et al.*, 1982). Apo C-I is a single polypeptide chain of 57 amino acids. Unlike apo C-III, apo C-I lacks carbohydrates. The amino acid sequence of the protein has been determined by Shulman *et al.* (1975) and Jackson *et al.* (1974) and has a MW of 6613. Apo C-II contains 79 amino acid residues (MW 8826) and its sequence has been determined by Hospattankar *et al.* (1984). Apo C-II is

involved in the activation of lipoprotein lipase, an enzyme that hydrolyses the triglycerides. Apo C-III represents ≃40% of the apo C content. It is a single polypeptide chain containing 79 amino acids, the Thr-74 is linked to a carbohydrate chain. Depending upon the terminal carbohydrate residue, apo C-III is catalogued as apo C-III-0, apo C-III-1, or apo C-III-2. Apo Cs undergo conformational changes following binding to phospholipids. Upon binding with the lipids the helical content of the apoprotein increases. For instance, in apo C-I/egg PC complexes the apoprotein was shown to have ≃70% α-helical content (Jackson *et al.*, 1974). The α-helical content of apo C-II and apo C-III increased from 23% to 60% and 22% to 54%, respectively, upon binding with phospholipids (Morrisett *et al.*, 1977; Morrisett *et al.*, 1978). Such lipid-protein interactions are believed to occur through the amphipathic α-helical segment of proteins (Segrest *et al.*, 1974).

Apo E is a single polypeptide chain containing 299 amino acids (MW of 34,200) (Rall *et al.*, 1982). Many polymorphic forms of apo E exist due to genetic mutations and polymorphic substitutions of sialylation of the peptide chain (Zannis *et al.*, 1982). A circular dichroism study has shown that the secondary structure is high in α-helical content, ≃45% in solution and ≃65% in association with phospholipid vesicles (Stanley *et al.*, 1986). Apo E is involved in receptor recognition (Mahley and Innerarity, 1983) and the binding region is between residues 129-194 (Innerarity *et al.*, 1983). For a detailed discussion about the involvement of apoproteins in the receptor recognition events the reader is referred to excellent articles by Brown and Goldstein. (1983), Mahley and Innerarity. (1983) and Dolphin. (1985).

A number of physical techniques have been used to study the surface structure of VLDL. These include fluorescence (Jonas, 1977; Schroeder *et al.*, 1979a; 1979b; Schroeder and Goh, 1979; Sklar *et al.*, 1980; Hale and Schroeder, 1981), Differential Scanning Calorimetery (DSC) (Deckelbaum *et al.*, 1977; Hale and Schroeder, 1981), ESR (Morrisett *et al.*, 1977), ^{1}H NMR (Hamilton *et al.*, 1983), ^{13}C NMR (Hamilton *et al.*, 1976; Hamilton *et al.*, 1974) and ^{31}P NMR (Cushley *et al.*, 1987).

Fluorescence quenching studies of β-parinaric acid and cholestatrienol with trinitrophenylglycine have shown that at least 94% and 81% of the probe molecules, respectively, were located in the surface monolayer of VLDL thereby substantiating the presence of a surface monolayer as proposed by Shen *et al*, 1978 (Schroeder *et al.*, 1979a; 1979b). In another study, the hydrophobic fluorescence probe, 1,6-diphenyl-1,3,5-hexatriene (DPH), was shown to locate predominantly in the core, with a small fraction (≃20%) locating between the phospholipid fatty acyl chains (Schroeder and Goh. 1979). In contrast, Jonas (1977) has shown that DPH locates exclusively in the lipid core of lipoproteins, with some adjacent to the surface apoproteins.

Fluorescence studies have shown the phospholipids in VLDL particles isolated from rat liver perfused with different fatty acids or from animals fed saturated diet showed a phase transition. The break points in the Arrhenius plot of β-parinaric acid incorporated into rat VLDL perfused with palmitate occured at 24°C and 32°C while that perfused with oleate occured at 17°C and 27°C suggesting that surface phospholipids display a lipid-dependent phase transition (Schroeder *et al.*, 1979b). Evidence for the phospholipid phase transition has also come from the ^{1}H NMR study of

VLDL isolated from non-human primates fed a saturated diet (Hamilton *et al.*, 1983).

Due to the complex ^{1}H NMR spectra of lipoproteins, there are few well resolved signals that allow the study of motional properties of the lipids (Hamilton and Morrisett, 1986). A ^{1}H NMR signal which can exclusively be assigned to phospholipids is the N-choline methyl group. This peak was shown to exhibit temperature-dependent linewidth and intensity changes in the spectra of VLDL (Hamilton *et al.*, 1983). Similar changes were also observed in the spectra of tripalmitin emulsions; models of VLDL. These results were compared with the earlier studies of vesicles where abrupt narrowing of the choline peak was observed to correspond with the gel to liquid crystalline phase transition. Hence, it was concluded that such a phospholipid phase transition could occur in the non-human primate VLDL (Hamilton *et al.*, 1983). In contrast, several investigators, using either fluorecence or DSC, have been unable to detect phase alterations in intact VLDL isolated from human plasma (Jonas, 1977; Castellino *et al.*, 1977; Deckelbaum *et al.*, 1977; Deckelbaum *et al.*, 1979). In these studies the lipid composition of the VLDL was not altered in a manner as described by Schroeder *et al.* (1979b) or Hamilton *et al.* (1983) thereby suggesting that the physical properties of VLDL particles are influenced by its lipid composition.

^{13}C NMR spectroscopy, in contrast to ^{1}H NMR spectroscopy, has been extensively used to study the molecular motions of lipids in lipoproteins. In a comparative study, the ^{13}C T_1 values of fatty acyl chains in VLDL were slightly longer than those of LDL and HDL (Hamilton *et al.*, 1974). Hence, it was concluded that the acyl chains in VLDL undergo faster

segmental motions compared to the acyl chains in other lipoproteins. Unfortunately, this technique fails to differentiate between phospholipid, cholesteryl ester and triglyceride acyl chains.

^{31}P NMR spectroscopy provides the motional information of the phosphate segments located at the lipoprotein surface. ^{31}P NMR spectroscopy has been sparingly used to study the surface structure of VLDL. In an earlier study, a single broad signal in the ^{31}P NMR spectra of VLDL was assigned to phosphatidylcholine (Assman *et al.*, 1974). We have employed ^{31}P NMR spectroscopy to measure the lateral diffusion coeffecient of phospholipid molecules across the surface of VLDL particles (Cushley *et al.*, 1987) (see Section V). In addition, we have used ^{31}P NMR spectroscopy to assess the size of VLDL particles following the incorporation of either selectively deuterated fatty acids or selectively deuterated phosphatidylcholine (see Section IV).

Very little is known about the organization of phospholipid acyl chains in VLDL. In a previous study, using a single nitroxide spin label, 12-doxyl stearic acid, it was shown that the orientational order in VLDL is considerably lower than that found in other lipoproteins (Morrisett *et al.*, 1977b). For instance, at 25°C, the orientational order in VLDL isolated from individuals on an *ad lib* diet was 0.488-0.578 while that in LDL was 0.588-0.638. Hence, it was concluded that the surface monolayer of VLDL is more disorderd compared to other lipoproteins (Morrisett *et al.*, 1977b). The major drawback to the use of bulky nitroxide spin labels is their perturbing effect on the membrane system (Seelig and Niederberger, 1974; Smith *et al.*, 1977). In contrast, ^{2}H NMR spectroscopy is a nonperturbing technique. Therefore, in the present study we have used selectively

deuterated phosphatidylcholines, labelled at the *sn*-2 position, and selectively deuterated palmitic acids to study the organization of phospholipid acyl chain in the surface monolayer of VLDL.

The core

Triglycerides and cholesteryl esters are approximately 55% and 13%, respectively, by weight of VLDL particle and represent the major constituents of the core. Small amounts of cholesterol is also partitioned in the lipid core (Miller and Small. 1982; Jandacek *et al.*, 1977). A number of methods have been employed to investigate the physical state of the core. The fluidity of triglycerides in VLDL has been studied by Morrisett *et al.* (1977b). From the temperature dependence study of TEMPO, 2,2,6,6-tetramethylpiperidine-1-oxyl, in VLDL has shown an increase in core fluidity from 0-40°C.

Other investigators have employed fluorescence and DSC techniques to study the core of VLDL. Schroeder and Goh. (1979a) using DPH and N-phenyl-1-napthylamine have shown how fluidity is effected by the fatty acid composition. From the break points in the Arrhenius plots, an indication of phase change, the authors have shown that rat VLDL perfused with palmitate displayed a phase transition over a temperature range of 10°C *i.e* between 28-39°C while VLDL perfused with oleate showed a phase transition between 20-30°C. This indicates that palmitate-enriched VLDL is less fluid than oleate-enriched VLDL. In both cases, triglycerides were enriched by 45% and 66.4% with palmitic and oleic acids, respectively. Similarly, Hale and Schroeder, (1981) using DSC, have shown that triglyceride extracts from intact rat VLDL perfused with palmitate and

oleate displayed similar DCS peaks. The multiplicity of the peaks has been explained in terms of the polymorphic behaviour of triglycerides. Larsen (1966) has shown that, for triglycerides which possess saturated and unsaturated fatty acids, the saturated fatty acids prefer to position themselves into different layers than unsaturated fatty acids. The phase transition of palmitate- and oleate-enriched VLDL were shown not to be effected by the presence of cholesteryl esters.

Gel to liquid crystalline phase transitions of triglycerides have also been shown by Hamilton *et al.* (1983) using high resolution ^{1}H NMR spectroscopy. By comparing the resonance peak area of fatty acyl chains in the aliphatic region of the spectrum to the allylic proton resonance the authors have shown the phase transition to occur on heating between 10 and 50°C in VLDL isolated from non-human primates fed on a saturated diet. The temperature-dependent increase in fatty acyl resonance was shown to closely match the integral of the DSC enthalpy curve. The above results are in contrast to the early investigations of Jonas and Jung, (1975), Jonas, (1977), Smith and Green, (1974) and Deckelbaum *et al.* (1977) who showed no phase behaviour in human VLDL.

The microviscosity of the lipid core of human serum lipoproteins has been determined with a fluorescence probe, DPH (Jonas, 1977). The microviscosity of VLDL at 25°C (1.0 Poise) was the lowest in comparison to the other lipoproteins. The microviscosity of the intact VLDL was not affected by the removal of proteins and the value was in agreement with isotropic oils. Hence, it was concluded that the fluorescence probe reflected the fluidity of the disordered triglycerides in the core.

The organization of cholesteryl esters in VLDL and LDL has been determined by calorimetric, X-ray scattering and polarizing microscopy techniques (Deckelbaum *et al.*, 1977). Unlike LDL, where the core cholesteryl esters undergo a phase transition between 20-40°C with peak at approximately at 37°C, intact VLDL does not. This is in contrast to its cholesteryl ester extracts. Further, the characteristic 3.6 nm maximum of cholesteryl esters in the liquid crystal domain in LDL were absent in VLDL suggesting that cholesteryl esters were dissolved in the triglyceride-rich core of VLDL. Similar conlusions have also been drawn from a ^{13}C NMR study. Hamilton *et al.* (1976) have shown the ratio of C3 to C6 linewidths of the cholesterol moiety of cholesteryl esters to be lower in VLDL compared to LDL. Further, the ^{13}C NMR spectra of VLDL were similar to that of cholesteryl esters dissolved in excess triolein. Hence it was concluded that the cholesterol moiety of cholesteryl esters had isotropic motions in VLDL because the esters were dissolved in triglycerides (Hamilton *et al.*, 1976).

Part 2. Cholesteryl esters in phospholipid membranes

Atherosclerosis is a disease that involves the thickening of the intimal layer of the artery wall through the deposition of cholesterol. Bulky plaques, formed following the accumulation of the lipids, restrict the flow of blood until a clot is formed. This obstructs the artery and leads to a heart attack or a stroke. The initial stage of the disease is characterised by fatty streaks that progressively become more complicated fibrous plaques following the further depositions of lipid material. Katz *et al.* (1976) have examined the chemical composition of various stages of

human atherosclerotic lesions and have shown cholesteryl esters to be the predominant lipid components. Fatty streaks have very high cholesteryl ester content (77±2%) and have been shown to exist as droplets (Lang and Insull, 1970; Katz *et al.*, 1974). Fibrous plaques, on the other hand, have low cholesteryl ester content (55.5±1.5%) and high cholesterol content (22.5±1.2%) compared to the fatty streaks.

Early investigations have involved the determination of the phase behaviour and organization of cholesteryl esters in phospholipid membrane systems. Janiak *et al.* (1974) using X-ray and polarising light microscopy have examined the incorporation of the cholesteryl ester, cholesteryl linolenate, in egg yolk lecithin-water mixtures. The incorporation of cholesteryl ester was observed to vary with the hydration of the phospholipids. For instance, an increase in water content from 10% to 15% caused the molar ratio of cholesteryl ester to lecithin to increase from 1:50 to 1:22. Between the water concentrations 15%-30%, the ratio remained unchanged (1:22). Upon increasing the water concentration to 42.5%, the lipid ratio was observed to decrease to 1:32. Several conformations of the cholesteryl ester in the bilayer were proposed. At 10% water concentration cholesteryl ester was proposed to be intercalated entirely within the hydrocarbon chains of the phospholipid bilayer. Whereas above 20% water concentration, the cholesteryl ester was proposed to adopted a 'horseshoe' conformation in which the polar cholesteryl ester group was facing the phospholipid-water interface and the hydrophobic cholesterol moiety and fatty acyl chain extended towards the interior of the phospholipid membrane.

Electron spin resonance (ESR) studies of cholesteryl 5-doxylpalmitate and cholesteryl 16-doxylstearate incorporated into egg PC mutilamellar bilayers have shown that the spin-labelled ester adopts a 'horseshoe' conformation in the bilayer (Grover *et al.*, 1979). The 5-doxyl ester in egg PC multilayers gave spectra characteristic of slow reorientation (correlation time $>10^{-8}$ s) and showed that the $2\pi p$ orbital of the nitroxide was aligned at an average angle of tilt of 47±1.5° with respect to the normal to the membrane surface. The 16-doxyl ester in egg PC multilayers gave spectra similar to that of 16-doxylstearic acid incorporated into the multilayers.

Although these results favour the 'horseshoe' conformation in phospholipid bilayers they are considered to give semiquantitative information because the bulky spin labels may reflect the perturbation more than the properties of unperturbed membrane (Taylor and Smith, 1983). Hence, several further studies have measured the dynamic structure of deuterated cholesteryl palmitate (CP) in dipalmitoylphosphatidylcholine (DPPC) (Cushley *et al.*, 1980; Gorrisen *et al.*, 1981). The results from these studies support the 'horseshoe' conformation of CE in phospholipid bilayers. A ^{13}C NMR T_1 study of egg PC incorporated with spin-labelled CP is also consistent with the cholesteryl esters adopting a 'horseshoe' conformation in the phospholipid bilayers (Treleaven *et al.*, 1983).

The permeability of Pr^{3+} and EDTA in egg PC vesicles containing CP or cholesteryl linoelate (CL) have been investigated with ^{31}P NMR spectroscopy (Forrest and Cushley, 1977). It was shown that CP increased the permeabilty of the membrane to both reagents while CL had no effect on membrane permeabilty.

A ^{2}H NMR study by Gorrissen *et al.* (1981) has shown that, in multilamellar dispersions of DPPC containing ≃5 mol% selectively deuterated CP, only about 0.5 mol% of the ester was incorporated into the bilayers at 50°C. This value compares well with the solubility of CP (0.2 mol%) in egg PC bilayers (Valic *et al.*, 1979). In contrast to the multilamellar bilayer studies, a ^{13}C NMR study by Hamilton and Small, (1982) have shown that [*carbonyl*-^{13}C]cholesteryl oleate has a slightly higher solubility (≃2 mol%) in egg PC vesicles.

In the present study we report the investigation of the orientational order of cholesterol moiety of several selectively deuterated CP in multilamellar dispersions of DPPC at 45°C and compare the results with the orientational order of cholesterol in the same membrane and temperature.

CHAPTER II

NMR THEORY

^2H NMR

^2H NMR has proven to be a very valuable technique to study the orientational order and dynamic behaviour of lipids in biological and model membrane systems (Stockton *et al.*, 1976; Seelig. 1977; Davis. 1983; Smith *et al.*, 1984). The advantage of this technique over other techniques arises from the fact that, coupled with low natural abundance (0.015%) and the ease with which certain protons can be replaced with a deuteron, the ^2H NMR spectrum produces signals that are assigned unambiguously. Furthermore, since the van der Waals radius of the deuteron is similar to that of the proton the replacement of proton by deuteron does not perturb the system. This is in contrast to ESR and fluorescence spectroscopy where bulky reporter groups are employed to report spectral information. Such groups have been shown to cause distortions in the membrane systems (Smith *et al.*, 1977; Taylor and Smith, 1981; Sklar *et al.*, 1981). The dominant relaxation mechanism in ^2H NMR is the quadrupolar relaxation. The magnetic moment of the nuclear spin of the deuteron is a factor 6.5X smaller than that of the proton such that dipolar interactions with the neighbouring nuclei are also reduced by a similar factor (Seelig, 1982a).

In the following chapter a simple account of ^2H NMR theory will be given. The reader interested in the detailed aspect of the theory is referred to excellent articles by Seelig. 1977; Mantsch *et al.*, 1977; Davis. 1983; Smith *et al.*, 1984. Details given here have been obtained from

these and other articles.

The powder pattern

In presence of an external static magnetic field, H_o, the deuterium nuclear magnetic moment interacts with the field, H_o, and acquires an energy E whose magnitude is given by

$$E = -\gamma\hbar H_o m \qquad (1)$$

where γ is the magnetogyric ratio of the deuteron, $\hbar$ is the modified planck's constant (= $h/2\pi$), and m is the spin quantum number which can have values I, I-1, ..., -I. Since deuterium is a spin I = 1 nucleus, the nuclear energy levels are split into 2I+1 energy states *i.e.* into the three Zeeman energy levels shown in Figure 2. The energy levels are equally spaced and the allowed transitions m = -1 to m = 0, and m = 0 to m = +1 give rise to a single signal. However, in addition to a magnetic moment, the deuterium nucleus also possess a non-spherical charge distribution and is said to possess an electrical quadrupole moment, Q. The electrostatic interaction between the quadrupole moment and the electric field gradient (EFG), due to the bonding electrons, at the site of the nucleus perturbs the Zeeman energy levels such that the degeneracy between the two transitions is removed. The energy of the corresponding energy levels is given by (Slichter, 1963)

$$E = -\gamma\hbar H_o m + (e^2qQ/h)/(4I(2I-1))\ ((3\cos^2\theta - 1)/2)\ [3m^2-I(I+1)] \qquad (2)$$

where eq is the EFG along the C-^{2}H bond axis and θ is the angle between the symmetry axis of the EFG and the applied magnetic field, H_o. With the selection rule for the allowed transition ($\Delta m = \pm 1$) and with $\Delta E = h\nu$, the

Figure 2: Energy levels for a spin I=1 system with and without quadrupole interactions. The insert describes, schematically, the interaction of a quadrupolar nucleus of ellipsoidal charge distribution with an array of four point charges for the three different spin orientations. Figure from Seelig, 1978.

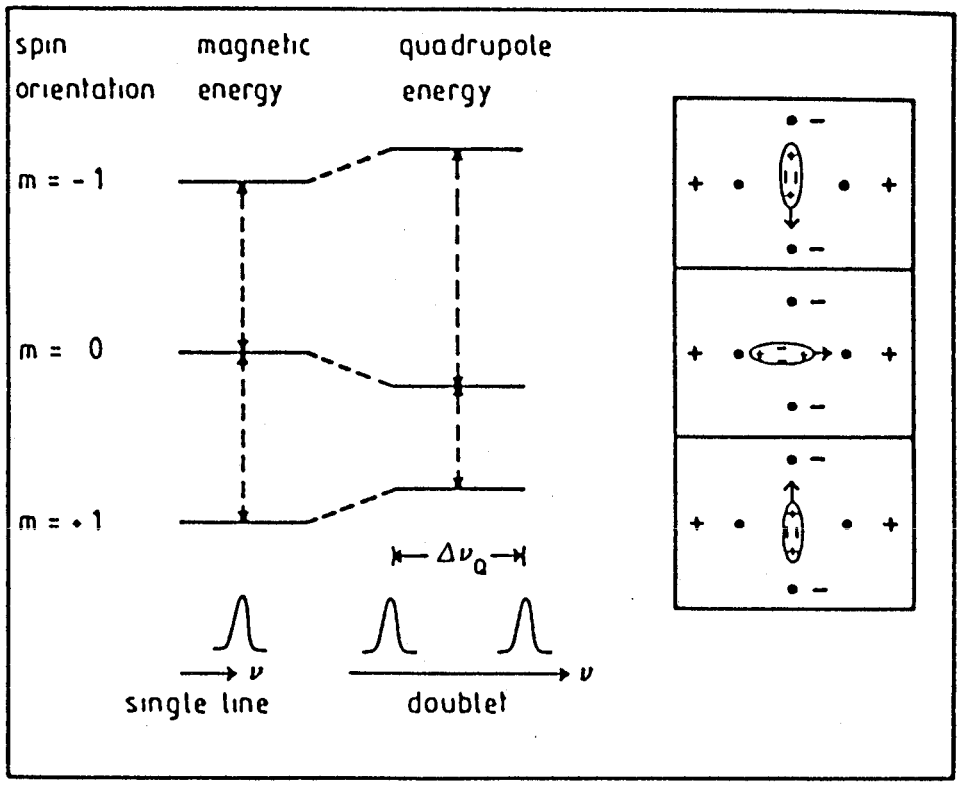

resonance frequencies (ν_1 and ν_2) of the allowed transitions correspond to

$$\nu_1 = \gamma H_0/2\pi + 3/4(e^2qQ/h)((3\cos^2\theta - 1)/2) \quad (3)$$

$$\nu_2 = \gamma H_0/2\pi - 3/4(e^2qQ/h)((3\cos^2\theta - 1)/2) \quad (4)$$

Both resonance frequencies are symmetrical about the Larmor frequency $\omega_0 = \gamma H_0/2\pi$, such that a spectral doublet is observed centered about ω_0. The frequency separation $\Delta\nu(\theta) = (\nu_1 - \nu_2)$ between the two signals is given by

$$\Delta\nu(\theta) = (3/2)(e^2qQ/h)((3\cos^2\theta - 1)/2) \quad (5)$$

In a polycrystalline sample, the C-^{2}H bond makes all possible orientations with respect to the H_0. The probability of finding a fraction of nuclei orientated between θ and $\theta+d\theta$ is given by (Seelig, 1977)

$$P(\theta) = (1/2)\sin\theta \, d\theta \quad (6)$$

The probability is maximum when $\theta = 90°$ and minimum when $\theta = 0°$, and $\theta = 180°$. Hence, in the resulting ^{2}H NMR spectrum the signal intensities are scaled according to equation 6 where the most intense peak corresponds to $\theta = 90°$ and least intense to $\theta = 0°$. A typical powder spectrum is shown in Figure 3. The frequency separation between the two intense peaks ($\theta = 90°$), called the quadrupole splitting ($\Delta\nu_Q$), is given by

$$\Delta\nu_Q = 3/4 \ (e^2qQ/h) \quad (7)$$

where e^2qQ/h is the static quadrupolar coupling constant. For C-^{2}H bonds of the methylene groups the static quadrupolar coupling constant is $\simeq$170 kHz (Burnett and Muller, 1971). For polycrystalline samples $\Delta\nu_Q$ is $\simeq$126 kHz.

Figure 3: A theoretical ^2H powder spectrum.

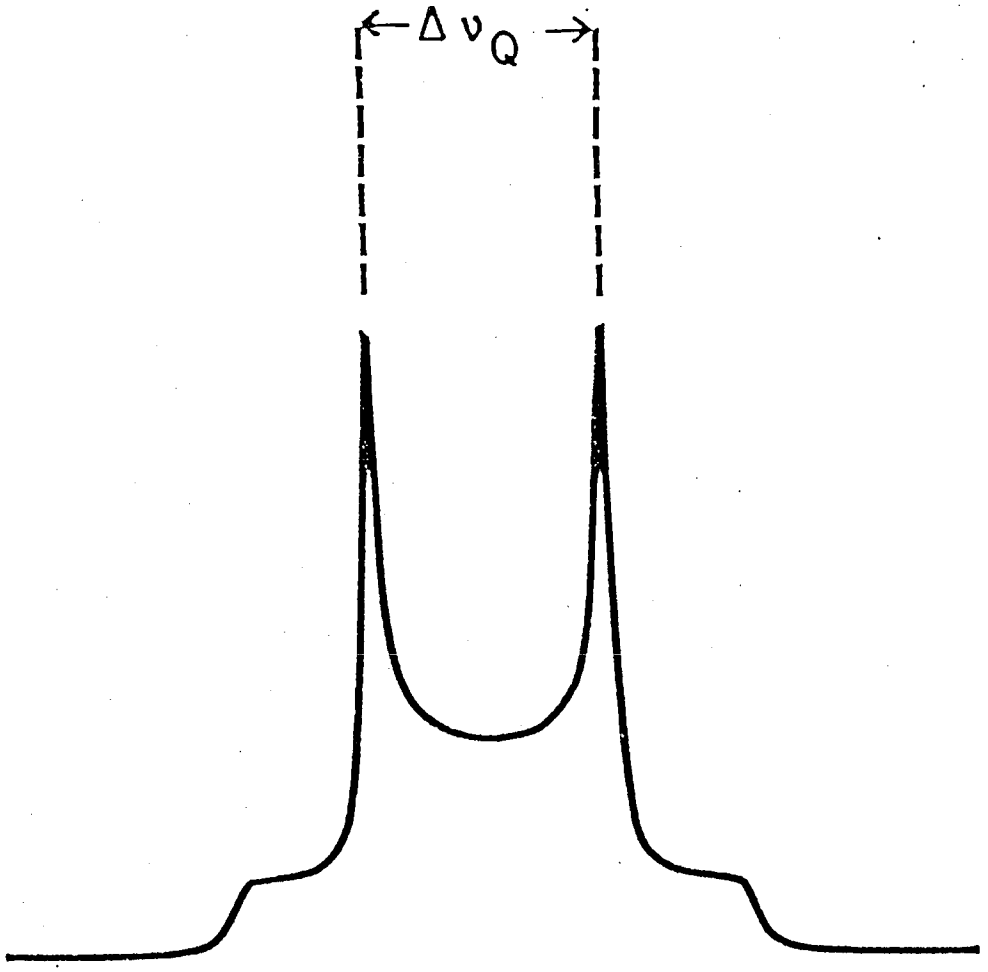

Phospholipid molecules are examples of liquid crystals and they exhibit both liquid and crystalline properties. In contrast to the crystalline compounds, phospholipid molecules in biological membranes are not immobile but undergo rapid anisotropic motions. Since phospholipids are rod-like in shape and have a tendency to align parallel to their long molecular axis, referred to as the director axis $\vec{n}$, rotations perpendicular to this long molecular axis are restricted while those about this axis are fast occurring at frequencies of 10^7-10^{10} s^{-1} (Seelig. 1977). In addition, the phospholipid acyl chains also undergo restricted angular excursions, due to gauche and trans isomerisation, about the director axis. The consequence of these motions is that the quadrupolar interactions become partially averaged reducing the static quadrupolar splitting. The angular fluctuations of the C-^{2}H bond about the director axis is characterised by the orientational order parameter, S_{ii}. This is defined by the following relationship (Seelig, 1977)

$$S_{ii} = (S_{ZZ} + 1/3\ \eta[S_{XX} - S_{YY}]) \qquad (8)$$

where the subscripts X,Y, and Z refer to the fluctuation of the C-^{2}H bond about the three principal axes of the molecule with respect to the director axis. Since $S_{ZZ} + S_{YY} + S_{XX} = 0$, two order parameters are required to describe the motion of a single deuterated molecule. The asymmetry parameter, η, describes the electric field gradient and is defined as $\eta = (V_{XX} - V_{YY})/V_{ZZ}$. By definition the principal axes of the electric field gradient, V, are chosen so that $V_{ZZ} \geqslant V_{XX} \geqslant V_{YY}$. Since $V_{ZZ} + V_{YY} + V_{XX} = 0$ η can have values between $0 < \eta < 1$. In the case of C-^{2}H bond in an

acyl chain, η is small (< 0.05) and the last term in equation 8 is neglected. Hence, S_{ii} becomes equal to S_{ZZ}. We define S_{ZZ} as S_{CD} the carbon-deuterium bond order parameter. The mean angular fluctuation calculated from the β, the C-^{2}H bond vector makes with the director axis is order parameter, S_{CD} (Seelig, 1977; Seelig and Seelig, 1980; Davis, 1983) by

$$S_{CD} = 1/2 \langle 3 \cos^2\beta - 1 \rangle \quad (9)$$

The angular brackets refer to the time averaged fluctuations of the C-^{2}H bond. The ^{2}H NMR spectrum of multilamellar phospholipid bilayers also resembles the spectrum shown in Figure 3 but the quadrupolar splitting is reduced by the factor S_{CD}, viz.,

$$\Delta\nu_Q = 3/4(e^2qQ/h)S_{CD} \quad (10)$$

S_{CD} is zero for isotropically reorienting system and one for a completely immobilized system. The order parameter in equation 10 has been interpreted in terms of a single molecular motion involving the trans-gauche chain isomerisation. However, other more complicated types of motions may also be present in membrane systems. Petersen and Chan (1977) have considered a case where lipid molecules in a bilayer perform two simultaneous types of motions that are independent of each other. In addition to the trans-gauche chain isomerisation, the hydrocarbon chain may also reorient as a whole rigid-body motion, about the director axis. This motion was assumed to be cylindrically symmetric about the director axis while the trans-gauche isomerisation motions are symmetric about an instantaneous position of the long molecular axis. The angles defining these motions are illustrated in Figure 4. Petersen and Chan (1977) have interpreted the order parameter in

Figure 4: Illustration of the angles defined by the orientation of the C-^{2}H bond. H_o is the direction of the applied magnetic field. The director, n, is normal to the bilayer surface. (Figure adapted from Petersen and Chan, 1977).

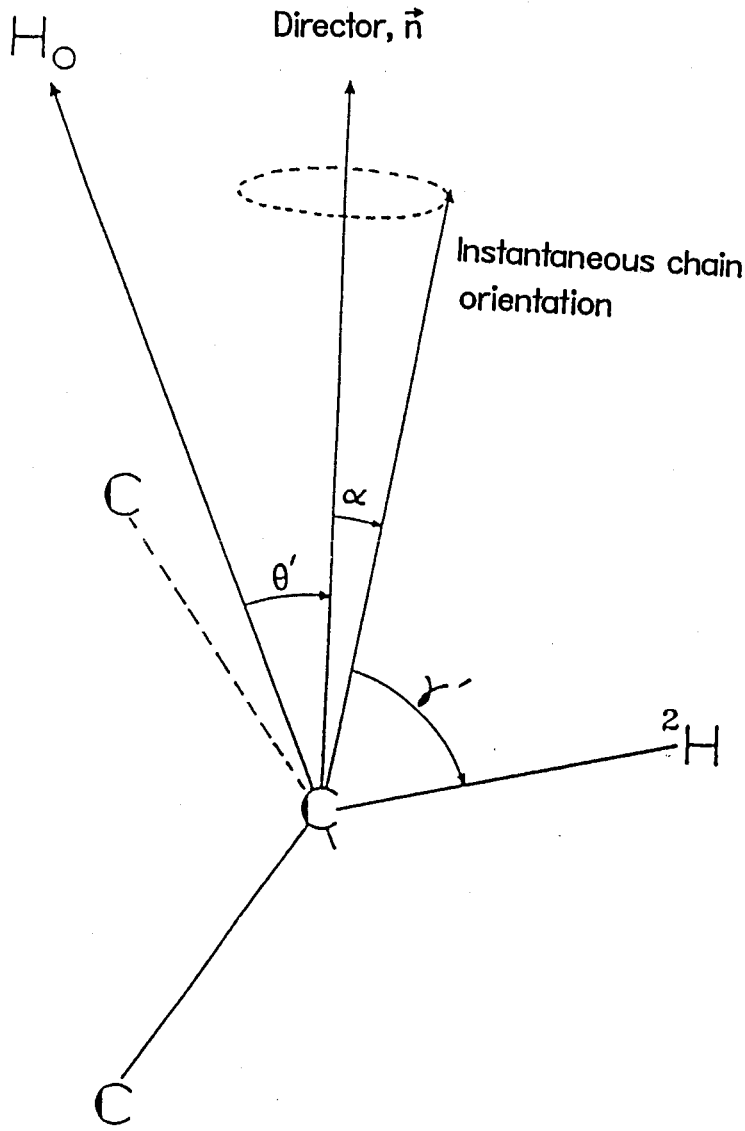

equation 9 in terms of having contributions from both types of fluctuations

$$S_{CD} = S_{\alpha}.S_{\gamma}' = 1/2\langle 3\cos^2\alpha - 1\rangle 1/2\langle 3\cos^2\gamma' - 1\rangle \quad (11)$$

where γ' is the angle between the C-^{2}H bond vector and the instantaneous chain reorientation, and α is the angle between instantaneous chain reorientation and the director axis (normal to the bilayer structure). Equation 11 shows that the S_{CD} value will have contributions not only from the angular fluctuations of the C-^{2}H bond, as a result of trans-gauche isomerisation, but also from the reorientation of the whole chain about the director axis.

For rigid structure such as cholesterol (Taylor *et al.*, 1981; Taylor *et al.*, 1982) or cyclopropane (Dufourc *et al.*, 1983), the angle γ', which is the angle between the C-^{2}H bond and the axis of rotational diffusion, is fixed such that equation 10 becomes:

$$\Delta\nu_Q = 3/4(e^2qQ/h)1/2\langle 3\cos^2\alpha - 1\rangle 1/2(3\cos^2\gamma' - 1) \quad (12)$$

In equation 12 the term in the angular brackets is called the molecular order parameter, S_{mol}. It is a measure of the time-averaged fluctuations of the axis of rotational diffusion ('wobbling') with respect to the director of overall ordering of the steroid moiety. S_{mol} describes the anisotropic motion of the rigid cholesteryl moiety which is fast on the ^{2}H NMR time scale.

Dufourc *et al.* (1983) have proposed two methods for evaluation of the separate order parameters S_{α} and S_{γ}' in equation 11. The first method uses the S_{CD} order parameters and the molecular atomic coordinates to calculate the ordering matrix in the molecule-fixed axis system, ζ. This matrix is

then diagonalized to the axially symmetric form, reflecting the properties of the model membrane system (Dufourc *et al.*, 1984). The second method is based on the fact that S_a is the same for all the deuterons linked to a rigid structure (Taylor *et al.*, 1981). The ratio of the quadrupolar splittings of C-i and C-j on the fused ring system is given by

$$\Delta\nu_{Qi}/\Delta\nu_{Qj} = (3\cos^2\gamma'_{i,n} - 1)/(3\cos^2\gamma'_{j,n} - 1) \qquad (13)$$

The angles $\gamma'_{i,n}$ and $\gamma'_{j,n}$ between each C-^{2}H bond and the axis of rapid rotational averaging, $\vec{n}$, of the sterol skeleton may be evaluated in terms of two new angles β and γ defining the position of $\vec{n}$ in the ζ-axis frame. The Appendix in their paper outlines how one can calculate the $(3\cos^2\gamma'_{i,n} -1)$ terms as a function of these two angles and, by comparison with equation 13, obtain the correct orientation of $\vec{n}$ in ζ. S_a is then obtained from equation 11.

The ^{2}H spectra of small, spherical systems *e.g.* unilamellar phospholipid vesicles (Stockton *et al.*, 1976; Parmar *et al.*, 1984) lipoproteins (Wassall *et al.*, 1982; Parmar, 1985; Treleaven *et al.*, 1986) and reconstituted HDL particles (Parmar *et al.*, 1983; Fenske *et al.*, 1988a) having specifically deuterated lipid molecules are characterised by Lorentzian lineshapes. The linewidths at half height vary with the position of the deuterium label. The collapse of the powder spectrum to a Lorentzian lineshape is due mainly to isotropic tumbling motions which have correlation rates greater than the static quadrupole coupling constant, *i.e* $\tau_c^{-1} >> (e^2qQ/h)$, thus averaging quadrupolar interactions. The order parameter, S_{CD}, can be obtained from Lorentzian lineshape using the second moment, M_2, of the powder spectrum. The second moment of the spectrum is

defined as

$$M_2 = \int_0^\infty (\omega - \omega_0)^2 \, f(\omega)d\omega / \int_0^\infty f(\omega)d\omega \qquad (14)$$

where ω_0 is the central frequency and ω is the frequency from the center of the pake doublet, and $f(\omega)$ represents the intensity of the NMR lineshape at frequency ω. The relationship between M_2 and the quadrupolar splitting $\Delta\nu_Q$ is given by (Davis, 1983)

$$M_2 = (4/5) \, \pi^2 \Delta\nu_Q^2 \qquad (15)$$

In vesicles and lipoprotein particles, particle tumbling and lateral diffusion of molecules are responsible for narrowing the ^2H NMR spectra to Lorentzian lineshapes. The linewidth at half height, $\Delta\nu_{1/2}$, for a Lorentzian line is related to M_2 by (Abragam, 1961)

$$\pi\Delta\nu_{1/2} = M_2\tau_e + C \qquad (16)$$

where C is a constant having contributions from magnetic field inhomogeniety and spin-lattice relaxation, and τ_e is the effective correlation time for the isotropic motions given by

$$1/\tau_e = 1/\tau_r + 1/\tau_d \qquad (17)$$

The time τ_d is the correlation time for diffusion in the surface plane and is related to the lateral diffusion coefficient, D_t, and the radius, R, from centre of the particle to the midpoint of the bilayer (for vesicles) or the surface monolayer (lipoprotein)

$$\tau_d = R^2/6D_t \qquad (18)$$

The time τ_r is the rotational correlation time for particle tumbling and is obtained from the Stokes-Einstein relationship

$$\tau_r = 4\pi\eta R^3/3kT \qquad (19)$$

where η is the solvent viscosity, T is the absolute temperature and k is the Boltzmann's constant.

The local anisotropic motions of the acyl chain reorientations partially average the static quadrupolar coupling constant by a factor S_{CD} such that the rigid lattice value of the second moment is reduced to a residual second moment M_{2_r}. With the assumption that rate of local molecular reorientations is faster than the isotropic motions represented by τ_e the linewidth may be given by

$$\pi\Delta\nu_{1/2} = M_{2_r}\tau_e + 1/T_1 \qquad (20)$$

where $1/T_1$ is the spin-lattice relaxation rate. It should be noted that the linewidth, $\Delta\nu_{1/2}$, in the equation 20 has contributions from two types of motions, fast trans-gauche isomerisations (T_1) and slow isotropic motions (particle tumbling and lateral diffusion of phospholipids across the surface plane of VLDL). Other slow anisotropic motions such as rigid-stick type motions have not been considered. If we assume the molecular motions of phospholipid molecules in the lipoprotein monolayer are axially symmetric about the normal to the lipoprotein surface then M_{2_r} can be written as

$$M_{2_r} = (4/5)\pi^2\Delta\nu_r^2 \qquad (21)$$

where $\Delta\nu_r$ is represented by equation 10. Substitution of equations 10 and 21 into equation 20 gives (Stockton *et al.*, 1976)

$$\Delta\nu_{1/2} = (9\pi/20)(e^2qQ/h)^2 S_{CD}^2 \tau_e + (1/\pi T_1) \quad (22)$$

Spin-lattice relaxation time

Measurement of the quadrupolar splitting and linewidth from a ^2H NMR spectrum provides information about the segmental ordering, a static measure of average molecular structure. Information about the molecular motions at the segmental level is obtained from the measurement of spin-lattice relaxation time, T_1.

T_1 is a measure of the return of the spins to thermal equilibrium following a radio frequency pulse. The mechanism by which spins of a system achieve thermal equilibrium is from the action of the local fluctuating fields. These can arise from neighbouring nuclei, paramagnetic ions, induced magnetic moments of chemical bonds and molecular motions. In the case of deuterium, relaxation results from the modulation of the interaction between the quadrupole moment and the EFG. Since the EFG is fixed in the molecular framework then the modulation of the interaction is achieved by the molecular motion of the molecule.

A general expression for the T_1 relaxation rate is given by (Jardetzky and Roberts, 1981).

$$1/T_1 = (3/80)(e^2qQ/\hbar)^2[J(\omega_0) + 4J(2\omega_0)] \quad (23)$$

where ω_0 is the Larmor frequency. $J(\omega)$ is the spectral density which is a measure of the energy of modulation available at a specific angular frequency ω. $J(\omega) = 2\tau_c/(1 + \omega^2\tau_c^2)$, where τ_c is the correlation time of the molecular motion(s). Under extreme narrowing condition ($\omega^2\tau_c^2 \ll 1$)

equation 23 is reduced to

$$1/T_1 = (3/8)(e^2qQ/\hbar)^2\tau_c \qquad (24)$$

Although equation 24 provides a reasonable first order approximation to the molecular motions in phospholipid bilayers, the C-^{2}H bond on the acyl chain does not undergo isotropic reorientation; instead it undergoes restricted angular fluctuations. Brown and Seelig (1979), assuming the molecular motions to be in the extreme narrowing limit, have derived an expression in terms of an orientational order parameter.

$$1/T_1 = (3/8)(e^2qQ/\hbar)^2(1 - S_{CD}^2)\tau_c \qquad (25)$$

However, their model was unable to account for the observed ^{2}H T_1 values of DPPC multilamellar dispersions as function of temperature and frequency (Brown, 1982). Alternative models were proposed to explain for the frequency dependence of T_1 (Peterson and Chan, 1977; Brown, 1982). In these models T_1 was suggested to have contributions from two types of motions, one being very fast ($1/T_{1f}$) and the other being much slower in magnitude ($1/T_{1s}$). Thus, T_1 is given by

$$1/T_1 = 1/T_{1f} + 1/T_{1s} \qquad (26)$$

In Brown's model, $1/T_{1f} = A\tau_f$, where A is a constant that corresponds to the trans-gauche isomerisations of the lipid acyl chains ($\tau_f = 10^{-11}$ s). $1/T_{1s} = BS_{CD}^2\omega_o^{-1/2}$, where B is a constant describing the collective bilayer motions. The $1/T_{1s}$ term determines the dependence of the relaxation rate on S_{CD} and frequency (ω_o). The modified T_1 expression, equation 26, quantitatively accounts for the observed ^{2}H NMR T_1 values of DPPC, in the

liquid crystalline state, and therefore is indicative of the fact that DPPC bilayers undergo collective-type fluctuations. These slow motions are veiwed as distribution of wave-like disturbances of phospholipid bilayers, analogous to twist and splay motions, with each having a characteristic amplitude, wavelength and correlation time (Brown, 1982; 1984; Brown *et al.*, 1983; Brown and Williams, 1985)

^{31}P NMR

^{31}P nuclear magnetic resonance spectroscopy has been employed extensively to study the dynamic and the polymorphic behaviour of membrane structures. ^{31}P NMR utilizes the natural abundance of the ^{31}P isotope of phosphate in the phospholipid head groups and is thus a non-perturbing technique. Phosphorus is a spin 1/2 nucleus and has a relative sensitivity of 0.06 compared to the proton nucleus (Buldt and Wohlgemuth, 1981).

The asymmetric ^{31}P NMR spectra observed in phospholipid membranes result from the combined effects of the Chemical Shift Anisotropy (CSA) of the phosphorus nuclei and the dipolar interactions with the methylene protons (Seelig *et al.*, 1978). By applying appropriate ^{1}H-decoupling techniques the dipolar interactions are removed and this then allows the determination of CSA. Measurement of CSA provides an insight into the headgroup structure in the membrane systems.

The electron density around the tetrahedral PO_4 segment, due to oxygen atoms, is not symmetrical but varies with respect to the molecular coordinate system of the phosphate group. The axis about which the electron density is small has less shielding and the axis with high electron density

has the largest shielding contribution (Seelig, 1982b). The orientation of the chemical shielding tensor about the phosphate segment has been determined for single crystals of phosphoethanolamine (Kohler and Klein, 1976) and barium diethylphosphate (Herzfeld *et al.*, 1978). ^{1}H-Decoupled ^{31}P NMR spectra of both crystals display two resonances originating from two magnetically inequivalent phosphate orientations in the unit cell. By monitoring the variation of the peaks as a function of crystal rotations with respect to the magnetic field, the magnitude and the orientation of the principal elements are determined. Figure 5a illustrates the principal orientations of chemical shielding tensors, σ_{11}, σ_{22} and σ_{33}, for the phosphate segment of the phosphodiester, barium diethylphosphate, (Herzfeld *et al.*, 1978). The σ_{11} axis is approximately perpendicular to the O(3)-P-O(4) plane, σ_{22} bisects the O(3)-P-O(4) angle and the σ_{33} is orthogonal to these two directions. The orientation of the principal axes in phospholipid molecules have proven difficult to measure due largely to the difficulties encountered in growing sufficiently large crystals necessary for the NMR investigations. Recently however, the principal axis orientations in a phospholipid analogue, 1-hexadecyl-2-deoxglycerophosphoric acid monohydrate, has been determined (Hauser *et al.*, 1988). The values are in close agreement with those reported for the phosphomonoester, phosphoethanolamine and deoxy 5'-monophosphate, and tend to deviate by 7-13° from the barium diethylphosphate orientations. The magnitude of the principal components in phospholipid molecules can however, be measured with less certitude from the ^{31}P NMR spectra of crystalline powders (Seelig, 1978). The completely immobilised phosphate groups yield typical spectra as shown in Figure 5b, where the magnitude of the principal components are obtained from the spectral edges and the central peak.

Figure 5a: Molecular orientation of ^{31}P chemical shift tensor in the molecular frame of phosphate segment according to the single crystal study of barium diethylphosphate. Figure from Herzfeld *et al.*, 1978.

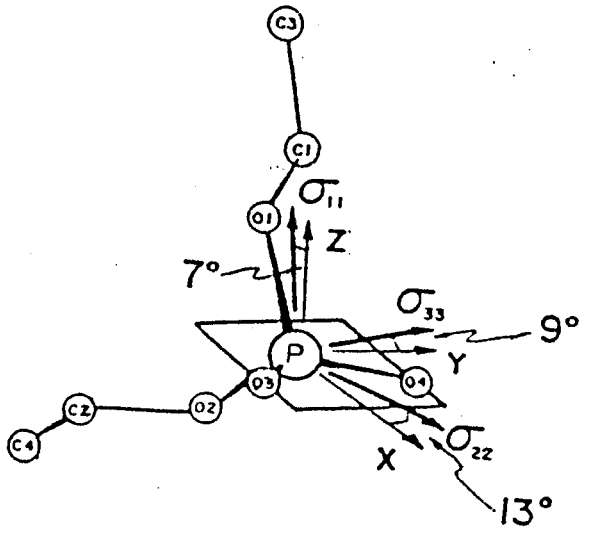

Figure 5b: ^{1}H-decoupled ^{31}P NMR spectra (118.5 MHz) of anhydrous 1,2-dipalmitoyl-*sn*-glycero-3-phosphocholine. Figure from Griffin, 1976.

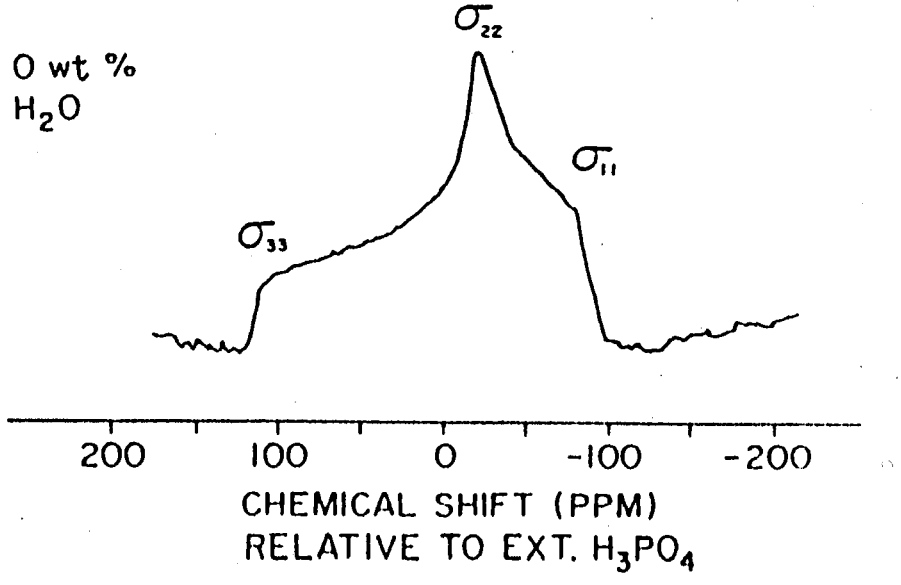

Figure 5b illustrates the ^{31}P NMR spectrum of 1,2-dipalmitoylphosphatidylcholine crystalline powder. A number of phospholipid monohydrate powders studied have yielded similar principal component values of approximately σ_{11} = -80, σ_{22} = -20 and σ_{33} = 110 ppm (Seelig, 1978), and are in close agreement with those of barium diethylphosphate (σ_{11} = -76, σ_{22} = -18 and σ_{33} = 110 ppm). Thus, the orientations of the principal axes in phospholipid molecules resemble those of either phosphoethanolamine or barium diethylphosphate.

The addition of water to the crystalline powder of 1,2-dipalmitoylphosphatidylcholine (σ_{11} = -98, σ_{22} = -34 and σ_{33} = 134 ppm) alters the completely immobilized spectrum such that the principal components are reduced (σ_{11} = -81, σ_{22} = -25 and σ_{33} = 110 ppm). Binding of one water molecule has been suggested to increase the phosphate symmetry (Griffin *et al.*, 1976). However, with further addition of water the spectrum increasingly assumes an axially symmetric lineshape. The addition of water does not change the chemical shift tensor since when the temperature is lowered to -110°C the spectrum reverts back to an asymmetrical lineshape with principal components of (σ_{11} = -81, σ_{22} = -21 and σ_{33} = 108 ppm) (Griffin, 1978).

Axially symmetric spectra are observed with phospholipid bilayers due to the rapid reorientations about the director axis (normal to the membrane) mentioned above, and the principal elements, σ_{22} and σ_{33}, become partially averaged (Seelig, 1978). The resonance is identical when the magnetic field H_0 is parallel to the σ_{22} and σ_{33} plane but vary when the magnetic field is perpendicular to the plane. Figure 6a illustrates a typical powder spectrum resulting from the rapid averaging of principal

elements σ_{22} and σ_{33}. The magnitude of the CSA is obtained from the frequency separation of $\sigma_{\parallel}$ (where the magnetic field is parallel to the bilayer normal) and $\sigma_{\perp}$ (where the magnetic field is perpendicular to the bilayer normal) as shown by

$$\Delta\sigma = \sigma_{\parallel} - \sigma_{\perp} \tag{27}$$

In membrane systems, in addition to the rapid axial reorientation of the phospholipid molecules, there are also tilting motions (wobbles) along the long axis of the phospholipid molecules. These motions are such that the $\sigma_{\parallel}$ and $\sigma_{\perp}$ are averaged to $\sigma_{\parallel}'$ and $\sigma_{\perp}'$. The effective tensor still has axial symmetry, but the spectrum has reduced CSA. The reduction in the CSA value is related to the amplitude of motion (Smith, 1984). Figure 6b illustrates the narrowing of the ^{31}P NMR spectrum due to additional motional states of the phospholipid head group. In general, $\Delta\sigma$ of phospholipid membranes above the gel to liquid-crystalline phase transition is between 40-50 ppm (Seelig, 1978). A quantitative measure of phosphate head group motion has been developed by Seelig (1978), where $\Delta\sigma$ has been related to the static chemical shielding tensors in terms of order parameters by the following expression

$$\Delta\sigma = S_{11}(\sigma_{11} - \sigma_{22}) + S_{33}(\sigma_{33} - \sigma_{22}) \tag{28}$$

where S_{11} is the order parameter for the axis connecting the esterified oxygen of the phosphate group and S_{33} is the axis that connects the nonesterified oxygen atoms. Although the measure of $\Delta\sigma$ provides information of the head group structure in the membranes, it cannot be analysed quantitatively as a measure of head-group motion, as two order parameters are required from just one experimental result ($\Delta\sigma$). However, by assuming

Figure 6a: Simulated ^{31}P NMR spectra of rapid axial motion of the long axis of phospholipid molecule in membrane lipids.

Figure 6b: Simulated ^{31}P NMR spectra of membrane lipids where in addition to rapid axial rotations the phospholipid molecules also undergoes tilting (wobbling) motions. Figure 6a and 6b from Smith, 1984.

ORDERED PHOSPHODIESTER
Rapid axial rotation

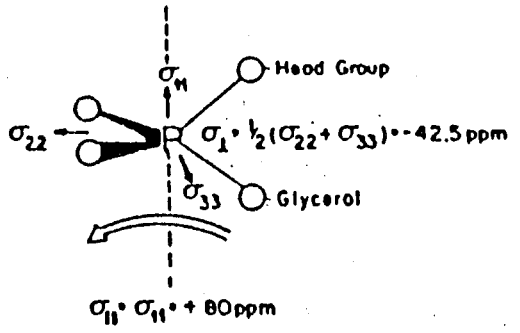

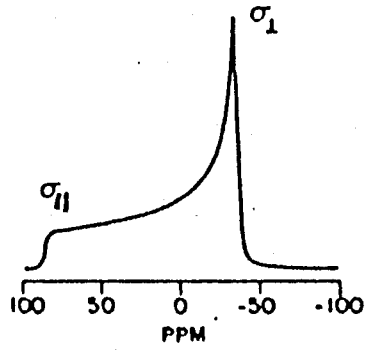

DISORDERED PHOSPHODIESTER
With rapid axial rotation

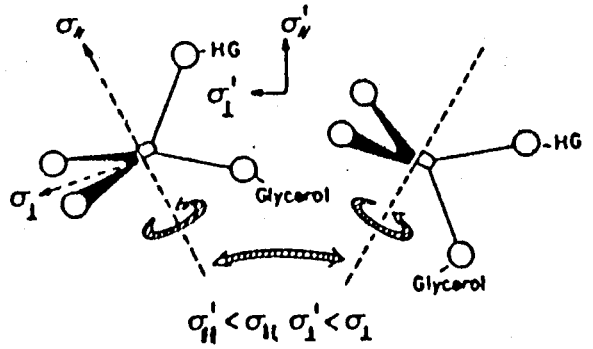

$\sigma_{||}' < \sigma_{||}$, $\sigma_\perp' < \sigma_\perp$

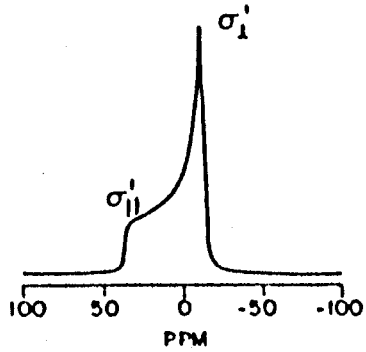

head group orientation and a model of motional averaging, the calculated $\Delta\sigma$ can be compared with the experimental data. Combination of this approach and with the information obtained from other techniques e.g. ^{2}H NMR can provide an understanding of the head group motions (Seelig and Gally, 1976).

Not all lipids when dispersed in water adopt a bilayer organization which is the generally accepted molecular model of biomembranes (Singer and Nicholson, 1972). There are lipids that adopt other types of molecular arrangements. Examples are the unsaturated phosphatidylethanolamines, monoglucosyldiglycerides and cardiolipins which, in the presence of Ca^{2+}, adopt hexagonal packed cylinders (Hexagonal II phase, Figure 7). The polar head groups of these molecules face towards the inside of the cylinder while the hydrocarbon chains face the hydrophobic phase (Cullis and de Kruijff, 1979). The ^{1}H-decoupled ^{31}P NMR spectra yield powder patterns of reverse asymmetry and with half the CSA of that found in bilayer membranes (see Figure 7). The reduced value of CSA arises from the motional averaging due to lateral diffusion of phospholipid molecules around the aqueous channels of the cylinders (Cullis and de Kruijff, 1979).

In unilamellar bilayer and lipoprotein structures the fast isotropic tumbling and lateral diffusion of the phospholipid molecules across the surface further averages the CSA such that the ^{31}P NMR spectra are narrow and display single Lorentzian lineshapes (see Figure 7). The linewidth at half height, $\Delta\nu_{1/2}$, is related to the second moment, M_2, by equation 16. M_2 of ^{31}P NMR powder spectra is related to the chemical shift anisotropy by (McLaughlin *et al.*, 1975)

Figure 7: ^{1}H-decoupled ^{31}P NMR spectra of egg yolk PC bilayer dispersions, hexagonal II phase (Soya bean PE) and 'isotropic motion' (mixture of Soya bean PE (85%) and egg yolk PC (15%). Figures from Cullis and de Kruijff, 1979.

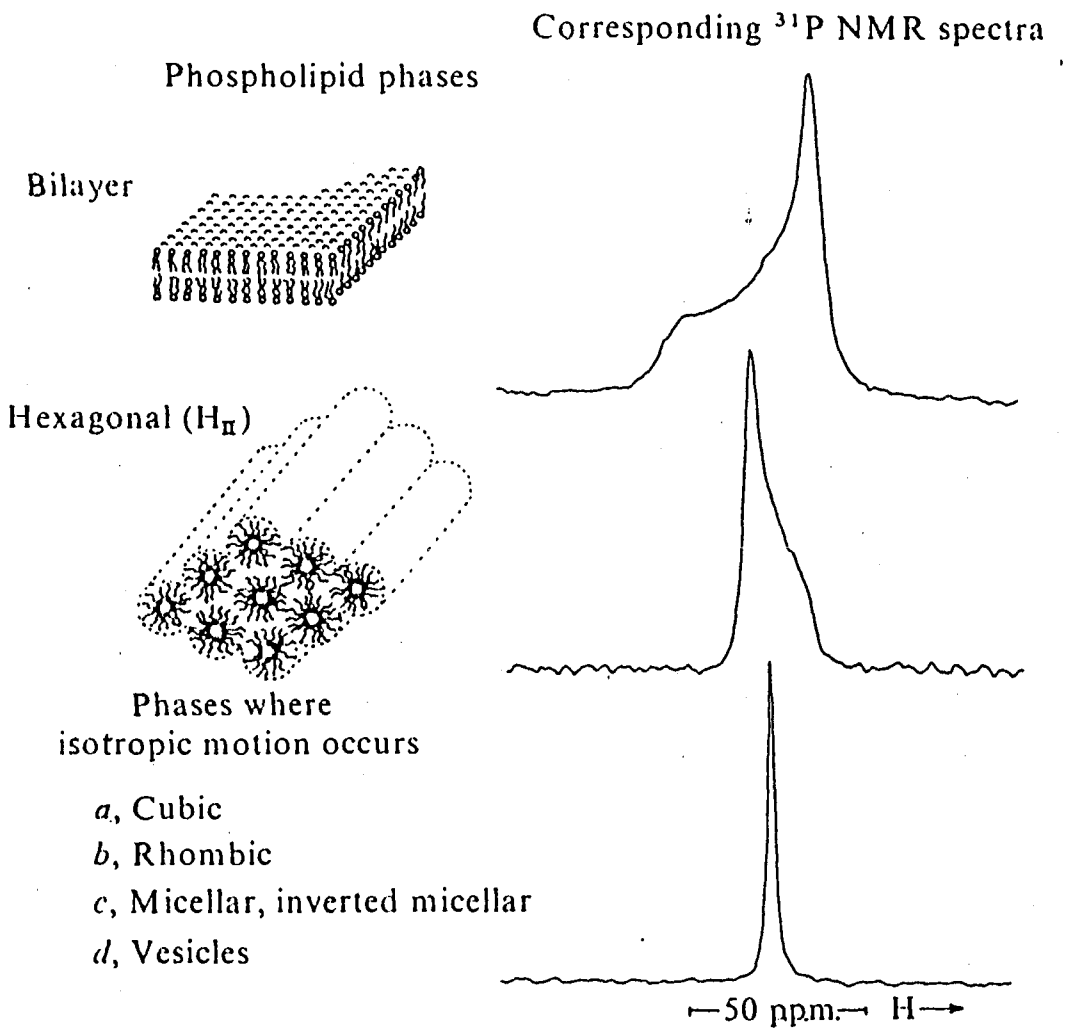

$$M_2 = (4/45)(2\pi\nu_0)^2\Delta\sigma^2 \quad (29)$$

where ν_0 is the resonance frequency of the ^{31}P nucleus (102.2 MHz on our spectrometer). Thus, by making appropriate substitutions for τ_e (equations 18 and 19) into equation 16 we obtain an equation that relates the variation of linewidth to solvent viscosity, and is given by

$$(\Delta\nu_{1/2} - C)^{-1} = \eta^{-1}(3kT/M_2 4R^3) + (\pi 6D_t/M_2R^2) \quad (30)$$

Note that M_2 can be obtained from the slope of equation 30 *i.e.* $M_2 = 3kT/((\text{slope})4R^3)$. A plot of $(\Delta\nu_{1/2} - C)^{-1}$ versus η^{-1} will yield D_t from the ratio of the intercept to the slope as shown by

$$D_t = ((\text{Intercept})kT/(\text{slope})R8\pi) \quad (31)$$

CHAPTER III

MATERIALS AND METHODS

Materials

Deuterium-depleted water, Egg yolk L-*α*-lysophosphatidylcholine (Egg yolk lysoPC), L-*α*-lysophosphatidylcholine (Palmitoyl), 1,1'-carbonyldiimidazole and triolein were purchased from Sigma Chemical Company. Sigma egg yolk lysoPC contains 66-68% palmitic acid, 24-26% stearic acid, and 6-10% other saturated acids (Thewalt *et al.*, 1985). [4,4-$^2H_2$]Palmitic acid and [7,7-$^2H_2$]stearic acid were generous gifts from the late Dr. A. P. Tulloch, Plant Biotechnology Institute, National Research Council of Canada, Saskatoon, Saskatchewan. Lithium aluminum deuteride, [5,5,6,6-$^2H_4$]- and [11,11,12,12-$^2H_4$]- palmitic acid were purchased from Merck, Sharp and Dohme, Canada Ltd. [2,2-$^2H_2$]Palmitic acid and [16,16,16-$^2H_3$]phosphatidylcholine were generous gifts from Dr. H. Gorrissen, BASF AG, Abt. Kunststofflabor, D-6700, Ludwigshafen, FRG. [N(CD_3)$_3$-$^2H_9$]PC and [$^2H_{31}$]Palmitic acid were a generous gift from from Drs. R. J. Cushley and W. D. Treleaven, respectively. Palmitic acid was obtained from Matheson, Coleman and Bell Canada. Cholest-5-en-3-one was purchased from Steraloid Incorporated. [2,2,4,4,6-$^2H_5$]Cholesterol and [7,7-$^2H_2$]cholesterol were generous gifts from Dr. I. C. P. Smith, Division of Biological Sciences, National Research Council, Ottawa, Ontario. "Baker analysed" Silica gel, 60-200 mesh, was purchased from J. T. Baker Chemical Company, Philipsburg, New Jersey. Aquacide II (Sodium salt of Carboxymethylcellulose) was obtained from Calbiochem. Pre-swollen Microgranular Anion Exchange DE52 (Diethylaminoethyl Cellulose) was obtained

from Whatman. Sepharose 4B chromatography gel was purchased from Pharmacia Fine Chemicals. AB Uppsala, Sweden. [1-^{14}C]Palmitic acid and [1-^{14}C]dipalmitoylphosphatidylcholine were purchased from New England Nuclear, Boston, Mass. Glycerol was purchased from Fisher Scientific Company. The lipid analysis kits for determining free cholesterol, total cholesterol and triglyceride were purchased from Boehringer Mannheim.

Isolation of Egg yolk phosphatidylcholine

Egg Yolk Phosphatidylcholine (egg PC) was isolated from 12 fresh hen egg yolks using the procedure of Singleton *et al* (1965). The crude product was purified by silica gel column chromatography as described by Richter *et al* (1977). The purified egg PC was dissolved in chloroform to a known concentration of 0.20g/mL. The sample was stored in the dark under N_2 at -20°C. The yield from 12 eggs was 8.3g.

Synthesis of Deuterated Phosphatidylcholines

Specifically deuterated phosphatidylcholines were synthesized by condensing specifically deuterated fatty acids to the *sn*-2 position of egg yolk lysoPC using the procedure of Grover and Cushley (1979). The following deuterated phosphatidylcholines were synthesised *sn*-2-[2,2-$^2H_2$]-, [4,4-$^2H_2$]-, [5,5-$^2H_2$]-, [5,5,6,6-$^2H_4$]-, and [11,11,12,12-$^2H_4$]-*sn*-1-palmitoyl(stearoyl)-3-phosphocholine, [$^2H_{31}$]-*sn*-1-palmitoyl-3-phosphocholine, and *sn*-2-[7,7-$^2H_2$]stearoyl-*sn*-1-palmitoyl(stearoyl)-3-phosphocholine. A revised procedure is illustrated for the synthesis of

sn-2-[2,2-$^2H_2$]palmitoyl-*sn*-1-palmitoyl(stearoyl)-3-phosphocholine. Following this, brief details regarding the synthesis of the other selectively deuterated phosphatidylcholines together with their analytical data are presented.

The mass spectra of the selectively deuterated PCs are characterised by two sets of peaks, one set centered at M - 183 (M minus $N(CH_3)_3$-$(CH_2)_2$-OPO_3:phosphocholine) m/e = 553 corresponding to phospholipids with palmitoyl *sn*-1 chain and one set at m/e = 582 corresponding to phospholipids with stearoyl *sn*-1 chains. In the case of [$^2H_{31}$]PC, there is one set of peaks at m/e = 580 corresponding to phospholipid with palmitoyl *sn*-1 chain.

All reactants were dried under high vacuum overnight prior to use. 1,1'-Carbonyldiimidazole (CDI) (64.35 mg, 0.39 mmol) was added to a continously stirring mixture of [2,2-$^2H_2$]palmitic acid (100 mg, 0.39 mmol) in dry benzene (25 mL) under a stream of N_2. Bubbles of carbon dioxide evolved as the reaction proceeded. Egg yolk lysoPC (191.8 mg, 0.39 mmol) was added after 45-60 min. The reaction mixture was stirred under increased flow of N_2 until all the benzene had evaporated. The sample was dried further under high vaccum ($\simeq$ 3 hr). The flask was heated under a continous flow of N_2 for 3 hr in an oil bath maintained at 80-82°C. The crude product was cooled and dissolved in petroleum ether (30-60)/95% ethanol (5/0.75, v/v) (3-4 mL) and precipitated in cold acetone (45-60 mL) with vigorous shaking. The mixture was allowed to stand overnight in the freezer at -20°C. Crude phospholipids were filtered from the solution, and precipitated once again. Following the final precipitation, the filterate was applied to a column (2.6 x 60 cm) packed with Baker Analysed silica

gel, 60-200 mesh, and eluted with chloroform/methanol/water (70:26:4, v/v). Approximately 7.5 mL fractions were collected from the column and examined for the presence of pure phospholipid by thin layer chromatography. Fractions showing the presence of pure phosphatidylcholine were pooled, and solvent was removed by rotary evaporation. Products were further dried under high vacuum overnight. Thin layer chromatogram of *sn*-2-[2,2-$^2H_2$]palmitoyl-*sn*-1-palmitoyl(stearoyl)-3-phosphocholine ([2,2-$^2H_2$]PC) developed in chloroform/methanol/water (70:26:4, v/v) showed a single spot at R_f = 0.21 while unreacted egg yolk lysoPC showed a single spot at R_f = 0.09. For comparison, DPPC obtained from Sigma showed single spots at R_f 0.21. Yield: 62.0 mg, 21.9%; mass spectrum: m/e (peaks between 500-640) 582 (13.7%), 581 (31.3%), 580 (40.0%), 579 (29.9%) 554 (33.4%), 553 (72.3%), 552 (100.0%), 551 (74.8%), 510 (18.0%), 509 (31.3%), 508 (36.4%).

[4,4-$^2H_2$]PC:

CDI (210.5 mg, 1.28 mmol), [4,4-$^2H_2$]palmitic acid (300.0 mg, 1.16 mmol) and egg yolk lysoPC (570.5 mg, 1.16 mmol) yielded 430.0 mg, 50.6%; m/e (peaks between 500-620) 582 (20.7%), 581 (34.4%), 580 (8.4%), 555 (22.0%), 554 (67.1%), 553 (100.0%), 552 (18.8%).

[5,5-$^2H_2$]PC:

CDI (210.5 mg, 1.28 mmol), [5,5-$^2H_2$]palmitic acid (300.0 mg, 1.16 mmol) and egg yolk lysoPC (570.5 mg, 1.16 mmol) yielded 548.2 mg, 64.5%; m/e (peaks between 500-620) 582 (18.2%), 581 (31.8%), 580 (5.0%), 555 (18.4%), 554 (63.0%), 553 (100.0%), 552 (14.3%), 511 (10.6%), 510 (29.8%).

[5,5,6,6-$^2H_4$]PC:

CDI (70.0 mg, 0.42 mmol), [5,5,6,6-$^2H_4$]palmitic acid (100.0 mg, 0.38 mmol) and egg yolk lysoPC (188.5 mg, 0.38 mmol) yielded 88.2 mg, 31.2%; m/e (peaks between 500-620) 584 (14.0%), 583 (30.2%), 582 (7.6%), 557 (12.3%), 556 (46.2%), 555 (100.0%), 554 (22.5%), 513 (14.8%), 512 (34.1%), 511 (17.0%), 510 (12.8%).

[7,7-$^2H_2$]PC:

CDI (190.4 mg, 1.15 mmol), [7,7-$^2H_2$]stearic acid (300.0 mg, 1.05 mmol) and egg yolk lysoPC (516.0 mg, 1.05 mmol) yielded 449.5 mg, 56.5%; m/e (peaks between 500-640) 610 (15.2%), 609 (29.2%), 583 (13.3%), 582 (51.1%), 581 (100.0%), 580 (17.9%).

[11,11,12,12-$^2H_4$]PC:

CDI (70.0 mg, 0.42 mmol), [11,11,12,12-$^2H_4$]palmitic acid (100.0 mg, 0.38 mmol) and egg yolk lysoPC (188.5 mg, 0.38 mM) yielded 63.0 mg, 22.3%; m/e (peaks between 500-640) 585 (7.5%), 584 (23.4%), 583 (38.7%), 582 (7.3%), 557 (20.1%), 556 (64.0%), 555 (100.0%), 554 (16.9%).

[$^2H_{31}$]PC:

CDI (320.0 mg, 1.94 mmol), [$^2H_{31}$]palmitic acid (556.0 mg, 1.94 mmol) and L-α-lysophosphatidylcholine (Palmitoyl) (988.0 mg, 2.00 mmol) yielded 780.0 mg, 51.1%; m/e (peaks between 500-640) 584 (7.5%), 583 (24.3%), 582 (56.9%), 581 (95.4%), 580 (100.0%), 579 (75.1%), 578 (35.1%), 577 (12.3%), 537 (12.2%).

DSC analysis of a [4,4-$^2H_2$]PC/water dispersion showed a pretransition at

32°C and a main gel to liquid crystalline phase transition at 42°C, while a [$^2H_{31}$]PC/water dispersion showed a pretransition and gel to liquid crystalline phase transition at 33°C and 41°C, respectively. These results are in good agreement with the DSC results for DPPC/water dispersions (Thewalt *et al*. 1985). The author is indebted to Dr. J. Thewalt and Mrs. Junshi Yue for obtaining the DSC analysis of deuterated phospholipids. The ^1H NMR spectra of [2,2-$^2H_2$]PC in chloroform/methanol (2:1, v/v) at 25°C is characterised by the presence of two doublets of doublets at δ = 4.13 and δ = 4.41 ppm for the 1CH_2OCO glycerol protons and the two protons of 3CH_2OP glycerol appear as a multiplet at δ = 4.0 ppm. The peak assignments were made as described by Birdsall *et al*, (1972) and Ponpipom and Bugianesi, (1980). The ^1H NMR spectrum of the selectively deuterated phospholipid was identical to the spectrum of DPPC obtained from Sigma and agrees with the published spectra of 1,2-distearoyl-*sn*-glycero-3-phosphocholine (Ponpipom and Bugianesi, 1980). Thereby indicating that in deuterated phospholipid the deuterated fatty acid chains are condensed at the *sn*-2 position. In the case of 1,3-distearoyl-*sn*-glycero-3-phosphocholine the CH_2OCO glycerol protons arising from the two equivalent fatty acids resonant as a doublet at δ = 4.24 ppm (Ponpipom and Bugianesi, 1980). We assume the remaining selectively deuterated phospholipids have the deuterated fatty acid chain condensed at the *sn*-2 position.

Synthesis of [3-$^2H_1$]Cholesterol

Cholest-5-en-3-one (1.87 g, 4.86 mmol), dissolved in anhydrous ether (50 mL), was introduced slowly into stirring $LiAl^2H_4$ (0.5 g) in anhydrous

ethereal solution (75 mL) over a period of approximately 40 min. The mixture was continously stirred for 3 1/2 hr at room temperature. The reaction was stopped by the following sequence of additions: H_2O (1.5 mL), freshly prepared 15% NaOH (0.5 mL) and H_2O (1.5 mL). The reaction mixture was further stirred for 30 min. The resulting white mixture was filtered using a Buchner funnel and the clear filtrate was collected. The cake was further extracted with ether (3 x 50 mL). The clear filtrates were pooled together and rotoevaporated to dryness and the solvent further removed overnight under high vacuum; the crude yield was 80%. The product was purified on TLC plates (Polygram Silica G) using a chloroform:methanol mixture (95:5) and yielded 0.88 g (0.23 mmol, 48%); m.p. 145.0-146.5°C. For mass spectral peaks between 0-640 mass units the relative abundance peak area are m/e 387 (90%), 369 (42%), 354 (38%), 301 (67%), 275 (70%), 245 (35%) and 214 (52%).

Synthesis of Deuterated Cholesteryl Esters

Cholesteryl esters were synthesized employing the procedure similar to the one used in the synthesis of selectively deuterated phospholipids. A brief outline of [3-$^2H_1$]cholesteryl palmitate synthesis will be presented and this will then be followed by the analytical data for the other cholesteryl esters synthesized.

1,1'-Carbonyldiimidazole (CDI) (80 mg, 0.49 mmol) was added to a stirring mixture of palmitic acid (122 mg, 0.48 mmol) in dry benzene (15 mL) under a flow of dry N_2 [3-$^2H_1$]Cholesterol (200 mg, 0.52 mmol) was added after 60 min and the reaction mixture was stirred under an increased flow of N_2 until all the benzene had evaporated. The solvent was further

removed under high vacuum (≃ 2 hr). The flask was sealed under a continous flow of N_2 and heated at 80-82°C for 3 hr. The product was dissolved in chloroform (20 mL) and washed with distilled water (3 x 20 mL). The chloroform extract was rotoevaporated to dryness and the product purified on Silica Gel G TLC plates in chloroform. [3-$^2H_1$]Cholesteryl palmitate showed a single spot, R_f = 0.61 on Silica Gel G TLC plates, using $CHCl_3$ as eluant. Yield: 234 mg (0.37 mmol, 72.4%); m.p. 72-73.5°C; m/e (peaks between 320-640) 627 (6%), 626 (16%), 533 (100%) and 445 (34%).

The m.p. of cholesteryl palmitate obtained from Sigma was 77-79°C. The literature m.p. of cholesteryl palmitate is 83.5°C (Ginsburg and Small, 1981).

[2,2,4,4,6-$^2H_5$]cholesteryl palmitate:

CDI (20.0 mg, 0.12 mmol). Palmitic acid (30.0 mg, 0.12 mmol) and [2,2,4,4,6-$^2H_5$]cholesterol (50.0 mg, 0.13 mmol) yielded 58.2 mg (0.09 mmol, 72%) of [2,2,4,4,6-$^2H_5$]cholesteryl palmitate; m.p. 75-77°C. A high resolution ^2H NMR spectrum was indentical with that reported ealier (Taylor *et al.* 1980) except that the resonance due to the slight (≃20%) amount of deuteration at the 3-position was shifted ≃1 ppm to lower field.

[7,7-$^2H_2$]cholesteryl palmitate:

CDI (17.0 mg, 0.10 mmol), palmitic acid (27 mg, 0.11 mmol) and [7,7-$^2H_2$]cholesterol (40 mg, 0.10 mmol) gave 36 mg (0.06 mmol, 56%) of [7,7-$^2H_2$]cholesteryl palmitate, m.p. 71-73°C, m/e (peaks between 500-700) 628 (24%), 627 (51%), 534 (31%) and 533 (100%).

[2,2,4,4,6-$^2H_5$]cholesteryl palmitate (8.0 mg) in ethanol/water (20.0 mL) (1:1, v/v) and potasium hydroxide (0.2 g) was refluxed for 3 days.

After acidifying with HCl, the mixture was extracted with chlorofrom (3 x 10 mL) and rotoevaporated to dryness. The [2,2,4,4,6-$^2H_5$]cholesterol was purified on the Silica Gel G TLC plates in $CHCl_3$; m/e (peaks between 200-400) 393 (11%), 392 (45%), 391 (100%), 390 (68%), 389 (20%), 302 (64%) 301 (69%) and 275 (48%). The mass spectrum of [2,2,4,4,6-$^2H_5$]cholesterol thus isolated agrees with the mass spectrum of the starting [2,2,4,4,6-$^2H_5$]cholesterol.

Isolation of Very Low Density Lipoproteins

Fresh human plasma, slightly turbid (non frozen and <3 days old), obtained from Canadian Red Cross, Vancouver, was centrifuged on Ti 50.2 rotor for 18-20 hr at 42,000 rpm and 5°C. Top fraction was collected and stored under N_2 in presence of NaN_3 at 5°C. In general, fractions from eight to ten units of plasma were pooled and dialysed exhaustively against 0.15 M NaCl, 0.02% NaN_3, 2.0 mM Na_2EDTA pH 7.4 reducing density to <1.006 g/mL. Following dialysis, the pooled fraction was centrifuged for 18-20 hr at 42,000 rpm in order to remove any trace amounts of LDL. The top fraction was isolated and subjected to further 30 min centrifugation on a Ti 60.0 rotor at 42,000 rpm at 5°C with brake in the off position. With a syringe, the bottom three-quarter fraction of VLDL sample was isolated from the centrifuge tube and stored under N_2 at 4°C until use.

Preparation of Phospholipid Unilamellar Vesicles

Unilamellar vesicles of specifically deuterated phosphatidylcholines were prepared by sonication. In a typical preparation 35-50 mg of

specifically deuterated phosphatidylcholine with trace amounts of [1-^{14}C]DPPC were co-dissolved in chloroform. The solvent was evaporated under a stream of N_2 and the thin film further dried under high vacuum for 3-4 hr. The dry lipids were dispersed in 5.0 mL of 0.15 M NaCl, 0.02% NaN_3 and 2.0 mM EDTA pH 7.4 which had been prewarmed to 45°C. The homogenous suspension was sonicated until clear for 20 min (2 min sonication followed by 1 min of cooling period) under N_2 using a Biosonic III probe-type sonicator at a power level of 40-50 Watts. The temperature was monitored by inserting a thermocouple directly into the sonication mixture and was maintained above the phase transition of the phospholipids (45-48°C). The solution was centrifuged on a clinical centrifuge for 15 min to remove the undispersed lipids and the titanium particles. The intregity of the phospholipids was checked by TLC. The vesicles were used immediately.

Isolation of Phosphatidylcholine Transfer Protein

The bovine liver phosphatidylcholine transfer protein was partially purified to step 4 of the procedure described by Kamp *et al* (1973). The method adopted was as follows: 12 Kg of bovine liver (fresh from the abattoir, J and L Meats Company Ltd., Surrey, B.C, Canada) was cut into small pieces and washed with 14 L of 0.25 M sucrose solution. The cut pieces were homogenized in 18 liter of 0.25 M sucrose solution using a Waring Blender. The homogenate was centrifuged on a Sorvall preparative centrifuge using a GS-3 rotor at 600g x 20 min (1,950 rpm) and the resulting solid discarded. The supernatant was further centrifuged at 14,000g x 25 mins (9,000 rpm). The pH of the resulting supernatant was brought to pH 5.1 by the addition of 3 M HCl. The sample was allowed to

stand for ≃4 hr. The resulting precipitate was sedimented and discarded. The supernatant was adjusted to pH 3 by the addition of 3 M HCl and dialysed overnight against 20 L of 0.25 M sucrose, 0.05 M Tris pH 9.1. A light brown precipitate developes within the supernatant. The sample was further dialysed until the supernatant pH was 6.8. The resulting precipitate was sedimented using a GSA-rotor at 15,000g for 10 mins (9,600 rpm) and discarded. To the supernatant, solid $(NH_4)_2SO_4$ (45 g/100 mL) was added slowly while stirring and allowed to stand overnight. The precipitate was isolated and dissolved in a minimum volume of 0.01 M sodium phosphate, 0.01 M β-mercaptoethanol pH 7.2 and dialysed in the same buffer (12 L x 3 exchanges) over a period of 24 hr. The dialysed solution (≃ 32 g with respect to protein) was filtered through glass wool and applied to a DEAE Column (6 x 65 cm) and eluted at a flow rate of ≃125 mL/hr. The ionic strength of the eluting buffer, 0.01 M sodium phosphate 0.01 M β-mercaptoethanol pH 7.2, was changed by addition of NaCl.

The transfer activity of the elution fractions collected were determined by using VLDL and vesicles. Egg PC vesicles (25 mg with respect to phospholipids) having trace amounts of [1-^{14}C]DPPC, VLDL (10 mg with respect to phospholipids), and 2 mL of each elution fraction collected were incubated for 1 hr at 37°C under an N_2 atmosphere. A control experiment without the addition of the elution fractions was also conducted. The VLDL particles were separated from the vesicles by centrifugation on a Ti 50.2 rotor at 42,000 rpm at 5°C for 20 hr. The top 15% of the centrifuge tube having the VLDL particles were isolated and analysed for radioactivity by liquid scintillation counting.

The elution fractions containing the transfer activity were pooled, solid $(NH_4)_2SO_4$ (65 g/100 mL) was added, and the mixture was allowed to stand overnight. The active protein precipitated and was isolated by centrifugation on GSA-rotor at 10,000g for 20 min (6,000 rpm) and dissolved in a minimum volume of 0.01 M citric acid 0.02 M Na_2HPO_4 0.01 M β-mercaptoethanol pH 5.0. The protein solution was stored in 50% glycerol at -22°C in 100 mL vials. Prior to each exchange experiment, glycerol was dialysed away against 0.01 M citric acid 0.02 M $NaHPO_4$ at pH 5.0 (6 liter x 3 exchanges) over a period of 24 hr at 4°C.

Incorporation of Selectively Deuterated Phosphatidylcholines into VLDL

Purified VLDL (100 mg with respect to VLDL phospholipids), deuterated PC vesicles (50 mg), and partially purified phosphatidylcholine exchange protein (35 mg) were suspended in 225 mL 0.15 M NaCl, 0.02% NaN_3 and 2.0 mM EDTA at pH 7.4 and incubated with occasional swirling under N_2 at 35-37°C. These proportions were maintained in all the incubations but the total amount occasionally varied. Following incubation period for 1-1.5 hr the VLDL particles were separated from the vesicles by centrifugation at 42,000 rpm in a Ti 50.2 rotor at 8.0°C for 18-20 hrs. The VLDL layer at the top of the centrifuge tube was collected and the mol % incorporation of specifically deuterated phosphatidylcholine determined by liquid scintillation counting. The chemical composition of the VLDL before and after the incorporation of selectively deuterated phospholipids was determined as descibed in the Analysis section, see below. Prior to the ^2H NMR experiments the residual ^2HOH was reduced by performing three exchanges using 15 mL of deuterium depleted water containing 0.15 M NaCl, 2.0 mM

EDTA and 2.0 M KBr at pH 7.4 by ultracentrifugation at 42,000 rpm at 5°C for 15-20 min. Frequently, a gel comprising of VLDL was obtained at top of the centrifuge tube and this was resuspended in deuterium depleted water containing 0.15 M NaCl, 2.0 mM EDTA and 2.0 M KBr at pH 7.4. The association of the deuterated phospholipids with VLDL particles was investigated by gel permeation chromatography.

Incorporation of Selectively Deuterated Palmitic Acid into VLDL

The procedure for incorporating selectively deuterated fatty acids into VLDL resembles that described by Wassall *et al* (1982). Briefly, an excess deuterated fatty acid (≃5-10 mg, representing an excess of 10 mol %) and a trace amount of [1-^{14}C]palmitic acid were co-dissolved in chloroform in a round bottom flask. The $CHCl_3$ was evaporated to leave a thin film of lipid using a rotory evaporation apparatus. The thin film was further dried overnight under high vacuum. VLDL sample, having undergone three 15 mL exchanged with deuterium depleted water containing 0.15 M NaCl, 2.0 mM EDTA and 2.0 M KBr at pH 7.4 was incubated, with agitation, on a thin film of deuterated fatty acid at room temperature. The transfer of fatty acid into VLDL was facilitated by gentle agitation. The mol % incorporation was monitored periodically by liquid scintillation counting. For a 10 mol % incorporation of deuterated fatty acid the incubation period was approximately 30-40 minutes. The labelled VLDL was subsequently filtered through glass wool to remove any floating particulate matter. The association of the fatty acid with VLDL particles was investigated by gel permeation chromatography (see Analytical section).

Preparation of Egg PC/TO Microemulsions

Egg PC/TO microemulsions were prepared according to the procedure described by Tajima *et al* (1983). The microemulsion sample for the lateral diffusion study was prepared by codissolving triolein and egg PC in choloroform in a ratio of 2.3:1.0 (w/w). The solvent was evaporated under a stream of N_2 and further removed under high vacuum overnight. The dry lipids were dispersed in 10 mL of 0.15 M NaCl in D_2O at pD 7.4 using a vortex mixer. Microemulsions for the phospholipid acyl chain order study consisted of triolein:egg PC (2.2:1, w/w). Specifically deuterated phospholipids were included at 10 mol % with respect to egg PC. The sample mixture was codissolved and dried as described. The dry lipids were dispersed in deuterium depleted water. Both samples were sonicated under a stream of N_2 for 65 minutes using a Heat System W-375 Sonicator at a power level of 65-75 Watts. The duty cycle was 5-10 min of sonication followed by 1-2 min of rest period. During sonication, cold tap water was continously run through the sonicating vessel jacket. The temperature, 40-45°C, was monitored by inserting a thermocouple directly into the sonicating suspension. The resulting slightly cloudy solution was centrifuged on a clinical centrifuge for 15 min to remove the titanium particles. The sample was then centrifuged on a Ti 75 rotor at 5°C and 42000 rpm for approximately 20 hr. A clear gel comprising of egg PC/TO microemulsions was obtained at top of the centrifuge tube. Microemulsions containing deuterated phospholipids were used without further purification. Microemulsions for the lateral diffusion study were resuspended into ≃7 mL 0.15 M NaCl in D_2O at pD 7.4 and subjected to an additional spin on a Ti 75 rotor with the brake off at 15000 rpm for 15 min. The bottom 80% of the

sample in the centrifuge tube was isolated using a syringe and stored in the fridge until use. The sample was examined for vesicle contamination by ^1H NMR at 400 MHz. The size of the particles was determined using a model 270 Nicomp Submicron Particle Sizer.

Analytical Methods

The amount of phospholipids in VLDL solution was determined by phosphorus analysis as described by Ames (1966). Cholesterol, cholesteryl ester and triglyceride were quantified using analytical enzyme kits obtained from Boehringer Mannheim. The amount of protein present in VLDL solution was determined by the method of Lowry *et al* (1951) as modified by Kashyap *et al* (1980), using egg albumin as a standard.

The association of deuterated phospholipids and deuterated fatty acids with the VLDL particles was confirmed by gel exclusion chromatography on Sepharose 4B using [1-^{14}C]DPPC and [1-^{14}C]palmitic acid, respectively. Typically, an aliquot of labelled VLDL solution, ≃20 mg protein/mL (PC labelled VLDL) and ≃10 mg protein/mL (palmitic acid labelled VLDL), was applied to the Sepharose 4B column (2.6 x 29 cm) and eluted with 0.15 M NaCl, 0.02% NaN_3 and 2.0 mM Na_2EDTA pH 7.4 at a flow rate of ≃17 mL/hr. The void volume of the column (43 mL) was determined using Blue Dextran (Pharmacia; MW = 2.0 x 10^6 Daltons). The total volume of the column was 161 mL. Approximately 4.0 mL elution fractions were collected from the column and examined for protein and radioactivity. The radioactivity was determined using a Wallac LKB 1217 Rackbeta liquid scintillation counter. The scintillation cocktail was prepared using napthalene (60 g), methanol (100 mL), ethylene glycol (20 mL), liquifluor (42 mL), and 1,4-dioxane made

to a volume of 1 L.

Electron Microscopy

Native VLDL, VLDL particles containing selectively deuterated phosphatidylcholines or palmitic acid, and egg PC:TO microemulsions containing [11,11,12,12-$^2H_4$]PC were sized by the negative staining method.

Copper grids, mesh 200, were washed in distilled water containing a dilute detergent solution by mild sonication using a Cole-Parmer Sonogen Automatic Cleaner. The grids were repeatedly rinsed with distilled water and with a final rinse in acetone. The clean grids were then air dried on ashless Whatman filter paper.

0.5% (w/w) Formvar in dichloromethane was used to coat the grids. The grids were placed on filter paper resting on a wire mesh immersed in distilled water. A microscope slide coated with a thin film of Formvar was carefully lowered into the water trough. A thin Formvar film separates and floats on top of the grids, lowering the water level caused the film to rest on the grids. The grids were than air dried on filter paper in a Petridish.

The Formvar-coated Cu grids were then carbon-coated with pointed carbon rods using a Varian NRC 3115 Vacuum evaporator. A thin film of carbon prevents discharging at the grid surface in the electron microscope.

Typically, ≃0.3 mg protein/mL of VLDL solution was applied on the grid and allowed to stand for ≃2 min. The excess fluid was desorbed using Whatman filter paper. A stain solution, 2% ammonium molybdate pH 8.0, was

then immediately applied for 2 min and removed as described above. The grids were generally air dried for 5-10 min before examining in the electron microscope. The electron micrographs were obtained with a Philips 300 electron microscope operating at 80 kV. Magnification was calibrated using a diffraction grating replica. Particle diameters were sized directly from the negatives.

Quasi-Elastic Light Scattering

Native VLDL, VLDL containing selectively deuterated lipids (phospholipids or fatty acids) and egg PC:TO microemulsions used in the lateral diffusion study were also sized using a Nicomp Model 270 Submicron Particle Sizer. The scattering angle was fixed at 90°. The autocorrelation function was analysed using 64 channels. The channel widths generally ranged between 5.0-8.9 μs (VLDL particles) and 7.9 μs (egg PC:TO microemulsions). The autocorrelation function is analysed simultaneously by either a Gaussian analysis or a Distribution analysis. The Gaussian analysis proceeds with the assumption that a single Gaussian particle distribution fits the autocorrelation function, with the goodness of fit analysed by the parameter chi-square. The Distribution analysis makes no assumptions and fits the autocorrelation function with several exponentially decaying functions to determine the actual size distribution of the particles. In this analysis the goodness of the fit is determined by the parameter fit error. The sizes measured in the above studies were determined from the Distribution analysis and are given in terms of the mean ± standard deviation. The data was usually obtained from 8-12 repeated runs on the same sample. For selectively deuterated phospholipids and fatty

acids in VLDL the chi-square values from the Gaussian analysis ranged between 0.5-409.4, with 47% of the values in the 0.5-1.5 range thus indicating that in most cases the Gaussian analysis is a poor fit to the autocorrelation function.

Polyacrylamide Gel Electrophoresis

Analysis of the apoproteins associated with VLDL before and after the incorporation of either deuterated phosphatidylcholines using partially purified transfer protein, or selectively deuterated fatty acids, was examined with SDS-polyacrylamide gel electrophoresis using the methodology of Laemmli (1970). Prior to gel electrophoresis all the lipoprotein samples (2-3 mL) were dialysed over a period of 12 hr in 0.85% NaCl, 0.1% EDTA, 0.05% L-leucine at pH 7.4 at 4°C (2 x 1 L) and concentrated to 2.0 mg protein/mL by the treatment with aquacide. The samples were then delipidated with anhydrous diethylether (30 x volume of protein solution) as described (Wu and Windmueller, 1978). To the partially delipidated lipoprotein samples an equal volume of 0.125 M Tris·HCl, pH 6.8 containing 4% SDS, 20% glycerol, 10% 2-mercaptoethanol and 0.1% bromophenol was added and heated in a boiling water bath for 90 s, following which they were cooled and stored at -20°C until used. Polyacrylamide gel electrophoresis was performed at room temperature on discontinuous gels in which the concentration of acrylamide was 4% in the stacking gel (1.5 cm) and 10% in the running gel (7.5 cm) (1.5 cm thick). The gels were placed in a vertical cell unit and subjected to a constant voltage of 85 V.

In some cases a continuous 4% polyacrylamide gel was used with a constant current of 8.5 mA. The running gel contained 1.5 M Tris-HCl 0.1%

SDS pH 8.8, while the stacking gel had 0.5 M Tris-HCl 0.1% SDS pH 6.8. Electrophoresis was performed in 0.025 M Tris pH 8.3 containing 0.192 M glycine and 0.1% SDS at room temperature. The gels were generally stained overnight (15-20 hr) with 0.125% Coomassie blue R-250 in fixative (50% methanol/10% acetic acid). Destaining was carried out in 50% methanol/10% acetic acid for about an hour followed by further destaining in 5% methanol/7% acetic acid until the gel was free from the background staining.

Lateral diffusion studies

For the lateral diffusion study of VLDL, VLDL was isolated from four fresh units of human plasma (<3 days old) and purified as described earlier. The VLDL sample thus obtained was further subjected to 20 min spin and the bottom three-quarter fraction was isolated and concentrated by centrifugation on Ti 60 rotor at 42,000 rpm for 18 hr at 5°C.

Egg PC/TO microemulsions prepared and subfracted as described earlier were concentrated by the treatment with acquacide. The solvent viscosities were increased by the addition of glycerol. The viscosities of the glyerol-0.15 M NaCl, 2.0 mM EDTA at pH 7.4, mixtures were determined at 25°C and 40°C using an Ostwald viscometer.

Preparation of NMR Samples

For phospholipid acyl chain organization study of VLDL, samples were generally concentrated prior to ^{2}H NMR study. VLDL labelled with selectively deuterated phospholipids were concentrated to ≃15-20 mg

protein/mL by ultracentrifugation while those labelled with selectively deuterated palmitic acid were concentrated to ≃35-40 mg protein/mL by the treatment with aquacide.

For cholesteryl ester study, multilamellar dispersions were prepared by dissolving 500 mg of dipalmitoyl **D,L**-α-phosphatidylcholine plus one of the following: [3-$^2H_1$]cholesterol (21.7 mg, 7.6 mol%), [3-$^2H_1$]cholesteryl palmitate (20.3 mg, 4.5 mol%), [2,2,4,4,6-$^2H_5$]cholesterol (23.1 mg, 8.0 mol%), [2,2,4,4,6-$^2H_5$]cholesteryl palmitate (21.5 mg, 4.8 mol%), [7,7-$^2H_2$]cholesterol (21.8 mg, 7.6 mol%) and [7,7-$^2H_2$]cholestery palmitate (20.3 mg, 4.5 mol%) in chloroform. The solvent was evaporated under a flow of N_2 and the sample further dried under high vacuum overnight. The dry lipids were dispersed in 500 mg of deuterium depleted water to give a 50 wt % dispersion through mixing using a spatula, with occasional warming, until the sample appeared homogenous.

Nuclear Magnetic Resonance

^2H NMR

^2H NMR spectra of VLDL and egg PC/TO microemulsions were acquired at 38.8 MHz using a Nalorac 5.9 T superconducting magnet and a home-built spectrometer. NMR signal collection and Fourier transformation of the free induction decays were performed on a Nicolet BNC-12 computer or a Vax Workstation. The temperature of all the experiments was controlled to an accuracy of ±0.5°C by a solid state temperature controller built by the Simon Fraser University electronic shop. The [16,16,16-$^2H_3$]PC spectra were obtained using a spinning probe while all other spectra were obtained on a broad band probe with a horizontally mounted coil. The samples were

equilibriated for 20-40 min at a given temperature before acquiring the data. The spectral parameters employed are listed in the Figure legends.

The spin-lattice relaxation times, T_1, were measured at 38.8 MHz by the inversion-recovery method $(180°-\tau-90°-T)_n$ (Vold *et al.* 1968). T_1 values were calculated from the expression $A_\tau = A_\infty (1 - 2e^{-\tau/T_1})$, where A_τ is the signal amplitude corresponding to a delay τ and A_∞ is the signal amplitude corresponding to $\tau >> T_1$. The delay times T was 0.20 s for [$^2H_2$]PC and [$^2H_4$]PC and 1.0 s for [$^2H_3$]PC at 25°C.

The deuterium powder spectra of selectively deuterated cholesterol and cholesteryl esters in DPPC multilamellar dispersions were obtained using the quadrupolar echo pulse sequence $(\frac{\pi}{2}|_{0°}-\tau-\frac{\pi}{2}|_{90°}-t)_n$. A Nicolet Explorer IIIA digital oscilloscope was used to acquire the NMR signals, which were subsequently transferred to a NIC BNC-12 computer where Fourier transforms were performed. In all cases the time delay τ between pulses was 75 μs unless otherwise indicated, the $\pi/2$ pulse length was 8 μs, and the sequence of pulses was repeated after a time t of 0.02 s. A phase-altering pulse sequence was used in order to cancel coherent receiver and pulse noise. The temperature for all the experiments was regulated at 45.0 ±0.5°C. Spectra were symmetrized by zeroing the 'out-of-phase' channel and folding over resulting in an increase in the signal to noise ratio of $\sqrt{2}$.

^{31}P NMR

^{31}P NMR spectra of VLDL and egg PC/TO microemulsions were acquired at 102.2 MHz on the home built spectrometer. The spectra were collected without proton decoupling using a broad band probe. T_1 were measured by the inversion-recovery method. The delay time T was 10.0 s and 7.0 s for

native VLDL and [^{2}H]PC labelled VLDL, respectively at 25°C.

^{1}H NMR

^{1}H NMR experiments were performed at 400 MHz on a Bruker WM-400 spectrometer to assess the contamination of egg PC/TO microemulsions (used in the lateral diffusion study) by vesicles. Aliqouts of stock solution of either shift reagent or broadening reagent were added directly into the NMR tube, containing either vesicle or microemulsion preparation, and vortexed. Data was acquired immediately following mixing. Data acquisition and Fourier transformations was facilitated by an Aspect 2000 computer. The temperature was controlled using a gas flow system to 30.0 ± 0.5°C. The author is indebt to Mrs. M. Tracey for obtaining the ^{1}H NMR spectra shown in Figures 47 and 48.

All the ^{2}H NMR and ^{31}P spectra shown were analysed using an iterative least-square fit to Lorentzian lineshape functions. The program was kindly furnished by Dr. K. E. Newman, and modified by Dr. W. D. Treleaven, both of Chemistry Department, Simon Fraser University. The author is indebt to Dr. W. D. Treleaven for the assistance and many helpful suggestions given during the simulation of the spectra. In order to simulate spectra, transformed spectra were uploaded to the IBM 3861-GX computer in the computing facility on campus at Simon Fraser University. In the simplest case, that of a single Lorentzian, theoretical spectra were compared to experimental data. The minimum parameters required to generate the theoretical spectrum were; baseline, chemical shift, signal amplitude, and full width at half-maximum signal intensity. Theoretical parameters were adjusted iteratively, by the computer, in order to achieve a least squares minimum fit to the data. In the case of superposed Lorentzian signals,

additional theoretical parameters were added to adequately describe chemical shift, signal amplitude, and linewidth of the additional signal.

CHAPTER IV

ACYL CHAIN ORGANIZATION IN THE SURFACE MONOLAYER OF VLDL AND EGG PC/TO MICROEMULSIONS

IVa. Selectively Deuterated Phosphatidylcholines in VLDL

RESULTS

Initial attempts to incorporate phospholipids into VLDL involved incubating VLDL with egg PC vesicles containing trace amounts of [1-^{14}C]DPPC. Egg PC vesicles were prepared by the modified procedure of Batzri and Korn, (1973). Egg PC containing trace amounts of radiolabel was dissolved in absolute ethanol and the mixture injected into rapidly stirring 0.15 M NaCl, 0.02% NaN_3, 2.0 mM Na_2EDTA at pH 7.4, prewarmed to ≃45°C. The resulting clear solution was incubated with VLDL, ethanol being <2% in final incubation volume, for varying periods of time (18-24 hr) at 37-40°C. Following this, the sample mixtures were dialysed against 0.15 M NaCl, 0.02% NaN_3, 2.0 mM Na_2EDTA at pH 7.4 over a period of 24-48 hr. Labelled VLDL was subsequently isolated by ultracentrifugation at 42,000 rpm for 18-20 hr at 5°C and monitored for radioactivity by liquid scintillation counting. The recovered radioactivity was found to be too low, and thus the method proved to be inadequate for incorporating large amounts of phospholipids into VLDL to allow easy detection by ^{2}H NMR spectroscopy.

Further attempts to incorporate phospholipids from egg PC vesicles containing trace amounts of [1-^{14}C]DPPC involved the use of exchange proteins present in lipoprotein free plasma. This method also proved

unsatisfactory. Although the procedure yielded high levels of incorporation (5-10 mol %) upon longer periods of incubations (20-28 hr), the incorporation varied with the isolation of lipoprotein free plasma. For instance, in one study a 1.5 mol % incorporation of [7,7-$^2H_2$]PC was obtained following incubation for 26 hr at 37±0.5°C. In order to avoid the variation of phospholipid incorporation using lipoprotein free plasma, a method yielding high incorporations in shorter periods was sought.

Jackson *et al.* (1979) have utilized bovine liver phosphatidylcholine transfer protein and demonstrated high degrees of incorporation occurred rapidly. We have adopted a similar procedure, using partially purified transfer protein, to incorporate selectively deuterated phospholipids into VLDL from vesicles. Phosphatidylcholine transfer protein was isolated from bovine liver to step 4 of the procedure described by Kamp *et al.* (1973). Partially purified transfer protein gave adequate levels of incorporation (3 mol % - 17 mol %) for relatively short periods of incubation (1-1 1/2 hr) (see Materials and Methods).

Gel permeation chromatography

In order to substantiate the association of deuterated phospholipids with VLDL particles following incorporation, as monitored by [1-^{14}C]DPPC tracer, the particles were subjected to gel permeation chromatography (see Materials and Methods). Figure 8 shows the results of gel permeation chromatography at 4°C of VLDL containing 7.0 mol % [4,4-$^2H_2$]PC and a trace amounts of [1-^{14}C]DPPC. The elution profile is characterised by the presence of two peaks. The first peak overlaps the second peak and elutes over a narrow volume range, 53.9-66.4 mL, and is centered at 58.1 mL. The second peak elutes over a wider volume range, 66.5-128.6 mL, and is

Figure 8: Elution profile of VLDL containing 7.0 mol % [4,4-$^{2}H_2$]PC and [1-^{14}C]DPPC on Sepharose 4B column. Approximately 20 mg protein/mL of labelled VLDL was applied on the column and eluted with 0.15 M NaCl, 0.02% NaN_3, 2.0 mM Na_2EDTA pH 7.4 at a flow rate of 17 mL/hr. Fractions were collected and examined for [1-^{14}C]DPPC activity (DPM, ■) by liquid scintillation counting and protein concentration (mg/Tube, ●) by the method of Lowry *et al.* 1951, as modified by Kashyap *et al.* 1980.

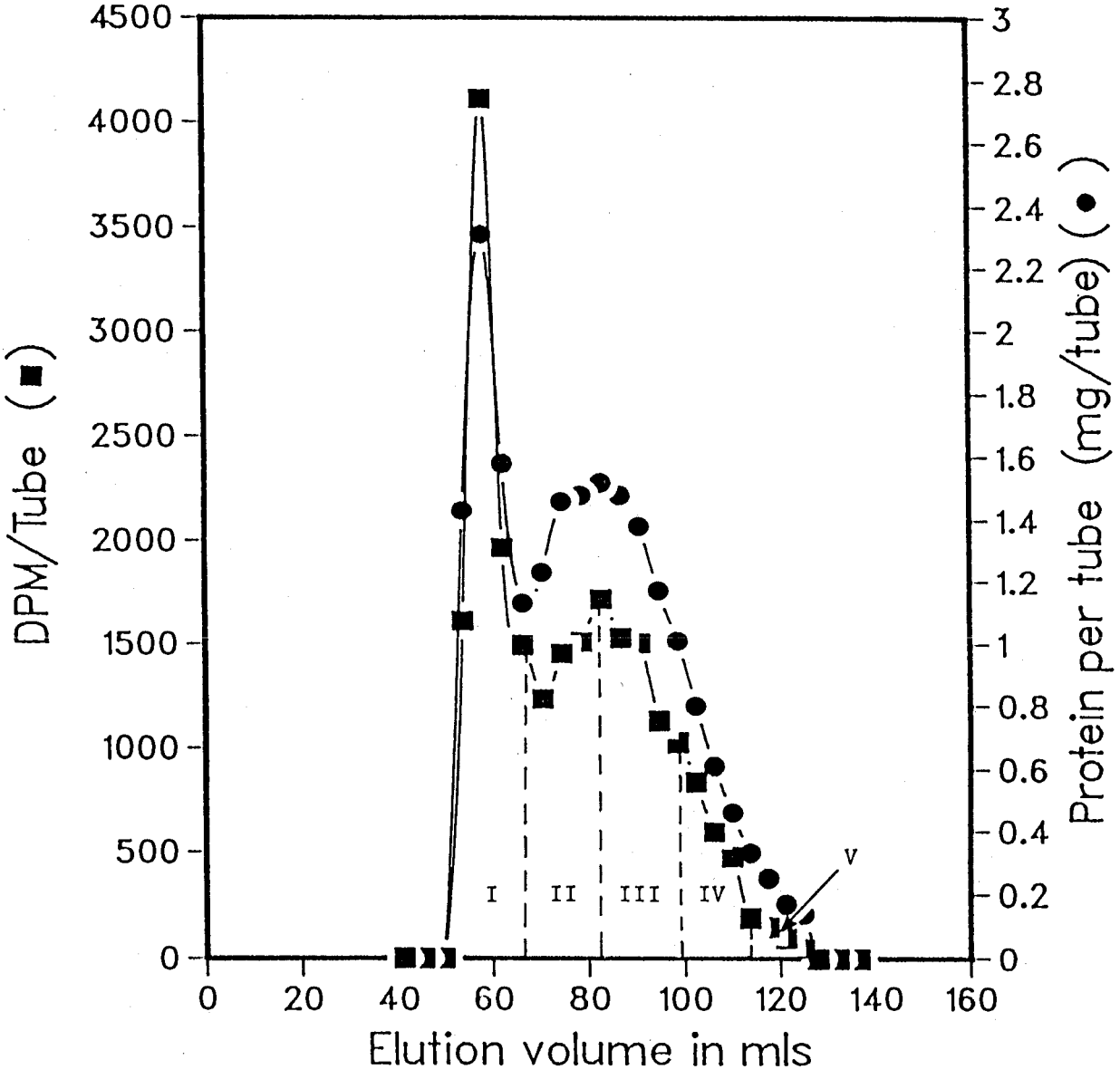
4500
4000
3500
3000
2500
2000
1500
1000
500
0
DPM/Tube (■)
3
2.8
2.6
2.4
2.2
2
1.8
1.6
1.4
1.2
1
0.8
0.6
0.4
0.2
0
Protein per tube (mg/tube) (●)
0
20
40
60
80
100
120
140
160
Elution volume in mls
I
II
III
IV
V

centered at 86.8 mL. The first peak contains ≃32% and ≃39%, and the second peak contains ≃67% and ≃57%, of the total protein and radioactivity recovered from the column, respectively. The first peak corresponds to the exclusion of large particles while the second peak corresponds to the elution of small particles. In order to confirm that both peaks were from the labelled VLDL particles rather from the vesicle contamination we have performed the following control studies with gel permeation chromatography.

Egg PC vesicles, prepared as described in Materials and Methods, at approximately 200 mg with respect to the phospholipids were eluted from the Sepharose 4B column under identical conditions as above. Approximately 4.8 mL fractions from the column were collected and examined under UV absorbance at 300 nm. The elution profile of egg PC vesicles is shown in Figure 9a and is also characterised by the presence of two peaks. The first peak elutes over a narrow volume range, 48.5-70.8 mL, and is centered at 57.2 mL, while the second peak elutes over a wider volume range, 70.9-147.9 mL, and is centered at 105.9 mL. From the elution profiles of the labelled VLDL (Figure 8) and egg PC vesicles (Figure 9a) it is obvious that while in both cases the first peak elutes over essentially the same volume range, the second peak elutes over a considerably different volume range. Had there been contamination by the smaller vesicles the second peak seen in Figure 8 would have eluted over a wider volume range. However, it may be argued that the first peak observed in the elution profile of labelled VLDL may arise from the contamination of larger vesicles. In order to disprove this we have performed the following:

a) The elution profile of labelled VLDL was subfractionated and examined for size and chemical composition.

Figure 9a: Elution profile of unilamellar egg PC vesicles. Approximately 200 mg of phosphatidylcholine was applied to a Sepharose 4B column and eluted with 0.15 M NaCl, 0.02% NaN_3, 2.0 mM Na_2EDTA pH 7.4. Fractions were collected and examined by UV absorbance at 300 nm (•).

Figure 9b: Elution profile of native VLDL. Approximately 25 mg protein/mL was applied on a Sepharose 4B column and eluted with 0.15 M NaCl, 0.02% NaN_3, 2.0 mM Na_2EDTA pH 7.4. Fractions were collected and examined by UV absorbance at 280 nm (•).

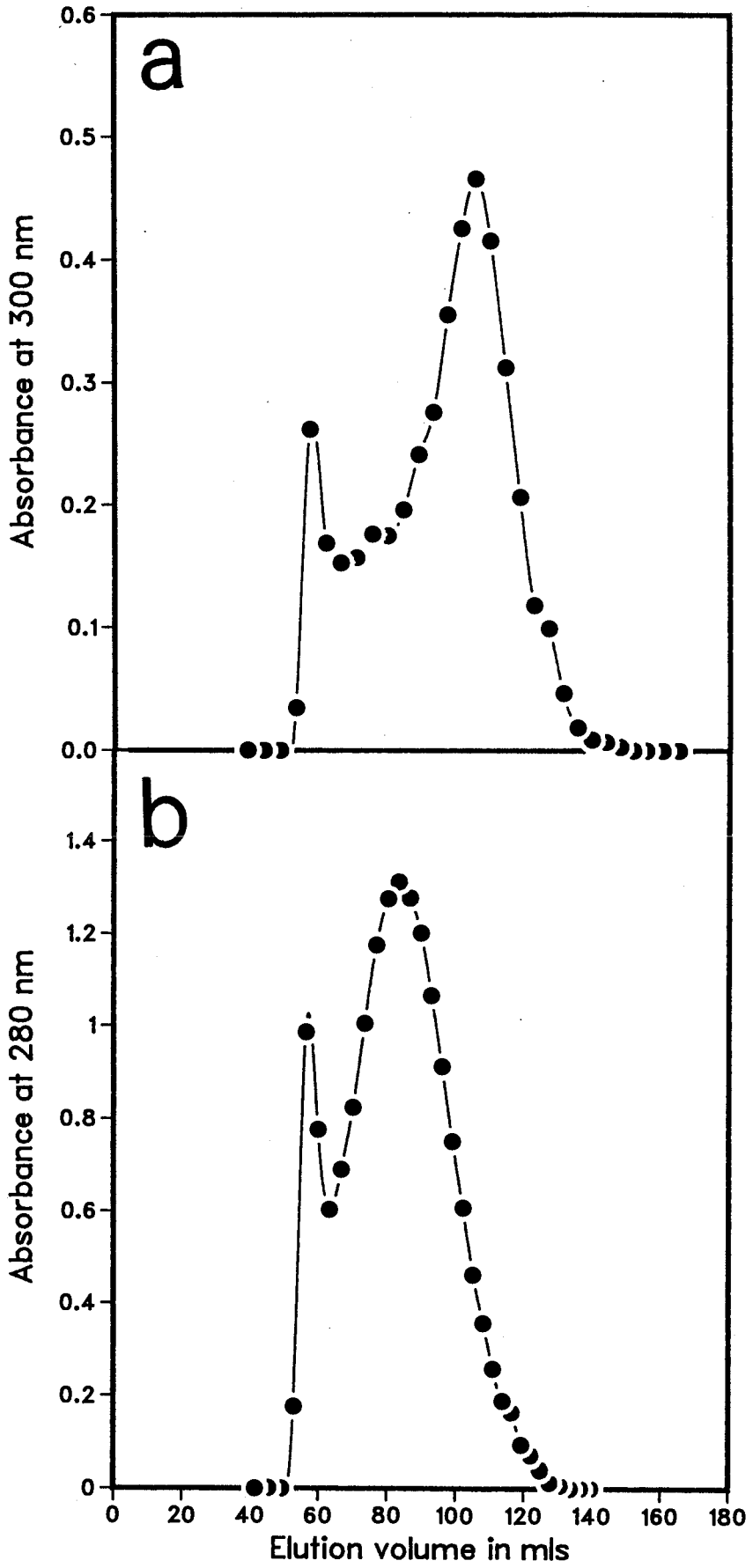
a
b
Absorbance at 300 nm
Absorbance at 280 nm
0.6
0.5
0.4
0.3
0.2
0.1
0.0
1.4
1.2
1
0.8
0.6
0.4
0.2
0
0 20 40 60 80 100 120 140 160 180
Elution volume in mls

b) Native VLDL was subjected to gel permeation chromatography.

The size and chemical composition of labelled VLDL subfractions isolated from the Sepharose 4B column are presented in Table 2.

A study by Miller and Small (1983) on human plasma lipoproteins isolated at a density <1.006 g/mL have shown the presence of a similar elution profile on a Bio-Gel A-150 (1% agarose) column. The subfractions isolated in that study showed similar chemical composition trends to our study except in the case of subfraction I where the chemical composition resembled the chylomicrons. In our case, subfraction I has the chemical composition that of VLDL. Therefore, based upon the size and the chemical composition of the subfractions presented in Table 2, and from the radio-labelled vesicles study, see below, we conclude that the first elution peak (elution volume 53.9-66.4 mL) results from the larger labelled VLDL particles. Further support for this comes from the elution profile of native VLDL (Figure 9b). Like that of the [^{2}H]PC-labelled VLDL the elution profile of native VLDL is also characterised by the presence of two peaks. The first peak elutes over a narrow volume range of 49.1-63.3 mL and is centered at 56.3 mL while the second peak elutes over a wider volume range of 63.4-130.6 mL and is centered at 83.4 mL. The elution profiles of both native and labelled VLDL are similar but the first peak is larger in labelled particles. The difference is attributed to the different sources of VLDL which made up our samples (History of subjects unknown). As shown below, the EM and QELS results indicate no difference between native and labelled particles.

In order to conclusively rule out the presence of vesicles in VLDL sample, egg PC vesicles containing trace amounts of [1-^{14}C]DPPC were

Table 2: Chemical composition of the subfractions of labelled VLDL (wt %).

Subfractions[a]	Size[b] (nm)	TG[c]	PL	TC	Pr	PL/TG	TC/TG	Pr/TG	PL/Pr
I	58.1±36.8	59.9	20.8	11.1	8.2	0.35	0.19	0.14	2.54
II	43.1±15.0	54.6	25.4	11.2	8.8	0.42	0.21	0.16	2.89
III	38.2±13.0	47.7	25.7	13.4	13.2	0.54	0.28	0.28	1.95
IV	36.2±12.5	45.3	27.6	8.5	18.6	0.61	0.19	0.41	1.48
V	-	49.4	26.0	-	24.6	0.53	-	0.50	1.06

[a] Subfractions of VLDL labelled with 7.0 mol % [4,4-$^2H_2$]PC isolated by gel permeation chromatography. The subfractions correspond to the following elution volumes; I (53.9-66.4 mL), II (66.5-83.4 mL), III (83.5-99.1 mL), IV (99.2-113.7 mL) and V (113.8-130.6 mL).

[b] Diameter measured by Quasielastic Light Scattering.

[c] Abbreviations; TG = Triglyceride, PL = Phospholipid, TC = Total Cholesterol and Pr = Protein. The chemical analyses were determined in duplicate.

prepared in 0.15 M NaCl, 0.02% NaN_3, 2.0 mM Na_2EDTA at pH 7.4 as described in Materials and Methods. Radio-labelled vesicles were centrifuged at 42,000 rpm at 5°C for 18 hr. The top 20% solution from the centrifuge tubes was removed and examined for radioactivity. The samples registered background counts only and therefore are consistent with no vesicles in the top 20% of the centrifuge tubes and hence, in VLDL sample.

Chemical composition of native VLDL and labelled VLDL

To demonstrate that the method of exchange had a negligible effect on VLDL structure, we have determined the chemical composition and the size of particles before and after the incorporation. Table 3 shows the physical properties of VLDL particles before and after the incorporation of deuterated phospholipids. The chemical composition data given represents the mean values from five separate chemical analyses, each analysis was performed in duplicate. The method of exchanging phospholipids does not appear to alter the VLDL structure appreciably. The largest change being in the ratios of PL/TG and CE/TG. The ratio of PL/TG increases from 0.40 to 0.43, while that of CE/TG decreases from 0.22 to 0.19 in the labelled VLDL particles.

Electron Microscopy and Light Scattering

The size of the particles was measured by quasielastic light scattering (QELS) and electron microscopy (EM). The values are also included in Table 3. Both techniques yield essentially identical size values. For instance, the diameter (mean ± standard deviation) of native VLDL measured by QELS is 42.2±11.5 nm while that of the labelled VLDL (VLDL containing [4,4-$^2H_2$]PC, [16,16,16-$^2H_3$]PC and [$N(C^2H_3)_3$]PC is 42.1±18.1 nm. Similar mean sizes were also measured by EM. An electron micrograph of VLDL containing 7.0 mol %

Table 3: Size and chemical composition of native VLDL and VLDL labelled with deuterated phospholipids.

	Native VLDL	Labelled VLDL
Mean Diameter (nm)		
QELS	42.2[a](±11.5[c])	42.1(±18.1)
EM	42.8[b](±10.3)	41.5(±9.3)
Composition (wt%)[d]		
Cholesterol	5.4(±0.7)	5.2(±0.6)
Cholesteryl ester	11.3(±1.8)	9.8(±2.1)
Phospholipid	20.7(±2.4)	22.2(±2.4)
Protein	11.4(±2.6)	10.9(±2.7)
Triglyceride	51.2(±4.2)	52.0(±4.2)

[a] size measured by quasielastic light scattering.

[b] size measured by electron microscopy. Approximately 300 particles of each sample, native and labelled VLDL (VLDL containing [4,4-$^2H_2$]PC and [16,16,16-$^2H_3$]PC), were counted.

[c] The number in parentheses represents the standard deviation.

[d] The data represents the mean values from five separate chemical analyses, each analysis was performed in duplicate.

[4,4-$^2H_2$]PC is shown in Figure 10. The particles are heterogenous in size and have a circular morphology. Included beneath the electron micrograph is a histogram depicting the size distribution of the labelled VLDL. However, the mean size measured by EM indicated slight variation from study to study. For instance, VLDL utilized for incorporating [4,4-$^2H_2$]PC had a diameter of 43.7±11.1 nm, and 43.1±10.3 nm following incorporation, while VLDL used for incorporating [16,16,16-$^2H_3$]PC had diameter 42.1±9.1 nm before and 40.0±7.2 nm following incorporation. Although there is a slight

Figure 10: Electron micrograph of VLDL containing 7.0 mol % [4,4-$^2H_2$]PC. Magnification = X167,000. Shown beneath the electron micrograph is a histogram depicting the size distribution for 300 particles counted. Mean diameter = 43.1±10.3 nm.

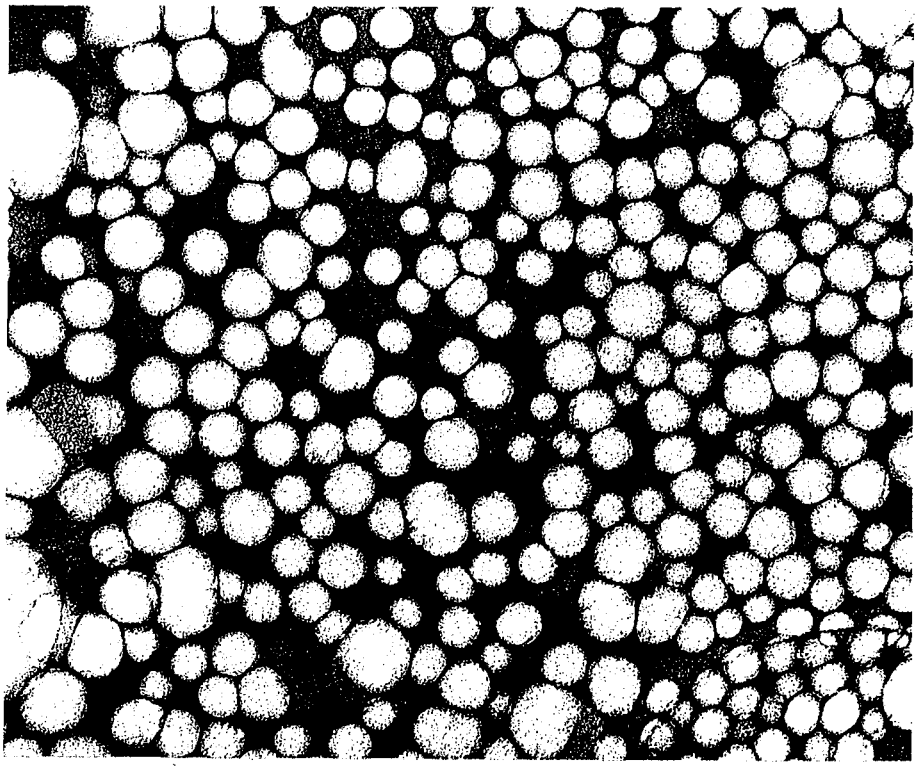

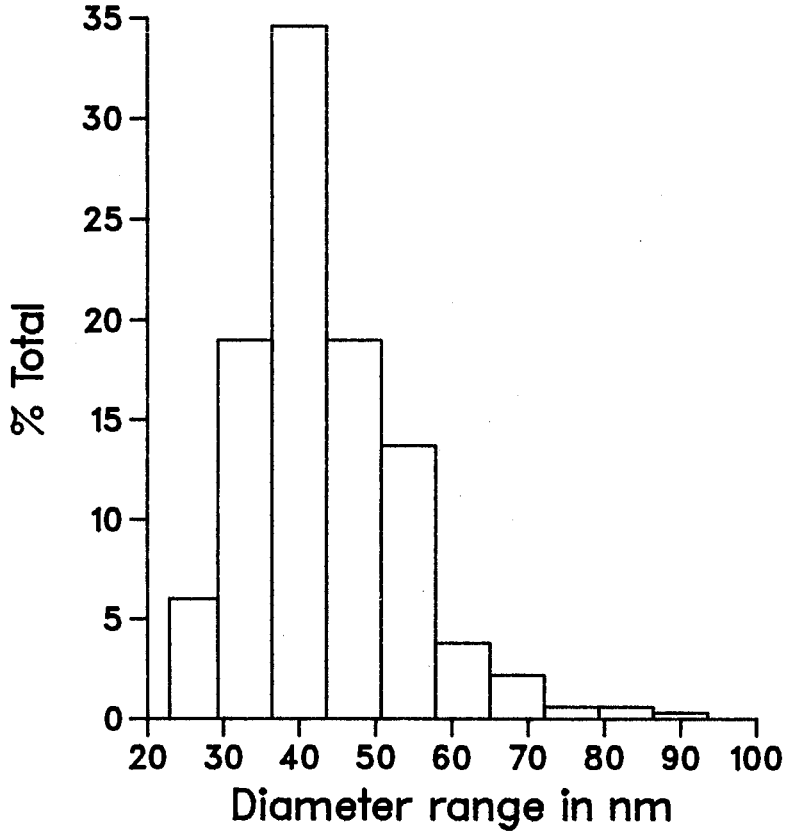
35
30
25
20
15
10
5
0
% Total
20
30
40
50
60
70
80
90
100
Diameter range in nm

difference in sizes found in the two studies, in both cases however, approximately 86% of the particles were within a diameter range of 30.0-50.0 nm. We have therefore combined the size measurements from both studies and have taken this to represent the mean size for all the studies. The size of native VLDL and labelled VLDL was determined by counting approximately 300 particles in each case and mean sizes of 42.8±10.3 and 41.5±9.3 nm were obtained, respectively.

^{31}P NMR

The effect of phospholipid incorporation on the particle size was also analysed by ^{31}P NMR spectroscopy. Figure 11 shows the representative ^{31}P NMR spectrum of native VLDL (Figure 11a) and VLDL containing 3 mol % [5,5,6,6-$^{2}H_4$]PC (Figure 11b) at 25°C. Unlike the ^{31}P NMR spectra of HDLs (Parmar, 1985) and LDL (Treleaven, 1985) where the sphingomyelin and phosphatidylcholine resonances are narrow, the ^{31}P NMR spectra of VLDL are comparatively broad and are primarily due to phosphatidylcholine. The % sphingomyelin associated with native VLDL was established to be <15% by ^{1}H-decoupled ^{31}P NMR spectra of total VLDL lipid extract in chloroform:methanol (2:1, v/v) (Figure 41). The spectra shown in Figure 11 were simulated as described in Materials and Methods. The solid line represents the best Lorentzian lineshape fit to the spectral data points (crosses). The contribution to the resonance from the sphingomyelin phospholipids (<15%), in both cases, was neglected in the fitting routine. Linewidths of 162.0 Hz and 172.7 Hz were obtained for the native and labelled VLDL, respectively. The linewidths are within ±10% of each other and are considered to be essentially the same. Similar ^{31}P linewidths confirm no change in size following the incorporation of selectively

Figure 11: ^{31}P NMR spectra of VLDL:

a) Native VLDL, ≃15 mg phospholipid/mL.

b) VLDL plus 3.0 mol % [5,5,6,6-$^{2}H_{4}$]PC, ≃20-25 mg phospholipid/mL.

The spectra were simulated by an iterative least-squares fit to a Lorentzian lineshape function (solid line) to the spectral datapoints (crosses). Spectral parameters for both cases: pulse width = 6.0 μs (90° flip angle), sweepwidth = 10,000 Hz, delay between pulses = 1.50 s, dataset = 4K zero filled to 8K, number of acquisitions 5,000 (a), 10,000 (b), linebroadening = 10.0 Hz, delay before acquisition = 10 μs. The sphingomyelin (<15.0%) contribution to the resonance was negected in the fitting routine.

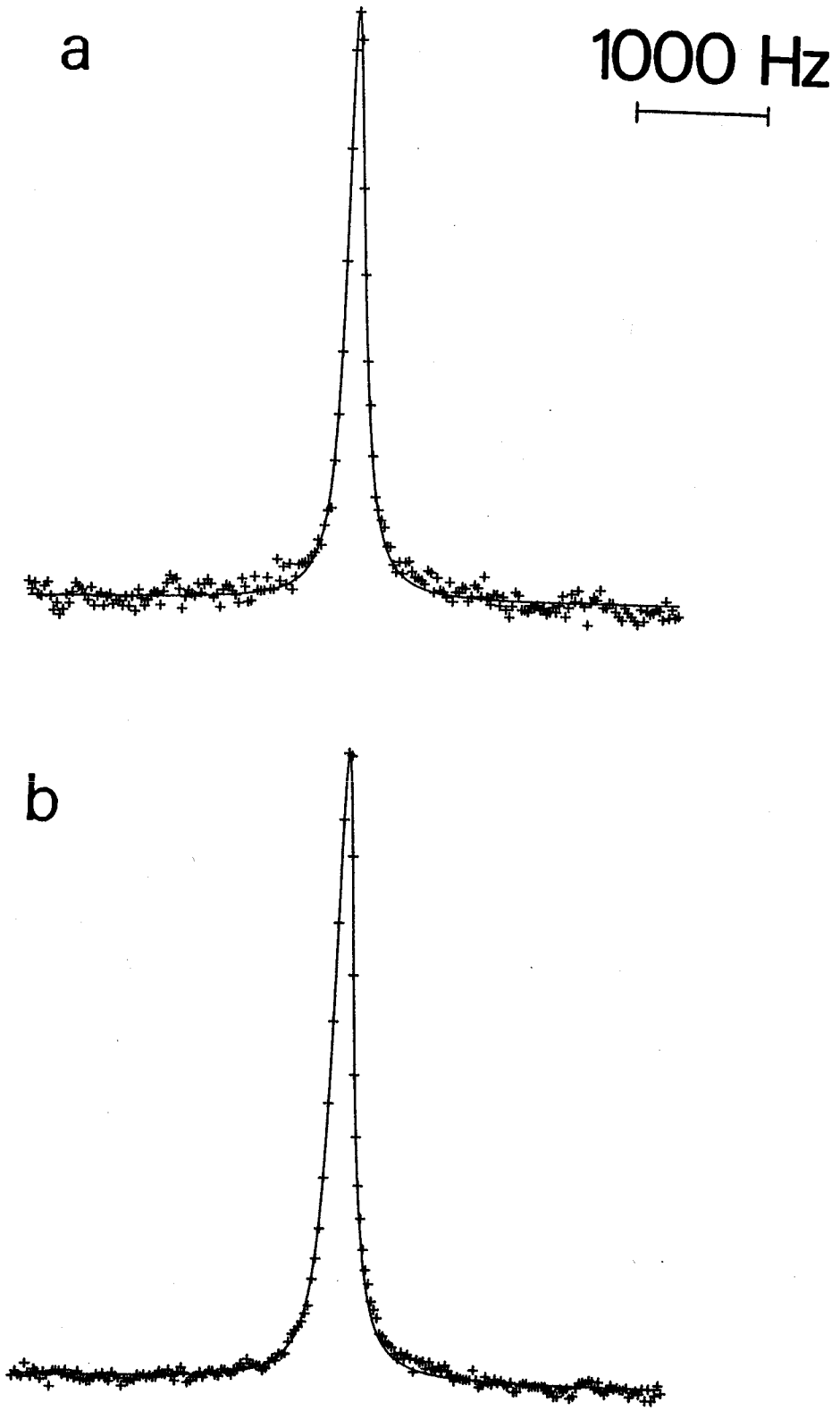
a
1000 Hz
b

deuterated phospholipids.

We have also examined T_1 of native VLDL and VLDL containing 7.0 mol % $[N(C^2H_3)_3]$PC at 25°C. Figures 12a and 12b show the plots of $\log(A_\infty - A_\tau)$ versus τ. A_∞ is the amplitude of magnetization in the z direction aquired when $\tau > 5\ T_1$. Figure 12a and 12b were analysed using a weighted least-squares routine courtesy of Dr. Ian Gay, Department of Chemistry, Simon Fraser University. Values of 1.36 s and 1.40 s were obtained for native and labelled VLDL, respectively. Thus, from the ^{31}P NMR linewidth and T_1 measurements we conclude that the size and the headgroup segmental motions are not affected following the incorporation of selectively deuterated phospholipids into VLDL particles.

Sodium dodecyl sulphate-polyacrylamide gel electrophoresis

In order to assess the effect of labelling procedure on VLDL apoproteins we have utilized sodium dodecyl sulphate-polyacrylamide gel electrophoresis (SDS-PAGE). Figure 13 shows the electrophoresis patterns of partially purified phosphatidylcholine transfer protein and apoproteins associated with native and labelled VLDL on a 10% polyacrylamide gel containing 0.1% SDS. The protein patterns in Lane 1 match with most of the bands seen in Lane 2, these bands are from the resuspended pellet which results following the separation of VLDL from vesicles. Lane 3 represents the mixture of six calibration protein standards whose molecular weights are shown on the left handside of the electrophoretogram. Lane 4 represents the apoprotein patterns associated with labelled VLDL particles and Lane 5 depicts the apoproteins associated with native VLDL particles. A calibration plot, Log MW and R_F, of the standard proteins allowed the determination of the type of apoproteins associated with VLDL particles.

Figure 12: Plots of ^{31}P NMR spin-lattice relaxation times of VLDL measured by inversion recovery method at 25°C at 102.2 MHz.
(a) Native VLDL.
(b) VLDL plus 7.0 mol % $[N(C^2H_3)_3]PC$.
Both Figures are plots of $\log(A_\infty - A_\tau)$ versus τ, where τ is in seconds. The solid line is a weighted least-squares fit to the experimental data points. Spectral parameters of Native VLDL: pulse width = 6.0 μs (90° flip angle), 12 μs (180° flip angle), sweepwidth = 10 KHz, dataset = 1K, number of acquisitons = 500, τ values ranged from 0.001-5.0 s; T = 10 s: Spectral parameters of VLDL plus 7.0 mol % $[N(C^2H_3)_3]PC$: pulse width as above, sweep width = 50 KHz, dataset = 4K, number of acquisition = 1500, τ value ranges from 0.01-4.0 s; T = 7.0 s: Delay before acquisition = 10 μs in both cases.

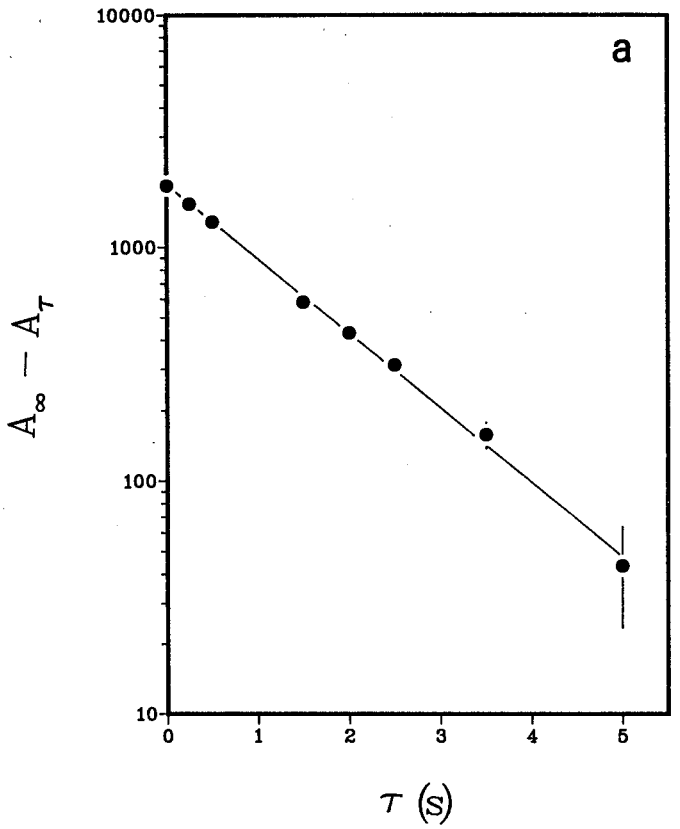
a
10000
1000
100
10
0
1
2
3
4
5
$A_\infty - A_\tau$
τ (s)

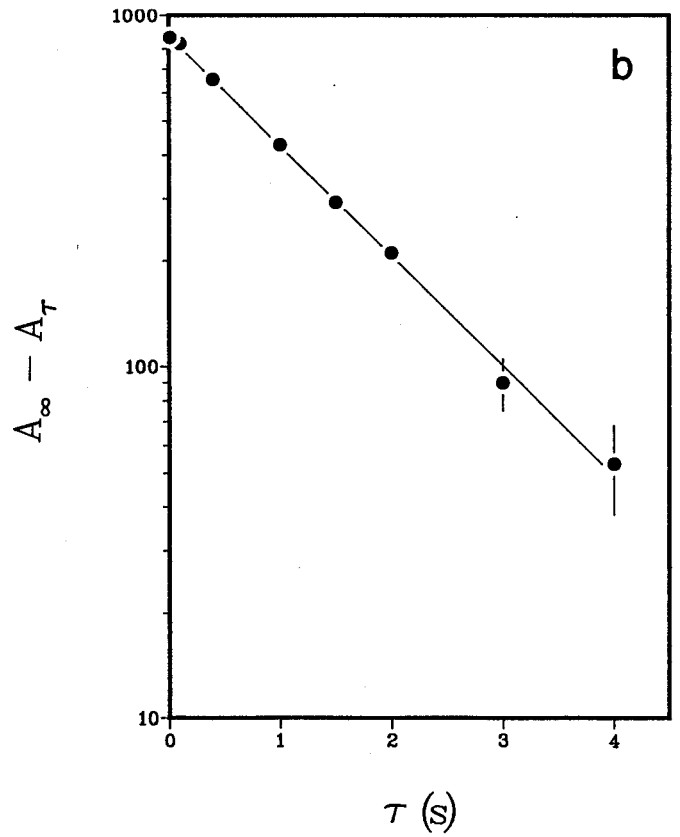
b
1000
100
10
0
1
2
3
4
$A_\infty - A_\tau$
τ (s)

Figure 13: Sodium Dodecyl Sulphate-10% polyacrylamide gel electrophoretogram of phosphatidylcholine transfer protein, native VLDL and PC labelled VLDL. Electrophoresis was performed as described in Materials and Methods. Lane 1.(10 μg) of crude bovine liver phosphatidylcholine transfer protein. Lane 2. (15 μg) protein from the lower fraction of the centrifuge tube containing the vesicles and the exchange protein. Lane 3. 10 μl of a 3 mg/mL mixture of calibration protein standards, from top to bottom, myosin (MW 205,000), β-galactosidase (MW 116,000), phosphorylase B (MW 97,000), bovine plasma albumin (MW 66,000), egg albumin (MW 45,000), and carbonic anhydrase (MW 29,000). The standards were obtained from Sigma (MW-SDS-200 kit). Lane 4. (15 μg) of protein isolated from VLDL labelled with [$^2H_2$]PC (*i.e.* after treatment with transfer protein). Lane 5. (15 μg) of protein isolated from native VLDL.

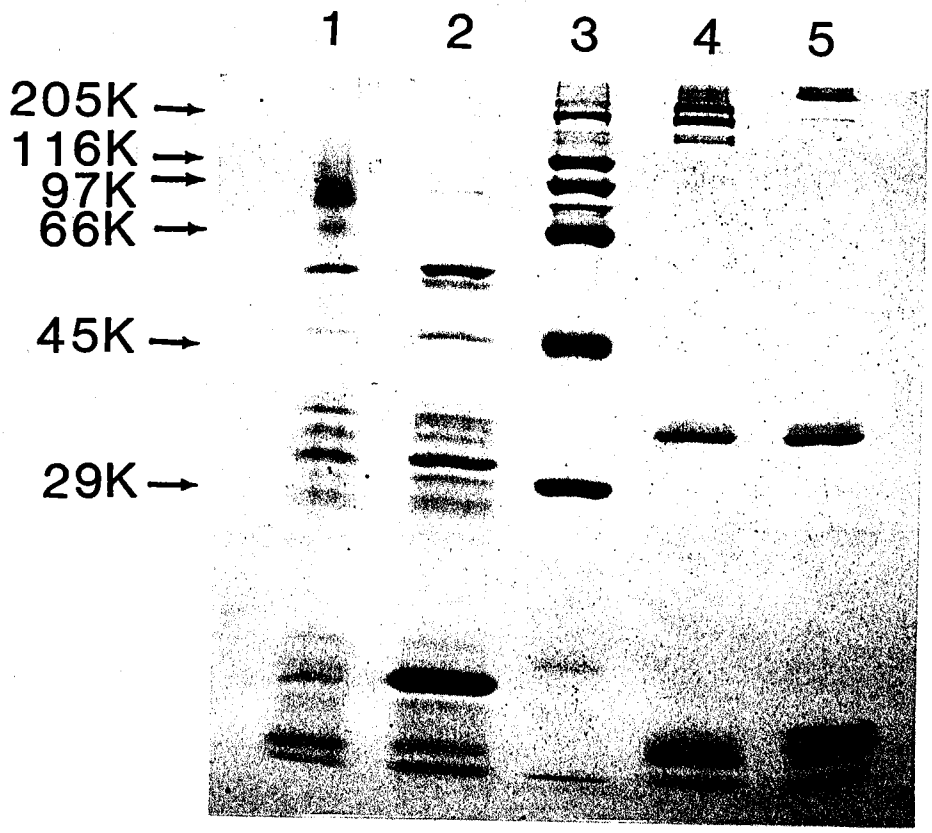
1
2
3
4
5
205K
116K
97K
66K
45K
29K

Further resolution of the apoB fragments was achieved on a 4% polyacrylamide gel containing 0.1% SDS. Figure 14 shows the apoB associated with native and labelled VLDL, and LDL. Lane 1 represents the mixture of calibration protein standards, their respective molecular weights are indicated on the left handside of the electrophoretogram. Lane 2 shows the apoB fragments associated with the labelled VLDL particles while Lanes 3 and 4 represent the apoB associated with the native VLDL and the native LDL particles, respectively. Since the abundant form of apoprotein in LDL particles is apo B-100 (Kane *et al.*, 1983; Sparks and Sparks, 1985), the protein band of Lane 3 whose R_F value is similar to the protein band in Lane 4 indicates that the major form of apoB associated with the VLDL particles is also apo B-100. From our 4% gel the two fragment observed in Lane 2 correspond to MWs of 240,000 and 200,000. These fragments are believed to result from cleavage of a single apo B-100 polypeptide chain.

Relative levels of apoproteins associated with VLDL particles were evaluated from the densitometric scans of SDS-10% polyacrylamide gels (Figure 13). The gels were scanned at 580 nm using a Hoefer Scientific Instruments GS 300 Scanning densitometer. Figure 15 shows the densitometric scans of apoproteins associated with the native VLDL (Figure 15a) and the labelled VLDL (Figure 15b). The major peaks corresponding to the R_F values of 0.018 (I), 0.509 (II), and 0.956 (III) were designated as apo B-100, apo E and apo C, respectively. Similar apoprotein bands have also been observed by Mahley and Innerarity (1983) on SDS-10% polyacrylamide gel. Peaks II and III in labelled VLDL have similar R_F values compared to the native VLDL particles. The two peaks corresponding to R_F values of 0.042 and 0.063 have been attributed to the two smaller fragments of apo B-100. The integrated intensities of the three apoprotein, apo B, apo E, and apo

Figure 14: Sodium Dodecyl Sulphate-4% polyacrylamide gel electrophoretogram showing the effect of phosphatidylcholine transfer protein on apoB-100 associated with VLDL. For comparison, apoprotein of LDL is also included. Electrophoresis was performed as described in Materials and Methods. Lane 1. 10 μl of 3mg/mL solution of calibration protein standards. Lane 2. (15 μg) of protein isolated from PC labelled VLDL. Lane 3. (15 μg) of protein isolated from native VLDL. Lane 4. (20 μg) of protein isolated from LDL.

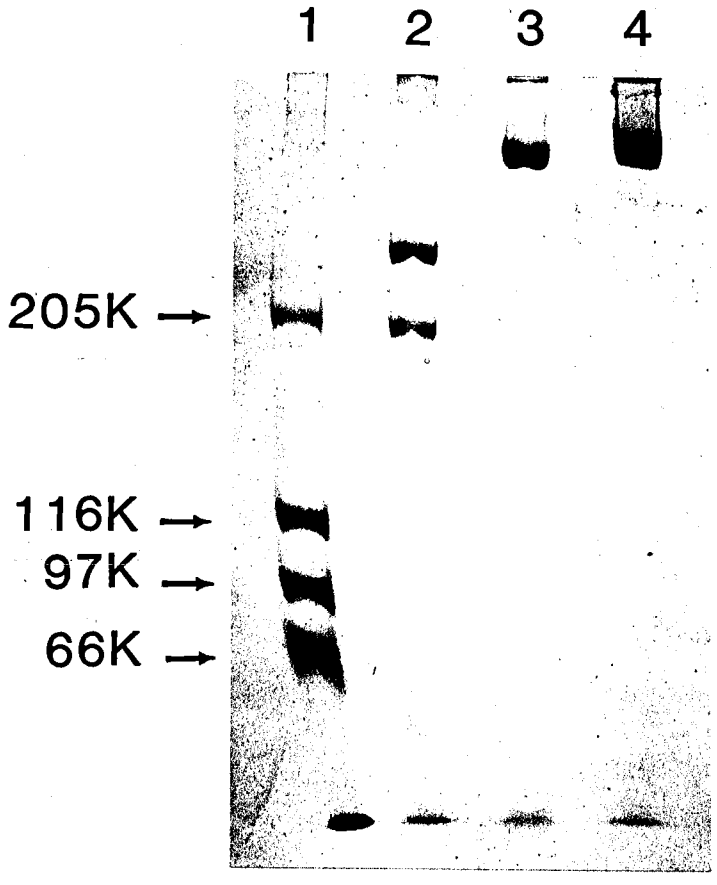
1
2
3
4
205K
116K
97K
66K

Figure 15: Densitometric scans of Native and Labelled VLDL obtained from Sodium Dodecyl Sulphate-10% polyacrylamide gel. The gels were stained with Coomassie brilliant blue R-250 and scanned at 580 nm using a Hoefer Scientific Instruments GS 300 Scanning Densitometer.

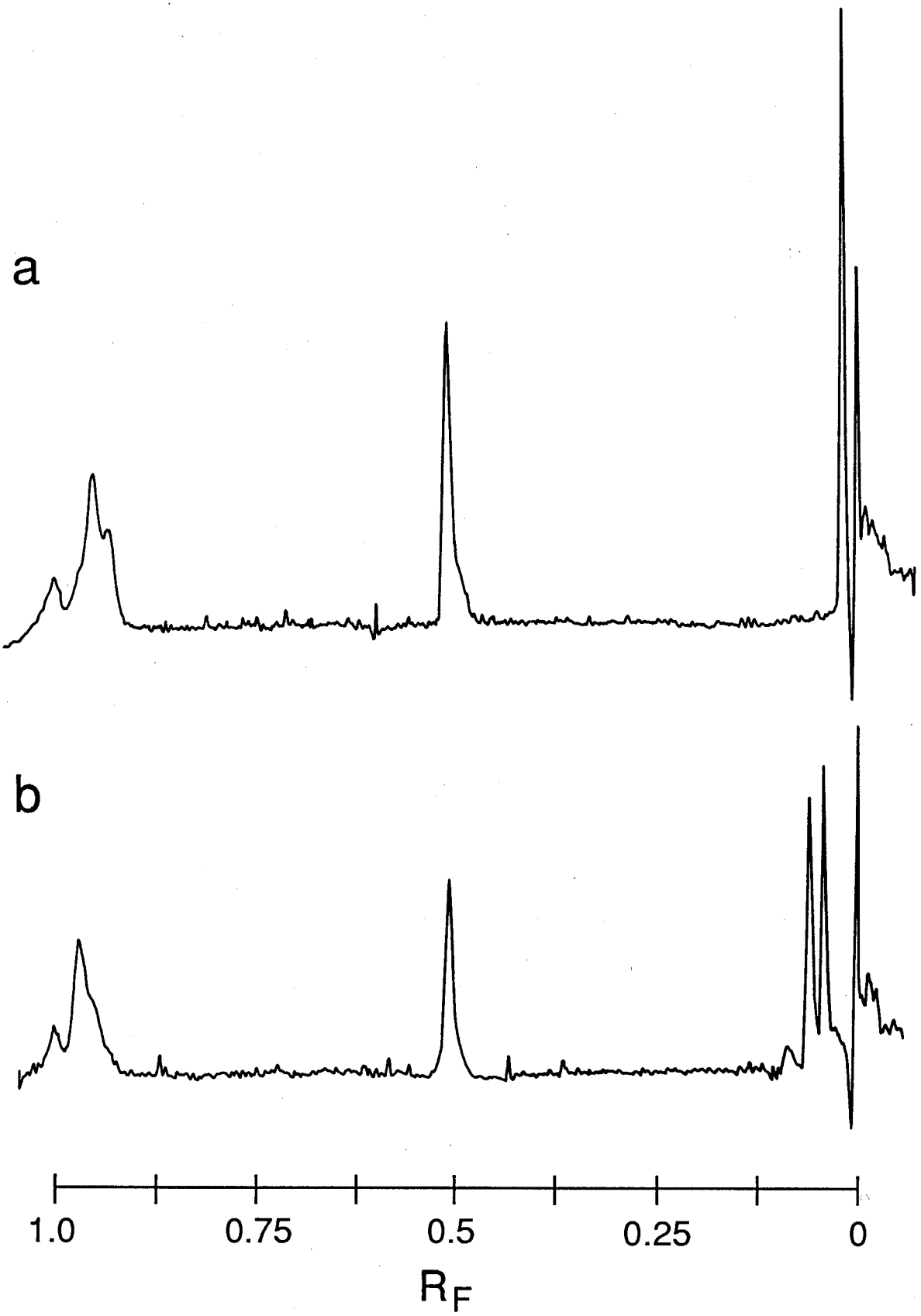
a
b
1.0
0.75
0.5
0.25
0
R_F

C, are listed in Table 4. In calculating the relative ratios of apoproteins we have assumed that the sum of the two apoB fragments represent the total apoB associated with labelled VLDL. From Table 4 it is observed that the percentages of apoB and apoC in native VLDL and labelled VLDL are within experimental error of each other whereas apo E is approximately 13% less in labelled VLDL. The relative ratios of apo B/apo C are in close agreement between the two VLDL while the apo B/apo E and apo E/apo C ratios deviate.

SDS-PAGE and densitometric studies demonstrate that following the incorporation of selectively deuterated phospholipids into VLDL particles using a partially purified transfer protein:

a) The proteins present in the crude preparation do not associate with VLDL particles.

b) Major apoproteins, apo B and apo C, are not depleted, whereas apo E is approximately 13% less in the [^{2}H]PC-labelled VLDL.

c) Apo B undergoes cleaveage into two fragments and these remain associated with the particles.

Inhibition studies

A possibility that cleaveage of apoB may be caused by the protease contaminants associated with VLDL particles or by the protease contaminants present in the partially purified phosphatidylcholine transfer protein was investigated. Two separate inihibition studies were performed using phenylmethylsulfonylfluoride (PMSF) and diisopropylfluorophosphate (DIFP). Varying amounts of inhibitors, (PMSF) 0.1 to 1.0 m$\underline{M}$ and (DIFP) 0.1 to 5.0 m$\underline{M}$, were added and incubated for 45 min with the crude enzyme preparation prior to use. VLDL (5 mL, 1.0 mg protein/mL), enzyme preparation containing the protease inhibitors (7.9 mL, 0.35 mg/mL protein) and buffer (7.1 mL,

Table 4: Apoprotein content of native VLDL and labelled VLDL (%).

Apoproteins	Native VLDL	Labelled VLDL
ApoB 100	31.4 (±1.5)	33.7 (±0.9)
ApoE	31.1 (±0.8)	27.1 (±0.9)
ApoC	37.5 (±0.7)	39.0 (±1.0)
ApoB/ApoE	1.02 (±0.08)	1.24 (±0.04)
ApoB/ApoC	0.84 (±0.06)	0.87 (±0.04)
ApoE/ApoC	0.83 (±0.01)	0.70 (±0.04)

Values are the mean ± standard deviation of duplicate densitometric traces of the apoproteins associated with native VLDL and labelled VLDL (VLDL containing [16,16,16-$^2H_3$]PC and [N(C^2H_3)$_3$]PC). The densitometric scans were obtained from SDS-10% polyacrylamide gel slabs (Figure 13).

0.15 M NaCl, 2.0 mM Na_2EDTA, 0.02% NaN_3 at pH 7.4) were incubated for 90 min at 35-37°C. In a separate study, VLDL (5.0 mL, 1.0 mg protein/mL) in buffer (15.0 mL) was incubated for 90 min at 35-37°C. Following incubation, VLDL particles were isolated by ultracentrifugation and subjected to SDS-PAGE. In Figure 16 are shown the protein pattern of VLDL obtained with the treatment with transfer protein in presence of PMSF (Figure 16a) and DIFP (Figure 16b). The gel patterns for proteins isolated from VLDL after incubation with transfer protein without inhibitors is found in Figure 16b (Lane 2). The inhibition studies with PMSF dissolved in ethanol, up to 1.0 mM concentration (Lane 4), were observed not to prevent cleaveage of apo B-100. At higher inhibitor concentration (3.0 mM) where ethanol was approximately 13.5% by volume in the final incubation media the VLDL

particles were found to denature. At the DIFP concentrations from 0.1 mM to 5.0 mM did not prevent the cleaveage of apo B-100 (Figure 16b, Lanes 3 to 5). Our results are in contrast to the findings of Krishnaiah and Wiegaudt (1974) who have reported the inhibition of protease activity associated with LDL_2 preparations against apo B with PMSF at 1.0 mM and DIFP at 5.0 mM.

Cholesteryl ester accumulation in macrophages

In order to assess whether cleavage of apo B-100 would alter the biological function of VLDL particles, a study was undertaken to measure the formation of cholesteryl esters in J774A.1 cells, a murine macrophage-like cell line. This study was not performed with the particles used in the ^2H NMR studies, here, VLDL was isolated and purified from fresh plasma (<3 days old), unlike in the ^2H NMR study where VLDL samples were pooled over a period of four to five week before purification. VLDL sample was treated with the partially purified transfer protein as described in the inhibition study section. The treated VLDL sample was isolated by ultracentrifugation at 42,000 rpm, 20 hr at 5°C. This sample was not spun further, 3 times at 42,000 rpm for 20 min, as was the case for the samples used in the ^2H NMR study. Palmitic acid (10 mol % with respect to VLDL phospholipid) was incorporated into VLDL as described in Materials and Methods. Particles were sized by QELS, native VLDL = 38.0±10.2, transfer protein treated VLDL = 38.4±11.6 and VLDL labelled with palmitic acid = 39.6±12.5. Prior to the biological assay, VLDL samples were dialysed against 0.15 M NaCl, 2.0 mM Na_2EDTA at pH 7.4 (3 x 2 L) overnight. The study was performed by Dr. Urs Steinbrecher and his staff, Division of Gastroenterology, Health Science Center Hospital, 2211 Wesbrook

Figure 16 : Sodium Dodecyl Sulphate-10% polyacrylamide gel electrophoretogram of VLDL incubated in presence of transfer protein containing phenylmethylsulfonylfluoride (PMSF) and diisopropylfluorophosphate (DIFP).

Figure 16 a: Lane 1. 20 μl of a 3 mg/mL mixture of calibration protein standards, from top to bottom, myosin (MW 205,000), β-galactosidase (MW 116,000), phosphorylase B (MW 97,000), bovine plasma albumin (MW 66,000), egg albumin (MW 45,000), and carbonic anhydrase (MW 29,000). The standards were obtained from Sigma (MW-SDS-200 kit). Lane 2. (20 μg) proteins isolated from VLDL. Lane 3. (20 μg) proteins isolated from VLDL after incubation with 0.1 m$\underline{M}$ PMSF. Lane 4. (20 μg) proteins isolated from VLDL after incubation with transfer protein and 1 m$\underline{M}$ PMSF. Lane 5. (20 μg) proteins isolated from VLDL after incubation with transfer protein and 0.5 m$\underline{M}$ PMSF.

Figure 16 b; only the upper part of the gel is shown. Lane 1. (15 μg) proteins isolated from VLDL. Lane 2. (20 μg) proteins isolated from VLDL after incubation with transfer protein. Lane 3. (20 μg) proteins isolated from VLDL after incubation with transfer protein and 0.1 m$\underline{M}$ DIFP. Lane 4. (15 μg) proteins isolated from VLDL after incubation with transfer protein and 1.0 m$\underline{M}$ DIFP. Lane 5. (15 μg) proteins isolated from VLDL after incubation with transfer protein and 5.0 m$\underline{M}$ DIFP.

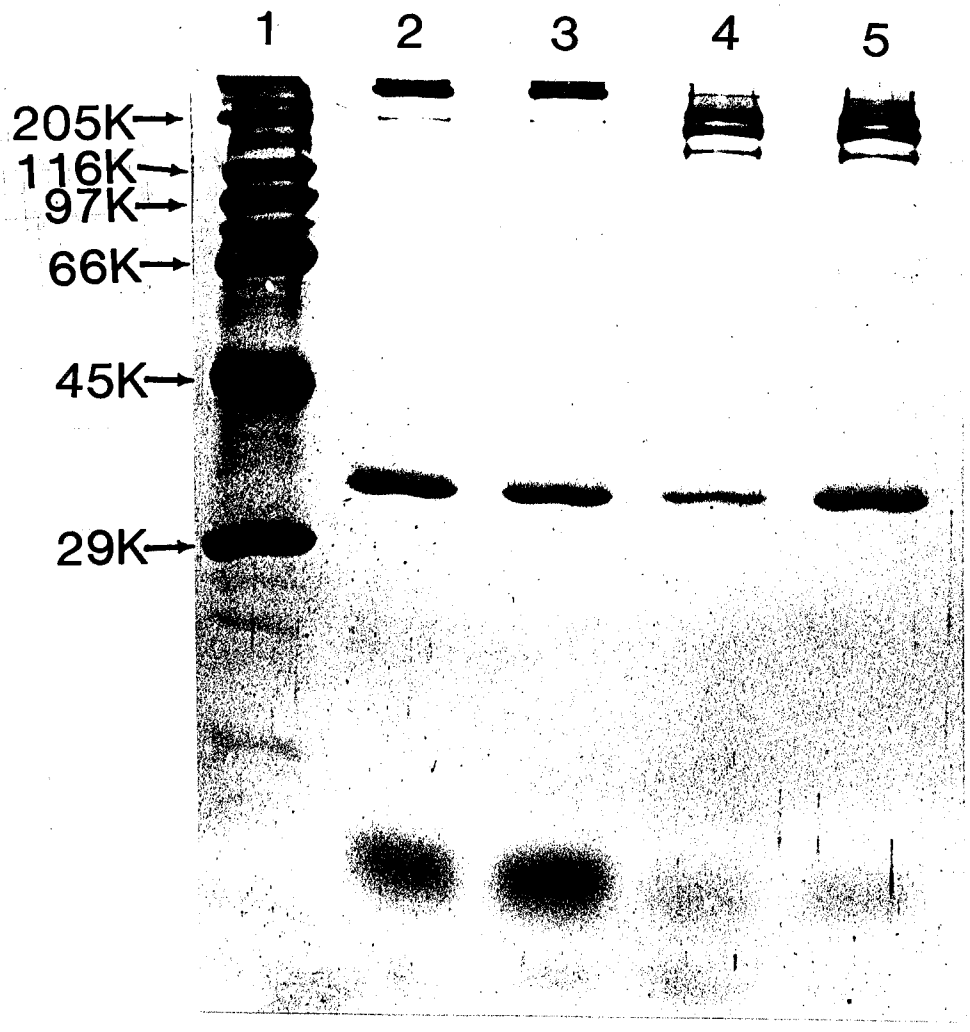
1
2
3
4
5
205K
116K
97K
66K
45K
29K

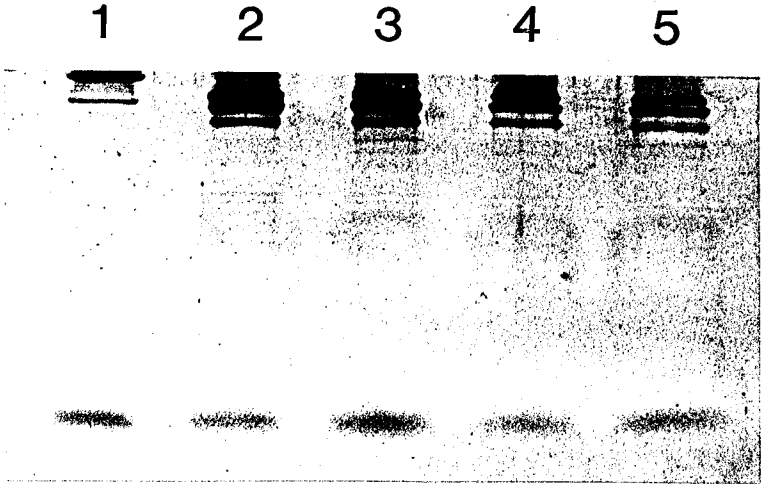
1
2
3
4
5

Mall, University of British Columbia, British Columbia, Canada. I am grateful to Dr. Steinbrecher for allowing me to present these results here.

Cholesterol esterification rate was assayed by measuring the conversion of [^{3}H]oleic acid into cholesteryl [^{3}H]oleate. The method involved the preincubation of J774A.1 cells (0.42 mg of cell protein) with increasing concentrations of native VLDL, transfer protein treated VLDL, and VLDL labelled with palmitic acid (15 to 100 μg/ml VLDL protein) overnight at 37°C in a 5% CO_2 incubator. BSA (2 g/l) complexed with 50μM [9,10-^{3}H]oleic acid was then added and incubated with the cells for a further 5 1/2 hr. The cells were then washed and the lipids were extracted with chloroform and methanol as described by Bligh and Dyer (1959). The lipids were separated on Whatman K6 250 silica gel TLC plates developed with hexane:ether:acetic acid (80:20:1 v/v/v) The cholesteryl ester zone was scraped and assayed for radioactivity. Figure 17 shows that all 3 VLDLs stimulated the formation of cholesteryl [^{3}H]oleate to a virtually identical extent.

The data presented in Figure 17 clearly demonstrate that the stimulated synthesis of cholesteryl [^{3}H]oleate in the macrophages was similar for all VLDL particles and proceeded through a saturable pathway. Thus, we conclude that the exchange procedure did not alter the biological function of VLDL particles in spite of the cleavage of apo B-100.

^{2}H NMR studies

The ^{2}H NMR spectra of selectively deuterated phospholipids, labelled in the methylene positions, incorporated into VLDL at 25°C are shown in Figure 18. In addition to the signal observed from the [^{2}H]PC resonance,

Figure 17: Dose-responce effect of native VLDL (solid line), transfer protein treated VLDL (dashed line), and VLDL labelled with palmitic acid (dotted line) on cholesteryl ester formation in J774A.1 cells, a murine macrophage-like cell line.

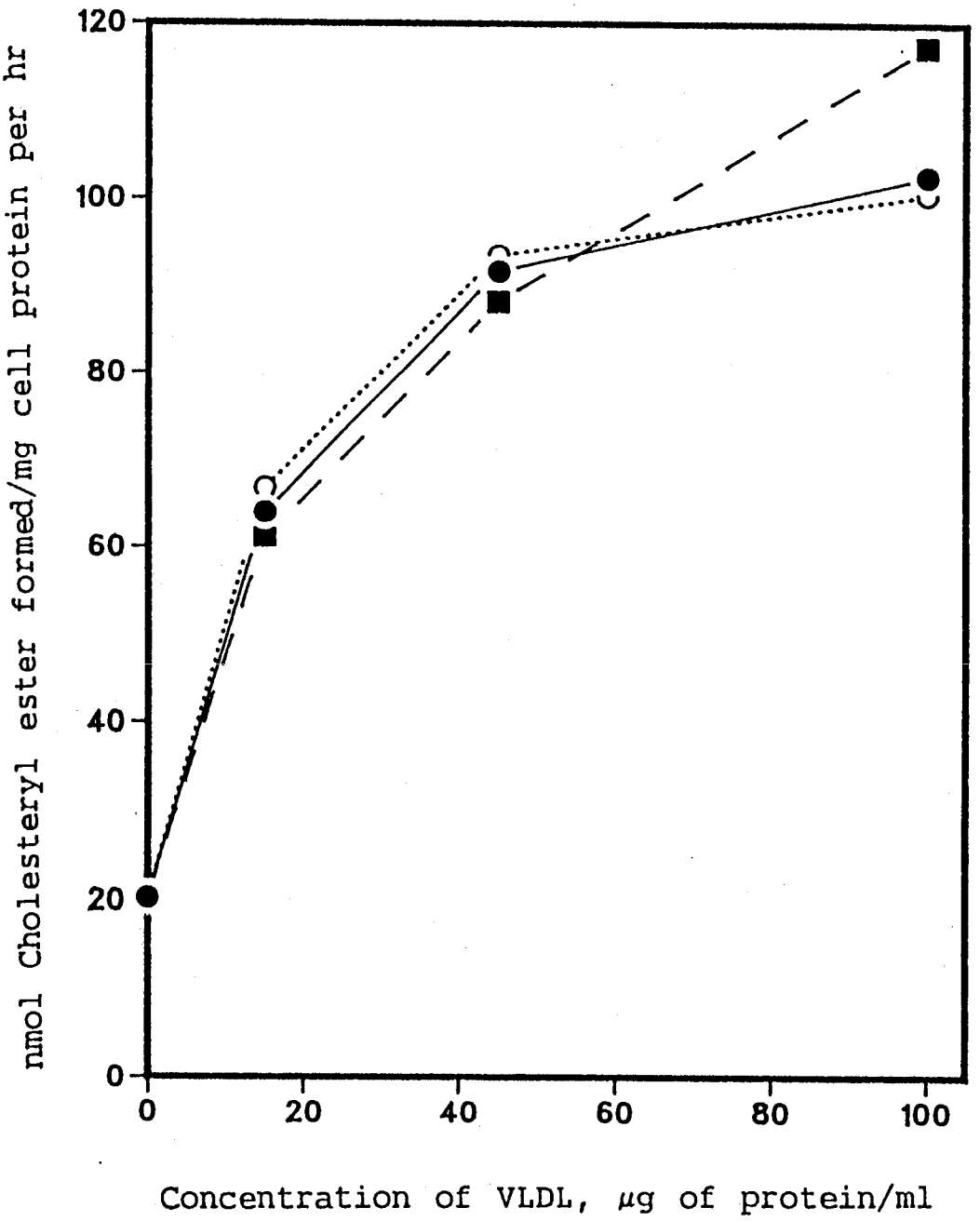
nmol Cholesteryl ester formed/mg cell protein per hr
120
100
80
60
40
20
0
0
20
40
60
80
100
Concentration of VLDL, μg of protein/ml

the spectra also contain a narrow resonance, ≃150 Hz downfield, due to the residual deuterium in water. In all cases, a Lorentzian lineshape provided excellent fits for the [^{2}H]PC resonances. The linewidths at half height of the [^{2}H]PC resonance from C2-C11,12-positions are roughly the same and range between 60-68 Hz (Table 5).

The ^{2}H NMR spectra of [2,2-$^2H_2$]PC and [4,4-$^2H_2$]PC in VLDL as a function of temperature are shown in Figure 19. The linewidths at 15°C are ≃79 Hz and decrease to ≃60 Hz at 35°C, in both cases. This is in contrast with the results obtained with the same probes in HDL_2 where the linewidths were observed to change drastically with temperature (Parmar, 1985). Since the change in linewidths with temperature of the two methylene positions was not drastic, the temperature dependence of ^{2}H NMR spectra of other selectively deuterated phospholipids were not examined. The linewidths determined for selectively deuterated phospholipids in VLDL are given in Table 5.

Figure 20 shows the ^{2}H NMR spectrum of [16,16,16-$^2H_3$]PC in VLDL as a function of temperature. In addition to the signal observed from the C^2H_3 resonance, the spectrum also shows the signal from residual deuterium in water, ≃150 Hz downfield. The spectra shown in Figures 20a, c, and e are least-squares fits to a Lorentzian lineshape for both water and PC. Visual inspection of the Figures 20a and 20c, reveals that the computer simulation failed to account for the intensity of the C^2H_3 signal, particularly at the top. Furthermore, the linewidths obtained from these spectra were 315 Hz (15°C) and 217 Hz (20°C) compared to the C^2H_2 segments whose average linewidth were 80 and 64 Hz at 15 and 25°C, respectively. In order to account for the amplitude we have used a three Lorentzian, nine parameter,

Figure 18: ^2H NMR spectra of phospholipids selectively deuterated in the methylene segments in VLDL at 25°C. The position of selective deuterations are given on the left hand side of each spectrum. The spectra were simulated by an iterative least-squares fit to a Lorentzian linshape function (solid line) to the spectral datapoints (crosses). Spectral parameters: all pulse widths = 90° flip angles; [2,2-$^2H_2$]PC, pulse width = 8.0 μs, sweep width = 20 kHz, delay between pulses = 0.2 s, number of aquisition = 100,000; [4,4-$^2H_2$]PC, pulse width = 8.0 μs; sweep width = 20 kHz, delay between pulses = 0.2 s number of aquisition = 400,000; [5,5,6,6-$^2H_4$]PC, pulse width = 7.5 μs; sweep width = 50 kHz, delay between pulses = 0.15 s number of aquisition = 400,000, left shifted twice; [7,7-$^2H_2$]PC, pulse width = 8.0 μs; sweep width = 50 kHz, delay between pulses = 0.11 s number of aquisition = 800,000; [11,11,12,12-$^2H_4$]PC, pulse width = 7.8 μs; sweep width = 50 kHz, delay between pulses = 0.16 s number of aquisition = 300,000, left shifted three times. Left shifts were performed to correct the base line abberations. Delay before acquisition = 10 μs, dataset = 4K zero filled to 8K; In all cases line broadening = 10 Hz.

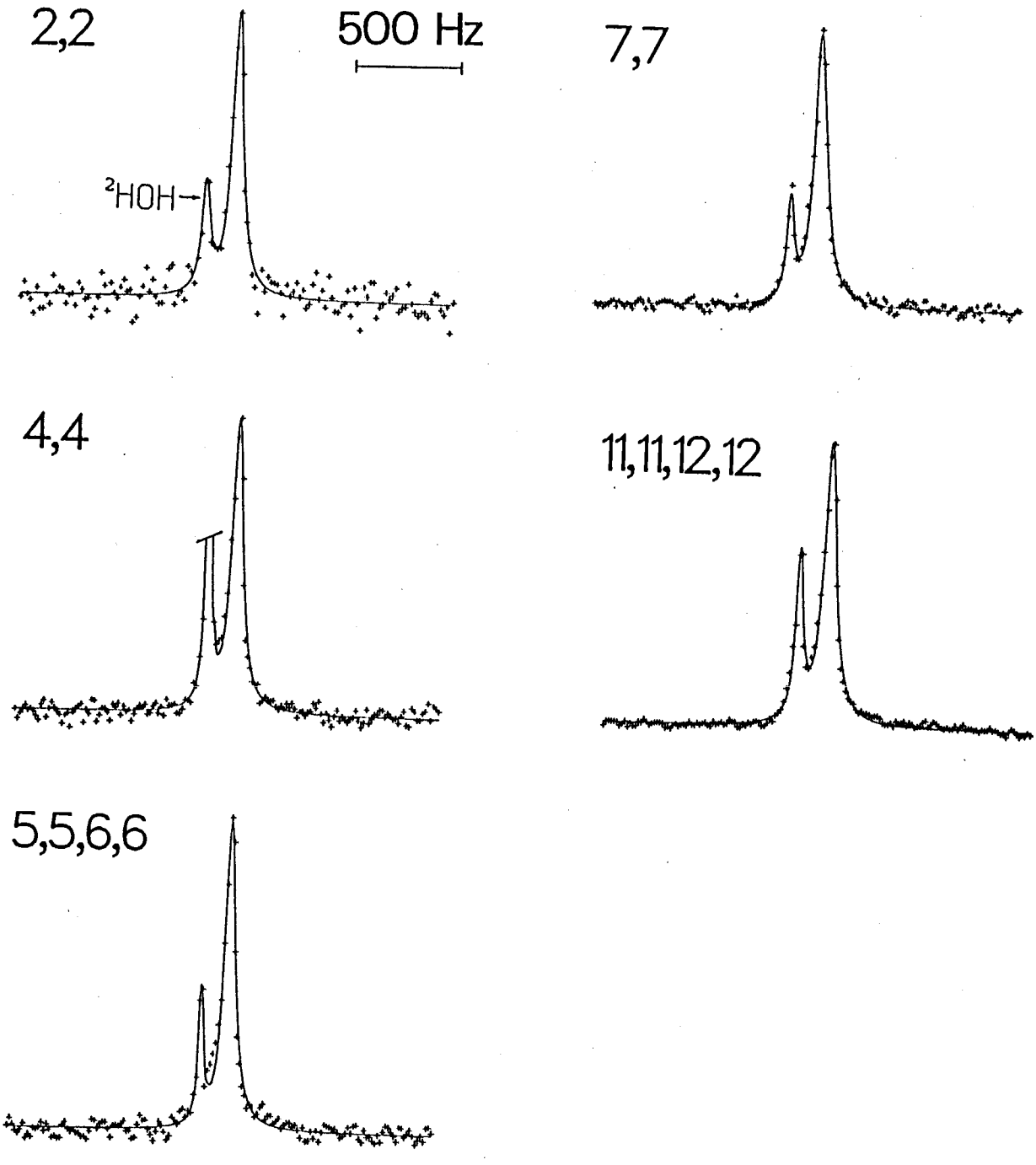
2,2
500 Hz
^{2}HOH
7,7
4,4
11,11,12,12
5,5,6,6

Figure 19: ^2H NMR spectra of [2,2-$^2H_2$]PC and [4,4-$^2H_2$]PC in VLDL at 15°C and 35°C. The position of selective deuterations are given on the left hand side of the spectrum. The spectra are iterative least-squares fit to a Lorentzian linshape function (solid line) to the spectral datapoints (crosses). Spectral parameters: pulse width = 8.0 μs (flip angle = 90°), sweep width = 20 kHz, delay between pulses = 0.2 s, number of aquisition = 225,000 (a), 100,000 (b), 200,000 (c and d), In all cases dataset = 4K zero filled to 8K, line broadening = 10 Hz, delay before acquisition = 10 μs.

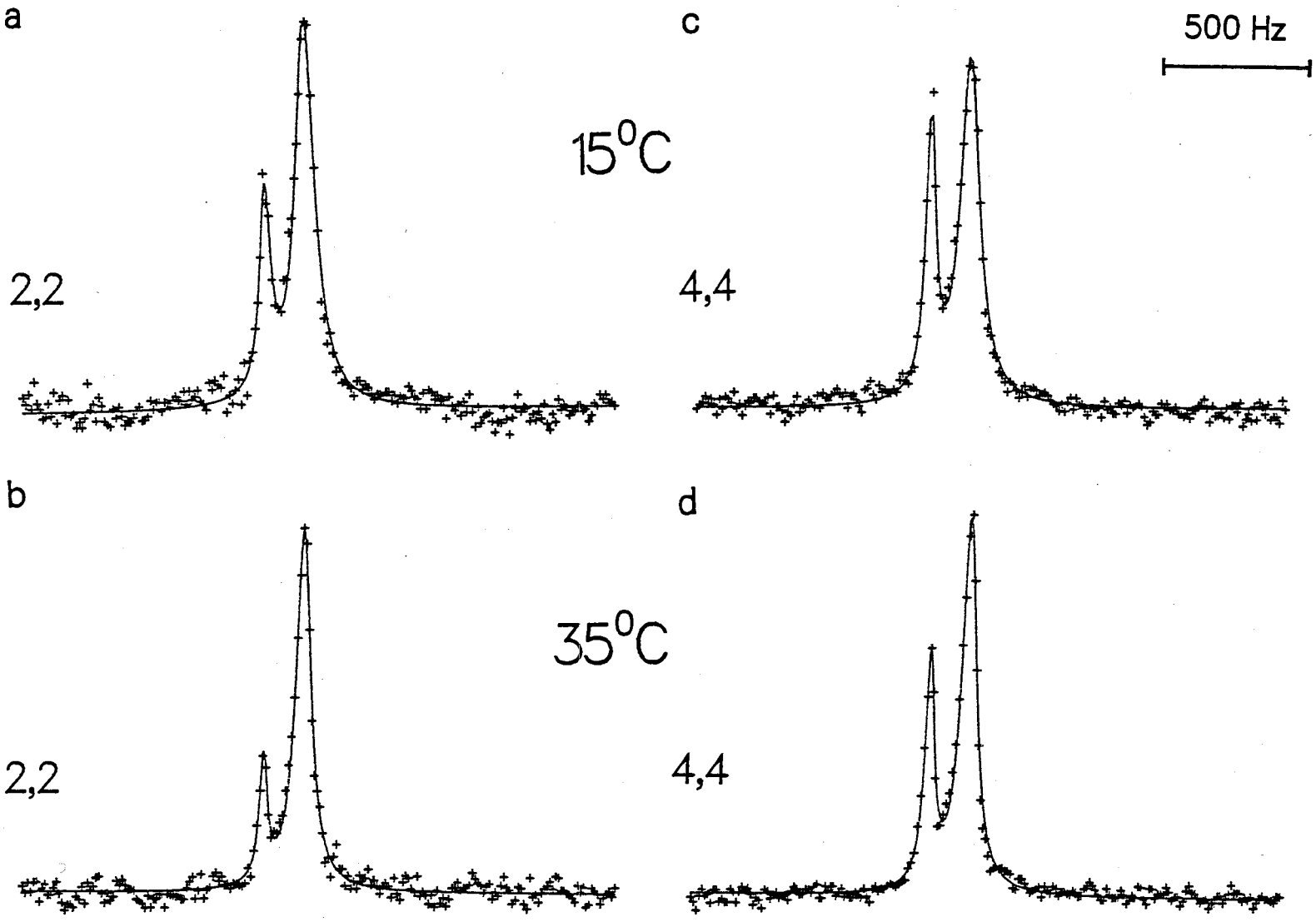
a
15°C
2,2
c
500 Hz
4,4
b
35°C
2,2
d
4,4

Table 5: ^2H NMR linewidths, $\Delta\nu_{1/2}$, of phospholipids selectively deuterated in the methylene segments in VLDL at selected temperatures.

Deuterated position	Incorporation (Mol %)	$\Delta\nu_{1/2}$ (Hz)[a]		
		15°C	25°C	35°C
2,2	5.0	79	60	62
4,4	7.0	-	63	-
4,4	17.0	80	62	61
5,5,6,6	3.0	-	60	-
7,7	1.5	-	69	-
11,11,12,12	10.7	-	68	-

[a] Linewidths are accurate to ±10% and were obtained from an iterative least squares fit to a [$^2H_2$]PC and [$^2H_4$]PC resonance.

iterative least-squares computer fit to [16,16,16-$^2H_3$]PC spectrum. The constraint imposed in the fitting routine was that the chemical shift for the phospholipid resonance from ^{2}HOH, the summation of two Lorentzian lines, was fixed. The amplitudes and the linewidths for the respective Lorentzian lineshapes were allowed to iterate. Figures 20b and 20d show the best nine parameter fit of [16,16,16-$^2H_3$]PC. The simulated spectrum yields a linewidths of 79 Hz (narrow component) and 613 Hz (broad component) at 15°C and 85 Hz (narrow component) and 571 Hz (broad component) at 20°C. The relative intensities of the spectral components were calculated from the linewidths and amplitudes of the signals as described by Stone, 1973.

The intensity ratios of narrow/broad spectral components were 16.8(±0.7)/83.2(±0.6) at 15°C and 25.9(±1.4)/74.1(±2.1) at 20°C (see Table 6). At 30°C we were unable to simulate the C^2H_3 resonance with the superposition of two Lorentzian lineshapes. The spectrum shown, Figure 20e, was simulated by a Lorentzian lineshape and a linewidth of 108 Hz was obtained. The failure to simulate the spectrum as the superposition of two Lorentzian lineshapes is expected if the linewidth difference between the two Lorentzian signals is small (Treleaven, 1985). Therefore the linewidth obtained represents an average of two domains.

We were unable to detect the broad spectral component for the C^2H_2 segments of phospholipids (Figures 18 and 19) because of insufficient signal to noise ratio and of the narrow sweep widths employed. This can be explained if we assume the order parameter of the broad component in the plateau region in VLDL to be similar to that measured for LDL, *i.e.* an average S_{CD} = 0.3. Then, for particles of mean diameter 41.5 nm, at a viscosity = 0.8711 cP (viscosity of 0.15 M NaCl, 2.0 mM Na_2EDTA, 2 M KBr at pH 7.4), temperature of 25°C, and D_t = (9.1±1.0) x 10^{-9} cm^2/s (see Section V), the linewidth calculated using equations 17 and 22 is 26.5 kHz. Thus, the sweep width employed together with poor signal to noise ratio did not allow us to measure such a broad component.

Using [$^2H_{31}$]PC we were able to demonstrate the presence of a broad component in the surface monolayer of VLDL. The spectra shown in Figure 21 clearly indicate the presence of a broad spectral component whose linewidth is 20 kHz at 25°C, and 5.3 kHz at 40°C. No meaningful conclusions can be made from the linewidth due to the composite nature of the signal as the average linewidth of the broad component is primarily due to the more

Figure 20: ^2H NMR spectra of [16,16,16-$^2H_3$]PC in VLDL as a function of temperature. The spectra were simulated by an iterative least-squares fit to a Lorentzian linshape (solid line) to the spectral datapoints (crosses) (Figures 11a, c and e) and superposition of two Lorentzian lineshapes for the C^2H_3 resonance (Figures 11b and 11d). Spectral parameters: pulse width = 15.0 μs (flip angle = 60°), sweep width = 10 kHz and 5 kHz (30°C), delay between pulses = 0.45 s and 0.5 s (30°C), number of aquisition = 20,000, In all cases delay before acquisition = 10 μs, dataset = 4K zero filled to 8K, line broadening = 10 Hz.

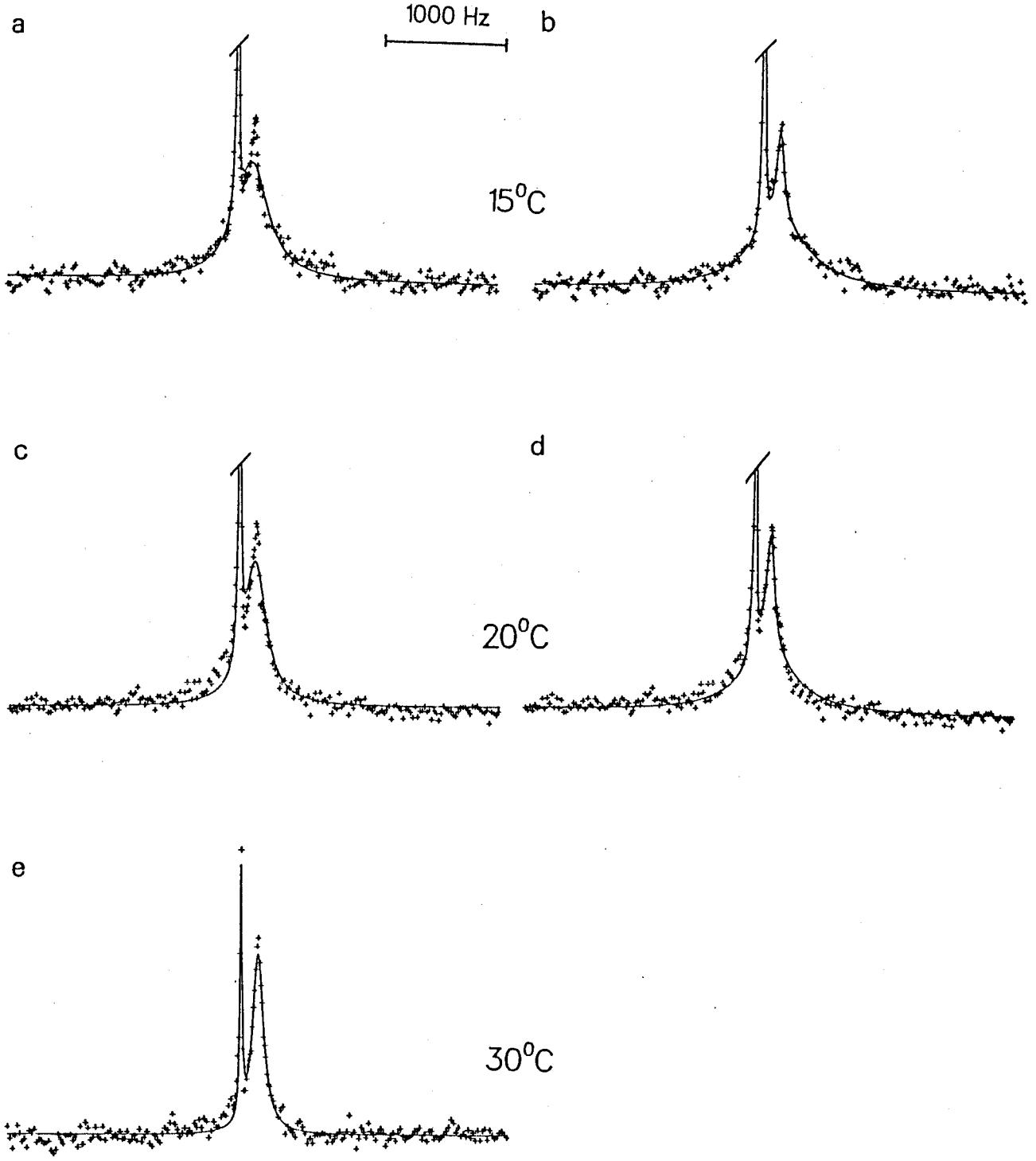
a
1000 Hz
b
15°C
c
d
20°C
e
30°C

Table 6: ^2H NMR linewidths, $\Delta\nu_{1/2}$, of [16,16,16-$^2H_3$]PC in VLDL.

Temperature °C	$\Delta\nu_{1/2}$ (Hz)[a]	$\Delta\nu_{1/2}$ (Hz)[b] Broad/Narrow	Ratio of [c] Broad/Narrow
15	315	613/79	83.2±0.6/16.7±0.7
20	217	571/85	74.1±2.1/25.9±1.4
25	147	256/73	74.4±1.8/25.6±1.8
30	108	-	-

Linewidths are accurate to ±10% and were obtained from an iterative least squares fit to the [$^2H_3$]PC resonance.

[a] Linewidths were obtained from a single Lorentzian lineshape fit to the C^2H_3 resonance.
[b] Linewidths were obtained from the superposition of two Lorentzian lineshapes to the C^2H^3 resonance.
[c] The ratio of the spectral components were calculated as described by Stone, 1973. The error in the values were calculated from the standard deviations obtained from the iterative least-squares fit.

disordered C-$^2H_2$ segments *i.e* the C-$^2H_2$ segments towards the terminal end of the acyl chains.

The dynamic behaviour of phospholipids in VLDL was investigated by measuring spin-lattice relaxation times, T_1. T_1 of selectively deuterated phosphatidylcholines in VLDL were measured by the inversion recovery method, $(180^\circ-\tau-90^\circ-T)_n$, (Vold *et al.*, 1968). Figure 23 shows the plots of $\log(A_\infty - A_\tau)$ versus τ for [^2H]PC. The solid line in each plot is a

Figure 21: ^2H NMR spectra of VLDL containing 6.0 mol % [$^2H_{31}$]DPPC at 25°C (a) and 40°C (b). Spectral parameters: pulse width = 6.5μs (73° flip angle), sweep width = ±100 kHz (a), ±50 kHz (b), dataset = 4K zerofilled to 8K, number of aquisition = 123,650 (a), 39,160 (b), delay between pulses = 0.5 s (a and b), line broadening = 50 Hz (a), 25 Hz (b), delay between acquisitions = 5 μs (a), 10 μs (b),

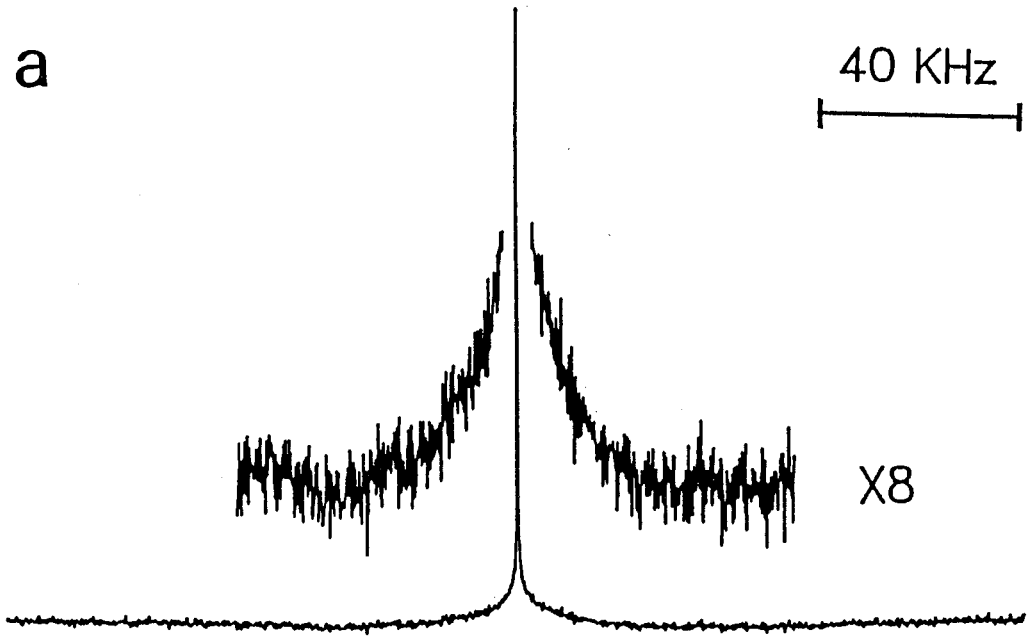
a
40 KHz
X8

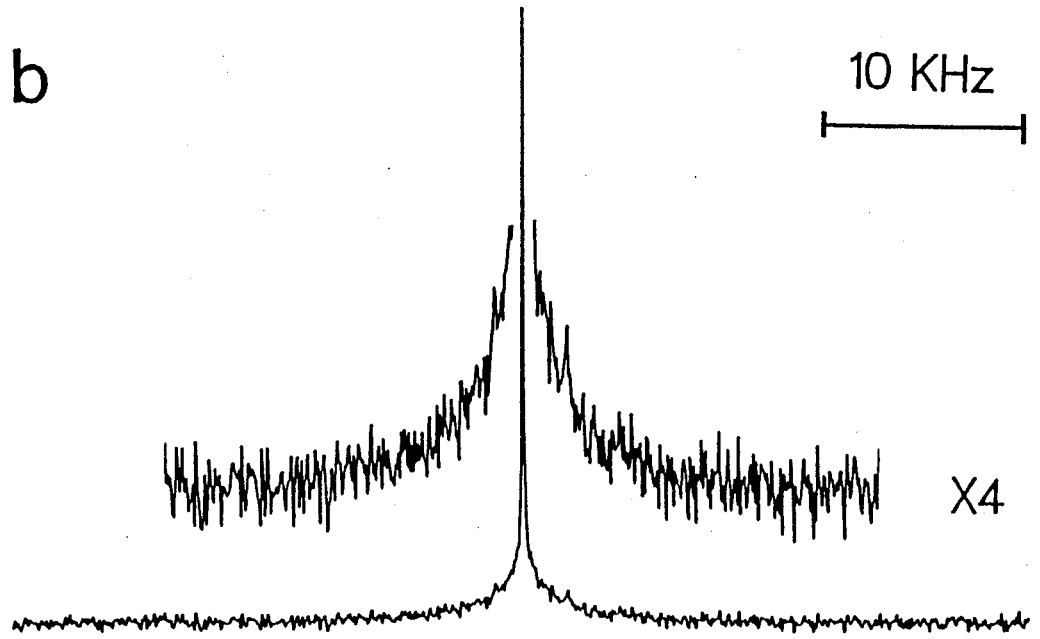
b
10 KHz
X4

weighted least-squares fit of the experimental data points. The T_1 values of the narrow component of selectively deuterated phosphatidylcholines in VLDL are given in Table 7. The errors associated with T_1 values were estimated from the standard deviations obtained from the weighted least squares plots.

Methylene segments exhibit constant T_1's of approximately 32 ms while the terminal methyl exhibits a longer T_1 of approximately 169 ms. The T_1 values of the methylene segments are approximately 50% larger than those of HDL_2 (Parmar. 1985) and LDL (Treleaven. 1985), whereas the T_1 of the [16,16,16-$^2H_3$]PC in VLDL is of comparable size.

IVb. Selectively Deuterated Palmitic Acid in Native VLDL

RESULTS

In a recent study, Wassall *et al.* (1982) have utilized perdeuterated palmitic acid to demonstrate the feasibility of fatty acids as probes to study the molecular organization of phospholipid chains in the surface monolayer of lipoproteins. Selectively deuterated palmitic acids have been used to determine the order profile of phospholipid chains in the surface monolayer of LDL (Treleaven, 1985), and HDL_2 and HDL_3 (Parmar, 1985). Selectively deuterated palmitic acids in HDL_2 gave complementary results to those obtained with selectively deuterated phospholipids (Parmar. 1985). We have taken a similar approach to study the surface monolayer of VLDL with selectively deuterated palmitic acids. Fatty acids are particularly useful in that they are readily avialable and can be incorporated into VLDL easily (see Materials and Methods).

Figure 23: Plots of ^2H NMR spin-lattice relaxation times of selectively deuterated phosphatidylcholines in VLDL at 25°C. T_1's were measured by inversion recovery method, $(180^\circ-\tau-90^\circ-T)_n$. The plots are of $\log(A_\infty - A_\tau)$ vs τ, where τ is in seconds. The solid line is the weighted least squares fit to the experimental data points. Spectral parameters: [2,2-$^2H_2$]PC (a), [4,4-$^2H_2$]PC (b) [5,5,6,6-$^2H_4$]PC (c) and [16,16,16-$^2H_3$]PC (d); pulse width = 8.0 μs (90° flip angle), 16.0 μs (180° flip angle) (a, b and d), pulse width = 7.5 μs (90° flip angle), 15.0 μs (180° flip angle) (c); sweep width = 20 KHz (a, b and c), 50 KHz (c); dataset = 4 K; number of acquisitions = 35,000 (a), 40,000 (b and c) and 20,000 (d); τ values ranged from 0.0025-0.06 s (a-b), 0.0025-0.055 s (c), and 0.001-0.24 s (d); T = 0.2 s (a-c) and 1.0 s (d); delay before acquisition = 10μs.

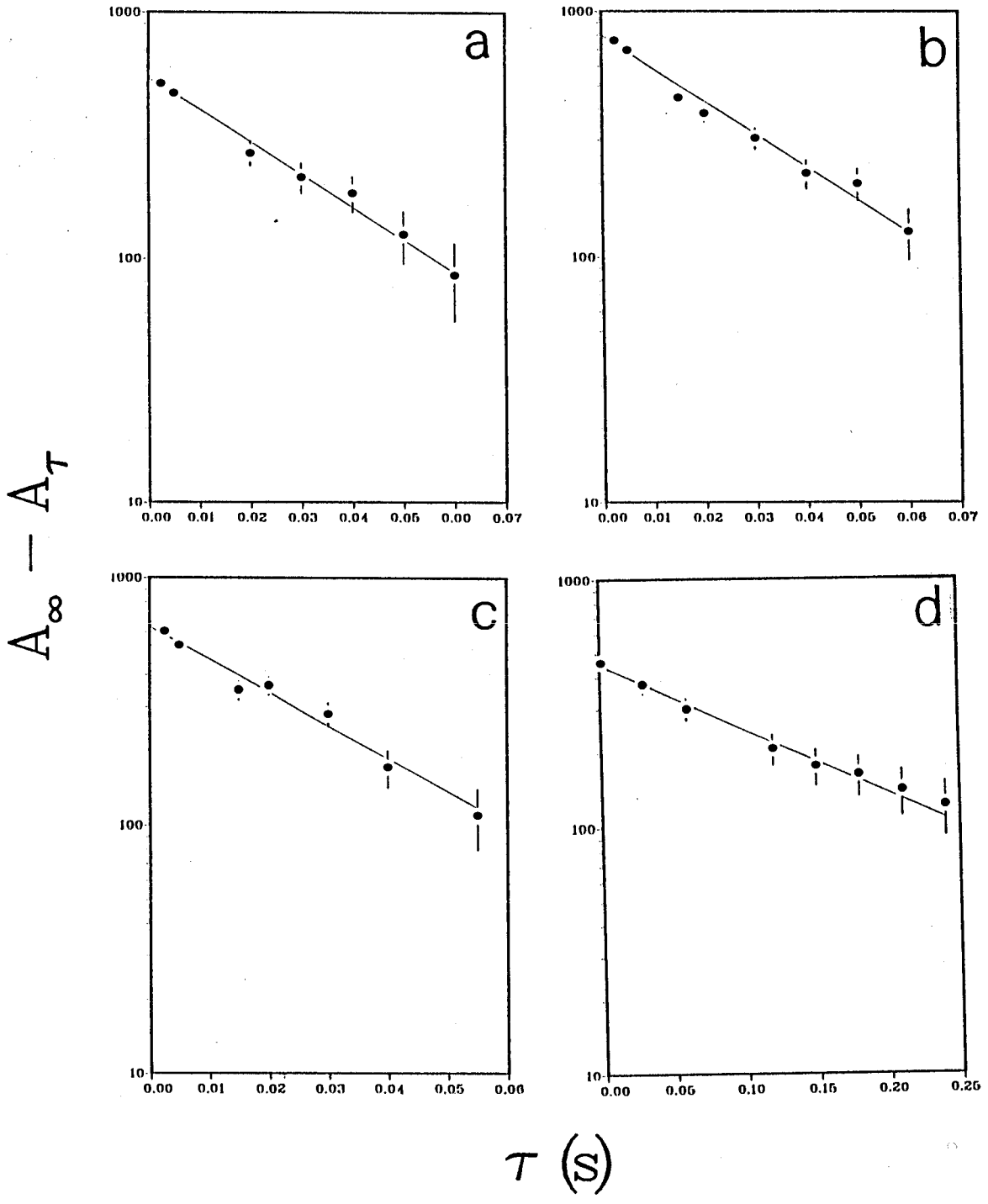
a
b
c
d
1000
100
10
0.00
0.01
0.02
0.03
0.04
0.05
0.06
0.07
0.10
0.15
0.20
0.25
$A_\infty - A_\tau$
τ (s)

Table 7: ^{2}H NMR spin-lattice relaxation times of selectively deuterated phospholipids in VLDL at 25°C.

Deuterated position	Incorporated (Mol %)	T_1 (ms)[a]
2,2	5.0	33±2
4,4	17.0	31±2
5,5,6,6	3.0	33±3
16,16;16	9.5	169±8

[a] The errors in T_1 values were estimated from the standard deviations obtained from weighted least-squares fits.

Gel permeation chromatography

Following the incorporation of deuterated palmitic acid, monitored using trace amounts of [1-^{14}C]palmitic acid ([1-^{14}C]PA) (see Materials and Methods), the intimate association of fatty acids with VLDL particles was established by gel permeation chromatography (see Materials and Methods). The elution profile of VLDL containing 6.7 mol % [4,4-$^{2}H_2$]palmitic acid and trace amounts of [1-^{14}C]PA at 4°C is shown in Figure 24. The elution profile is characterised by the presence of two peaks. The first peak elutes over a narrow volume range, 50.9-66.5 mL, and is centered at 54.8 mL while the second peak elutes over a wider volume range, 66.1-121.1 mL, and is centered at 86.0 mL. The first peak contains ≃38% and ≃21%, and the second peak contains ≃61% and ≃72% of the total protein and radioactivity recovered from the column, respectively. The elution profile of fatty acid

Figure 24: Elution profile of VLDL containing 6.7 mol % [4,4-$^{2}H_{2}$]palmitic acid and [1-^{14}C]PA on Sepharose 4B column. Approximately 10 mg protein/mL of labelled VLDL was applied on the column and eluted with 0.15 M NaCl, 2.0 mM EDTA, 0.02% NaN_3 at pH 7.4. Fractions were collected and examined for [1-^{14}C]PA activity (DPM, ■) by liquid scintillation counting and protein concentration (mg/Tube, •) by the method of Lowry *et al.* 1951, as modified by Kashyap *et al.* 1980.

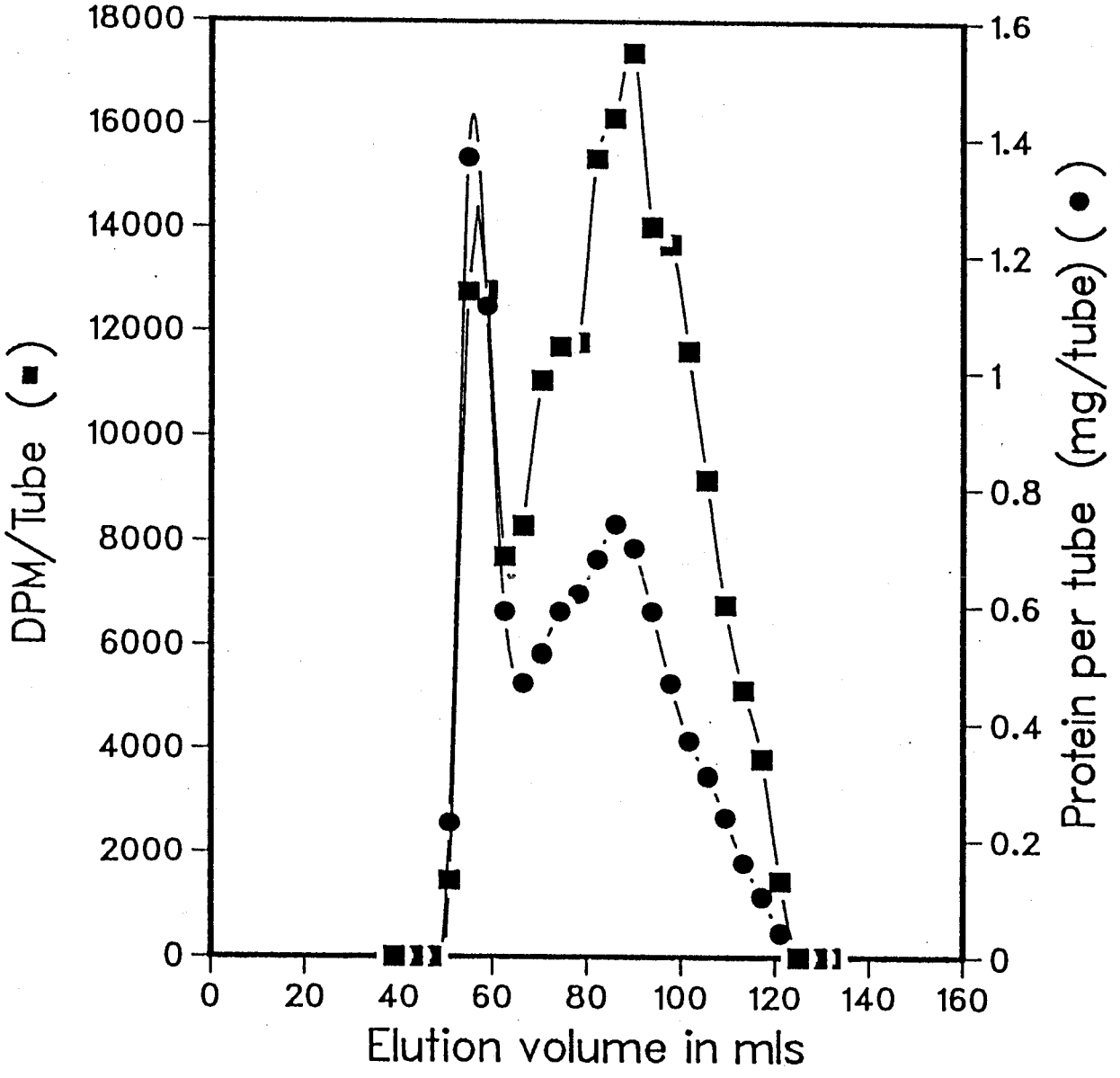
18000
16000
14000
12000
10000
8000
6000
4000
2000
0
DPM/Tube (■)
1.6
1.4
1.2
1
0.8
0.6
0.4
0.2
0
Protein per tube (mg/tube) (●)
0
20
40
60
80
100
120
140
160
Elution volume in mls

labelled VLDL resembles that of phospholipid labelled VLDL (see Figure 8). However, there are slight differences between the two elution profiles. For instance, from the radioactivity associated with the peaks, 72% of palmitic acid is associated with smaller VLDL particles unlike phospholipid labelled VLDL where ≃57% of phospholipids are associated with smaller particles. In both cases, however, all the radioactivity was recovered from the column in the VLDL fraction and therefore demonstrated that no protein-free structures were formed in either of the methods employed to incorporate deuterated lipids.

Further confirmation regarding association of fatty acids with VLDL particles was obtained by precipitation. VLDL particles containing trace amounts of [1-^{14}C]PA were precipitated with Pr^{3+} ions. Following precipitation, VLDL sample was isolated by centrifugation and washed repeatedly. The pale white solid was resuspended into solution by adding Na_2EDTA and examined for radioactivity by liquid scintillation counting. Approximately 97% of the counts were recovered and therefore indicates that fatty acid were intimately associated with the VLDL particles.

Electron Microscopy and Light Scattering

The effect of fatty acid incorporation on particle size was monitored by QELS and EM. Both techniques yield essentially identical sizes before and after the incorporation. For instance, the diameter (mean ± standard deviation) of native VLDL measured by QELS is 40.1±9.8 nm while that of labelled VLDL (VLDL containing [5,5,6,6-$^2H_4$]palmitic acid and [11,11,12,12-$^2H_4$]palmitic acid) is 39.4±12.1 nm. The diameter of native VLDL measured by EM is 38.8±7.3 nm while that of labelled VLDL (VLDL containing [11,11,12,12-$^2H_4$]palmitic acid) is 39.0±8.0 nm. An electron

micrograph of VLDL containing 10 mol % [11,11,12,12-$^2H_4$]palmitic acid is shown in Figure 25. The particles are heterogenous in size and have a circular morphology. Approximately 85% of the particles fall within a diameter range of 30-50 nm.

^{31}P NMR

The effect of fatty acid incorporation on the particle size was also analysed by ^{31}P NMR spectroscopy. The ^{31}P NMR spectra of native VLDL and VLDL containing 10.0 mol % [11,11,12,12-$^2H_4$]palmitic acid at 25°C is shown in Figure 26. In each case, a Lorentzian lineshape provide an excellent fit to the spectrum. As with the ^{31}P NMR spectrum of phospholipid labelled VLDL (Figure 11b) the contribution of sphingomyelin phospholipids to the ^{31}P resonance was neglected in the simulation routine. VLDL labelled with palmitic acid yielded a linewidth of 166 Hz and this is in excellent agreement with the linewidth of native VLDL (162 Hz). This result indicates that size and headgroup conformation at the surface of VLDL particles are not affected by the incorporation of fatty acids.

^2H NMR

The presence of a broad spectral component for the deuterated methylene segments at 25°C was demonstrated using [11,11,12,12-$^2H_3$]palmitic acid. Figure 27 shows the best computer fit spectrum, sum of two Lorentzian lineshapes, of VLDL containing 10 mol % [11,11,12,12-$^2H_4$]palmitic acid. The linewidth obtained for the broad component is 15.9 kHz.

The ^2H NMR spectra of [16,16,16-$^2H_3$]palmitic acid in VLDL as a function of temperature are shown in Figure 28. In addition to the signal from C^2H_3 the spectra also have a signal from residual deuterium in water,

Figure 25: Electron micrograph of VLDL containing 10 mol % [11,11,12,12-$^2H_4$]palmitic acid. Magnification = X157,000. Shown beneath the electron micrograph is a histogram depicting the size distribution for 300 particles counted. Mean diameter = 39.0±8.0 nm.

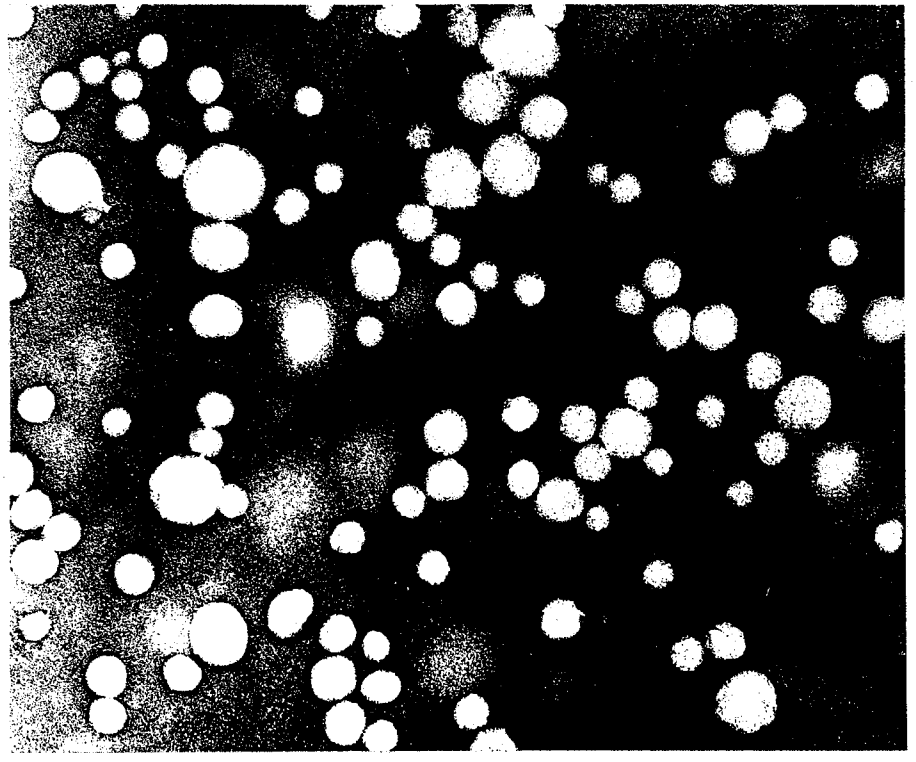

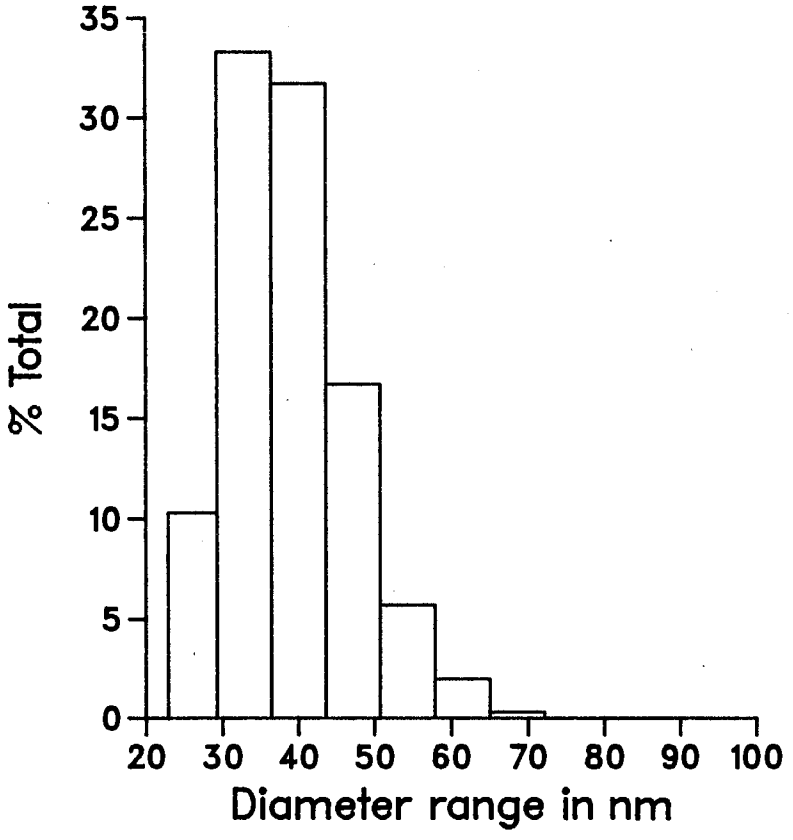
35
30
25
20
15
10
5
0
% Total
20
30
40
50
60
70
80
90
100
Diameter range in nm

Figure 26: ^{31}P NMR spectra of VLDL.

a) Native VLDL, ≃15 mg phospholipid/mL

b) VLDL plus 10.0 mol % [11,11,12,12-$^{2}H_4$]palmitic acid, ≃ 25 mg phospholipid/mL.

The spectra were simulated by an iterative least-squares fit to a Lorentzian lineshape (solid line) to the spectral datapoints (crosses). Spectral parameters: Native VLDL as described in Figure legend 11a: Labelled VLDL; pulse width = 6.0 μs (90 ° flip angle); sweep width = 10 KHz; delay between pulses = 1.7 s; number of acquisitions = 3000; delay before acquisition = 10 μs; line broadening = 5 Hz. The contribution of the sphingomyelin phospholipid (<15%) to the ^{31}P resonance was neglected in the fitting routine.

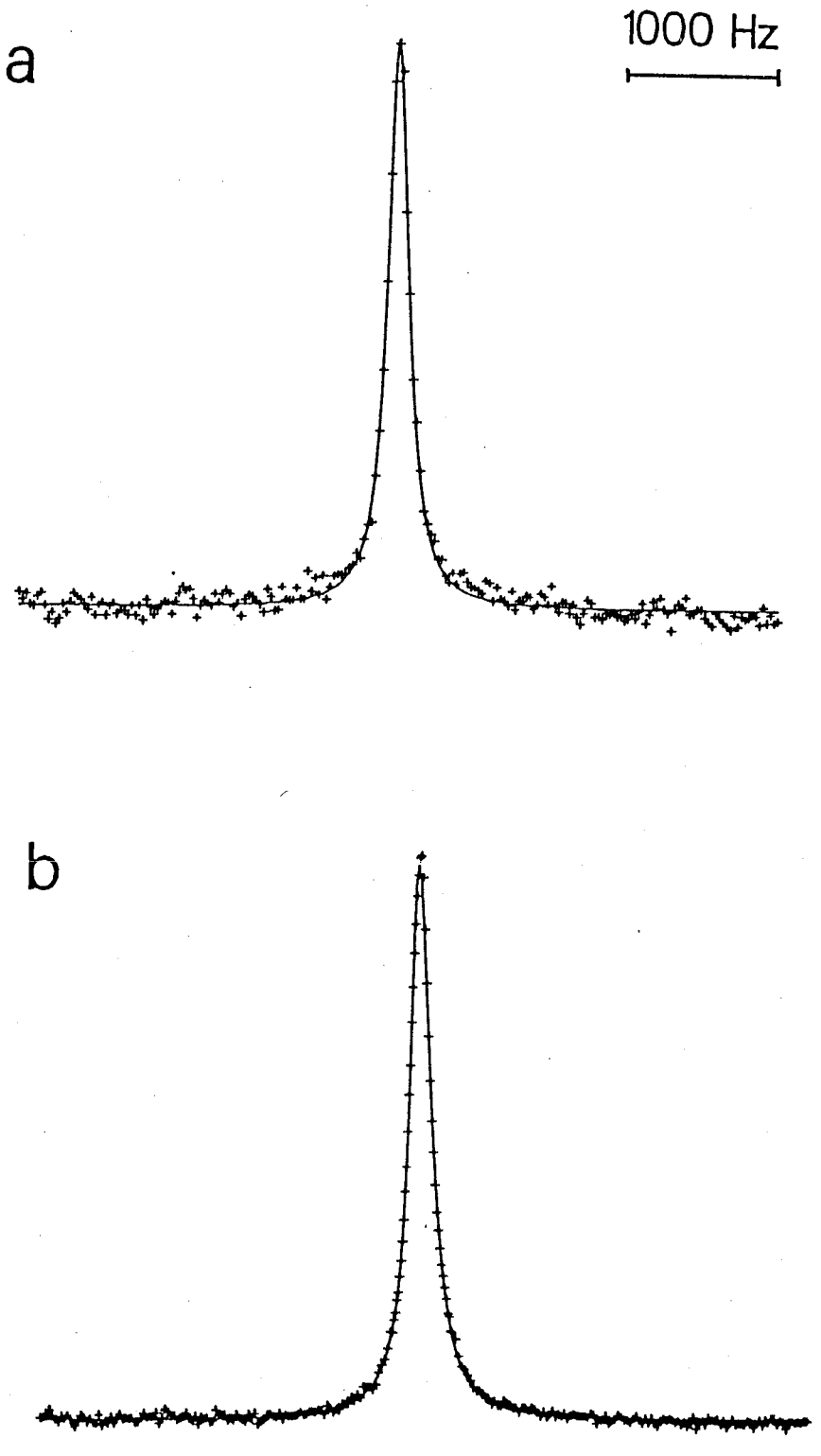
a
1000 Hz
b

Fpgure 27: ^2H NMR spectra of 10 mol % [11,11,12,12-$^2H_4$]palmitic acid in VLDL at 25°C. The spectrum is the best computer fit to the superposition of two Lorentzian lineshapes (solid line) to the spectral data points (crosses). Spectral parameters: pulse width = 6.0 μs (flip angle = 68°), sweep width = 100 KHz, delay between pulses = 0.08 s, number of acquisitions = 500,000, line broadening = 400 Hz, dataset = 4K zerofilled to 8K, delay before acquisition = 5.0 μs.

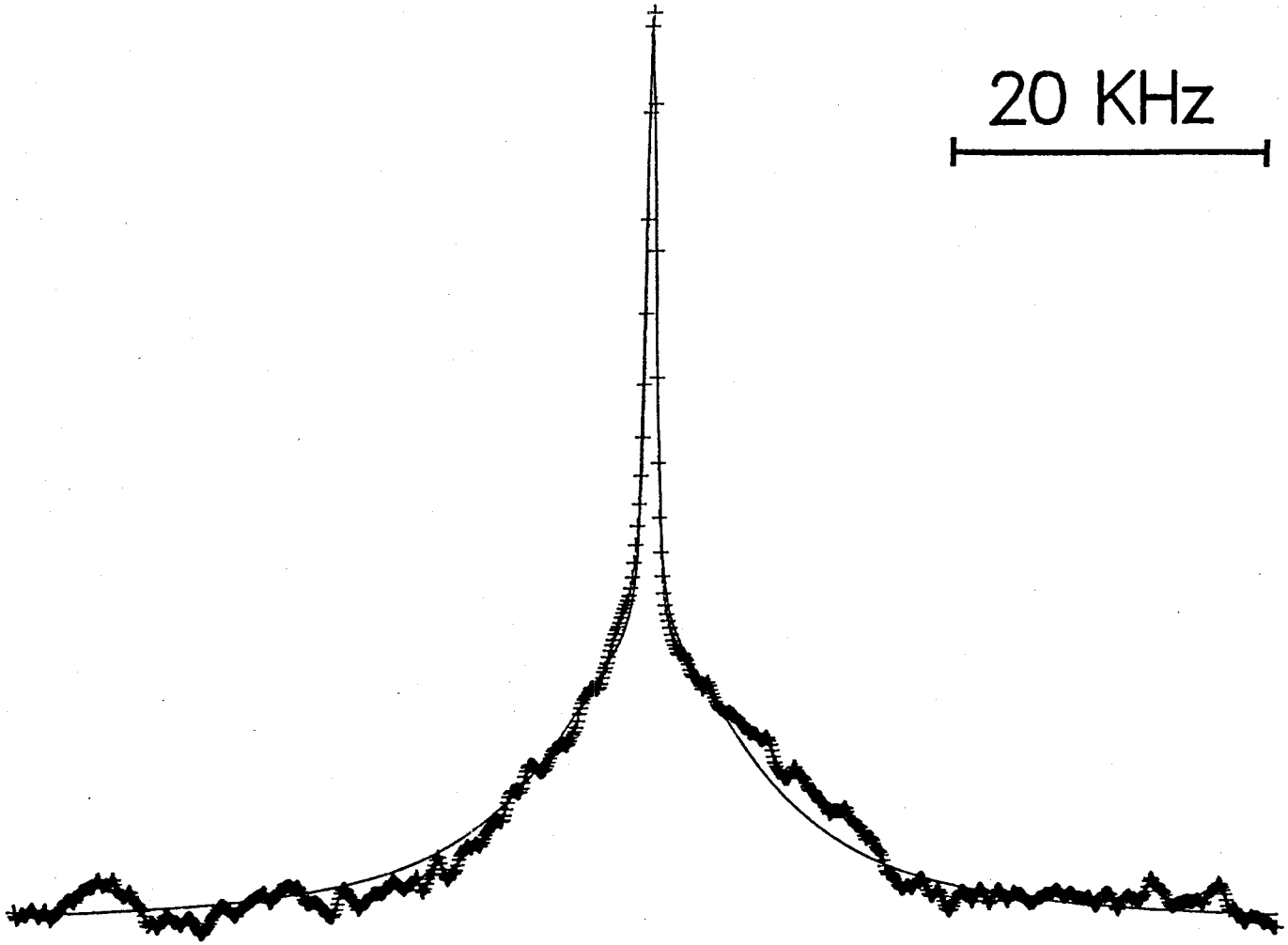
20 KHz

Table 8: ^2H NMR linewidths, $\Delta\nu_{1/2}$, of palmitic acids selectively deuterated in the methylene segments in VLDL at selected temperatures.

Deuterated position	Incorporation (Mol %)	$\Delta\nu_{1/2}$ (Hz)[a]		
		15°C	25°C	35°C
4,4	6.7	80	69	64
5,5,6,6	10.0	-	66	-
11,11,12,12	10.0	-	63	62

[a] Linewidths are accurate to ±10% and were obtained from an iterative least squares fit to the [$^2H_2$]palmitic acid and [$^2H_4$]palmitic acid resonance.

≃150 Hz downfield. A Lorentzian lineshape fit to both peaks is shown in Figures 28a, 28c and 28e. Visual inspection of these spectra reveals the poorness of the fit particularly at the top of the C^2H_3 signal. The linewidth of 234 Hz (15°C) and 148 Hz (25°C) were obtained from these simulations. These linewidths are considerably larger then the methylene segments whose average linewidths were 80 Hz (15°C) and 66 Hz (25°C) (Table 8). In order to account for the intensity of the C^2H_3 signal, the spectra were simulated as described earlier for [16,16,16-$^2H_3$]PC in VLDL. Figures 28b and 28d show the best fit for sum of two Lorentzian lineshapes for the C^2H_3 signal. The linewidths of [16,16,16-$^2H_3$]PA as a function of temperature are given in Table 9. The linewidths obtained from these simulations were 81 Hz (narrow component) and 679 Hz (broad component) at 15°C, and 59 Hz (narrow component) and 300 Hz (broad component) at 25°C.

Figure 28: ^2H NMR of VLDL containing [16,16,16-$^2H_3$]palmitic acids in VLDL as a function of temperature. The spectra were simulated by an iterative least-squares fit to a Lorentzian lineshape (a, c and e) and a superposition of two Lorentzian lineshapes (b and d) for the C^2H_3 signal. Spectral parameters: pulse width = 6.0 μs (flip angle = 68°), sweep width = 50 KHz, delay between pulses = 0.6 s, line broadening = 10 Hz, number of acquisitions = 20,000 (a and c) and 60,000 (b), dataset = 4K zerofilled to 8K, delay before acquisition = 10 μs.

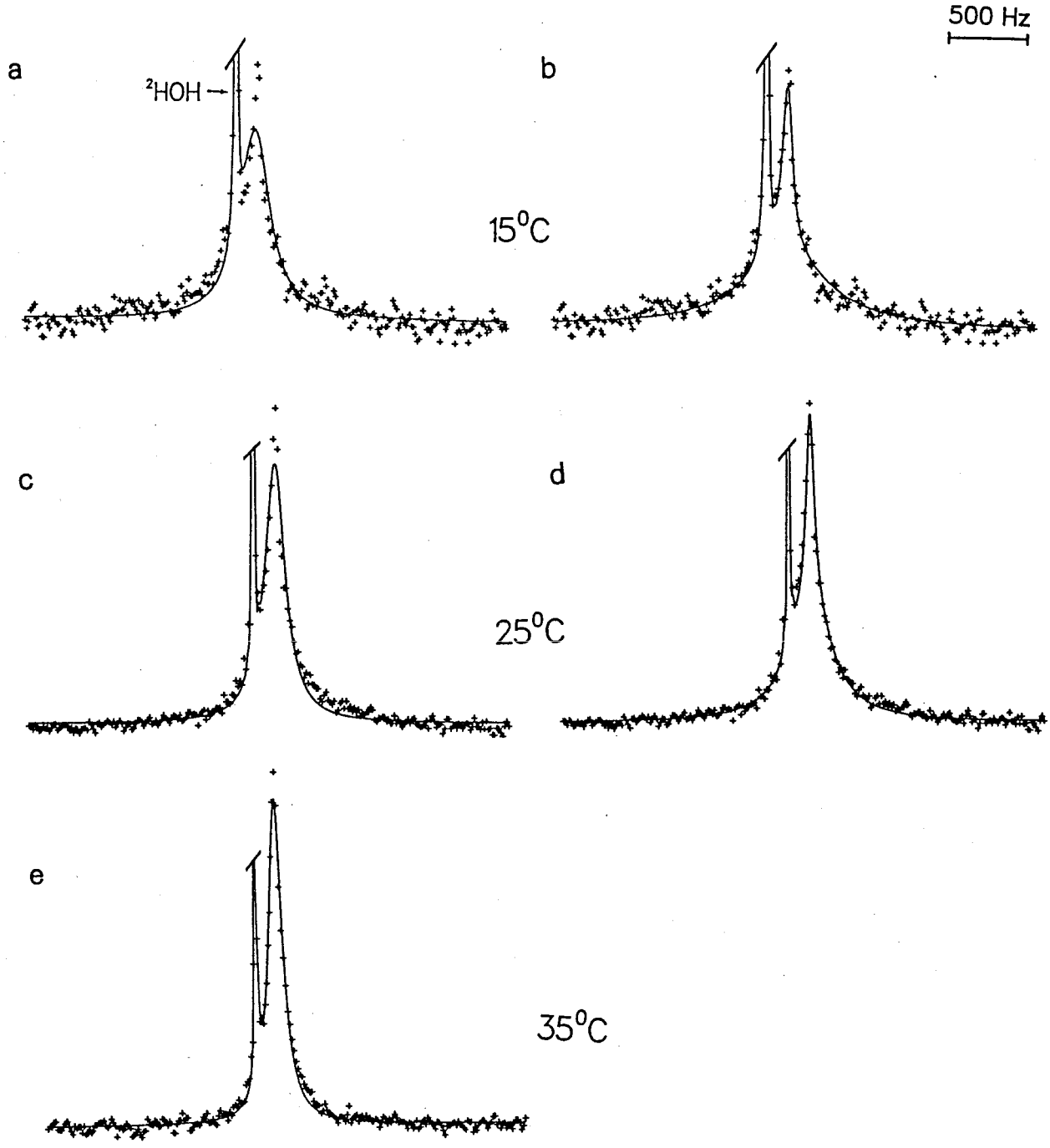
500 Hz
a
^{2}HOH
b
15°C
c
d
25°C
e
35°C

The relative intensities of the two spectral components were estimated as described by Stone, (1973) and are given in Table 9. At 35°C the superposition of two Lorentzian lineshapes proved difficult to fit the data, and hence a Lorentzian lineshape simulation was used. A linewidth of 106 Hz was obtained from this fit and represents an average of two domains.

We were unable to measure the linewidth of [5,5,6,6-$^2H_4$]palmitic acid in VLDL at 25°C because the spectrum was highly distorted in lineshape. However, upon increasing the temperature to 40°C the linewidth of the broad spectral components decreased considerably. Figure 29 shows the ^2H NMR spectra of [5,5,6,6-$^2H_4$]palmitic acid and [11,11,12,12-$^2H_4$]palmitic acid in VLDL at 40°C. Both spectra were simulated by the superposition of two Lorentzian lineshapes, one for the narrow component and one for the broad component. In both cases, the signal from the residual deuterium in water was small and ignored in the simulation (see inset spectra). The linewidth of the broad spectral components of [5,5,6,6-$^2H_4$]palmitic acid and [11,11,12,12-$^2H_4$]palmitic acid at 40°C were 4307 and 2157 Hz, respectively (Table 10).

The inset spectra in Figure 29 are the horizontal expansions of the narrow signals of [$^2H_2$]palmitic acid and residual deuterium in water, ≃150 Hz downfield. These spectra were acquired at narrow sweepwidths and a Lorentzian lineshape provided an excellent fit for the [^2H]palmitic acid resonance. The linewidth and the relative ratio of the spectral components determined as described by Stone (1973) are given in Table 10.

The segmental reorientational rate of [4,4-$^2H_2$]palmitic acid and [16,16,16-$^2H_3$]palmitic acid in VLDL was investigated by measuring the

Table 9: ^2H NMR linewidths, $\Delta\nu_{1/2}$, of [16,16,16-$^2H_3$]palmitic acid in VLDL as a function of temperature.

Temperature °C	$\Delta\nu_{1/2}$ (Hz)[a]	$\Delta\nu_{1/2}$ (Hz)[b] Broad/Narrow	Ratio of [c] Broad/Narrow
15	234	679/81	77.2±3.2/22.8±2.3
25	148	300/59	76.4±1.8/23.6±1.5
35	106	-	-

Linewidths are accurate to ±10% and were obtained from an iterative least squares fit to the [$^2H_3$]palmitic acid resonance.

[a] Linewidths were obtained from a Lorentzian lineshape fit to the C$^2H_3$ resonance.

[b] Linewidths were obtained from the superposition of two Lorentzian lineshape fit to the C$^2H_3$ resonance.

[c] The ratio of the spectral components were calculated as described by Stone, 1973. The error in the values were calculated from the standard deviations obtained from the iterative least-squares fit.

spin-lattice relaxation time, T_1. Figures 30a and 30b show the plots of $\log(A_\infty - A_\tau)$ versus τ. The solid line is a weighted least-squares fit to the experimental data points. T_1 values of 20±1 and 185±18 ms were obtained for [4,4-$^2H_2$]palmitic acid and [16,16,16-$^2H_3$]palmitic acid in VLDL at 25°C respectively.

The T_1 value of [4,4-$^2H_2$]palmitic acid is approximately 50% smaller than that of [4,4-$^2H_2$]PC in VLDL. However, it is comparable to [4,4-$^2H_2$]palmitic acid in LDL (Treleaven. 1985) and HDLs (Parmar. 1985). [16,16,16-$^2H_3$]palmitic acid has a long T_1 which is within the experimental

Figure 29: ^2H NMR spectra of selectively deuterated [5,5,6,6-$^2H_4$]palmitic acid and [11,11,12,12-$^2H_4$]palmitic acid in VLDL at 40°C. The spectra were simulated by an iterative least squares fit to a superposition of two Lorentzian lineshapes. Spectral parameters: [5,5,6,6-$^2H_4$]palmitic acid; sweep width = ±50 KHz; delay between pulses = 0.15 s; number of acquisitions = 500,000; line broadening = 20 Hz; Spectral parameters of the inset: sweep width = ±10 KHz; delay between pulses = 0.25 s; number of acquisitions = 340,100; line broadening = 5.0 Hz; Spectral parameter: [11,11,12,12-$^2H_4$]palmitic acid; sweep width = ±50 KHz; delay between pulses = 0.15 s; number of acquisitions = 540,000; line broadening = 20 Hz; Spectral parameters of the inset: sweep width = ±10 KHz; delay between pulses = 0.25 s; number of acquisitions = 316,100; line broadening = 5.0 Hz; In all cases, the pulse width = 6.5 μs (flip angle = 73°); delay before acquisition = 10 μs; dataset = 4K.

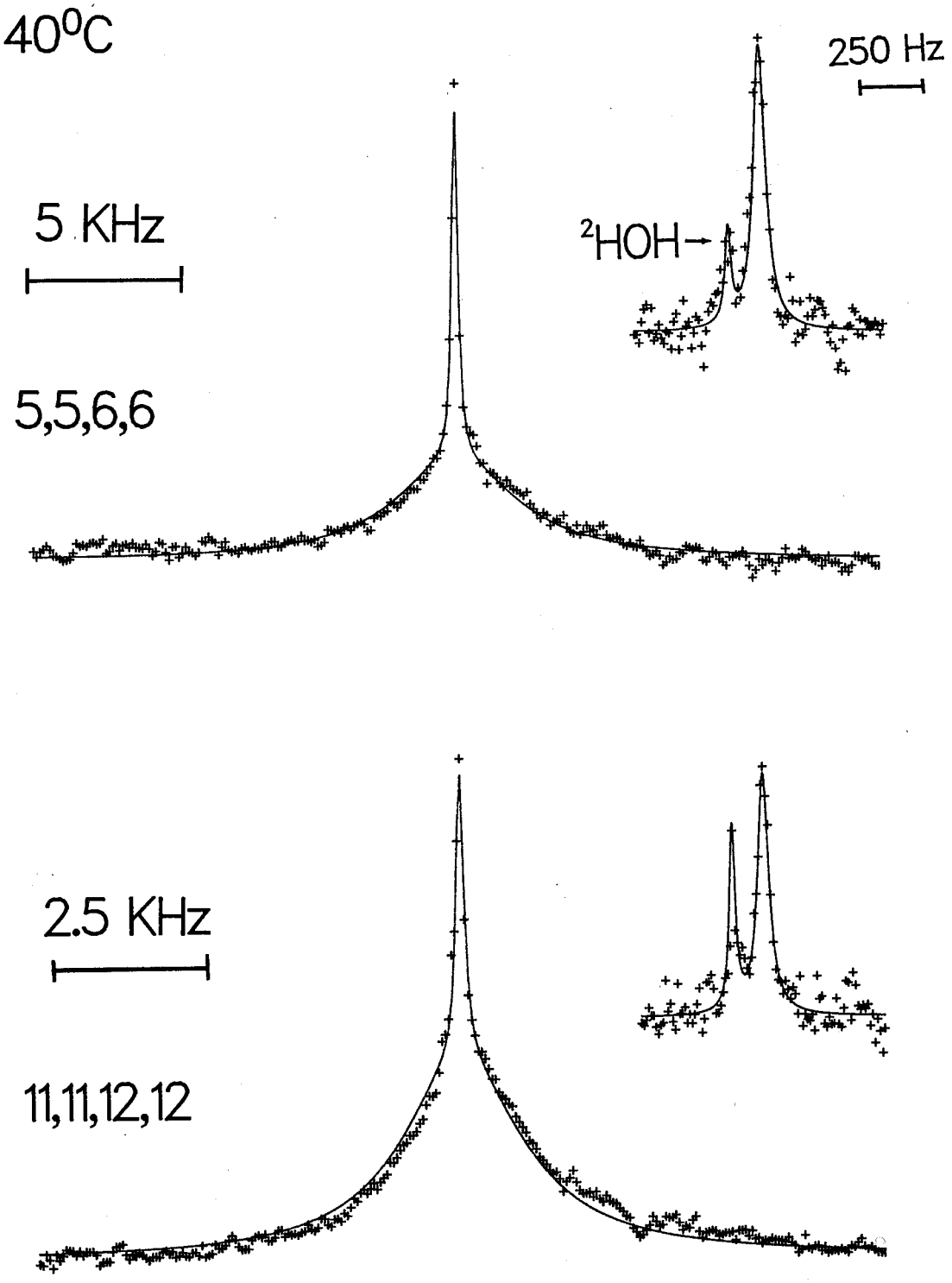
40°C
250 Hz
5 KHz
^{2}HOH
5,5,6,6
2.5 KHz
11,11,12,12

Table 10: ^2H NMR linewidths, $\Delta\nu_{1/2}$, of selectively deuterated palmitic acid in VLDL at 40°C.

Deuterated position	Incorporation (Mol %)	$\Delta\nu_{1/2}$ (Hz)[a]	Broad/Narrow[c] component
5,5,6,6	10.0	59 (4307[b])	85.1±0.6/14.9±0.5
11,11,12,12	10.0	56 (2157)	91.2±0.4/8.8±0.6

[a] Linewidths are accurate to ±10% and were obtained from an iterative least squares fit to the [$^2H_4$]palmitic acid resonance.
[b] Linewidths of broad spectral components.
[c] The ratio of the spectral components were calculated as described by Stone, 1973. The error in the values were calculated from the standard deviations obtained from the iterative least-squares fit.

error of [16,16,16-$^2H_3$]PC in VLDL (see Table 7), and agrees with the values found in LDL and HDLs.

Selectively Deuterated Palmitic Acid in Treated VLDL

The method of incorporating specifically deuterated phospholipids into VLDL from vesicles using partially purified transfer protein was demonstrated to cause cleavage of apoprotein B-100 into two smaller fragments (see Figures 13 and 14). This appears to be due to some protease contaminant present in the crude enzyme preparation. Protease inhibitors, PMSF and DIFP, were employed without success (see section IVa on the

Figure 30: Plots of ^2H NMR spin-lattice relaxation times of selectively deuterated palmitic acid in VLDL at 25°C. T_1's were measured by inversion recovery method, $(180^\circ-\tau-90^\circ-T)_n$. The plots are of $\log(A_\infty - A_\tau)$ vs τ, where τ is in seconds. The solid line is the weighted least squares fit to the experimental data points. Spectral parameters: [4,4-$^2H_2$]palmitic acid (a) and [16,16,16-$^2H_3$]palmitic acid (b); pulse width = 8.0 μs (90° flip angle), 16.0 μs (180° flip angle); sweep width = 20 KHz; dataset = 4 K; number of acquisitions = 40,000 (a) and 20,000 (b); τ values ranged from 0.0025-0.06 s (a) and 0.015-0.24 s (b); T = 0.2 s (a) and 1.0 s (b); delay before acquisition = 10 μs.

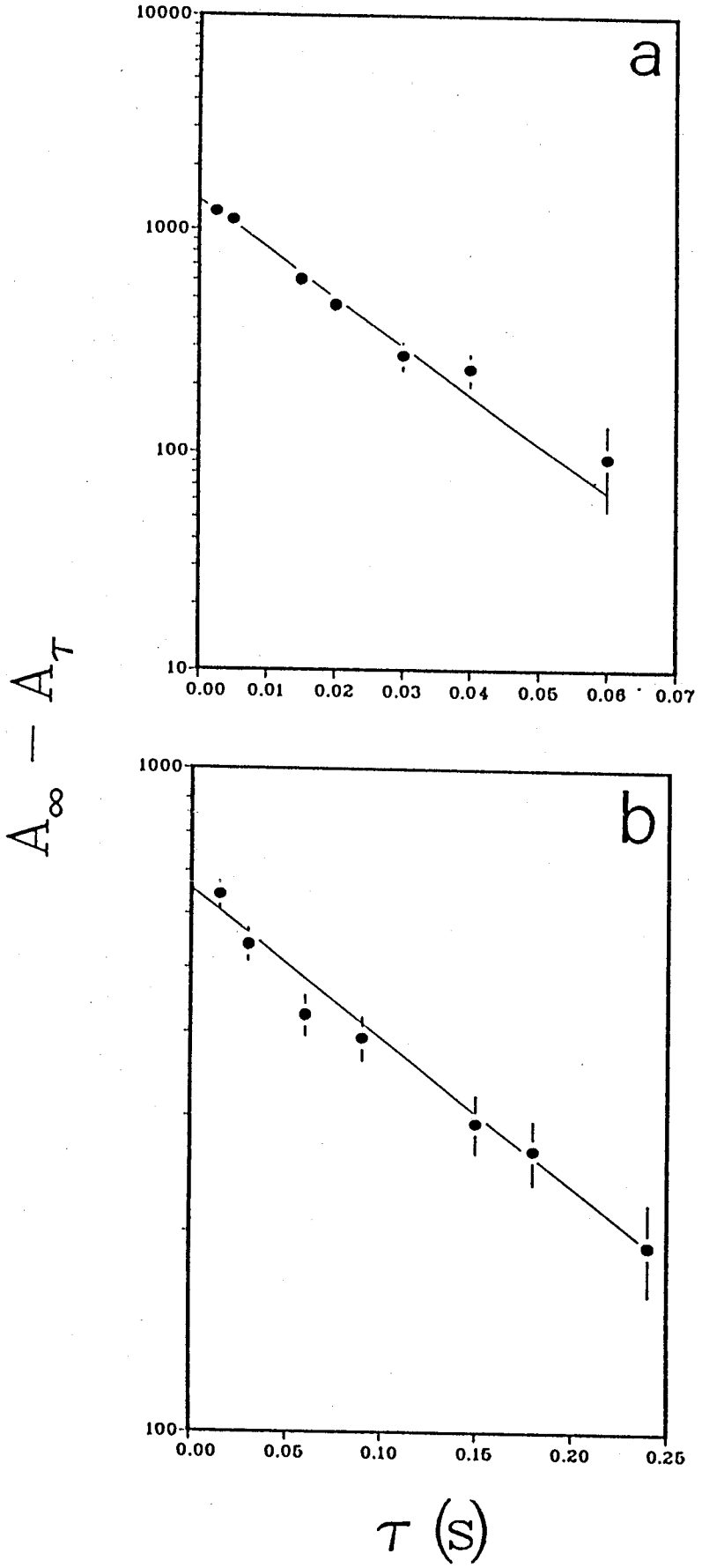
a
b
10000
1000
100
10
1000
100
0.00
0.01
0.02
0.03
0.04
0.05
0.06
0.07
0.00
0.05
0.10
0.15
0.20
0.25
$A_\infty - A_\tau$
τ (s)

inhibition studies). In order to examine whether cleavage of apo B-100 had an affect on the ^2H NMR spectra we have undertaken another study with VLDL particles that have been treated with partially purified transfer protein.

Purified VLDL was incubated with partially purified phosphatidylcholine transfer protein at 35-37°C for 90 min. Following this, VLDL was isolated by ultracentrifugation and examined by SDS-PAGE. The apoprotein B-100 was observed to be cleaved into two fragments. VLDL thus isolated is referred to as treated VLDL. Following deuterium depleted water exchanges (deuterium depleted water containing 0.15M NaCl, 2.0mM Na_2EDTA, 2.0M KBr at pH 7.4) treated VLDL was incorporated with [5,5,6,6-$^2H_4$]palmitic acid and [11,11,12,12-$^2H_4$]palmitic acid and trace amounts of [1-^{14}C]PA. Mol % incorporation of fatty acid was monitored by liquid scintillation counting (see Materials and Methods).

The effect of palmitic acid incorporation on the integrity of native VLDL and treated VLDL apoproteins was investigated by SDS-PAGE. Figure 31 show a 10 % SDS-PAGE of VLDLs containing palmitic acid. The protein bands of VLDLs containing and not containing the fatty acid are similar in all cases and thus indicate that fatty acids have no effect on the integrity of VLDL apolipoproteins.

^2H NMR spectra were acquired at 40°C since at this temperature, as seen in the previous section, both spectral components can be measured with ease. Figure 32 shows the ^2H NMR spectra of treated VLDL containing [5,5,6,6-$^2H_4$]palmitic acid or [11,11,12,12-$^2H_4$]palmitic acid at 35°C and 40°C. The spectra shown provide excellent fit to a sum of two Lorentzian lineshapes, one for the broad and one for the narrow spectral component. In both cases, the signal from the residual deuterium in water was not

Figure 31: Sodium Dodecyl Sulphate-10% polyacrylamide gel electrophoretogram of native VLDL and treated VLDL containing 10 mol % [11,11,12,12-$^2H_4$]palmitic acid. Electrophoresis was performed as described in Materials and Methods. Lane 1. 10 μl of a 3 mg/mL mixture of calibration protein standards, from top to bottom, myosin (MW 205,000), β-galactosidase (MW 116,000), phosphorylase B (MW 97,000), bovine plasma albumin (MW 66,000), egg albumin (MW 45,000), and carbonic anhydrase (MW 29,000). The standards were obtained from Sigma (MW-SDS-200 kit). Lane 2. (10 μg) protein isolated from native VLDL. Lane 3. (10 μg) protein isolated from VLDL containing palmitic acid. Lane 4. (10 μg) protein isolated from VLDL treated with transfer protein. Lane 5. (10 μg) protein isolated from VLDL treated with transfer protein containing palmitic acid.

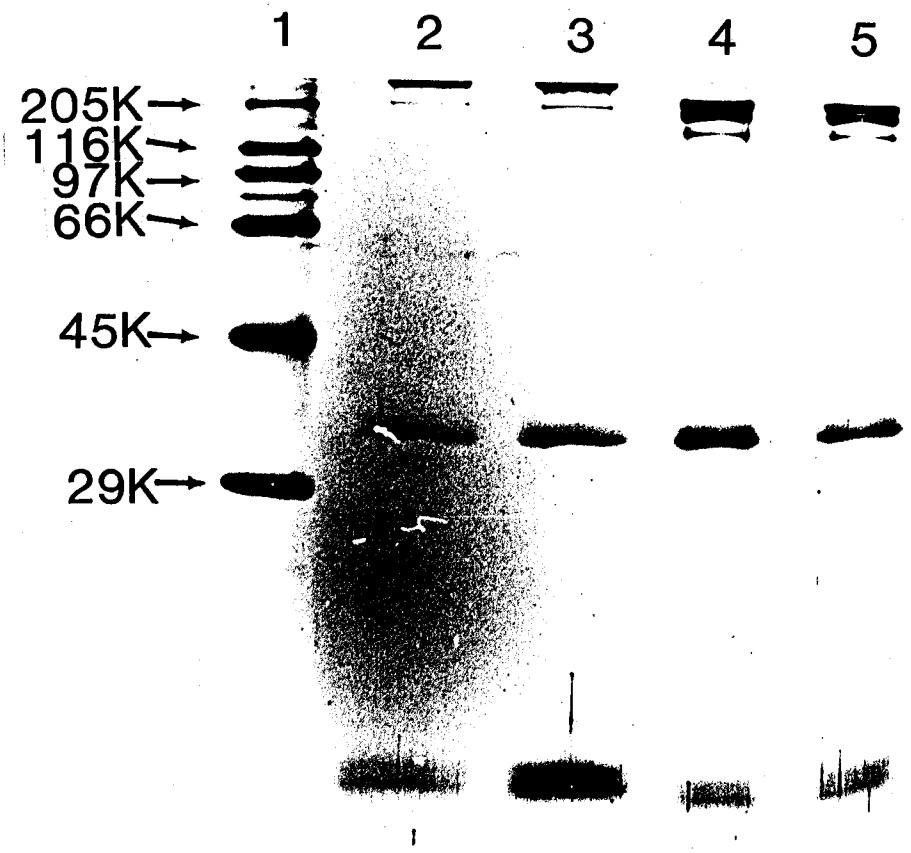
1
2
3
4
5
205K
116K
97K
66K
45K
29K

Figure 32: ^2H NMR spectra of [5,5,6,6-$^2H_4$]palmitic acid and [11,11,12,12-$^2H_4$]palmitic acid in native and treated VLDL particles at selected temperatures. The spectra were simulated by an iterative least squares fit to a superposition of two Lorentzian lineshapes. Identical spectral parameters were employed in both cases. Spectral parameter: [5,5,6,6-$^2H_4$]palmitic acid; number of acquisitions, native VLDL = 500,000, treated VLDL =492,160; plot width = 25 KHz; [11,11,12,12-$^2H_4$]palmitic acid: number of acquisitions, native VLDL = 540,000, treated VLDL = 482,090; In all cases, pulse width = 6.5 μs (flip angle =73°); sweep width = ±50 KHz; delay between pulses = 0.15 s; line broadening = 20 Hz; delay before acquisition = 10 μs; dataset = 4K.

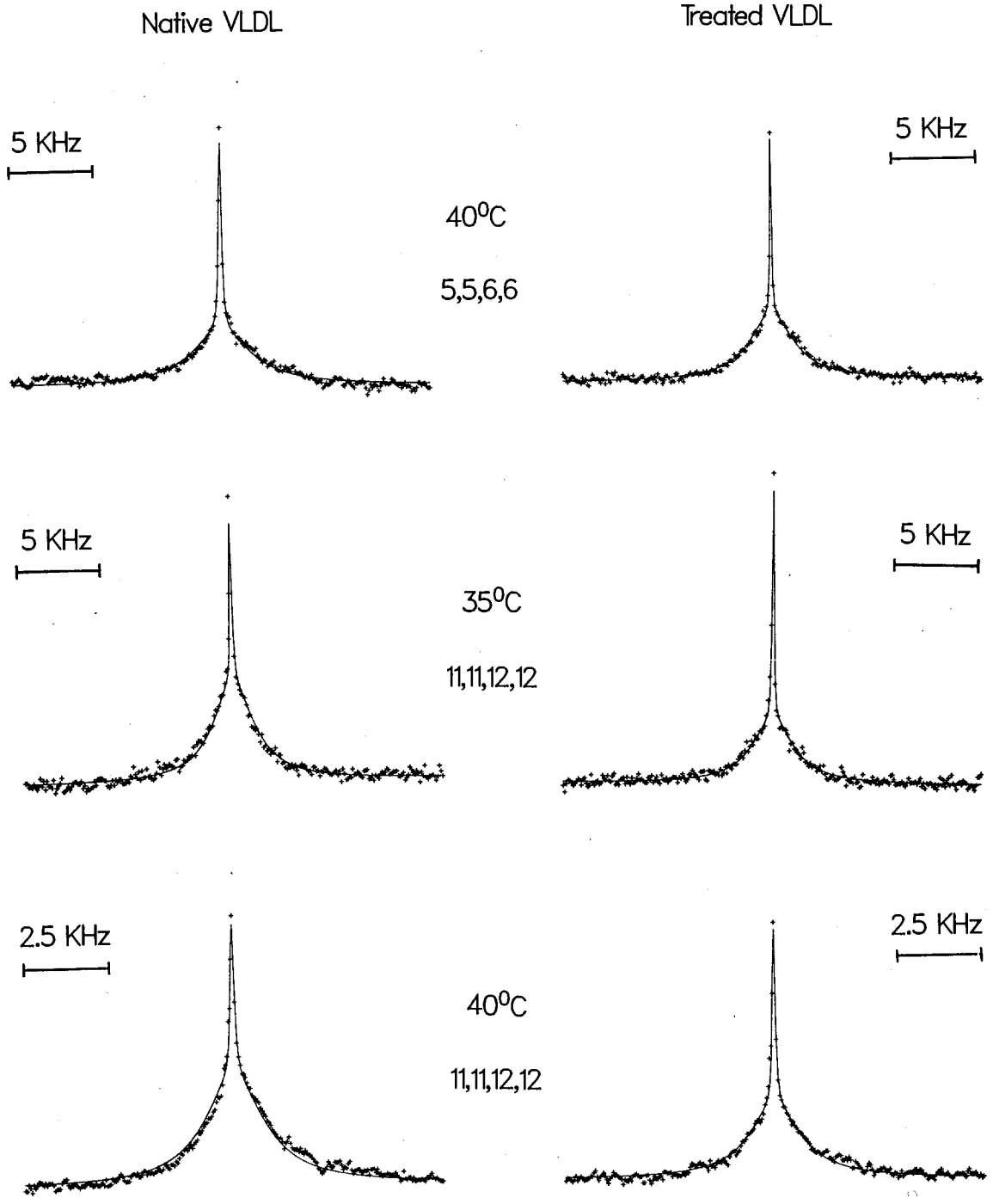
Native VLDL
Treated VLDL
5 KHz
40°C
5,5,6,6
5 KHz
5 KHz
35°C
11,11,12,12
5 KHz
2.5 KHz
40°C
11,11,12,12
2.5 KHz

significant and thus was ignored in the fitting routine. For the purposes of comparison we have also included the simulated spectra of [5,5,6,6-$^2H_4$]palmitic acid and [11,11,12,12-$^2H_4$]palmitic acid incorporated into native VLDL. The linewidths and the ratio of spectral intensities are given in Table 11.

IVc. Selectively Deuterated Phosphatidylcholines in Egg PC/TO Microemulsions

RESULTS

In recent years model systems of native lipoprotein particles have been used to gain a better understanding of lipid-lipid and lipid-protein interactions in native lipoproteins (Ginsburg *et al.*, 1984; Mims *et al.*, 1986; Atkinson 1986 and references therein; Fenske *et al.*, 1988a) Similarly, in order to understand the occurence of two phospholipid domains in the surface monolayer of VLDL we have utilized protein-free egg PC/TO microemulsions as simple models of VLDL to study the phospholipid chain order in the surface monolayer.

Egg PC/TO microemulsions, similar in size to VLDL, were prepared using egg PC/selectively deuterated PC/triolein (90:10:220, w/w) in deuterium depleted water using the method described by Tajima *et al.*, 1983 (see Materials and Methods). The preparations were examined by the shift reagent, Pr^{3+}, and were observed to be free of vesicle contamination.

The ^2H NMR spectra shown in this section were obtained by Dr. Parmar and simulated by the author. I am greatful to Dr. Parmar for allowing me to present this data.

Table 11: ^2H NMR linewidths, $\Delta\nu_{1/2}$, and intensity ratios of selectively deuterated palmitic acid in native VLDL and treated VLDL.

	Native VLDL		Treated VLDL	
Deuterated position	$\Delta\nu_{1/2}$ (Hz)[a]	Broad/Narrow component	$\Delta\nu_{1/2}$ (Hz)[a]	Broad/narrow component
5,5,6,6	4307[b]	85.1±0.6/14.9±0.4	3211[b]	91.6±0.3/8.4±0.3
11,11,12,12	2997[c]	91.6±0.3/8.4±0.4	3041[c]	86.5±0.6/13.5±0.4
11,11,12,12	2157[b]	91.2±0.4/8.8±0.6	1880[b]	88.0±0.7/12.0±1.3

[a] Linewidths are accurate to ±10% and were obtained from an iterative least squares fit to the [$^2H_4$]palmitic acid resonance.

[b] Linewidths obtained at 40°C.

[c] Linewidths obtained at 35°C.

[d] The ratio of the spectral components were calculated as described by Stone, 1973. The error in the values were calculated from the standard deviations obtained from the iterative least-squares fit.

^2H NMR spectra of selectively deuterated phosphatidylcholines in egg PC/TO microemulsions were recorded at 25°C and 40°C and are presented in Figures 33 and 34, respectively. All the spectra shown, except the [2,2-$^2H_2$]PC spectra, were simulated by a sum of two Lorentzian lineshapes, one for the broad and one for the narrow [^2H]PC spectral component. For the [2,2-$^2H_2$]PC spectra at 25°C and 40°C, a third Lorentzian lineshape was added to account for the signal arising from the residual deuterium in the water. The inset spectra shown in Figures 33 and 34 include a simulation for residual deuterium in water.

The ^2H NMR linewidths obtained from the simulated spectra together with the relative ratios of the spectral components are listed in Table 12.

In order to calculate the order parameter, S_{CD}, it is essential to know the size of the microemulsions. We have measured the size of egg PC/TO microemulsions containing [11,11,12,12-$^2H_4$]PC by EM. The electron micrograph is shown in Figure 35. The particles are heterogeneous in size and have circular morphology. The size distribution depicted beneath the electron micrograph was constructed by counting 200 particles directly from the electron micrograph negatives which were taken from different fields of measurement. The mean diameter (42.1±6.6 nm) was taken to represent the mean size of all the other microemulsions studied since the lipid composition and sonication conditions were similar in all cases.

Figure 33: ^2H NMR spectra of selectively deuterated phospholipids in egg PC/TO microemulsions at 25°C. The spectra were simulated by an iterative least squares fit to a superposition of two Lorentzian lineshapes. Spectral parameters: [2,2-$^2H_2$]PC; sweep width = 50 KHz, number of acquisitions = 100,000, delay between the pulses = 0.06 s, line broadening = 30 Hz: [11,11,12,12-$^2H_4$]PC; sweep width = 50 KHz, number of acquisitions = 160,000, delay between the pulses = 0.06 s. line broadening = 30 Hz; In both cases, pulse width = 8.0 μs (90° flip angle), dataset = 4K zerofilled to 8K, delay before acquisition = 10 μs. For the inset spectra line broadening was 5 Hz throughout.

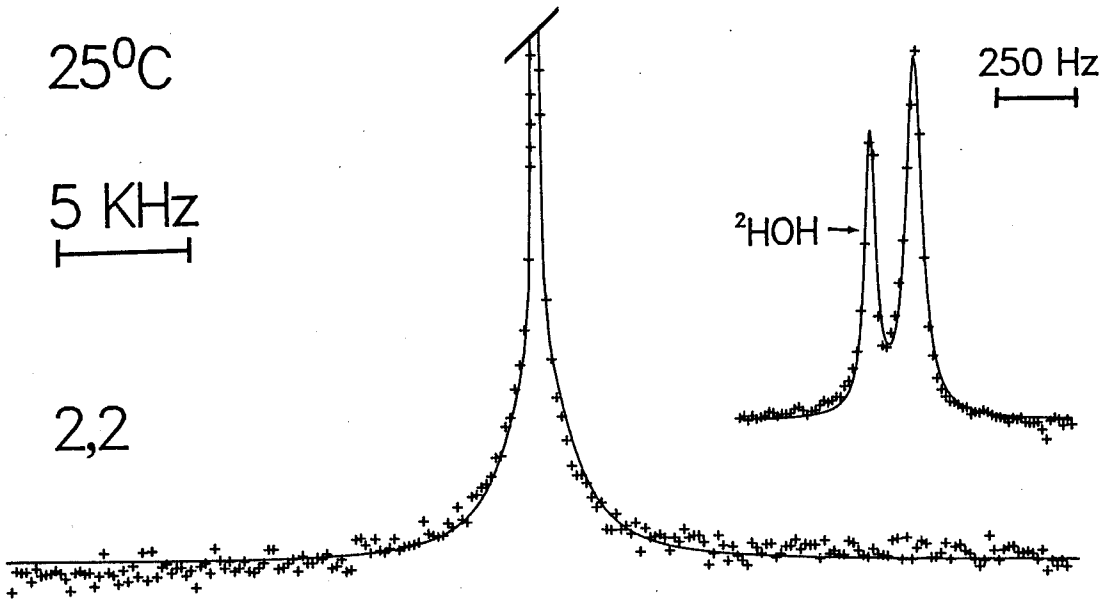
25°C
5 KHz
2,2
250 Hz
²HOH

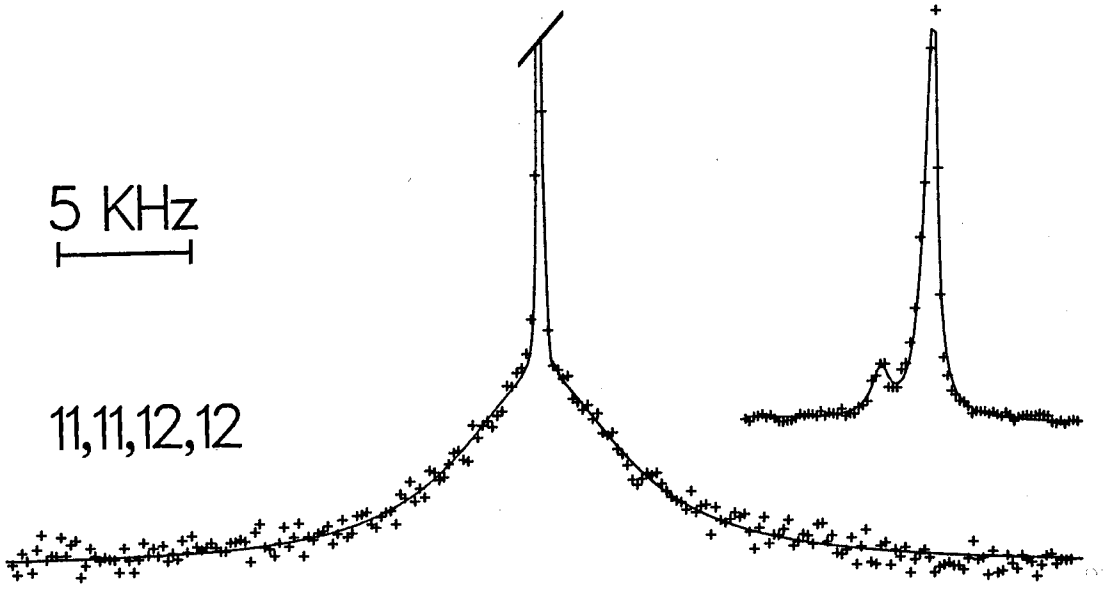
5 KHz
11,11,12,12

Figure 34: ^2H NMR spectra of selectively deuterated phospholipids in egg PC/TO microemulsions at 40°C. The spectra were simulated by an iterative least-squares fit to a superposition of two Lorentzian lineshapes. Spectral parameters: [2,2-$^2H_2$]PC; pulse width = 8.0 μs (90° flip angle), sweep width = 50 KHz, delay between pulses = 0.06 s, number of acquisitions = 175,000, line broadening = 10 Hz: [5,5,6,6-$^2H_4$]PC; pulse width = 4.5 μs (51° flip angle), sweep width = 100 KHz, delay between pulses = 0.01 s, number of acquisitions = 500,000, line broadening = 50 Hz: [11,11,12,12-$^2H_4$]PC; pulse width = 8.0 μs (90° flip angle), sweep width = 50 KHz, delay between pulses = 0.06 s, number of acquisitions = 210,000, line broadening = 30 Hz. In all cases, dataset = 4K zerofilled to 8K, delay before acquisition = 10 μs. For the inset spectra the line broadening was 5 Hz throughout.

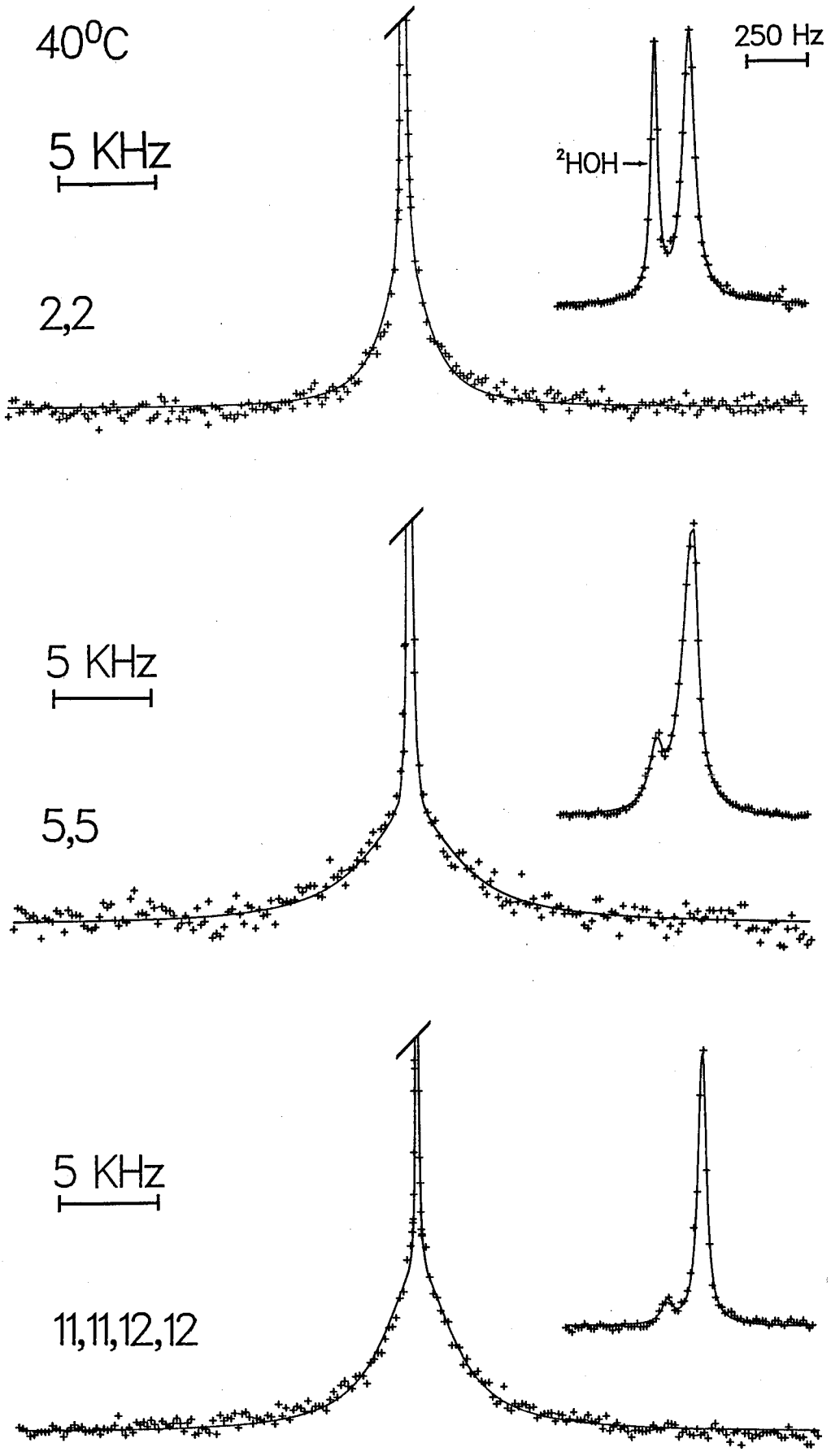
40°C
5 KHz
2,2
250 Hz
²HOH
5 KHz
5,5
5 KHz
11,11,12,12

Table 12: ^{2}H NMR linewidths, $\Delta\nu_{1/2}$, of selectively deuterated phosphatidylcholines in the egg PC/TO Microemulsions at 25°C and 40°C.

	25°C		40°C	
Acyl chain position	$\Delta\nu_{1/2}$ (Hz)[a]	Broad/Narrow[b] component	$\Delta\nu_{1/2}$ (Hz)[a]	Broad/Narrow[b] component
2,2	58 (2805[c])	79.3±0.4/20.7±0.3	55 (2795[c])	68.6±1.1/31.4±0.5
5,5	- (-[d])	-	73 (5925[c])	67.3±1.1/32.7±0.2
11,11,12,12	45 (7470[c])	88.8±0.3/11.2±0.1	39 (4190[c])	87.9±0.3/12.1±0.1

[a] The Linewidths are accurate to ±10% and were obtained from an iterative least-squares fit.

[b] The ratio of peak areas determined from the spectral linewidths and signal amplitudes as described by Stone, 1973. The error in the values were calculated from the standard deviations obtained from the iterative least-squares fit.

[c] The broad spectral component.

[d] Too broad to measure.

Figure 35: Electron micrograph of egg PC/TO microemulsion containing 10 mol % [11,11,12,12-$^2H_4$]PC. Magnification = X171,000. Shown beneath the electron micrograph is a histogram depicting the size distribution for 200 particles counted. Mean diameter = 42.1±6.6 nm.

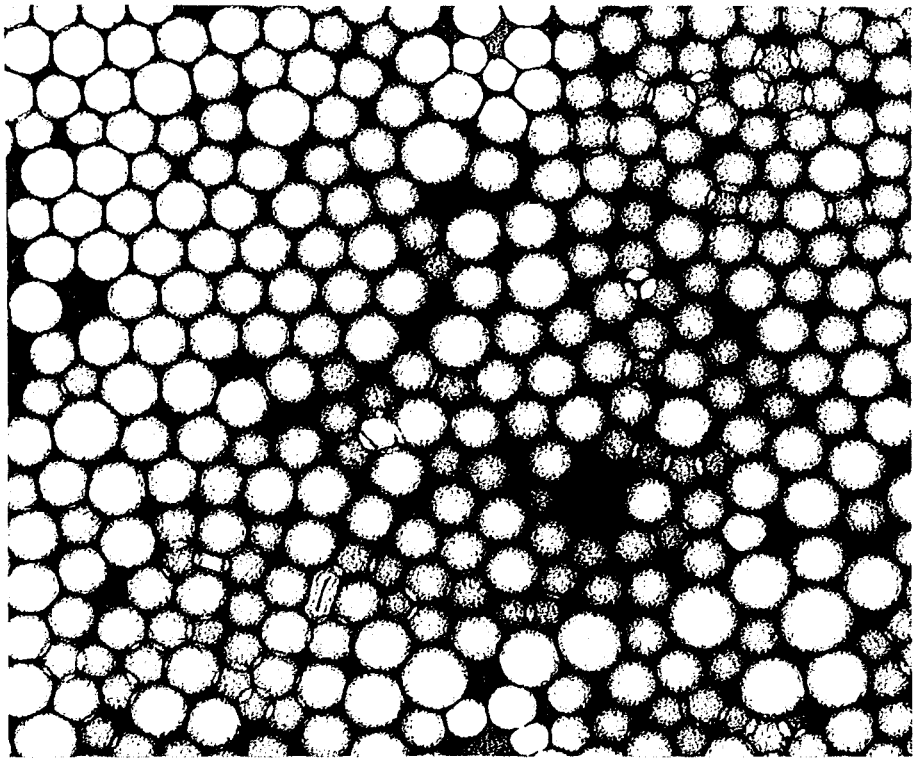

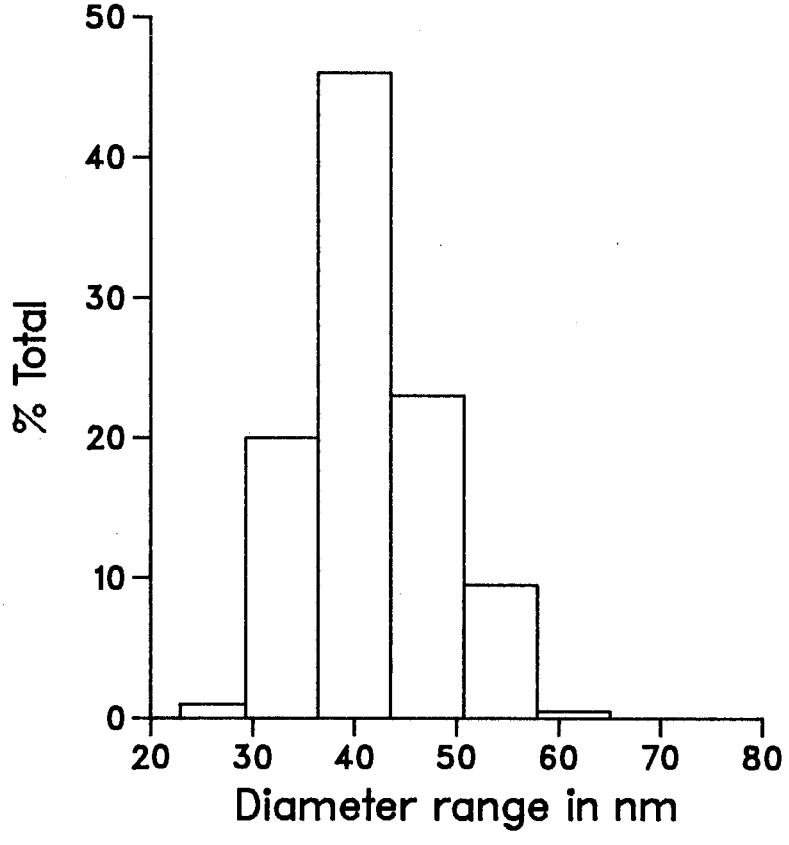
50
40
30
20
10
0
% Total
20
30
40
50
60
70
80
Diameter range in nm

DISCUSSION

Selectively deuterated phosphatidylcholines

Selectively deuterated PCs were prepared from egg yolk lysoPC and a selectively deuterated palmitic acid or, in the case of [7,7-$^2H_2$]PC, stearic acid, inserted at the *sn*-2 position. The *sn*-1 position of egg yolk lysoPC contains 66-68% palmitoyl, 24-26% stearoyl and 6-10% other acyl chains. Hence, the behaviour (DSC, thin layer chromatography, etc) of selectively deuterated PCs is very much like that of DPPC (Thewalt *et al.*, 1985). We have incorporated selectively deuterated phospholipids from vesicles into VLDL using the method described by Jackson *et al.*, 1979. In our method, we have utilized partially purified phosphatidylcholine transfer protein, isolated from bovine liver, to transfer phospholipids from vesicles to VLDL. In an effort to assess what effects, if any, the phospholipid incorporation would have on VLDL structure we have analysed the chemical composition, the size, and the apoprotein composition of the particles. From the chemical composition data presented in Table 3 a slight change in the ratio of PL/TG and CE/TG following the incorporation of phospholipids was observed. The PL/TG ratio had increased from ≃0.40 to ≃0.43 and the CE/TG ratio had decreased from ≃0.22 to ≃0.19 while the C/TG and Pr/TG ratios had essentially remained unchanged. The slight variation in the chemical composition does not appear to affect the size of the particles. This was demonstrated by EM and QELS. The mean particle size measured by EM was 42.8±10.3 nm and 41.5±9.3 nm for the native VLDL and PC labelled VLDL, respectively. The mean size determined by QELS was also very similar to those established by EM. With mean sizes of 42.2±11.5 nm and 42.1±18.1 nm for native VLDL and PC labelled VLDL, respectively, being

obtained. ^{31}P NMR spectroscopy which has been used to monitor the size and the headgroup conformation of lipoprotein particles (Treleaven, 1985; Parmar, 1985) was also utilized to examine the VLDL particles following the incorporation of phospholipids. The ^{31}P NMR linewidths of native VLDL (162 Hz) and PC labelled VLDL (173 Hz) were within experimental error, suggesting that both the particles were of equal size, a result in agreement with the size determinations by EM and QELS. Taken together, the results of chemical composition analysis, size measurements, and ^{31}P NMR spectroscopy indicate that the method utilized to incorporate selectively deuterated phospholipids does not alter the particle size and structure in a significant manner.

Since we were employing vesicles as vehicles to exchange phospholipids into VLDL particles, we considered the possibility that the apoproteins of VLDL may migrate to vesicles during the incubation procedure. This consideration is justified because it is known that apoproteins, with the exception of apo B-100, are able to exchange between lipoprotein particles during their metabolism (Schaefer *et al.*, 1978; Dolphin, 1985; Atkinson *et al.*, 1986). To examine this, we have analysed the composition of apoproteins associated with VLDL particles before and after the incorporation of phospholipids by SDS-PAGE. Upon performing gel electrophoresis (see Figures 13 and 14) it was observed that the largest apolipoprotein, apo B-100, had cleaved into two smaller polypeptide fragments of MW 240,000 and 200,000, and further, there was also a minor loss of apo E (13%) (Table 4). The cleaved apo B-100 fragments remained associated with the VLDL particles. In spite of using the protease inhibitors PMSF and DIFP in the incubation mixture we were unable to prevent the cleavage of apo B-100. The loss of apo E in PC labelled

particles could have resulted from ultracentrifugation since DDW exchanges were performed by ultracentrifugation (see Materials and Methods). Similar observations have been made with rat VLDL where ultracentrifugation at density 1.21 g/mL was shown to cause a minor depletion of apo E (Fainaru *et al.*, 1977). In order to prevent this, an alternative method involving millipore immersible-CX ultrafilters was employed. Treleaven (1985) and Parmar (1985) have successfully used millipore immersible-CX ultrafilters to perform DDW exchanges of labelled LDL and HDL particles. However, in our case, this method proved unsuccessful since VLDL particles were observed to aggregate and fuse to form irregularly shaped particles. A ^{31}P NMR study of these particles produced axially symmetric powder spectra similar to those observed for phospholipid bilayers. This was in contrast to the ^{31}P NMR spectra of VLDL particles, following untracentrifugation, which gave Lorentzian lineshaped spectra (cf. Figure 11). Therefore, the best and the most efficient method to perform DDW exchanges proved to be by ultracentrifugation.

In order to assess whether fragmentation of apo B-100 would have an effect on the biological activity of VLDL particles a study was conducted to examine the synthesis of cholesteryl [^{3}H]oleate in cultured macrophage cells. From Figure 17 it was observed that, although there was a slight increase in the synthesis of cholesteryl [^{3}H]oleate in macrophages with transfer protein treated VLDL particles at the saturating concentration of 100 μg/mL VLDL protein, all the VLDL samples studied, native VLDL, transfer protein treated VLDL and palmitic acid labelled VLDL, were observed to yield similar profiles of cholesteryl [^{3}H]oleate synthesis, demonstrating that the stimulated synthesis of cholesteryl [^{3}H]oleate in the macrophages was similar for all VLDL particles and proceeded through a saturable

pathway.

In conclusion, the use of partially purified phosphatidylcholine transfer protein has allowed us to incorporate large amounts of selectively deuterated phospholipids (3 mol % to 17 mol %) in relatively short incubation periods (1-1.5 hr) with minimal structural alterations in the size, shape, chemical composition and biological activity of the particles. Furthermore, the SDS-PAGE gels (Figure 13) demonstrated that the proteins present in the crude enzyme preparation did not associate with VLDL during the incubation procedure. The exchange procedure did not alter the biological function of VLDL particles in spite of the cleavage of apo B-100.

Since phospholipids are surface-active molecules possessing a zwitterion we expect them to associate with the surface monolayer of VLDL particles. Support for this conclusion has come from the fluorescent quenching studies of Johnson *et al.*, 1980. Using a fluorescent phospholipid, dansyl phosphatidylethanolamine, the authors have demonstrated its association with the surface monolayer and not with the apolar triglyceride core of VLDL particles. The intimate association of selectively deuterated phospholipids with VLDL particles was confirmed by gel exclusion chromatography on a Sepharose 4B column (Figure 8). All the radioactivity ($\simeq$96%) was observed to coelute with the VLDL protein peak, thus demonstrating that no small protein-free structures were formed during the incorporation procedure.

The ^2H NMR spectra of PCs selectively deuterated in the C2-, C4-, C5,6-, C7-, and C11,12- segments of the *sn*-2 palmitoyl chain in VLDL particles (Figure 18 and 19) yielded extremely narrow signals having

linewidths of ≃80 Hz at 15°C, 60-69 Hz at 25°C, and ≃62 Hz at 35°C (see Table 5). While the ^2H NMR spectra of the C16-position (Figure 20a) simulated by a Lorentzian lineshape yielded a linewidth of 147 Hz at 25°C. Compared to the bilayer studies it is very surprising that the C^2H_2 linewidths are less then the terminal C^2H_3. The narrow linewidths observed in VLDL (Table 5) are much smaller than the linewidths observed in other lipoprotein particles which are smaller in size. Furthermore, comparison with similar sized unilamellar vesicles (Parmar *et al.*, 1984) reveals that VLDL has smaller linewidths for all the methylene positions. The variation of linewidths with position of deuteration in HDLs and vesicles showed a plateau of constant linewidths spanning from C2- to C5,6-positions and decreasing to a minimum at the terminal methyl position (Parmar *et al.*, 1984; Parmar *et al.*, 1983; Parmar, 1985). This is in contrast to the results obtained in VLDL where a plateau was not observed.

Examination of the Lorentzian lineshape simulation of C16-positions in VLDL revealed that the simulation had failed to account for the C^2H_3 resonance intensity particularly at the top of the signal, this is clearly apparent in the spectra acquired at 15°C and 20°C (Figures 20a and 20c). In order to account for the missing intensity, it was necessary to simulate the C^2H_3 resonance with the sum of two Lorentzian lineshapes, one for the narrow component and one for the broad component. The linewidths of the narrow component were 79 Hz and 73 Hz, while those of the broad component were 613 Hz and 256 Hz at 15°C and 25°C, respectively (Table 6). This indicates there are two significantly different phospholipid domains in the surface monolayer of VLDL. Since the methylene position should also exhibit two spectral components, and only a single narrow component was observed, it was suspected that signal arising from the methylene segments was too

broad to be detected, possibly due to the spectral conditions employed and to the insufficient signal to noise. In order to demonstrate the presence of a much broader spectral component, [$^2H_{31}$]PC was incorporated into VLDL. [$^2H_{31}$]PC contains more disordered methylenes (C12 to C15) which are expected to yield smaller linewidths than those in the plateau region. This was indeed observed as shown in Figure 21. Mean linewidths of 20 kHz at 25°C, and 5.3 kHz at 40°C were measured for a broad component in addition to the narrow signal seen earlier.

Selectively deuterated palmitic acids

The method of incorporating phospholipids into VLDL using partially purified phosphatidylcholine transfer protein resulted in the cleavage of apo B-100 into two smaller fragments (see Figures 13 and 14). In spite of using protease inhibitors, PMSF and DIFP, in the incubation mixture the cleavage of apo B-100 could not be prevented. Such a cleavage may alter the phospholipid packing and the protein-lipid interactions at the surface monolayer of VLDL. Therefore, we have incorporated selectively deuterated palmitic acid into VLDL to monitor the phospholipid acyl chain organization and dynamics. The method of incorporating palmitic acid into VLDL resembles that described by Wassall *et al.* (1982). The method essentially involves the incubation of VLDL particles with a thin film of fatty acid coated on the flask container (see Materials and Methods). This method is least perturbing and hence is not expected to cleave the apoprotein in VLDL particles, in particular apo B-100. This was demonstrated by SDS-PAGE (see Figure 31) where no fragmentation of apo B-100 was observed. Fatty acids have been used to investigate the molecular organization of phospholipid acyl chains in biological membranes (Davis, 1979), model membranes

(Stockton *et al.*, 1976; Pauls *et al.*, 1983), and lipoprotein membranes (Wassall *et al.*, 1982; Parmar, 1985; Treleaven, 1985). A detailed study by Pauls *et al.*, (1983) showed that the carbon-deuterium order parameter of deuterated palmitic acids, up to 20 mol %, in DPPC multilamellar liposomes yielded values which were within 10% of those obtained from the deuterated phospholipids themselves. Similar findings have also been made with PCs and palmitic acids incorporated into HDL_2 particles (Parmar, 1985) where both molecules were shown to yield similar order parameter values.

Based on the amphiphilic nature of the fatty acids we expect them to intercalate into the VLDL monolayer. We favour a conformation in which the carbonyl groups are anchored towards the aqueous phase and the fatty acyl chains are aligned parallel to the apolar phospholipid chains. Support for this conclusion has come from the fluorescent quenching studies of parinaric acid (Schroeder *et al.*, 1979b, Sklar *et al.*, 1980). Both *cis* and *trans* isomers of parinaric acid were shown to locate in the surface monolayer of the particles (Sklar *et al.*, 1980). The intimate association of selectively deuterated fatty acids with VLDL particles was confirmed on a Sepharose 4B column containing [1-^{14}C]palmitic acid (Figure 24). All the radioactivity (93%) was observed to coelute with the VLDL protein peak, suggesting that no protein-free structures were formed during the incorporation procedure.

The effects of fatty acid incorporation on the particle size was examined by EM, QELS, and ^{31}P NMR spectroscopy. These techniques have shown that the size of VLDL particles essentially remained the same as those found for the native VLDL particles following the incorporation of fatty acids. For instance, the mean size measured by EM was 38.8±7.3 nm and

39.0±8.0 nm for the native VLDL and palmitic acid labelled VLDL, respectively. Similarly, the ^{31}P NMR study of the respective particles yielded spectra whose linewidths were within experimental error of each other and therefore indicated that both particles had similar size. Similar conclusions have also been made from ^{31}P NMR studies of LDL (Treleaven, 1985) and HDLs (Parmar, 1985) incorporated with selectively deuterated fatty acids.

^{2}H NMR spectra of selectively deuterated palmitic acids in VLDL are presented in Figures 27,28 and 29. The computer fit necessitated a double Lorentzian lineshape simulation of a broad and narrow resonance signals in Figures 27,28 and 29. The extremely narrow signals had linewidths of 80 Hz at 15°C, 63-69 Hz at 25°C, and 62-64 Hz at 35°C (Table 8). The narrow linewidths for all the positions are similar in size to that found when PC was incorporated. The linewidth of the broad [11,11,12,12-$^{2}H_4$]palmitic acid resonance was 15.9 kHz at 25°C and 2157 Hz at 40°C, while that of the [5,5,6,6-$^{2}H_4$]palmitic acid was 4307 Hz at 40°C. We were unable to measure the broad component of [5,5,6,6-$^{2}H_4$]palmitic acid at 25°C. The ^{2}H NMR spectra of [16,16,16-$^{2}H_3$]palmitic acid, presented in Figure 28, shows that a Lorentzian lineshape simulation failed to account the $C^{2}H_3$ intensity and yielded broader linewidths compared to those obtained for methylene segments (narrow component) (see Table 8). However, upon simulating the $C^{2}H_3$ resonance with the superposition of two Lorentzian lineshapes, linewidths of 81 and 59 (narrow component) and 679 and 300 (broad component) at 15 and 25°C, respectively, were obtained. Similar results were also obtained with [16,16,16-$^{2}H_3$]PC. This result demonstrates that cleavage of apo B-100 had no effect on the organization of phospholipids, at least at the C16 position. Since the spectra of $C^{2}H_2$ segments of PC

also showed narrow linewidths similar to those observed with palmitic acid it may further be suggested that fragmention of apo B-100 has no effect on the organization of PC acyl chains in the less ordered domain.

In an effort to assess whether fragmentation of apo B would effect the organization PC acyl chains in the high order domain, [5,5,6,6-$^2H_4$]palmitic acid and [11,11,12,12-$^2H_4$]palmitic acid were incorporated into VLDL particles that had been treated with partially purified transfer protein. At 40°C, the ^2H NMR linewidths of [5,5,6,6-$^2H_4$]palmitic acid and [11,11,12,12-$^2H_4$]palmitic acid were within ≃25% and ≃13%, respectively, of those found in the native VLDL particles. At 35°C, the linewidths of [11,11,12,12-$^2H_4$]palmitic acid in both particles were essentially the same (Table 11). Although, the linewidths of the C11,12-position in both particles can be considered to be within the experimental error, the linewidths of the C5,6-positions in treated VLDL are slightly smaller than those obtained in native VLDL. The variation of the linewidths between the two particles cannot be attributed to the size differences since the measured mean sizes were similar. This linewidth is marginally larger than the bounds of uncertainty and we hasten to point out this accounts for a calculated uncertainty in S_{CD} of 14% (see below).

Thus, the ^2H NMR studies with selectively deuterated PCs and selectively deuterated palmitic acid provide evidence for the presence of two significantly different phospholipid domains in the amphiphilic monolayer of VLDL (Figures 20, 27, 28 and 29, Tables 6, 9 and 10). Furthermore, if exchange occurs between the two domains it must be slow on the ^2H NMR time scale since, if the exchange rate were fast then a single broad signal representing an average order in the two domains would be

observed.

Calculation of order parameters, S_{CD}

In order to calculate the segmental order parameter, S_{CD}, for the PCs and palmitic acid in VLDL, it is imperative that the effective correlation time, τ_e, for the isotropic motions of the particle are known. Examination of equation 17 reveals that τ_e has contributions from particle tumbling, τ_r, and lateral diffusion, τ_d. The former was calculated from the Stokes-Einstein equation in which the solvent viscosity, particle radius and temperature are required. In the case of τ_d, the knowledge of particle radius and lateral diffusion coefficient of phospholipid molecules across the VLDL surface are required. In our calculations, we have taken the mean diameters determined from EM for VLDL particles containing selectively deuterated phospholipids (41.5 nm) and selectively deuterated palmitic acids (39.0 nm), solvent viscosity of 0.8711 cP (25°C) and 0.6822 cP (40°C) of 0.15 M NaCl, 2.0 mM Na_2EDTA, 2.0 M KBr in DDW at pH 7.4. Using these values, τ_r of 7.9 X 10^{-6} s at 25°C for PC labelled VLDL and 6.6 X 10^{-6} s at 25°C, and 4.9 X 10^{-6} s at 40°C for palmitic acid-labelled VLDL were obtained. In these calculations we have assumed the mean size of VLDL particles to be independent of temperature. This assumption is valid since a recent study with rat VLDL has shown no evidence that the mean size of particles had changed upon heating the particles to 58°C (Bennett-Clark *et al.*, 1982). The contribution to τ_e from τ_d was evaluated by measuring the lateral diffusion coefficient of phospholipid molecules across the VLDL surface monolayer by ^{31}P NMR spectroscopy using the method described by Cullis (1976) (see section V). Using the lateral diffusion coefficient values of (9.1±1.0) X 10^{-9} cm^2/s at 25°C and (1.2±0.2) X 10^{-8} cm^2/s at

40°C, we have calculated a τ_e of 7.2 X 10^{-6} s for PC labelled VLDL at 25°C. For the palmitic acid-labelled VLDL particles values of 6.0 X 10^{-6} s at 25°C, and 4.5 X 10^{-6} s at 40°C were found.

The absolute order parameter values of the selectively deuterated phospholipids and palmitic acids in VLDL were calculated using equation 22 and the ^{2}H NMR linewidths given in Tables 5, 6, 8, 9, 10 and 11. In the calculations the contributions from other slow motions, such as reorientations of the entire acyl chains also referred to as "rigid stick motions" (Petersen and Chan, 1977), which contribute to line narrowing, have not been considered. Hence, the S_{CD} values reported are of upper limit. The S_{CD} values calculated are listed in Table 13 and 14.

Further confidence in the calculated S_{CD} values of the broad spectral component was obtained by analysing the ^{2}H NMR spectra of [5,5,6,6-$^2H_4$]palmitic acid and [11,11,12,12-$^2H_4$]palmitic acid at 40°C as descibed by Parmar *et al.* (1984). In their analysis, the spectra are simulated by superLorentzian lineshapes which are statistically weighted in intensity according to the size distribution of the particles determined from electron microscopy and with the assumption that all particles within a size range have identical S_{CD} values. Theoretical lineshapes were obtained according to the following equation (Parmer *et al.*, 1984)

$$S(\nu) = A\sum_{i=1}^{n} \frac{F_i \bar{R}_i^2}{W_i} \frac{1}{1 + (4\nu^2/W_i^2)} \qquad (32)$$

where F_i is the fraction of VLDL particles in the size category i, and W_i is the linewidth (equation 22) for the ith size. The term $\bar{R}_i^2$ compensates for the fact that large VLDL particles have a greater number of phospholipid molecules and the term A is a scaling factor. The amplitude of

Table 13: Order parameters, S_{CD}, of selectively deuterated phosphatidylcholines in VLDL at various temperatures.

	Temperature (°C)				
Deuterated position	15[a]	20[b]	25[c]	30[d]	35[e]
$N(C^2H_3)_3$	-	-	0.010	-	-
2,2-	0.015	-	0.013	-	0.016
4,4-	0.015	-	0.013	-	0.016
5,5,6,6-	-	-	0.013	-	-
7,7-	-	-	0.014[f]	-	-
11,11,12,12-	-	-	0.015	-	-
16,16,16-	0.015 (0.042)[g]	0.016 (0.042)	0.015 (0.029)	0.019	-

[a] Based upon τ_e = 8.3 X 10^{-6} s. In the calculation of τ_e at 15°C, 20°C, 30°C and 35°C the lateral diffusion coefficient value of 9.1 X 10^{-9} cm^2/s was used.
[b] Based upon τ_e = 7.8 X 10^{-6} s.
[c] Based upon τ_e = 7.2 X 10^{-6} s.
[d] Based upon τ_e = 6.5 X 10^{-6} s.
[e] Based upon τ_e = 6.1 X 10^{-6} s.
[f] In this calculation a T_1 value of 33 ms was assumed.
[g] The values in parenthesis refer to the broad spectral component.

the broad component to which superLorentzian lineshapes were constructed was that obtained from the Lorentzian lineshape simulation of the respective spectra. Plots of varying S_{CD} values, generally ranging between 0.05 to 0.2 in steps of 0.01 units were constructed to this amplitude

Table 14: Order parameters, S_{CD}, of selectively deuterated palmitic acids in VLDL at the indicated temperatures.

	Temperature (°C)			
Deuterated position	15[a]	25[b]	35[c]	40[d]
4,4	0.017	0.015	0.015	-
5,5,6,6	-	0.014[e](-[f])[g]	-	0.018 (0.15)
11,11,12,12	-	0.016 (0.25)	0.017 (0.12)	0.017 (0.11)
16,16,16	0.017 (0.049)	0.015 (0.035)	0.023	-

[a] Based upon $\tau_e = 7.0 \times 10^{-6}$ s. In the calculation of τ_e at 15°C, and 35°C the lateral diffusion coefficient value of 9.1×10^{-9} cm²/s was used.
[b] Based upon $\tau_e = 6.2 \times 10^{-6}$ s
[c] Based upon $\tau_e = 5.1 \times 10^{-6}$ s
[d] Based upon $\tau_e = 5.0 \times 10^{-6}$ s
[e] In this calculation a T_1 value of 21 ms was assumed.
[f] Too broad to measure.
[g] The values in parenthesis refer to the broad spectral component.

using the VLDL sizes determined from the electron micrograph (Figure 25). The statistical weighting was performed for seven VLDL size categories, VLDL size in nm with the fraction of total F_i in the parenthesis, are given in the legend of Figure 36. Figure 36 shows the simulated spectra of [5,5,6,6-$^2H_4$]palmitic acid and [11,11,12,12-$^2H_4$]palmitic acid in VLDL, at 40°C. The solid line represents the best fit for the S_{CD} values of 0.16 and 0.12, respectively. These order parameter values were found to be <5%

Figure 36: Deuterium NMR spectrum of approximately 10 mol % [5,5,6,6-$^2H_4$]palmitic acid (a) and [11,11,12,12-$^2H_4$]palmitic acid (b) in VLDL at 40°C. The solid line represents the best visual fit to a superposition of Lorentzian lineshapes to a broad spectral component by the order parameter S_{CD} of 0.16 (a) and 0.12 (b). VLDL radii, in nm, with fraction of total F_i given in the parenthesis, determined from negative staining electron micrographs are 12.86(0.10), 16.43(0.33), 20.00(0.37), 23.57(0.17), 27.15(0.06), 30.72(0.02) and 34.29(0.003).

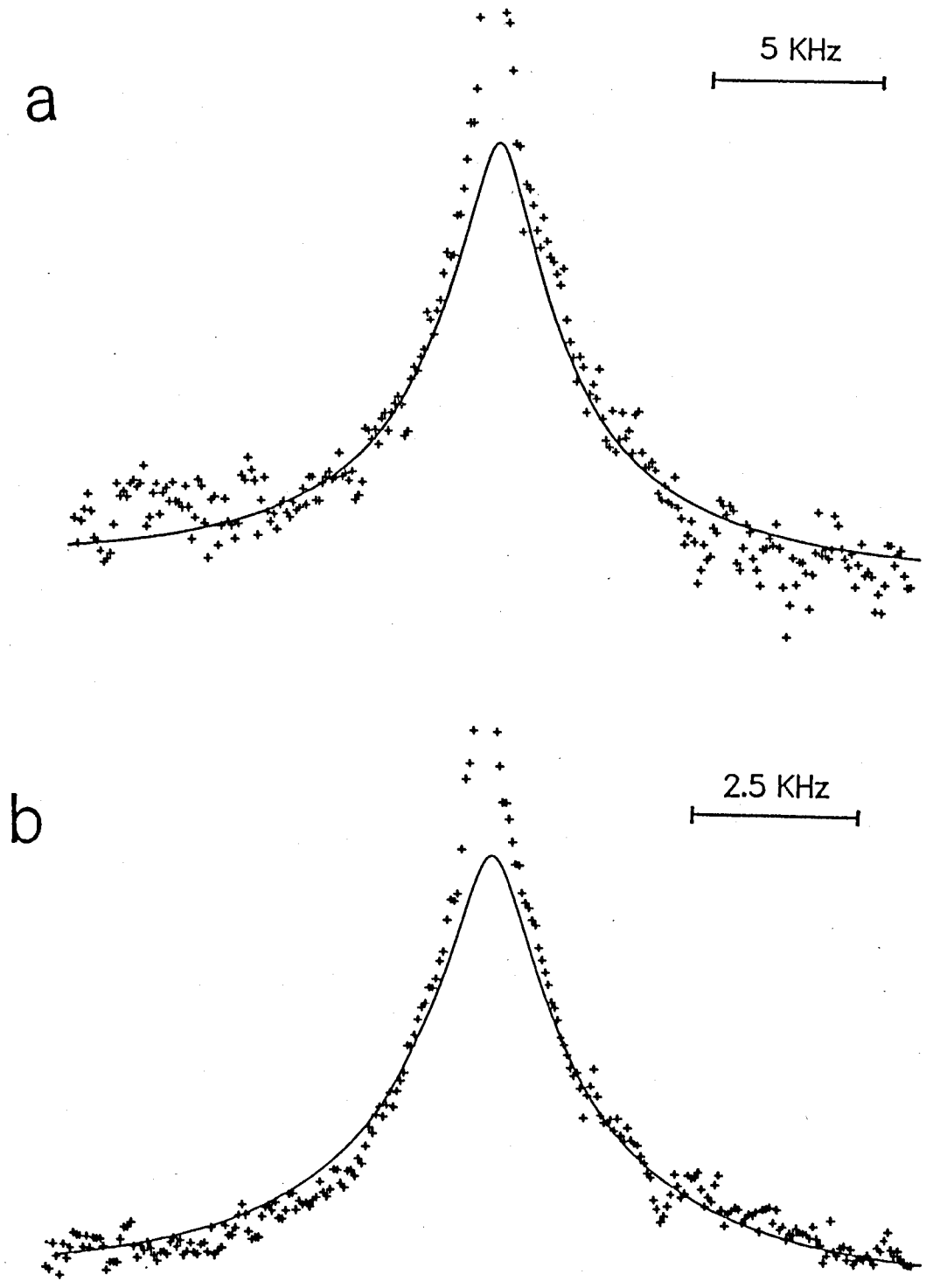
a
5 KHz
b
2.5 KHz

for [5,5,6,6-$^2H_4$]palmitic acid and <12% higher for [11,11,12,12-$^2H_4$]palmitic acid than the Lorentzian estimates, hence, the S_{CD} values obtained from equation 22 are reported (Table 13 and 14).

In the less ordered domain of VLDL, the order parameters obtained with PCs and palmitic acids, are essentially constant over the entire acyl chain length. For example, at 25°C, the S_{CD} values range between 0.013-0.016 for PCs from C2-C16 and 0.014-0.016 for palmitic acid from C4-C16. The S_{CD} values are ≃4-5 times lower than those measured by Treleaven (1985) for the less ordered domain in LDL and ≃5-8 times smaller than those measured by Parmar *et al.*, (1984) in unilamellar vesicles composed of egg PC/SPM (85:15).

The S_{CD} of the more ordered domain obtained with [11,11,12,12-$^2H_4$]palmitic acid in VLDL is in good agreement to those found in LDL, HDL_2 and HDL_3 (Table 15). Whereas, it is ≃3.6 times and ≃1.5 times higher than those found in egg PC/SPM vesicles (85:15) and egg PC liposomes, respectively, and is in good agreement with the ESR order parameter measured by 12-doxylstearate in human VLDL at 21°C ($S_{ESR} = 2S_{CD}$ = 0.488-0.578) (Morrisett *et al.*, 1977b).

The S_{CD} values of the C16-positions in VLDL, 0.029 (obtained with PC) and 0.035 (obtained with palmitic acid) (see Tables 13 and 14, respectively), are slightly higher than those found in egg PC/SPM vesicles, egg PC multilamellar liposomes and LDL, and slightly less than those found in HDL_2, and HDL_3 (see Table 15).

The S_{CD} values of the less ordered domain show no order variation with temperature unlike the more ordered domain. For instance, the S_{CD} value of

Table 15: Order parameter of phospholipid bilayers and lipoproteins.

Deuterated position	LDL[a]	HDL_2[b]	HDL_3[b]	vesicles[c]	liposomes[b]
2,2-	0.31 (0.06)	0.27	0.38	0.08	0.12
4,4-	0.34 (0.06)	0.30	0.38	0.09	0.24
5,5,6,6-	0.28 (0.07)	0.30	0.37	0.10	0.23
11,11,12,12-	0.24 (0.05)	0.23	0.23	0.07	0.17
16,16,16-	0.02	0.04	0.05	0.015	0.02

[a] Obtained from Treleaven. 1985.

[b] Obtained from Parmar. 1985.

[c] Obtained from Parmar *et al.*, 1984.

The values in parenthesis refer to the narrow spectral component.

the C11,12-position decreased from 0.25 to 0.11 upon raising the temperature from 25 to 40°C (Table 14). The change in the linewidth with temperature cannot be attributed to the change in the effective correlation time as a consequence of reduced solvent viscosity. Assuming that the S_{CD} value of [11,11,12,12-$^2H_4$]palmitic acid (0.25) remains unchanged at 40°C, then the expected linewidth as a result of the change in the effective correlation time can be evaluated using equation 22. Using a lateral diffusion coefficient value of 1.2 X 10^{-8} cm^2/s, particle diameter of 39.0 nm, and viscosity η = 0.6822 cP we calculate a linewidth of 11.8 kHz. The calculated linewidth is clearly much larger than the experimental linewidth of 2157 Hz, suggesting that the change in the S_{CD} value with temperature results as a consequence of the ordering effects and not because of the change in the effective correlation time. A similar change of the order

parameter with temperature has been reported with nitroxide spin label in VLDL (Morrisett *et al.*, (1977b). For instance, the ESR order parameter reported with 12-doxyl-stearate in VLDL, obtained from individuals on an *ad lib* diet, decreased from 0.488-0.578 to 0.158-0.178 upon raising the temperature from 21°C to 36°C. The order parameter is also observed to change in HDL_2 with temperature (Parmar, 1985). The S_{CD} value of C11,12-position changes from 0.21 to 0.15 upon increasing the temperature from 25°C to 40°C. The change in S_{CD} value is not as large as seen in VLDL.

A recent study by Ekman *et al.* (1988) has shown that, at pH 7.4, approximately 8% of oleic acid was dissolved into the triglyceride core of egg PC/TO microemulsions while the remainder was associated with phospholipid monolayer. Thus, it is possible that the narrow component (low order domain) we observe in the ^2H NMR spectra of fatty acids may result from the partitioning of fatty acids into the more fluid triglyceride core. The liquid crystalline state of the triglycerides in VLDL core has been demonstrated in VLDL particles isolated from fasting humans (Deckelbaum *et al.*, 1977; Hamilton *et al.*, 1976). A DSC study by Deckelbaum *et al.* (1977) of such particles showed no thermal transition between 10°C and 60°C, and a ^{13}C NMR study on a similar type of particle also showed that triglycerides were in their liquid state at about 35°C (Hamilton *et al.*, 1976). Similar observations have also been made in rabbit VLDL, here a ^1H NMR study has shown that the core lipids were disordered over the temperature range of 20°C to 50°C (Kroon and Seidenberg. 1982). The physical state of triglycerides in the VLDL core can be affected by the fatty acid composition of dietary fats such that they may exhibit thermal transitions at higher temperatures (Small *et al.*, 1980; Bennett-Clark *et al.*, 1982; and

Hamilton *et al.*, 1983).

In contrast to the above, the cholesteryl ester cores of LDL (Treleaven *et al.*, 1986), reconstituted HDL particle (Parmar *et al.*, 1984), and model lipoproteins composed of cholesteryl oleate, DMPC and apo E (Mims *et al.*, 1986) are highly ordered. For instance, ^2H NMR studies by Treleaven *et al.* (1986) have shown the acyl chain order to be 0.2 at the C2' position and 0.12 at the C5' position. S_{CD} values of C2'-C6' of cholesteryl palmitate in the core of reconstituted HDL particles prepared from apo HDL/egg PC yielded S_{CD} of $\simeq$0.35 (Parmar *et al.*, 1983). The presence of triglycerides in LDL particles was suggested to be responsible for lowering the S_{CD} values compared to those observed in reconstituted HDL particles. Therefore, if fatty acid are dissolved in the core they will reflect the core order, which is expected to be lower than that found for LDL core.

The fact that PC also show a region of low order domain argues against the solublization of PCs into the core. Ekman *et al.* (1988) have also demonstrated that phospholipid molecules are associated with the surface monolayer and not with the core of egg PC/TO miroemulsions. Further agreement of the surface location of PCs comes from the fluorescent quenching studies where phospholipids were shown to partition into the amphiphilic monolayer rather than into the hydrophobic triglyceride core of VLDL particles (Johnson *et al.*, 1980). Therefore, we believe that both PCs and palmitic acids are similarly located in the surface monolayer of VLDL.

It may be argued that the low order domain in the surface monolayer of VLDL is due to the presence of apoproteins. The hydrocarbon chains of the phospholipid molecules surrounding the apoproteins may become disordered through lipid-protein interactions. A small fraction of VLDL phospholipids

(3-10%) are known to intimately associate with apoproteins (Reman *et al.*, 1978). A number of techniques have been utilized to investigate the lipid-protein interactions. Optical rotatory dispersion studies of apo B have shown a decrease in the α-helical content by $\simeq$27% following the removal of phospholipids (Scanu *et al.*, 1968; Scanu *et al.*, 1968). In addition to the presence of amphipathic α-helical regions in apo B-100 evidence also suggests the presence of a hydrophobic proline rich region (DeLoof *et al.*, 1987). The secondary structure at the proline rich regions in apo B-100 has been suggested to form amphiphatic β-strands such that they may be able to interact with the lipids. Recently, Osterman *et al.* (1984) have shown that synthetic amphipathic β-strand peptides were able to organize lipids into a LDL-type particles, and further had the ability to tightly bind with the plasma LDL. Thus, it is possible that in apo B-100 both amphipathic α-helical region and amphiphatic β-strand region may be involved in binding with the lipids. In the case of apo C-I, apo C-II and apo C-III, conformational changes in the apoprotein structure are also observed following the binding of phospholipids. For instance, in apo C-I/egg PC complexes the apoprotein was shown to have $\simeq$70% α-helical content (Jackson *et al.*, 1974a). The α-helical content of apo C-II and apo C-III increased from 23% to 60% and 22% to 54%, respectively, upon binding with the phospholipids (Morrisett *et al.*, 1973; Pownall *et al.*, 1979). Such lipid-protein interactions are believed to occur through the amphipathic α-helical segments of the proteins (Kaiser and Kezdy. 1974; Segrest *et al.*, 1974). Although the nature of lipid-protein interactions in the surface monolayer of VLDL is not known, from the above considerations it is possible that such interactions may take place.

In the case of LDL, ^{1}H NMR (Finer *et al.*, 1975) and ^{31}P NMR studies (Yeagle *et al.*, 1977) have shown the presence of immobilized phospholipid head groups. We have not observed such immobilised phospholipid headgroups in VLDL particles by ^{31}P NMR spectroscopy. ^{31}P spectra with sweep width up to 50 kHz show no evidence of broad component nor does the F.I.D.

It is also not known whether immobilization of phospholipid headgroups would restrict the motions of phospholipid acyl chains. ^{2}H NMR studies have provided no evidence that proteins can have an ordering effect on the acyl chains of phospholipid molecules. Instead, studies with deuterated phospholipids, selectively labelled on the *sn*-2 position, to which proteins and polypeptide chains, gramicidin A, bacteriophage f1 coat protein, beef brain myelin proteolipid apoprotein, cytochrome b_5, and cytochrome c oxidase, have been added, were shown to disorder the acyl chains (Oldfield *et al.*, 1978; Kang *et al.*, 1979; Rice and Oldfield. 1979). Taken together these studies suggest that lipid-protein interactions are likely and that the result is to disorder the boundary PC acyl chains. However, there is no evidence in the literature where lipid-protein interactions have been shown to disorder the PC acyl chains to the extent necessary to give isotropic spectra. Although the effect of lipid-protein interactions on PC acyl chains cannot be neglected, such interactions do not appear to be totally responsible for the low order domain in the monolayer of VLDL.

Selectively deuterated phosphatidylcholine in egg PC/TO microemulsions

In an attempt to understand the occurrence of two domains in the surface monolayer of VLDL we have extended our investigations to the model particles - microemulsions composed of egg PC/triolein (TO). Egg PC/TO microemulsions containing 10 mol % selectively deuterated

phosphatidylcholines are similar in size (diameter = 42.1 ±6.6 nm) to the native VLDL particles (diameter = 42.8 ±10.3 nm) and can thus be considered as simple models of VLDL. The simplicity of the model also resides in the chemical composition of the system, as these particles lack cholesterol, cholesteryl esters and apoproteins.

Based on the amphipathic character of the phospholipid molecules they are expected to surround the neutral triglyceride core of the microemulsion. Support for this comes from the enzymatic studies of Tajima *et al.*, (1983). Utilizing phospholipase A_2 they have shown that all the phospholipid molecules in egg PC/TO microemulsions were digested; unlike unilamellar vesicles where only the phospholipids on the outer surface were accessible to the enzyme. Studies by Ekman *et al.* (1988) have also shown that phospholipid molecules are associated with the surface and are not found in the apolar triglyceride core.

From the ^2H NMR spectra shown in Figures 33 and 34, and the linewidth measurements listed in Table 12, it is clear that, like the VLDL surface phospholipids, the phospholipids of egg PC/TO microemulsions also exhibit two spectral components, one broad and one narrow, of vastly order. The broad component linewidths vary with the position of deuteration along the acyl chain analogous to the variation of the quadrupole splitting in phospholipid multilamellar dispersions (Parmar, 1985). In contrast, the linewidths of the narrow component show minor variation (Table 12). The narrow component linewidths in microemulsions are in good agreement with those measured in VLDL with PC and palmitic acid (see Tables 5 and 8).

We have calculated S_{CD} for microemulsions using equation 22 and the linewidths listed in Table 12 for selectively deuterated

phosphatidylcholines in egg PC/TO microemulsions at 25°C and 40°C. Using the egg PC/TO microemulsion radius of 21.05 nm measured by EM (Figure 35), with η = 0.8904 cP (25°C) and 0.6529 cP (40°C) we obtain τ_r = 8.5 x 10^{-6} s (25°C), and 5.9 x 10^{-6} s (40°C). In these calculations we have assumed that the size of egg PC/TO microemulsions is independent of temperature. Together with the lateral diffusion coefficient, D_t = (2.5±0.4) x 10^{-8} cm²/s, determined from the viscosity dependence of ^{31}P NMR linewidths (see Section V), we have calculated τ_e = 6.6 x 10^{-6} s (25°C). The D_t value of egg PC/TO microemulsions is not known at 40°C. However, we have demonstrated that the coefficient of lateral diffusion in VLDL changes marginally over this temperature range (see Section V). Therefore, in applying equation 22 at 40°C, we have used the value of D_t of (2.5±0.4) x 10^{-8} cm²/s. The S_{CD} values calculated at 25°C and 40°C are listed in Table 16. Here, in calculating S_{CD} we have ignored the contribution to the linewidth resulting from local segmental motions (*i.e.* the $1/T_1$ in the equation 22) and other slow motions. Therefore, the S_{CD} values reported are of upper limit. Further confidence in the calculated S_{CD} values was attained by analysing the spectra as described by Parmar *et al.* (1984). The broad spectral components of [11,11,12,12-$^2H_4$]PC spectra at 25°C and 40°C was simulated as described earlier for VLDL. Figure 37 shows the superLorentzian lineshape simulation of [11,11,12,12-$^2H_4$]PC spectra at 25°C and 40°C, solid line representing the best fit for the S_{CD} values of 0.16 (25°C) and 0.14 (40°C). Since the S_{CD} values obtained from the superLorentzian lineshape fits are in excellent agreement with those measured from the Lorentzian lineshape simulations, the S_{CD} values reported in Table 16 are from eqaution 22.

Figure 37: Deuterium NMR spectrum of approximately 10 mol % [11,11,12,12-$^2H_4$]PC in egg PC/TO microemulsion at 25°C (a) and 40°C (b). The solid line represents the best visual fit to a superposition of Lorentzian lineshapes to a broad spectral component by the order parameter S_{CD} of 0.16 (a) and 0.14 (b). Egg PC/TO microemulsion radii, in nm, with fraction of total F_i given in the parenthesis, determined from negative staining electron micrographs are 12.86(0.01), 16.43(0.20), 20.00(0.46), 23.57(0.23), 27.15(0.095) and 30.72(0.005).

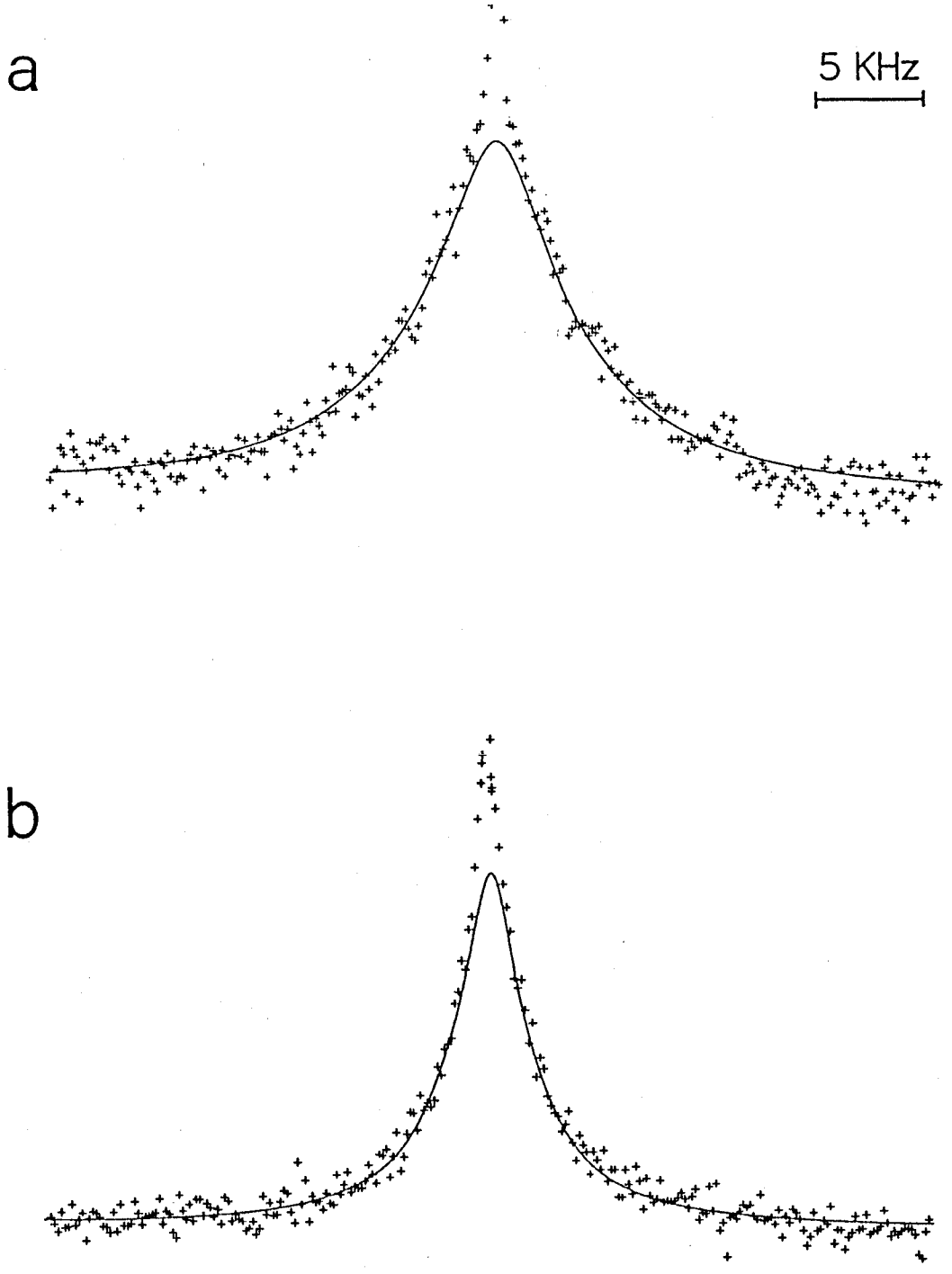
a
5 KHz
b

From Table 16 it is apparent that all the positions studied show the presence of two significantly different orders of phospholipid domains in the surface monolayer of egg PC/TO microemulsions. For instance, the order parameter for the more ordered domain of C11,12-position is 0.17 and 0.013 for the less ordered domain at 25°C.

Although the results from egg PC/TO microemulsions cannot be extrapolated directly to the VLDL results because of the simplicity of the model system, both particles however, share common structural feature as far as size, hydrophobic core and hydrophilic monolayer are concerned. It is anticipated that egg PC/TO microemulsions will closely resemble the physical state of lipids in VLDL and hence, offer an analogy with the native particles. The S_{CD} values of the less ordered domain of microemulsions are in excellent agreement with those measured in VLDL at 25°C and 40°C (Table 13 and 14). For instance, at 40°C, the mean S_{CD} value of 0.017 for C2- to C11,12-positions in microemulsions is in excellent agreement with the S_{CD} values of similar positions in VLDL (0.018). Earlier it was mentioned that the isotropic component we observe in the ^2H NMR spectrum of VLDL may arise from the possible lipid-protein interactions. However, our observations with the protein-free microemulsions lead us to conclude that the narrow spectral component we detect by ^2H NMR in both VLDL and microemulsions is not a consequence of lipid-protein interactions but must arise from another mechanism.

We may compare the S_{CD} values of the more ordered domain of egg PC/TO microemulsions (Table 16) with those of egg PC multilamellar dispersions at 25°C (Table 15). In both cases the S_{CD} values, at the equivalent acyl chain positions, are very similar. For example, the mean S_{CD} of 0.12 for

Table 16: Order parameter of selectively deuterated phosphatidylcholines in egg PC/TO microemulsions.

Deuterated position	Temperature°C 25	40[a]
2,2-	0.015 (0.10[b])	0.017 (0.12)
5,5-	-	0.019 (0.17)
11,11,12,12-	0.013 (0.17)	0.014 (0.14)

[a] Contribution from lateral diffusion measured at 25°C has been used in the calculation of these S_{CD} values.
[b] The value in parenthesis refers to the broad spectral component.

the 2-position of phosphatidylcholine in egg PC multilamellar dispersions is in excellent agreement with the S_{CD} value (0.10) in egg PC/TO microemulsions. Since S_{CD} values along the phospholipid acyl chain in egg PC/TO microemulsions (C2 and C11,12) are essentially the same as for the egg PC multilamellar dispersions, the phospholipids in the surface monolayer of egg PC/TO microemulsions appear to have acyl chain packing similar to that found in bilayer membranes.

We may also compare the S_{CD} values of the more ordered domain of egg PC/TO microemulsions with those obtained for unilamellar vesicles composed of egg PC/SPM (85:15) (Table 15). The order parameters of the corresponding positions on the *sn*-2 chain of phosphatidylcholine in egg PC/TO microemulsions are higher than the order parameter values of unilamellar vesicles. For instance, the S_{CD} value for the C2-position in microemulsions is approximately 1.25 times higher than that found in vesicles at 25°C

while the C11,12-positions are approximately 2.4 times higher. This seems particularly interesting since, as suggested by Parmar *et al.* (1984), the acyl chain order in vesicles may arise from the packing contraints imposed on the phospholipid acyl chains as a consequence of particle curvature. Egg PC/TO microemulsions are approximately the same size as vesicles and yet show order parameters significantly higher. This difference may be explained by considering the structure of the particles. Egg PC/TO microemulsions, unlike vesicles, contain a triglyceride core and this may stabilize the phospholipid acyl chain packing at the surface by interdigitation of TO chains into the monolayer.

Speculations into the origins of low PC acyl chain order in egg PC/TO microemulsion and VLDL

While a definitive explanation for the occurence of the low PC acyl chain order domain in both particles cannot be given, several possibilities must be considered.

(1). The egg PC/TO microemulsion preparation may be contaminated with very small vesicular-type structures whose rapid tumbling will yield narrow lines. We have searched for contamination by such structures and consider the possibility of their presence to be highly remote. The electron micrographs of varying concentrations of egg PC/TO microemulsions stained with 2% ammonium molybdate at pH 8.6 did not show the presence of small vesicular structures. However, as seen from the electron micrograph (Figure 35) very few large vesicular-type structures (<1%) were observed and hence are not expected to give the narrow lineshapes. Furthermore, the absence of small vesicular-type structures in the egg PC/TO microemulsion preparation was demonstrated using lanthanide shift reagents. All the ^{31}P NMR signal

due to the phosphatidylcholines was shifted downfield upon the addition of Pr^{3+} ions. In support of our finding Tajima *et al.* (1983), in a similar preparation, have shown the absence of vesicular-type structures in the egg PC/TO microemulsion preparation.

In the case of VLDL, the formation of the small structures during the incorporation of either PCs or palmitic acid was also rejected because the gel permeation chromatography of both labelled particles showed no evidence for the presence of small, protein-free structures (see Figure 8 and 24). Further support for this observation came from the examination of the electron micrographs of the labelled particles (Figures 10 and 25) where no evidence was found for the presence of small structures.

(2). Egg phosphatidylcholine and triolein are the only constituents of the microemulsion, thus an interaction between these two components must be responsible for giving rise to the low acyl chain order. In unlike unilamellar vesicles or multilamellar liposomes composed of egg PC only one domain, of PC acyl chain order, is observed (Table 15). A number of studies have shown that triglycerides are soluble to a limited extent in the phospholipid monolayer. Phase equilibrium studies with triglyceride emulsions have shown that approximately 2-5% of the triglycerides were located in the surface monolayer (Miller and Small, 1980; Miller and Small. 1983b). Similar studies by Ekman *et al.*, (1988), using an ultracentrifugation technique to separate the surface and core phases, have shown the association of triolein (2-6%) with the surface phase in egg PC/TO microemulsions. Miller and Small, (1982; 1983b) have also shown that emulsions with chemical composition similar to those present in chylomicrons and VLDL had approximately 2-5% triglyceride localized in the

surface phase. Limited solubility of triglyceride molecules in phospholipid bilayers has also been demonstrated by ^{13}C and ^{2}H NMR. A ^{13}C NMR study has shown that approximately 2.5 mol % triolein partitioned into the egg PC vesicle bilayers. The three carbonyl groups were orientated towards the aqueous phase while the acyl chains extended into the phospholipid bilayer (Hamilton and Small, 1981). Similarly, a ^{2}H NMR study has also shown that approximately 2.5 mol % triolein was incorporated into egg PC multilamellar dispersions (Gorrissen *et al.*, 1982). Thus, from the evidence presented above, it is possible that in both egg PC/TO microemulsions and VLDL a small amount of core triglycerides are present in the amphiphatic surface monolayer. Our proposal contrasts with those of Shen *et al.* (1977) where the triglycerides were said to reside exclusively in the core of the particles. From an intuitive point of view, the presence of the core constituents at the surface monolayer of lipoprotein particles seems reasonable. The enzymatic interactions of lipases and exchange/transfer protein with their substrate molecules will occur at the surface-water interface rather than within the particle or in the aqueous phase where the lipoprotein lipids are known to have low solubility (Small, 1970). Therefore, it is possible that areas of VLDL and microemulsion surface may have triglyceride rich regions that may disorder the phospholipid acyl chains. Another possibility is that triglyceride molecules may cause bulging at some regions in the surface. These areas would be so highly curved that diffusion rate may be fast enough to average the deuterium signal.

Speculations into the origin of high order domain in egg PC/TO microemulsions and VLDL

We may also compare the S_{CD} values of the high ordered domain of microemulsions (Table 16) with those obtained for VLDL (Table 14). The order parameter of the corresponding positions on the *sn*-2 chain of phosphatidylcholine in microemulsions are considerably lower than the order parameter values in VLDL at 25°C. For instance, the S_{CD} values for the C11,12-positions in microemulsions is approximately 32% smaller than that found in VLDL. Possible reasons for the high order parameter values in VLDL compared to those found in microemulsions may be explained by considering the differences in the structural composition of the two monolayers.

The high orientational order in the surface monolayer of VLDL may be explained by considering the effects of sphingomyelin (SPM), apoproteins, and cholesterol (surface components, other than phospholipids, in VLDL particles) and also by considering the possible monolayer/core interactions.

SPM, represents <15% of the total phospholipid content of VLDL (see Section V) and may be responsible for ordering the PC acyl chains. Naturally occuring SPM have long, heterogenous fatty acyl chains and, in general, have significantly higher gel to liquid crystalline phase transitions then phospholipids (Boggs, 1987). Thus, it is possible that the more ordered SPM may induce higher order of the PC acyl chains in the VLDL monolayer. Recently, the effect of SPM on phospholipid acyl chain order has been investigated in egg PC vesicles. Egg PC vesicles in the presence and in the absence of 15% SPM were observed to yield similar linewidths and hence order parameter values (Parmar, 1985). Vesicles, however, have an

aqueous core and the interior of the bilayer has very low order. In VLDL monolayer the long SPM acyl chains (C20-C24) may protrude deep into the triglyceride core and, as a result, may restrict the motions of the PC acyl chains and give rise to higher order parameter values.

The presence of apoproteins in the surface monolayer of VLDL is not expected to order the phospholipid acyl chains. A recent ^2H NMR review on numerous phospholipid/protein model membranes has shown that proteins do not have an appreciable ordering effect on the phospholipid acyl chains (Bloom and Smith. 1985).

In an effort to assess what effects, if any, cleavage of apo B-100 would have on the high order domain we have examined the C5,6- and C11,12-positions in transfer protein-treated VLDL. Examination of Table 17 shows that, at 40°C, the S_{CD} values of the C5,6-positions and C11,12-positions are within ≃14% and ≃7%, respectively, of those found in native VLDL. At 35°C, the S_{CD} values of the C11,12-positions in both particles are essentially the same. The S_{CD} value of the C5,6-position in treated VLDL is marginally larger then that of native VLDL. Based upon the results shown in Table 17, cleavage of apo-B into two fragments does not appear to have a substantial effect on the PC acyl chain order. A result in agreement with early investigations of phospholipid/protein systems (Bloom and Smith. 1985).

The monolayer/core interactions in the VLDL particles may also be responsible for ordering the PC acyl chains at the surface monolayer. The PC acyl chains may interdigitate with the triglyceride acyl chains such that the PC acyl chain motions become restricted. Monolayer/core interactions have recently been demonstrated in HDL sized particles and

Table 17: Order parameters of selectively deuterated palmitic acids in native and treated VLDL.

Deuterated position	Native VLDL	Transfer protein treated VLDL
5,5,6,6[a]	0.15	0.13
11,11,12,12[b]	0.12	0.12
11,11,12,12[a]	0.11	0.10

[a] S_{CD} measured at 40°C. Based upon τ_e = 4.5 X 10^{-6} s
[b] S_{CD} measured at 35°C. Based upon τ_e = 5.0 X 10^{-6} s

were shown to become pronounced at lower temperatures (Fenske *et al.*, 1988a). In these particles the monolayer/core interactions were observed to take place as high as the C5-position of the acyl chain. Even in the larger LDL sized particles such effects have been suggested to play an important role in the lateral diffusion of the phospholipid molecules across the surface of the particle. The PC lateral diffusion coefficient in LDL increased by ≃10 fold following the increase in temperature from 25°C to 45°C (Fenske, 1988b). The slower diffusion at 25°C was explained by the fact at 25°C the core is in the midst of a phase transition (Tm ≃20-40°C). Similar findings have also been reported in larger model systems composed of cholesteryl oleate, dimyristoylphosphatidylcholine and apolipoprotein E (Mims *et al.*, 1986). Thus, if such interactions are operative they are expected to be equivalent in both VLDL and egg PC/TO microemulsions.

The order parameter of the C16-position in HDL_2 was shown to remain unaltered following a temperature change from 25°C to 15°C (Parmar, 1985).

Therefore, assuming that the order parameter of the C16-position in VLDL remains as that found at 25°C, we have calculated theoretical linewidths using equation 22 at 15°C and 20°C based upon the change of correlation time of particle tumbling. From Table 18, it is observed that the experimental linewidths are considerably higher than the calculated linewidths. This suggests that the methyl group is in an environment where the angular excursions have become restricted. We suggest that the C16-positions of the PC and palmitic acid acyl chains are in contact with the core constituents which become more ordered following a change of temperature from 25°C to 15°C.

Another possible reason for the high order in the surface monolayer of VLDL may be due to the presence of cholesterol. Although the amount of free cholesterol in the surface monolayer of VLDL is not known, calculations by Eisenberg and Olivecrona 1979, based on the phase diagram of free cholesterol, cholesteryl ester and phospholipids, have shown that in VLDL particles of molecular weight 56.3 X 10^6 and 8.2 X 10^6 Daltons $\simeq$67% and $\simeq$82% of cholesterol, respectively, was localized in the surface monolayer. From the chemical composition data given in Table 3, in our labelled VLDL, the ratio, based on the wt % per particle, of cholesterol to phospholipid is 0.26 and this corresponds to $\simeq$35-42 mol % cholesterol in the surface monolayer. The effect of cholesterol on the phospholipid acyl chain order has been studied extensively in phospholipid bilayers. Stockton and Smith (1976) have analysed the effect of cholesterol (0 to 33.4 mol %) on the order of perdeuteriostearic acid intercalated into egg PC bilayers. It was observed that, upon the addition of cholesterol, the S_{CD} value for C11-C18 acyl chain segments increased linearly. Thus, it is expected that cholesterol will also order the phospholipid acyl chain in the surface

Table 18: Experimental and theoretical linewidths of C16-position in VLDL as a function of temperature.

Temperature (°C)	PC linewidths (Hz)		PA linewidths (Hz)	
	Observed	Calculated	Observed	Calculated
15	613	286[a]	679	348[c]
20	571	266[b]	-	-
25	256	-	300	-

[a] Based upon $\tau_e = 8.3 \times 10^{-6}$ s

[b] Based upon $\tau_e = 7.8 \times 10^{-6}$ s

[c] Based upon $\tau_e = 7.0 \times 10^{-6}$ s

In the τ_e calculations, a lateral diffusion coefficient value of 9.1×10^{-9} cm^2/s was used.

monolayer of VLDL unlike microemulsions which have no cholesterol.

At 40°C, the order parameter of C5,6- and C11,12-positions in egg PC/TO are marginally higher than those found in VLDL (see Tables 14 and 16). The presence of ≃40 mol % cholesterol in the VLDL monolayer does not appear to have an effect on the PC acyl chain order at 40°C. This may be due, at least in part, to the solubilization of small amounts of cholesterol in the triglyceride core since, Jandacek *et al.* (1977) have shown that in triolein-water systems the solubility of cholesterol increases by a small amount from 1.9 wt% to 3.2 wt% upon increasing the temperature from 21°C to 37°C. However, not all the cholesterol at the VLDL surface is expected to dissolve into the triglyceride core and account for the disorder of the phospholipid acyl chains. An alternative mechanism that

may perhaps explain why VLDL phospholipids are disordered up to C5,6-positions is by considering the interdigitation of the core components. At higher temperature the triglyceride core becomes disordered such that their ordering effect on the phospholipid acyl chains would be reduced.

Spin-lattice relaxation times

The ^2H spin-lattice relaxation times of selectively deuterated PCs incorporated into VLDL at 25°C are given in Table 7. It should be emphasized that the T_1 values measured for the C^2H_3 groups have a mixture of both narrow and broad spectral components. The weighted least squares fit to the plots of $\log(A_\infty - A_\tau)$ versus τ shows a straight line thus suggesting the presence of a single exponential decay. Therefore, the relaxation rate of the broad component may be similar to that of the narrow component although the signal to noise ratio for the broad component is too low to ascertain this possibility. The relaxation rates are approximately constant at 31 s^{-1} for the C2 to C5,6 segments and fall to $\simeq$6 s^{-1} at the terminal methyl end. The relaxation rate exhibits a profile where the plateau region, at least from C2 to C5,6 segments, remains constant and than falls to the terminal methyl end. This is in contrast to the S_{CD} values of the narrow component where no order profile was observed. The trend of the relaxation rate is very similar to that shown by the dipalmitoylphosphatidylcholine membranes in their liquid crystalline state (Brown *et al.*, 1979). In the DPPC bilayers the $1/T_1$ relaxation rates were approximately 30 s^{-1} from C3 to C6 segments and decreased to $\simeq$7 s^{-1} at the C15 segment suggesting that the phospholipids in the surface monolayer of VLDL exhibit similar segmental motions as those observed in DPPC bilayers. However, comparison of the $1/T_1$ relaxation rates with the selectively

deuterated phospholipids in HDL_2 (Parmar, 1985) indicate that, apart from the terminal methyl group, the rate of relaxation from C2 to C7 segments are more than 2X greater than the phospholipids of VLDL. Similarly, the relaxation rates of palmitic acid in LDL labelled at the C5,6-position, is 50 s^{-1} while that of the terminal methyl group is $\simeq$5 s^{-1}. The lower spin lattice relaxation rates observed for the phospholipid acyl chains in VLDL particles suggest that the molecular motions are comparatively faster than those observed in either HDL_2 or in LDL. The T_1 value measured for palmitic acid labelled at the 4-position in VLDL (20±1 ms) is in contrast to the phospholipid labelled at the equivalent position (T_1 = 31±2 ms) while the T_1 values of the terminal methyl group, in both cases, were wihtin experimental error.

CHAPTER V

LATERAL DIFFUSION COEFFICIENT (D_t) AND CHEMICAL SHIFT ANISOTROPY ($\Delta\sigma$) IN VLDL AND EGG PC/TO MICROEMULSIONS

Va. Measurement of D_t and $\Delta\sigma$ in VLDL at 25°C and 40°C.

RESULTS

We have measured the lateral diffusion of phospholipid molecules across the surface monolayer of VLDL and egg PC/TO microemulsions using ^{31}P NMR. The VLDL study comprised one part of a total lipoprotein study (Cushley *et al.*, 1987). The lateral diffusion coefficients of phospholipids in lipoprotein paricles and egg PC/TO microemulsions have been determined by following the increase in ^{31}P NMR linewidths as a function of solvent viscosity according to the procedure described by Cullis (1976).

Initial attempts to measure the lateral diffusion coefficient in native VLDL sample proved difficult. At high glycerol concentrations the ^{31}P NMR spectra became increasingly asymmetrical in lineshape. Figure 38 illustrates the ^{31}P NMR spectra of native VLDL at three solvent viscosities. At η = 5.64 cP, the spectrum shows the superposition of a narrow central peak with a broad asymmetrical lineshape at the baseline. At η = 28.10 cP, the spectrum has a pronounced asymmetrical lineshape. The asymmetrical lineshapes observed at high solvent viscosities can be explained by the presence of a range of correlation times arising from the heterogenous size distribution of the particles in the sample under study. The size distribution of native VLDL particles is shown by the electron micrograph in Figure 39a. From the histogram (Figure 39b) a mean diameter

of 46.1±11.7 nm was calculated. To illustrate the range of correlation times, we have calculated the effective correlation time, τ_e, for a range of particle sizes at η = 28.10 cP and temperature = 25°C. For particles of mean diameter = 30±5 nm, $\tau_e = 2.8 \times 10^{-5}$ s, while particles of diameter = 45±5 nm, $\tau_e = 7.1 \times 10^{-5}$ s and particles of diameter = 60±5 nm, $\tau_e = 1.3 \times 10^{-4}$ s. The size distribution is such that the τ_e values are approximately an order of magnitude in range. Burnell *et al.*, 1980, have examined the effect of τ_e on the ^{31}P NMR lineshapes of dioleoylphosphatidylcholine (DOPC) vesicles. The spectra were shown to become non-Lorentzian at $\tau_e < 8.2 \times 10^{-5}$ s. The authors have further shown that the size of the particles is very important in determining the lineshape of the spectrum. Based on the known values of the CSA, D_t, and η the ^{31}P NMR spectra were shown to acquire asymmetrical lineshapes with increasing vesicle size and symmetrical lineshapes were only observed for smaller vesicles. Thus, in order to avoid the difficulties encurred with the asymmetrical lineshapes, the native VLDL sample was subfractionated (see Materials and Methods) so as to remove the large VLDL particles.

An electron micrograph of the subfractionated VLDL together with its histogram depicting the size distribution is shown in Figure 40a and 40b, respectively. The mean size of the subfractionated VLDL was 38.8±15.7 nm. Subfractionation of native VLDL does not lead to particles of differing chemical composition. Table 19 illustrates the chemical composition of subfractionated and native VLDL. Very little change is observed between the two chemical compositions and thus, we conclude that we are dealing with a narrow distribution of small VLDL particles.

Figure 38: Representative ^{31}P NMR spectra of native VLDL at three solvent viscosities to demonstrate the asymmetry in the lineshape. Spectral parameters: pulse width = 6.5μs (73° flip angle); Sweepwidth 10 KHz (a) and 50 KHz (b-c); datset = 4k zerofilled to 8k; delay between pulses = 1.5 s; number of of acquisitions = 5,000 (a), 30,000 (b) and 50,000 (c); line broadening = 5 Hz (a), 10 Hz (b) and 50 Hz (c).

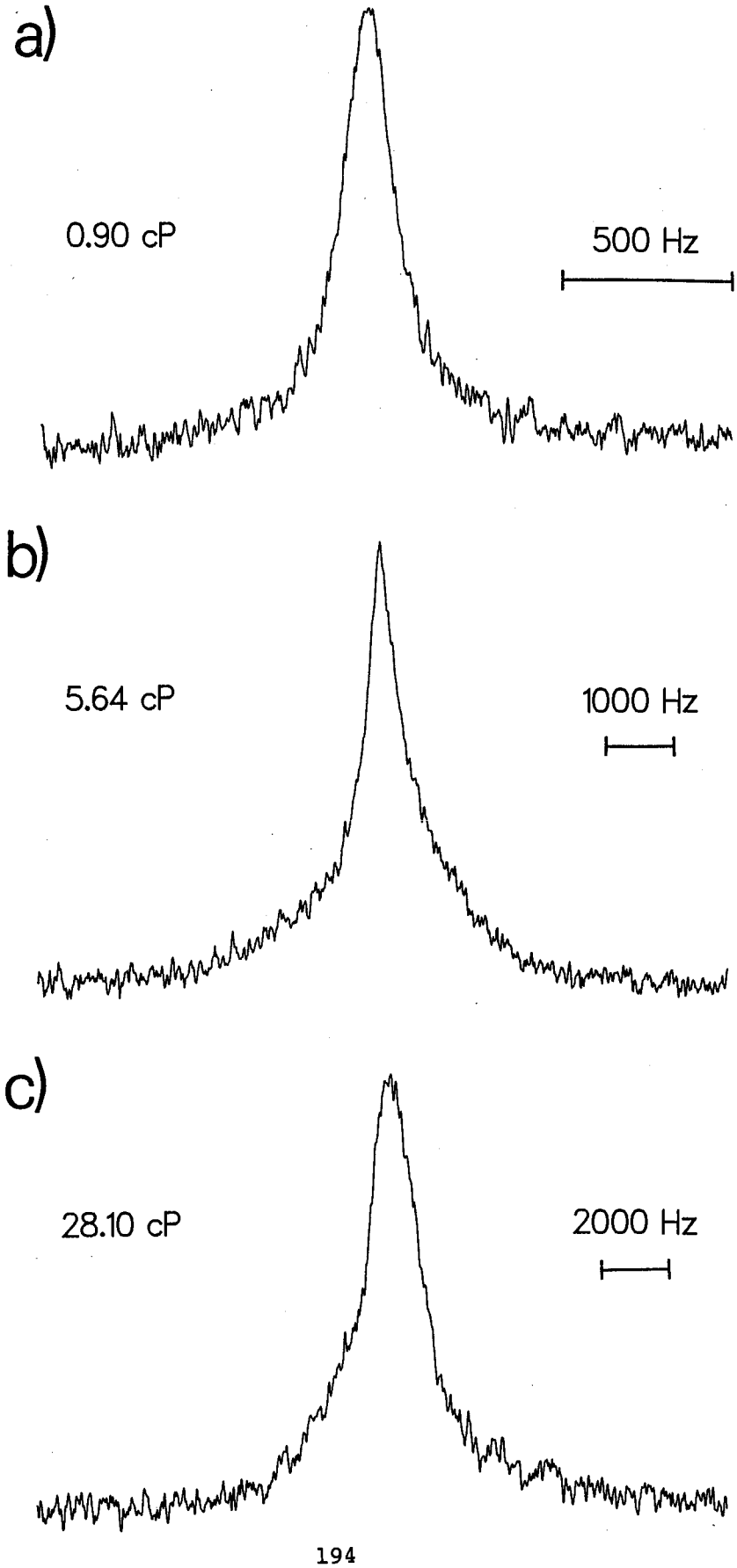
a)
0.90 cP
500 Hz
b)
5.64 cP
1000 Hz
c)
28.10 cP
2000 Hz

Figure 39: a) Electron micrograph of native VLDL. Magnification = X137,000. b) Histogram depicting size distribution for 350 particles counted is given below the electron micrograph. Mean diameter = 46.1±11.7nm.

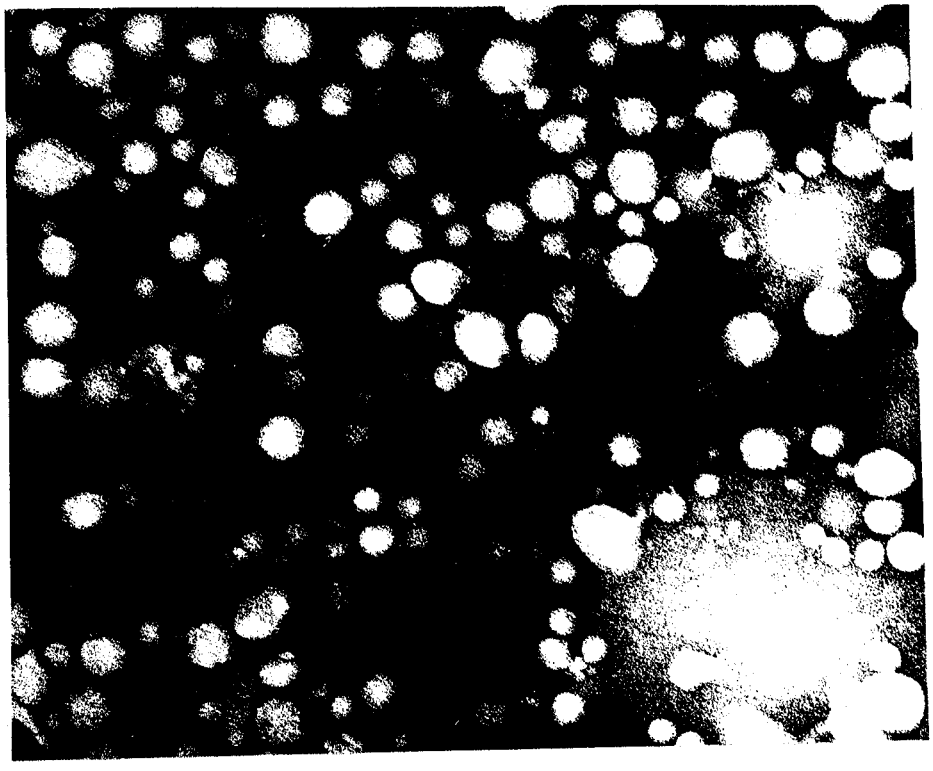

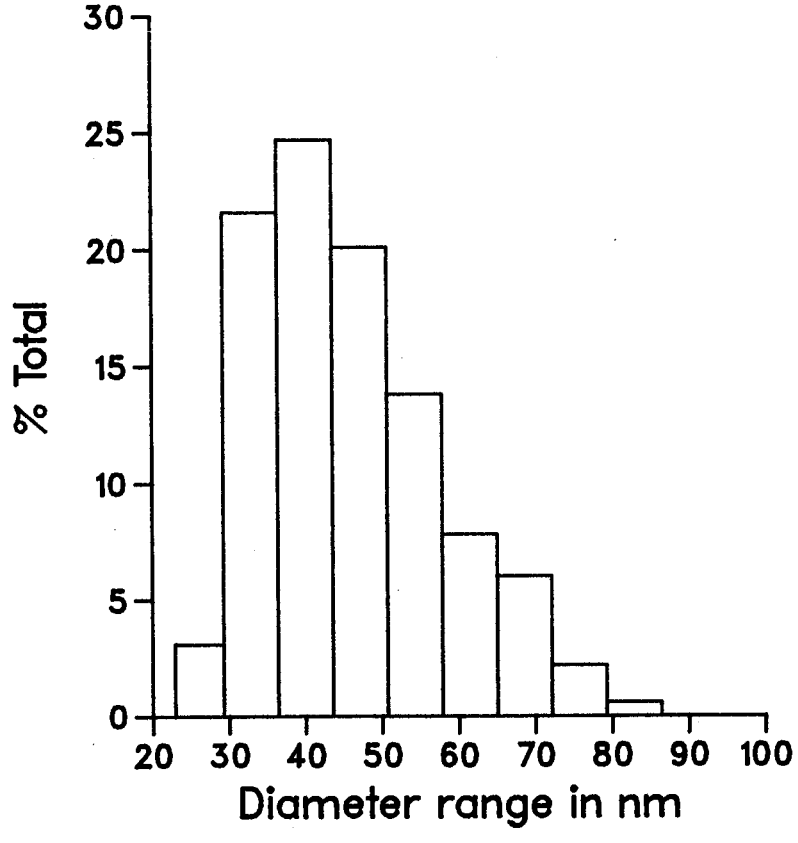
30
25
20
15
10
5
0
% Total
20
30
40
50
60
70
80
90
100
Diameter range in nm

Figure 40: a) Electron micrograph of subfractionated VLDL. Magnification = X137,000. b) Histogram depicting the size for 510 particles counted is given below the electron micrograph. Mean diameter = 38.8±15.7 nm.

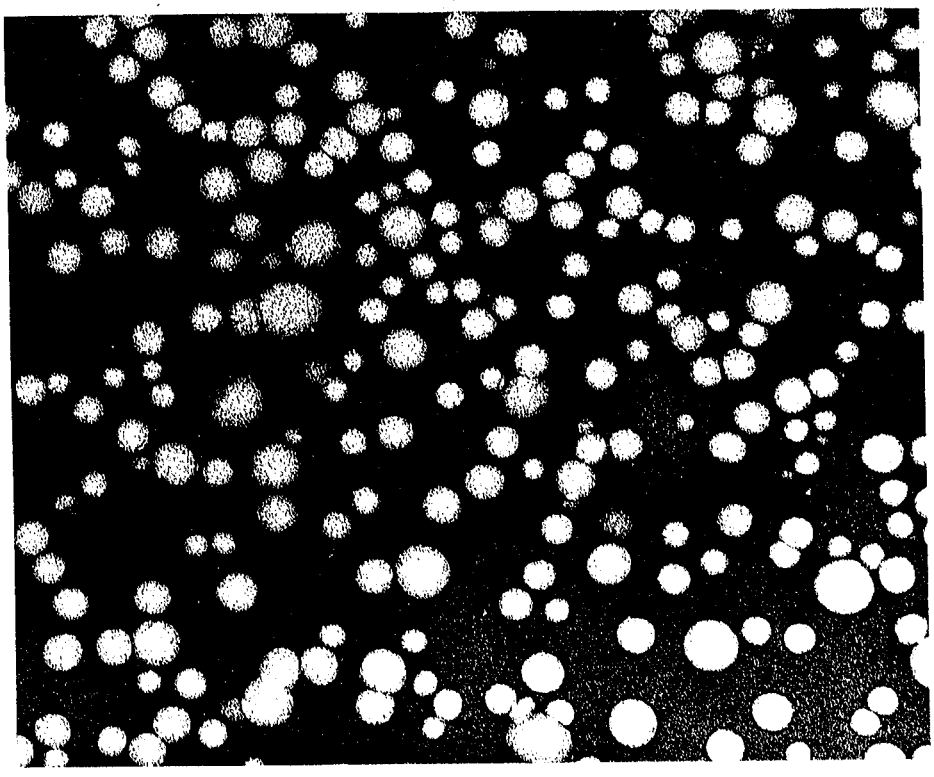

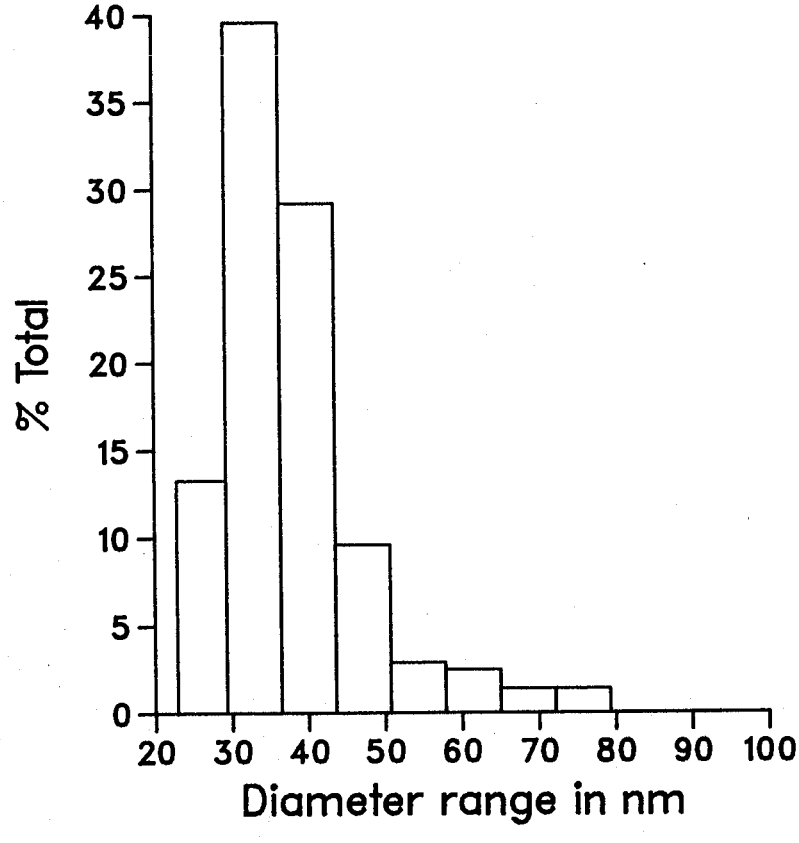
40
35
30
25
20
15
10
5
0
% Total
20
30
40
50
60
70
80
90
100
Diameter range in nm

Table 19: Comparison of chemical composition of native VLDL and subfractionated VLDL.

Composition	Native VLDL	Subfractionated VLDL
Phospholipid	21.1	22.2
Triglyceride	46.5	45.9
Cholesterol	5.6	6.1
Cholesteryl ester	13.3	11.6
Protein	13.7	14.2

All the values quoted are % by weight. The estimated errors in all cases, duplicate analysis of each sample, are ±2%.

Figure 41 illustrates the ^{1}H-decoupled ^{31}P NMR of total VLDL lipid extract (≃2.0 mg/mL w.r.t. phospholipid). The prominent PC peak is centered at -0.16 ppm and the SPM peak is centered at 0.77 ppm relative to the external 85% phosphorus acid. The chemical shifts of respective lipids in VLDL were confirmed using standard lipids, PC and SPM, obtained from Sigma Chemical Company. From the integration of the spectrum, ≃86% of VLDL phospholipids were established to be PC and the remainder to be SPM.

Representative ^{31}P NMR spectra of subfractionated VLDL particles in the presence of increasing solvent viscosities at 25°C are shown in Figure 42. The spectra are iterative least-squares fits of a single Lorentzian lineshape function (solid line) to the spectral data points (crosses). The spectra at high solvent viscosities give particularly good fits to single Lorentzian lineshape function despite the fact that 14% of the intensity is from the SPM. In order to account for the SPM contribution to the

Figure 41: ^{1}H-decoupled ^{31}P NMR spectra of VLDL lipid extract (≃2.0mg/ml, w.r.t VLDL phospholipid) in chloroform:methanol (2:1, v/v) at 25°C. Spectral parameters: pulse width = 30 μs (90° flip angle); sweep width = 1.3 KHz; dataset = 8k; number of acquisitions = 2470; repetition time = 4 s; line broadening = 5 Hz. Chemical shifts are with respect to an external H_3PO_4 (85%) reference. Resonance frequency = 116.8 MHz

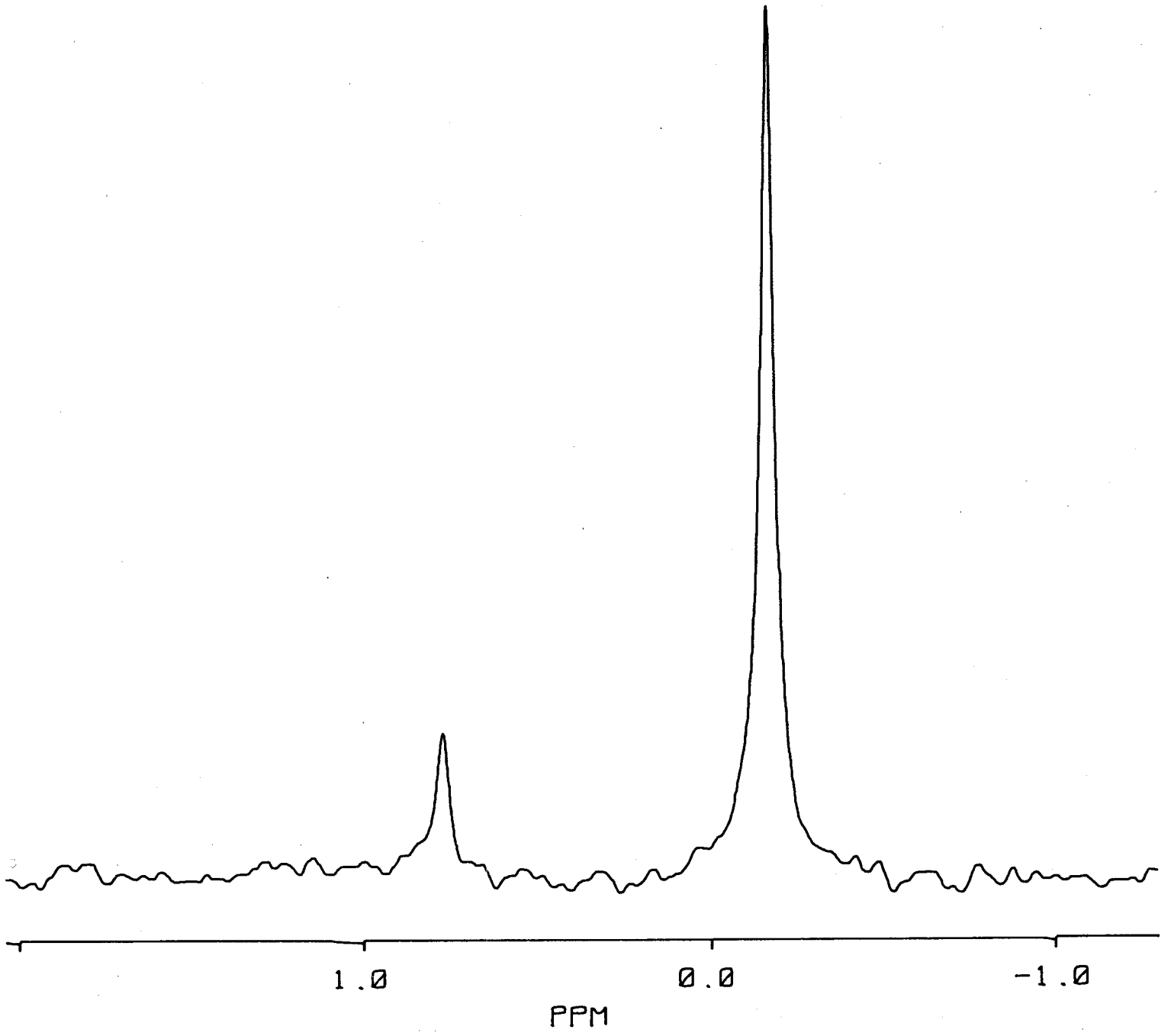
1.0
0.0
-1.0
PPM

Figure 42: Representative ^{31}P NMR spectra of subfractionated VLDL in the presence of increasing concentrations of glycerol at 25°C. The spectra are iterative least-squares fit to a single Lorentzian lineshape function (solid line) to the spectral data points (crosses). The concentrations of glycerol (weight-%) were 0 (a), approximately 36 (b), 56 (c) and 68 (d). Spectral parameters: pulse width = 6.5 μs (73° flip angle); sweep width = 20 KHz (a) and 50 KHz (b-d); dataset = 4k zerofilled to 8k; number of acquisitions = 8,000 (a), 30,000 (b), 40,000 (c) and 50,000 (d); delay between pulses = 1.5 s; line broadening = 5 Hz (a), 15 Hz (b), 25 Hz (c) and 150 Hz (d); delay before acquisition = 10 μs. For a clear representation of the fits every 3rd (spectra a, b), 4th (c) and 5th (d) spectral data points, respectively, are shown.

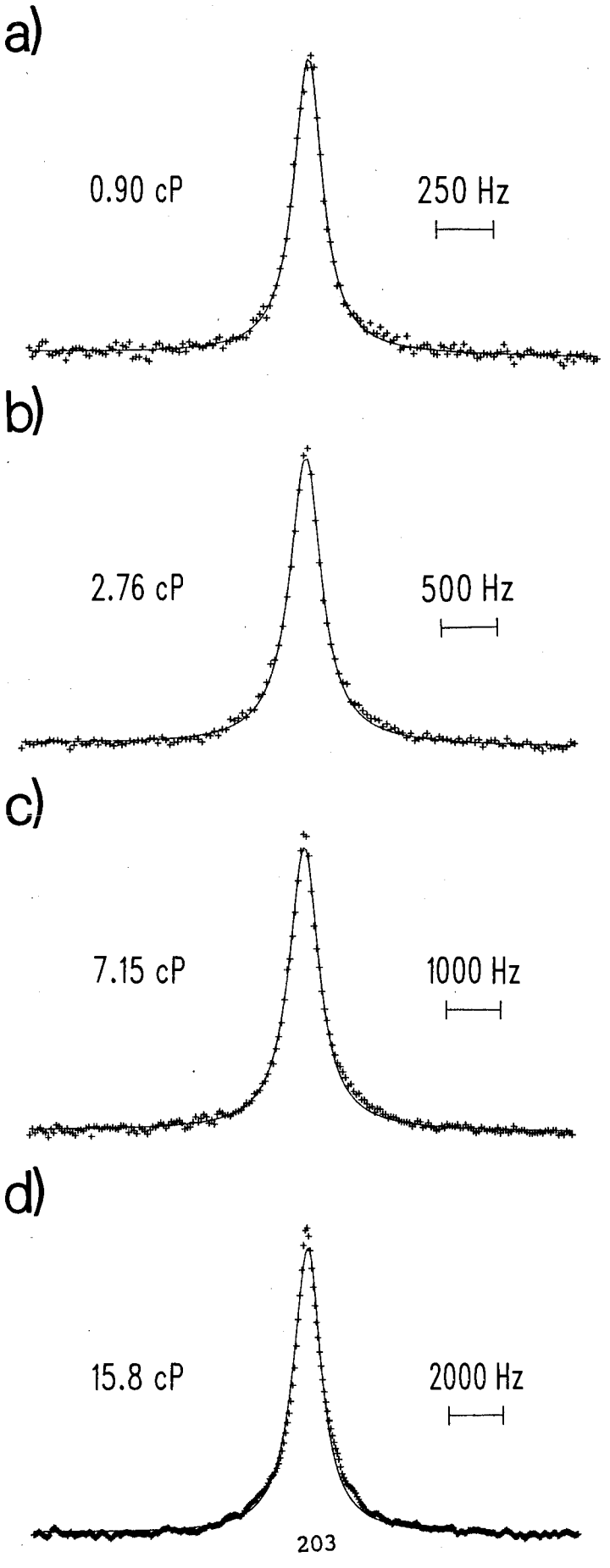
a)
0.90 cP
250 Hz
b)
2.76 cP
500 Hz
c)
7.15 cP
1000 Hz
d)
15.8 cP
2000 Hz

spectrum, Figure 42a was also fit with a double Lorentzian lineshape function. The following constraints were imposed in the computer routine to fit the spectrum: a) The linewidths due to SPM and PC were kept the same. This assumption is reasonable because both HDL and LDL, where the PC and SPM peaks are resolved (at a ratio of 4:1 and 3:2, respectively), show equal linewidths and suggest the lipids to be homogenoeus mixed (Parmar, 1985 and Cushley *et al.*, 1987). Another study utilizing SPM:DPPC mixture (1:1, wt/wt), has also demonstrated that lipids are homogenously mixed (Villalain *et al.*, 1988). Thus, SPM in VLDL is assumed to be homogenously mixed in the phospholipid matrix; b) The intensity of the SPM peak was kept at 14% that of PC peak. It is assumed that the T_1's of both lipids in VLDL are identical since the respective T_1s in LDL are similar (Yeagle *et al.*, 1977); c) The chemical shift between SPM and PC peaks was fixed at 65 Hz. The spectra (Figure 42a.) simulated by a single or a double Lorentzian lineshape function yielded indistinguishable spectra. Based on this, all the spectra were fit with a single Lorentzian lineshape function. The exclusion of SPM may slightly overestimate linewidths but the errors are expected to be small. The linewidths obtained from the ^{31}P NMR spectra at respective solvent viscosities are listed in Table 20.

The lateral diffusion coefficient, D_t, was calculated from equation 31. The ratio of intercept to slope was obtained from a plot of $(\Delta\nu_{1/2} - C)^{-1}$ versus η^{-1}, as shown in Figure 43, where the solid line is the weighted least-squares fit to the experimental data points. To calculate D_t both the size of VLDL and the value of constant C are required. The size of VLDL particles was determined by two techniques: 1) EM which gave a mean diameter of D = 38.8±15.7 nm (see Figure 40) and 2) QELS of VLDL particles in 0.15 M NaCl, 2.0 mM Na_2EDTA at pH 7.4 (D = 36.8 nm). The

Table 20: ^{31}P NMR linewidths of VLDL as a function of glycerol concentration at 25°C.

% Glycerol	Viscosity (cP)	linewidth (Hz)
0	0.90	152
10	1.19	203
20	1.59	253
28	2.06	289
36	2.76	330
46	4.27	457
56	7.15	635
64	11.80	863
68	15.81	1066
72	21.61	1117

The linewidth measurements have approximately ±10% uncertainty.

constant C has contributions from both the field homogeniety and fast motions. Its value is taken as the isotropic linewidth of phosphatidylcholine (15 Hz). This has been measured by dissolving egg phosphatidylcholine in chloroform:methanol (2:1, v/v) in the presence of 2 mM Na_2EDTA (Parmar, 1985). From Figure 43 D_t value of 9.1±1.0 x 10^{-9} cm^2/s was calculated for VLDL particles at 25°C. The data presented in Figure 43 was also analysed by linear regression analysis. This yielded a D_t value of 1.0±0.1 x 10^{-8} cm^2/s. Since both values are essentially the same, all the D_t values we report here are from the weighted least-squares analysis.

In order to examine how the calculated value of D_t and $\Delta\sigma$ compare with the experimental linewidths, we have calculated the theoretical ^{31}P NMR

Figure 43: Plot of $(\Delta\nu_{1/2} - C)^{-1}$ versus η^{-1} for the ^{31}P NMR linewidths of VLDL at 25°C. The straight line is a weighted least-squares fit to the data points.

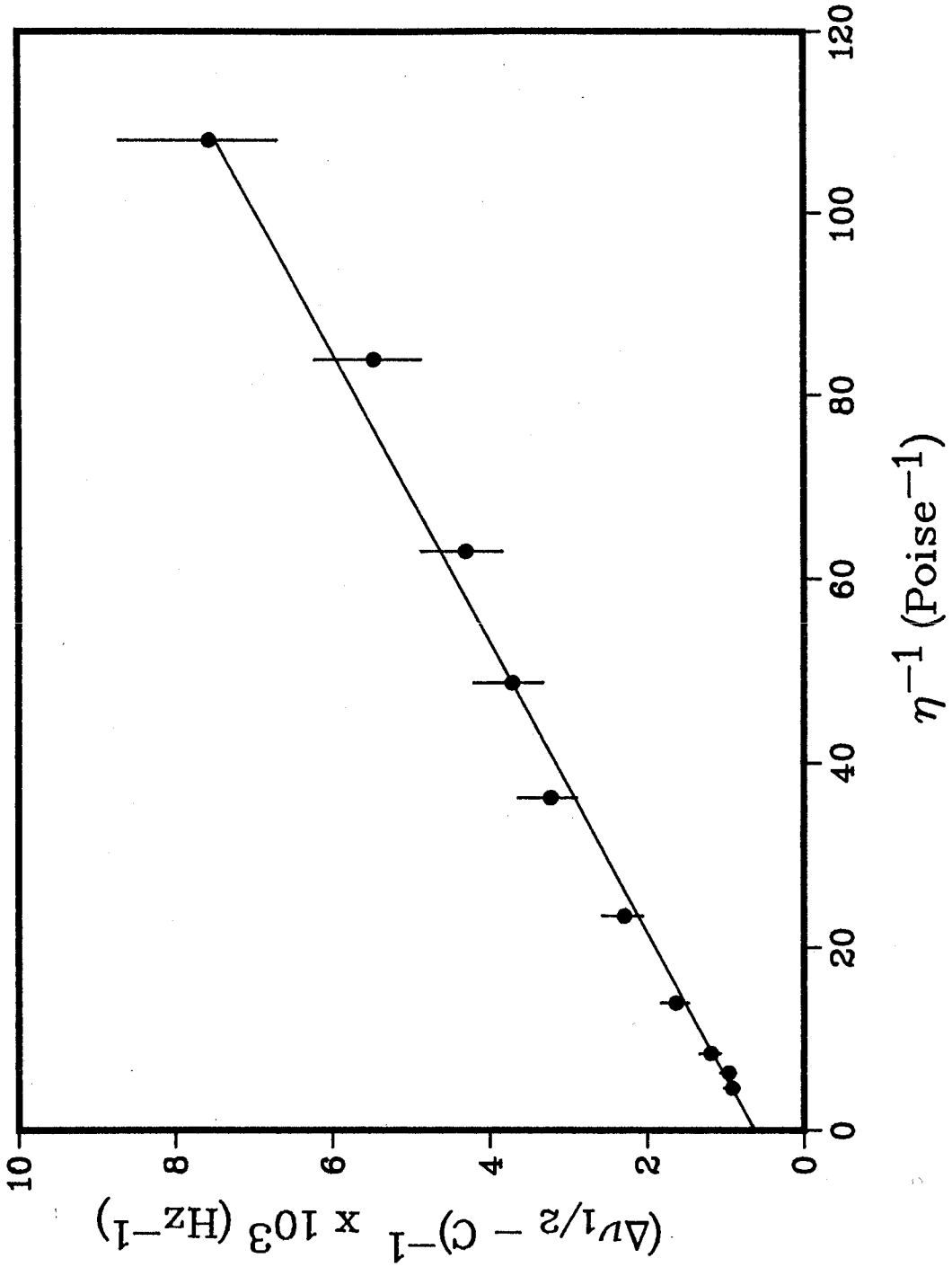
$(\Delta\nu_{1/2} - C)^{-1}$ x 10^3 (Hz^{-1})
0
2
4
6
8
10
0
20
40
60
80
100
120
η^{-1} (Poise^{-1})

linewidths for D_t = 0.5 x 10^{-8}, 0.9 x 10^{-8}, and 2.0 x 10^{-8} cm^2/s. The theoretical linewidths were calculated using a VLDL radius of 18.4 nm and a second moment, M_2, = 2.58 x 10^7 s^{-2}. M_2 was calculated from equation 29, $\Delta\sigma$ was taken as 47 ppm and ν_0 as 102.2 MHz. The variation of the ^{31}P NMR linewidths as a function of solvent viscosity for respective D_t values is shown in Figure 44. The linewidths increase and begin to level off at high glycerol concentrations indicating that the lateral diffusion has become the dominant line narrowing mechanism. The best fit to the experimental linewidths is observed for the experimentally determined D_t value of 9.1 x 10^{-9} cm^2/s and the D_t values of 0.5 x 10^{-8} and 2.0 x 10^{-8} cm^2/s fall outside the range of experimental linewidths at most of the viscosities.

LDL particles exhibit an order of magnitude increase in D_t from 1.4 x 10^{-9} to 1.1 x 10^{-8} cm^2/s upon increasing the temperature from 25°C to 45°C (Fenske, 1988). Similar changes in diffusion have also been observed in phospholipid bilayers of DPPC (Cullis, 1976) and DMPC (Yeagle, 1987). The increase in diffusion correlates with the gel-to-liquid crystalline phase transition of the lipids. In order to examine if a similar behaviour was observed in VLDL we have measured D_t at 40°C. Table 21 lists the ^{31}P NMR linewidths as a function of solvent viscosity. D_t was calculated from the ratio of the intercept to the slope, obtained from a plot of $(\Delta\nu_{1/2} - C)^{-1}$ versus η^{-1} shown in Figure 45. The solid line is the weighted least-squares fit to the experimental data points. A D_t = (1.2±0.2) x 10^{-8} cm^2/s and $\Delta\sigma$ = 41±1 ppm was obtained for VLDL at 40°C. Although the D_t values at respective temperatures are within experimental error, the $\Delta\sigma$ decreases from $\simeq$ 47 ppm to 41 ppm. This is in contrast to LDL, where D_t values change by an order of magnitude and $\Delta\sigma$ remained unchanged.

Table 21: ^{31}P NMR linewidths of VLDL as a function of glycerol concentration at 40°C.

% Glycerol	Viscosity (cP)	Linewidth (Hz)
10	0.95	137
20	1.12	151
28	1.35	169
36	1.80	206
46	3.00	244
62	6.30	423
64	6.95	429
68	8.60	503
72	11.20	620
76	15.50	789

The linewidth measurements have approximately ±10%

The value of $\Delta\sigma$ = 47±1 ppm, from the viscosity measurements, was calculated using equations 29 and 30 and is very similar to the $\Delta\sigma$ = 45±5 ppm for DPPC bilayers at 48°C (Seelig, 1978). However, the high glycerol concentrations employed may affect the surface structure and hence, the headgroup conformations of the phospholipid molecules in VLDL. To examine this, we have carried out the following investigations:

a) A control experiment was set up and this involved the reexamination of the size and the ^{31}P NMR linewidth of particles following an exhaustive dialysis of a 75% glycerol sample in 0.15 M NaCl, 2.0 mM Na_2EDTA at pH 7.4. No obvious changes in either the size or the ^{31}P NMR linewidths was observed when compared to the native VLDL particles.

b) From equation 16 and 29, it can be seen that

Figure 44: ^{31}P NMR Linewidths of VLDL as a function of solvent viscosity at 25°C for $D_t = 5.0 \times 10^{-9}$ (a) $D_t = 9.1 \pm 1.0 \times 10^{-9}$ (b) and $D_t = 2.0 \times 10^{-8}$ (c) cm^2/s. The CSA = 47 ppm and $M_2 = 2.58 \times 10^7\ s^{-2}$ was used to determine the theoretical linewidths.

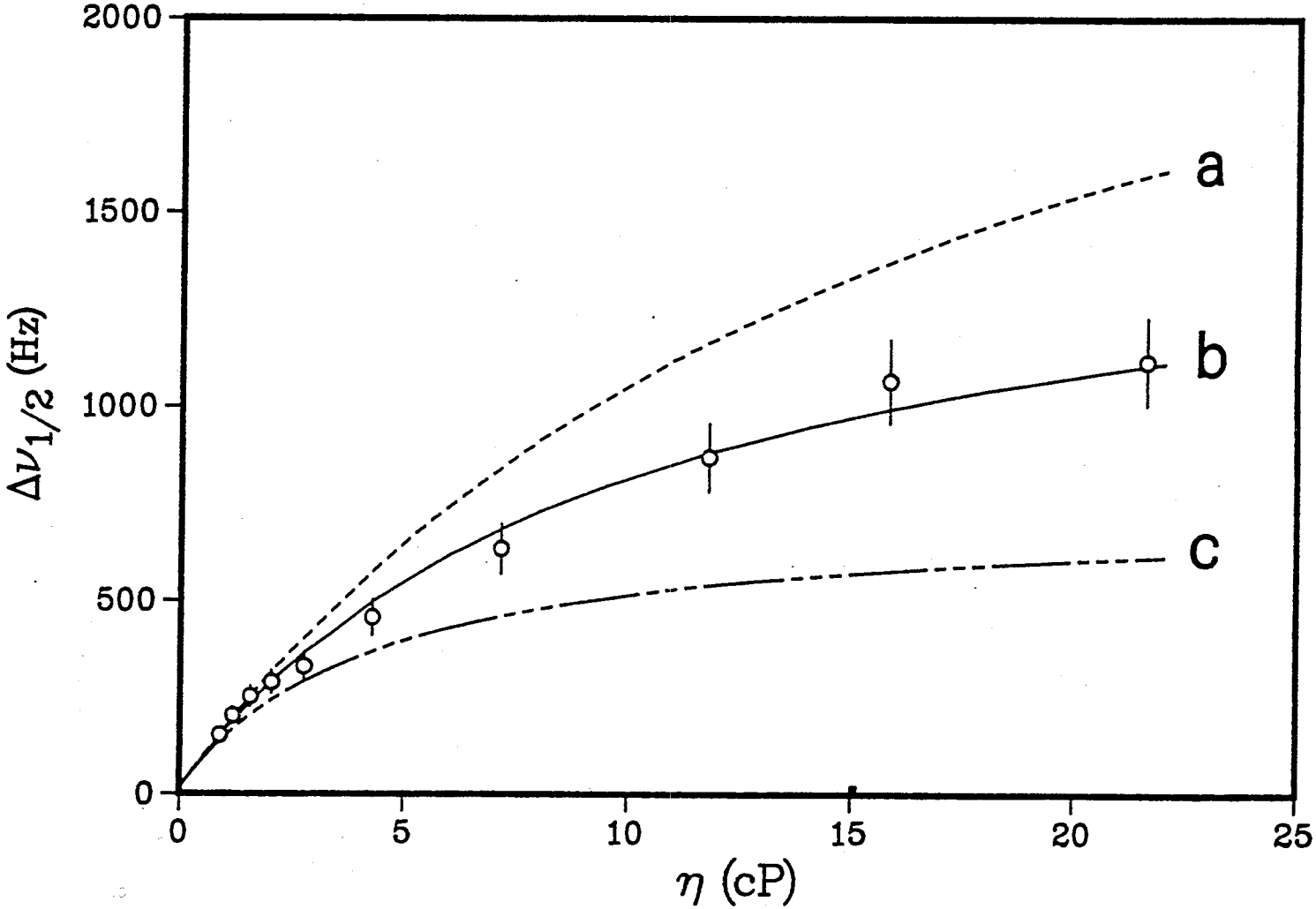
2000
1500
1000
500
0
$\Delta\nu_{1/2}$ (Hz)
0
5
10
15
20
25
η (cP)
a
b
c

Figure 45: Plot of $(\Delta\nu_{1/2} - C)^{-1}$ versus η^{-1} for the ^{31}P NMR linewidths of VLDL at 40°C. The straight line is a weighted least-squares fit to the data points.

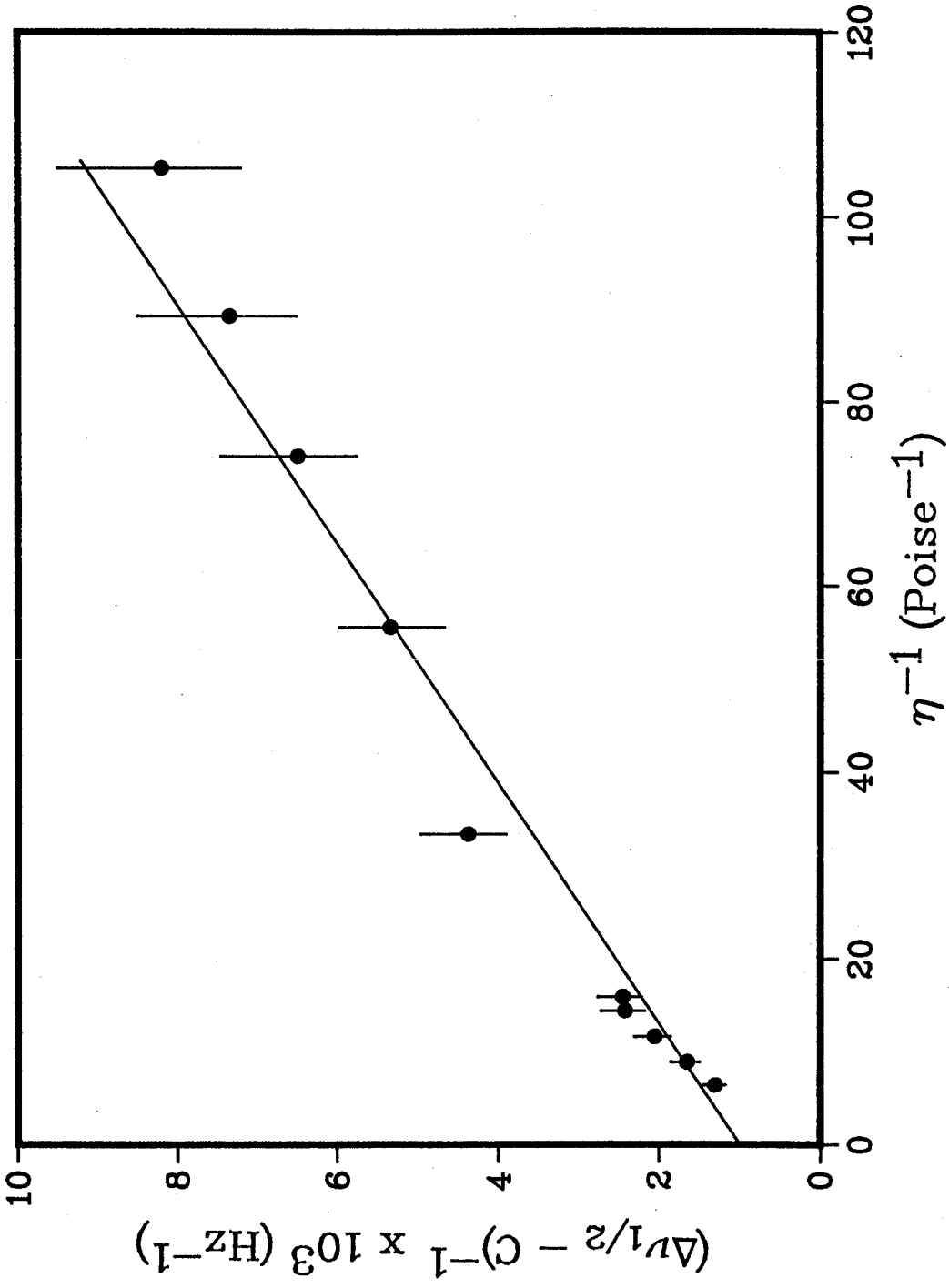
$(\Delta\nu_{1/2} - C)^{-1} \times 10^3$ (Hz^{-1})
0
2
4
6
8
10
0
20
40
60
80
100
120
η^{-1} (Poise^{-1})

Table 22: ^{31}P NMR linewidths of VLDL as a function of resonance frequency at 25°C.

ν_0 (MHz)	$\Delta\nu_{1/2}$ (Hz)
40.5	40
102.2	152
161.8	340

$$(\Delta\nu_{1/2} - C) = (16/45)\pi\nu_0^2\Delta\sigma^2\tau_e \qquad (33)$$

$\Delta\sigma$ was calculated from the field dependence of the ^{31}P NMR linewidths of VLDL using equation 33. The ^{31}P NMR spectra were recorded at three magnetic field strengths and the linewidths obtained from the spectra are given in Table 22. A plot of $(\Delta\nu_{1/2} - C)$ versus ν_0^2, shown in Figure 46, was analysed by weighted least-squares analysis. The resulting slope = 1.2432 x 10^{-2}, and using the mean value of τ_e = 5.22 x 10^{-6} s, $\Delta\sigma$ = 46±0.5 ppm was calculated.

The $\Delta\sigma$ values from both the viscosity and field dependence studies are in excellent agreement. This is further indication that high glycerol concentration has a minimal/or no affect on the surface orientation of phospholipid headgroups. High glycerol concentrations have also been shown not to affect the particle structures of LDL and HDL_3 (Fenske, 1988b) and HDL_2 (Parmar, 1985). These observations are in agreement with those reported by Cullis (1976) who showed that phospholipid vesicles maintain the same inside to outside ratio and permeability barrier to the cations at high glycerol concentrations that they did in the absence of glycerol.

Figure 46: Plot of ^{31}P NMR linewidth ($\Delta\nu_{1/2}$ - C) as a function of ν_0^2 for VLDL at 25°C. The estimated error in the Linewidths is ±10%. The straight line is a weighted least-squares fit to the data points.

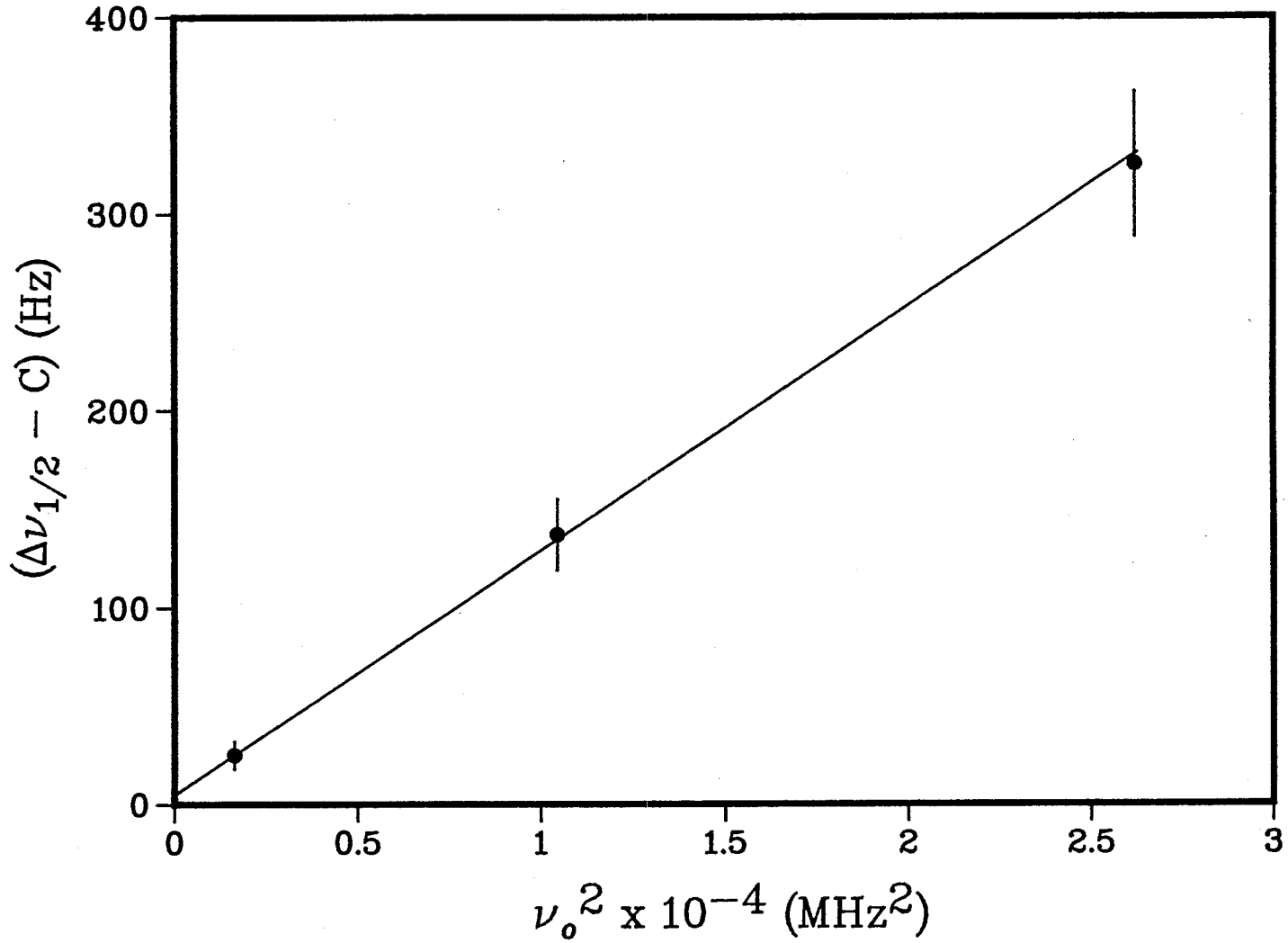
400
300
200
100
0
0
0.5
1
1.5
2
2.5
3
$(\Delta\nu_{1/2} - C)$ (Hz)
ν_o^2 x 10^{-4} (MHz^2)

Vb. Measurement of D_t and $\Delta\sigma$ in egg PC/TO microemulsions at 25°C

RESULTS

Although vesicles have been regarded as simple models of lipoproteins, they nevertheless are bilayer structures without any lipid core. As mentioned earlier, Egg PC/TO microemulsions are considered as simple models of VLDL as they possess a phospholipid monolayer surrounding a neuteral triglyceride core.

Egg PC/TO microemulsions, of similar size to VLDL, were prepared in 0.15 M NaCl in D_2O at pD 7.4 as described by Tajima *et al.*, (1983) (see Materials and Methods). The microemulsion preparation was examined for vesicle contamination by high resolution ^1H NMR at 400 MHz. Phospholipid vesicles are enclosed bilayer structures. The polar head groups of phospholipid molecules face the aqueous phase while the hydrocarbon chains from the semi-permeable barrier.

Paramagnetic ions are routinely used as broadening and shift reagents to distinguish between the NMR signals arising from the phospholipid headgroups of the inner and the outer monolayer of vesicular structures. (Bystrov *et al* 1971, Bystrov *et al* 1972, Sheetz *et al* 1972, and Shapiro *et al* 1975). The paramagnetic ions most commonly used are the Mn^{2+}, Co^{2+}, Ni^{2+}, Eu^{3+} and Pr^{3+} ions. The Mn^{2+} ions have a broadening affect on the choline N-methyl proton resonance (Bystrov *et al* 1971), whereas the Eu^{3+} and Pr^{3+} ions cause the resonance to shift upfield and downfield, respectively (Bystrov *et al* 1971 and Bystrov *et al* 1972). Due to the low permeability of paramagnetic ions across the vesicle bilayer, resonances of

only the outer monolayer headgroups are affected while those of the inner monolayer remain unchanged. Egg PC/TO microemulsions, on the other hand, are monolayer structures. The phospholipid molecules in these structures surround the triglyceride core such that all of the phospholipid head groups are exposed to the aqueous phase.

The affect of broadening and shift reagents on the vesicle head groups is shown in Figure 47. The spectra in Figure 47a, d and g illustrate the choline N-methyl proton resonance of the inner (δ = 3.13 ppm) and outer (δ = 3.15 ppm) phospholipid headgroups in the absence of paramagnetic ions. The chemical shifts quoted are with respect to external DSS (Sodium 2,2-dimethyl-2-silapentane-5-sulphonate) standard. Addition of Mn^{2+} to the vesicle preparation caused the outer choline N-methyl proton resonance to broaden (Figure 47b) while the inner choline N-methyl resonance remained unaffected. At 2.07 x 10^{-4}M the outer peak broadens into the baseline (Figure 47c). These observations are in agreement with those reported by Bystrov *et al* 1971. Addition of Eu^{3+} to the vesicle preparation caused the outer choline N-methyl proton resonance to shift towards high field passing over the inner choline N-methyl proton resonance. At 4.17 x 10^{-4}M Eu^{3+} the two resonances are well resolved (Figure 47e). In order to demonstrate that only the outer peak was shifted, 1.76 x 10^{-4}M Mn^{2+} was added to the vesicle preparation containing the Eu^{3+} ions. The shifted, outer choline N-methyl proton resonance broadens in a manner similar to that observed in Figure 47b. The effects of Pr^{3+} are opposite to that observed with the Eu^{3+} ions. The outer choline N-methyl resonance shifts towards the low field end of the spectrum. Thus, addition of 3.33 x 10^{-4} M Pr^{3+} results in well separated proton resonances (Figure 47i).

Figure 47: ^1H NMR spectra of Choline N-methyl head groups of phospholipids in vesicles with Mn^{2+} (a), Eu^{3+} (b) and Pr^{3+} (c).

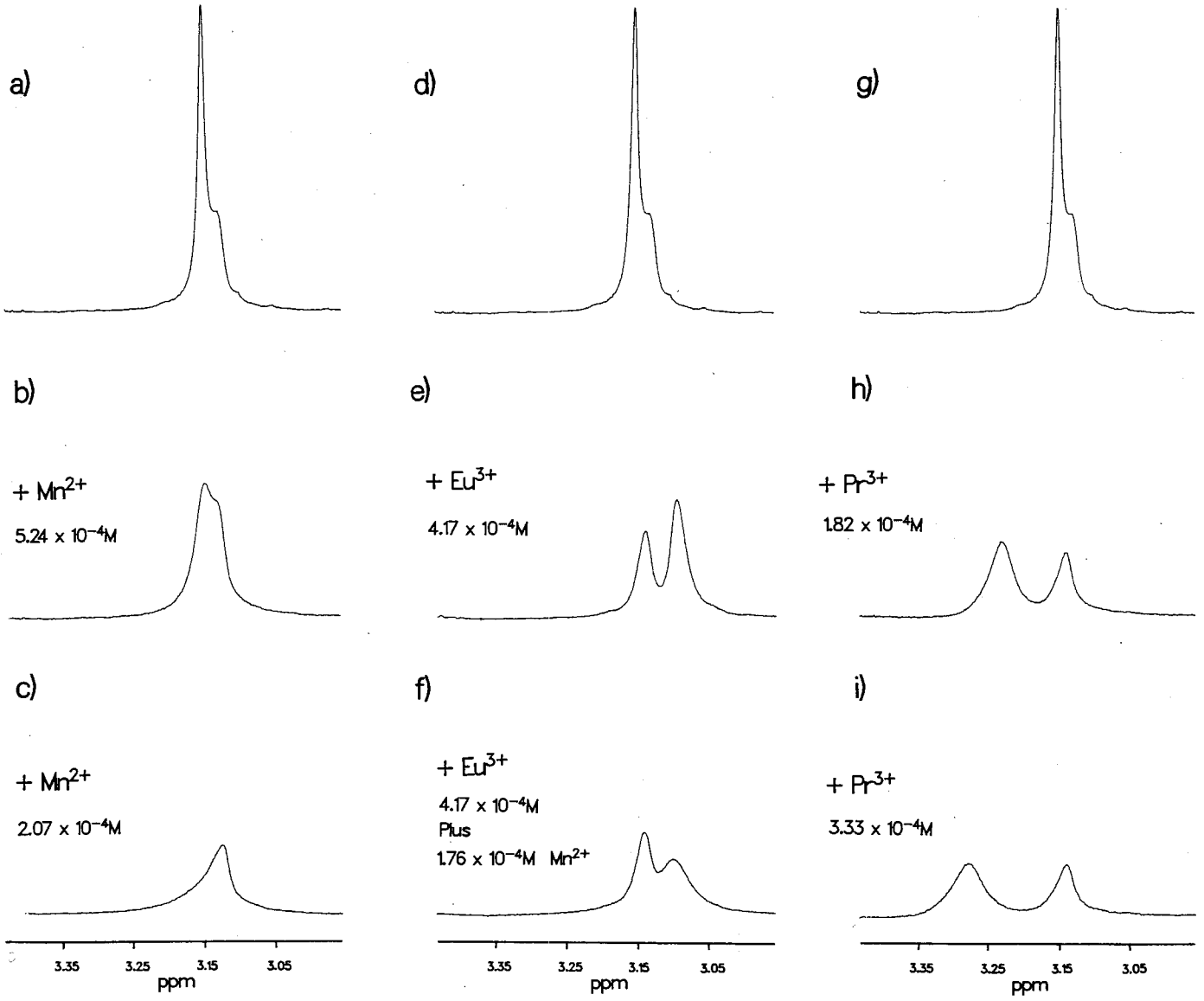
a)
d)
g)
b)
+ Mn^{2+}
5.24×10^{-4}M
e)
+ Eu^{3+}
4.17×10^{-4}M
h)
+ Pr^{3+}
1.82×10^{-4}M
c)
+ Mn^{2+}
2.07×10^{-4}M
f)
+ Eu^{3+}
4.17×10^{-4}M
Plus
1.76×10^{-4}M Mn^{2+}
i)
+ Pr^{3+}
3.33×10^{-4}M
3.35
3.25
3.15
3.05
ppm

The contamination of egg PC/TO microemulsion preparation by vesicles was investigated with broadening and shift reagents. Figure 48a, d and g shows the ^{1}H NMR spectrum of choline N-methyl protons of phospholipids in egg PC/TO microemulsions in the absence of paramagnetic ions. A series of Mn^{2+} ion concentrations added to the egg PC/TO microemulsion preparation resulted in the gradual broadening of the peak. At 6.75×10^{-4} M Mn^{2+} the peak totally broadens into the baseline of the spectrum (Figure 48c). Thus, from the Mn^{2+} ion study it appears that no bilayer contaminants (vesicles) were present in the preparation. However, this is not the case. Conclusive proof regarding this was obtained using the shift reagents Eu^{3+} and Pr^{3+}. Addition of Eu^{3+} causes choline N-methyl proton resonance to shift towards the high field end of the spectrum. At 9.26×10^{-4} M two peaks are observed (Figure 48f). The shifted peak is due to the outer choline N-methyl resonance since this peak broadens upon the addition of Mn^{2+}. The small non-shifting peak (Figure 48f) is due to the inaccessible inner choline N-methyl protons suggesting the coexistance of vesicular structures and microemulsions. The ^{1}H NMR spectrum in presence of Pr^{3+} ions also reveals two well resolved peaks (Figure 48i). The amount of vesicle contamination of the egg PC/TO microemulsion preparation was estimated (by cutting and weighing the respective peaks) to be $\simeq$10%. Thus, $\simeq$10% of ^{31}P NMR resonance in the microemulsion preparation is due to the vesicles. Such a small amount will have negligible effect upon viscosity measurements.

Figure 49 shows representative ^{31}P NMR spectra of egg PC/TO microemulsions in increasing concentrations of glycerol. The solid line represents the iterative least-squares fit of a Lorentzian lineshape function to the experimental data points (crosses). The ^{31}P NMR linewidths obtained from the spectra at the respective viscosities are given in Table

Figure 48: ^1H NMR spectra of Choline N-methyl head groups of phospholipids in egg PC/TO microemulsions with Mn^{2+} (a), Eu^{3+} (b) and Pr^{3+} (c).

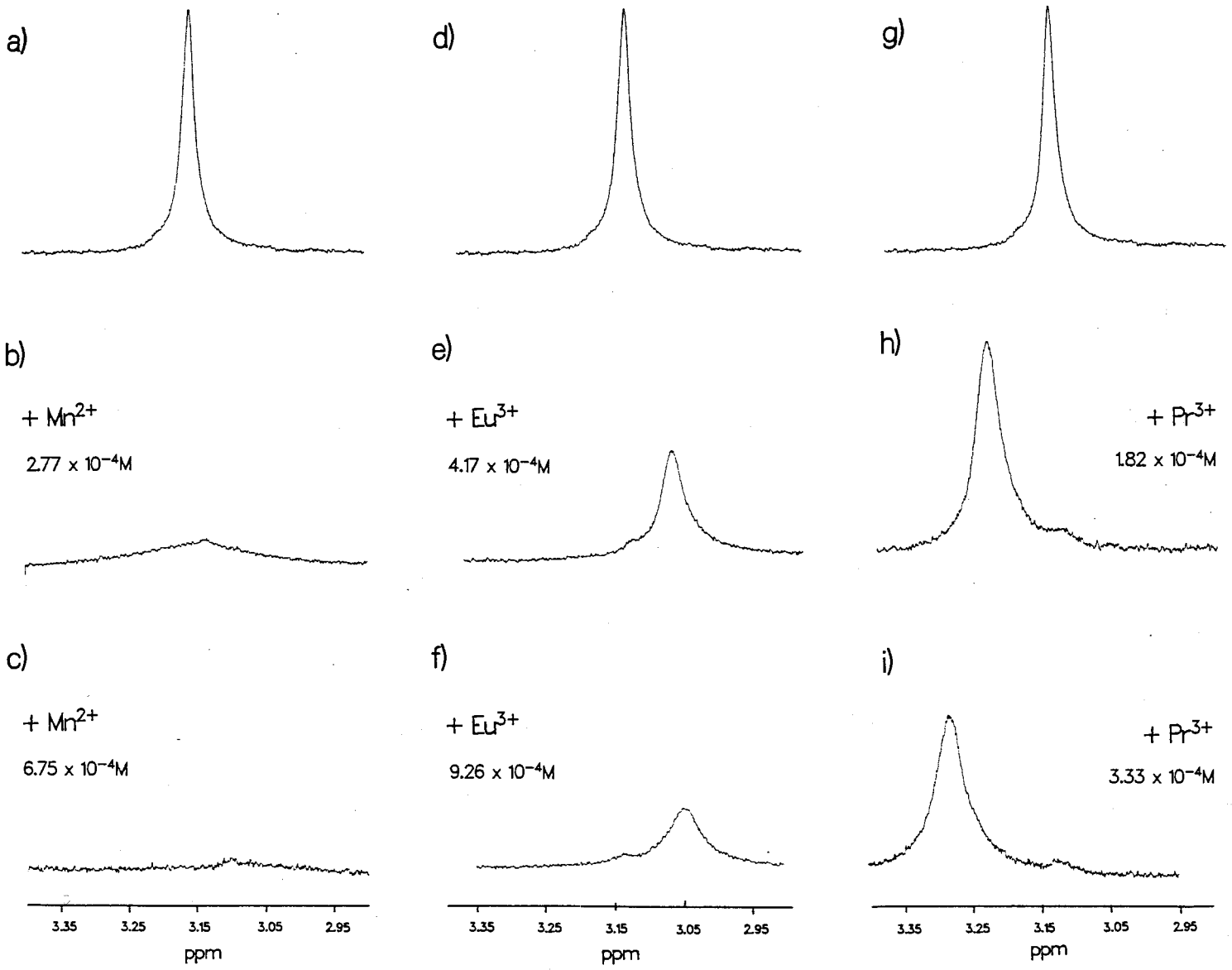
a)
d)
g)
b)
+ Mn^{2+}
2.77 x 10^{-4}M
e)
+ Eu^{3+}
4.17 x 10^{-4}M
h)
+ Pr^{3+}
1.82 x 10^{-4}M
c)
+ Mn^{2+}
6.75 x 10^{-4}M
f)
+ Eu^{3+}
9.26 x 10^{-4}M
i)
+ Pr^{3+}
3.33 x 10^{-4}M
3.35
3.25
3.15
3.05
2.95
ppm

Figure 49: Representative ^{31}P NMR spectra of egg PC/TO microemulsion in presence of increasing concentrations of glycerol at 25°C. The spectra are iterative least-squares fit to a Lorentzian lineshape function (solid line) to the spectral data points (crosses). The concentration of glycerol (weight-%) were 0 (a), approximately 36 (b), 56 (c) and 64 (d). Spectral parameters: pulse width = 5.0 μs (56° flip angle); sweep width = 20 KHz (a), 50 KHz (b-d); dataset = 4k zerofilled to 8k; number of acquisitions = 2,300 (a), 10,000 (b-d); delay between pulses = 1.5 s; linebroadening = 10 Hz (a), 20 Hz (b-d); delay before acquisition 10 μs. For a clear representation of the fits every 3rd (spectra a-d) spectral data points are shown.

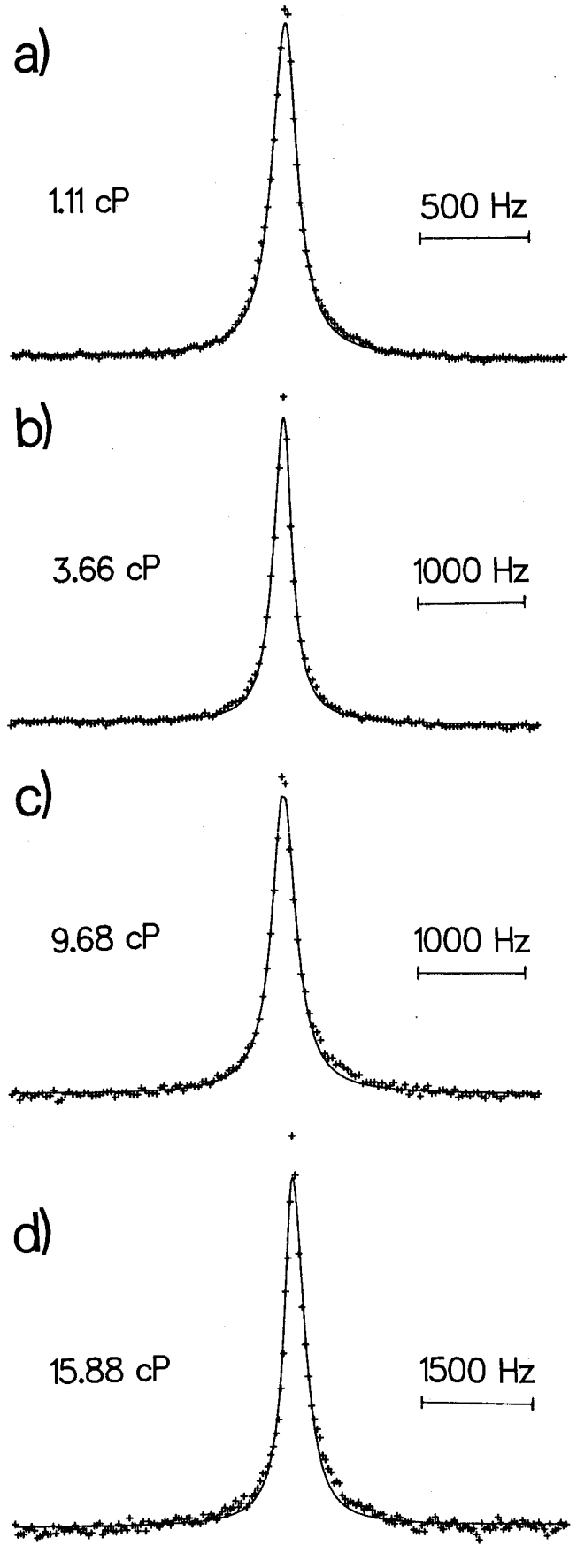
a)
1.11 cP
500 Hz
b)
3.66 cP
1000 Hz
c)
9.68 cP
1000 Hz
d)
15.88 cP
1500 Hz

Table 23: ^{31}P NMR Linewidths of egg PC/TO microemulsions as a function of glycerol concentration at 25°C.

% Glycerol	Viscosity (cP)	linewidth (Hz)
0	1.11	138
10	1.50	140
20	2.10	189
28	2.66	215
36	3.66	211
46	5.69	242
56	9.68	276
64	15.88	323
68	21.01	376
72	28.96	409

The linewidth measurements have approximately ±10% uncertainty.

23. A plot of $(\Delta\nu_{1/2} - C)^{-1}$ versus η^{-1} is shown Figure 50. From the ratio of intercept to slope, together with the size of microemulsions (Radius = 24.15 nm), determined from quasielastic light scattering, we calculate D_t = 2.5±0.4 x 10^{-8} cm²/s. The D_t value of the microemulsions is similar in magnitude to that determined for egg PC vesicles (2.6 x 10^{-8} cm²/s) at 50°C (Cullis, 1976). Using equations 29 and 30 we have determined the $\Delta\sigma$ of 28±1 ppm. Both the D_t and $\Delta\sigma$ values of egg PC/TO microemulsion are in excellent agreement with those measured for egg PC vesicles (Cullis, 1976; MacLaughlin *et al.*, 1975).

Figure 50: Plot of $(\Delta\nu_{1/2} - C)^{-1}$ versus η^{-1} for the ^{31}P NMR linewidths of egg PC/TO microemulsions at 25°C. The straight line is a weighted least-squares fit to the data points.

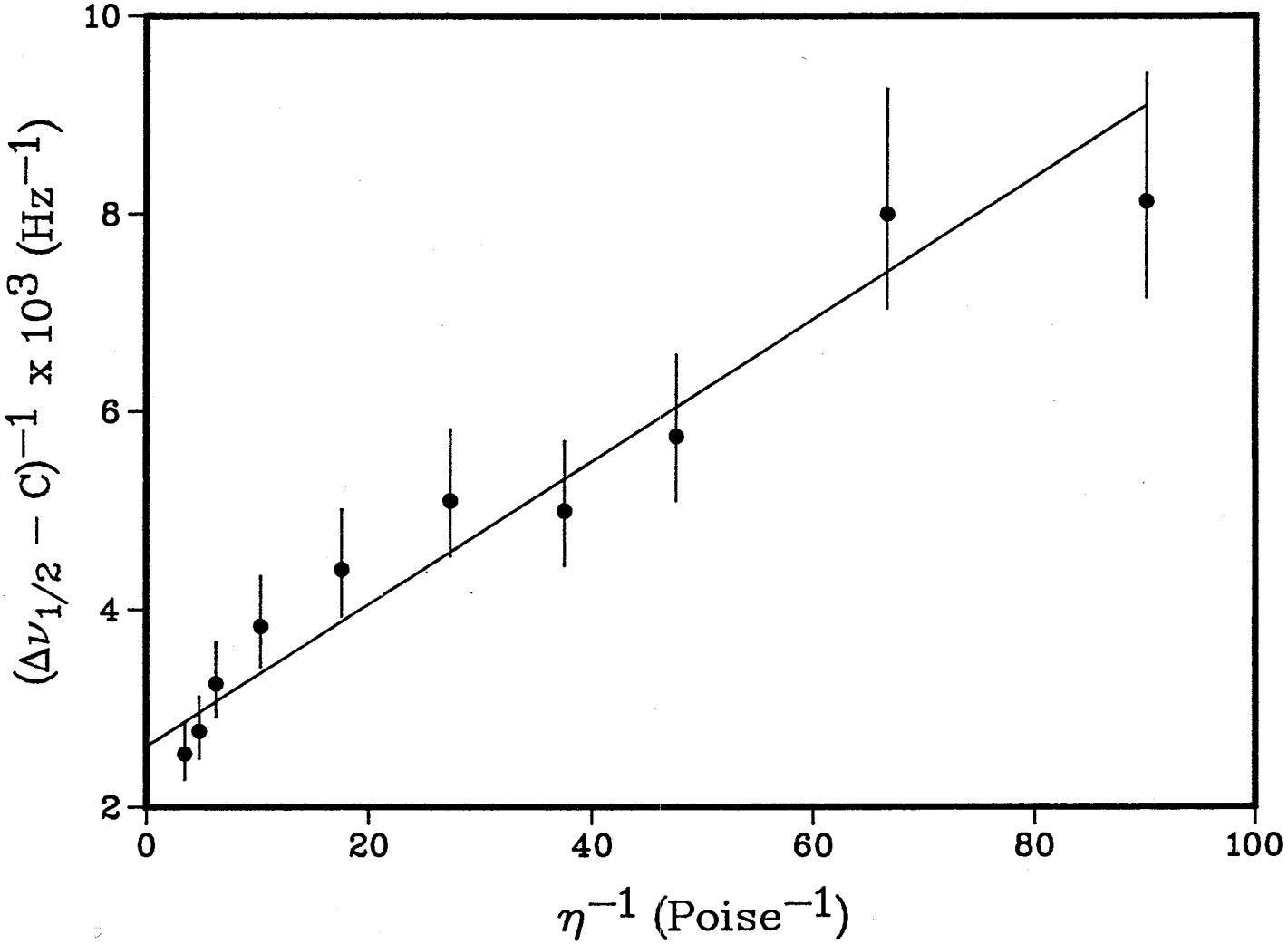
10
8
6
4
2
0
20
40
60
80
100
$(\Delta\nu_{1/2} - C)^{-1}$ x 10^3 (Hz^{-1})
η^{-1} (Poise^{-1})

Table 24: Comparison of D_t and $\Delta\sigma$ for Human Serum Lipoproteins, Microemulsions and Phospholipid Bilayers.

Lipoprotein	T (°C)	D_t (cm^2/s)	$\Delta\sigma$ (ppm)	
			viscosity	field-dependence
VLDL	25	(9.1±1.0) $x10^{-9}$ *	47±1	46±0.5
VLDL	40	(1.2±0.2) $x10^{-8}$ *	41±1	
LDL	25	(1.4±0.5) $x10^{-9}$ a	49±1[b]	50±4[b]
LDL	45	(1.1±0.2) $x10^{-8}$ b	52±2[b]	
HDL_2	25	(1.8±0.3) $x10^{-8}$ a	75±10[d]	≃69[d]
HDL_3	25	(2.3±0.8) $x10^{-8}$ b	136±11[b]	156±2[b]
egg PC/TO microemulsions	25	(2.5±0.4) $x10^{-8}$ *	28±1	
egg PC/vesicles	30		45[e]	
egg PC/vesicles	50	2.6 $x10^{-8}$ c	32[e]	
DPPC liposomes	30		56±10[e]	
DPPC liposomes	50		45±10[e]	

a Cushley *et. al* (1987).
b Fenske (1988b).
c Cullis (1976).
d Parmar (1985).
e McLaughlin *et. al* (1975).
* This work.

DISCUSSION

The values of D_t and $\Delta\sigma$ of VLDL and egg PC/TO microemulsions are presented in Table 24. For comparison purposes, D_t values of LDL, HDL_2, HDL_3 and phospholipid bilayers are also included. From Table 24 it is observed that the diffusion of the egg PC/TO microemulsions (D_t = 2.5 x 10^{-8} cm^2/s) is similar to that found in egg PC vesicles at 50°C (D_t = 2.6 x 10^{-8} cm^2/s; Cullis,1976), and agrees with those reported for the phospholipid bilayer structures where the D_t values range from (1-7) x 10^{-8} cm^2/s (MacKay *et al.*, 1978 and references therein). The diffusion of protein-free microemulsions is also in good agreement with those found in smaller, protein-rich, HDLs (Table 24) but significantly faster than those found in VLDL and LDL.

The D_t value of (9.1±1.0) x10^{-9} cm^2/s for VLDL particles at 25°C (Table 24) is ≃3 times slower than the corresponding value of egg PC/TO microemulsions and ≃2 times slower than that found in HDLs. The slower diffusion in VLDL particles compared to egg PC/TO microemulsions, vesicles and HDLs can be explained by the presence of cholesterol. Approximately 67-82% of the cholesterol in VLDL is associated with the phospholipid-protein monolayer (Eisenberg *et al.*, 1979). The ratio of cholesterol to phospholipid in the VLDL studied is 0.27 (Table 19) while that in HDL_2 and HDL_3 is less than 0.15 (Shen *et al.*, 1977). The effect of cholesterol on phospholipid diffusion in egg PC vesicles has been investigated by ^{31}P NMR (Cullis, 1976). That study showed that the diffusion of phospholipid molecules decreased by approximately two-fold in the presence of 30 mol % cholesterol *i.e* the D_t value of 2.6x10^{-8} cm^2/s falls to 1.4x10^{-8} cm^2/s, while further addition, up to 50 mol %, had no

substantial effect. Similar effects of high cholesterol concentration on phospholipid diffusion have also been observed by other investigators (Fahey *et al.*, 1977; Wennerstrom and Lindblom, 1979; Rubenstein *et al.*, 1979; Kuo and Wade. 1979). For instance, Kuo and Wade (1979) utilizing orientated samples of egg PC and dilaurylphosphatidylcholine (DLPC) showed a reduction in phospholipid diffusion by 50% and 40%, respectively, following the addition of 30 mol % cholesterol. Cholesterol is also known to have opposite effects on phospholipid diffusion. For instance, at <10 mol % cholesterol phospholipid diffusion in DPPC bilayers was observed to increase (Kuo and Wade, 1979). Thus, from the above considerations, the presence of ≃40 mol % cholesterol in the surface monolayer of VLDL is predicted to lower the diffusion rate compared to its model structure where no cholesterol is present.

The diffusion in the surface monolayer of LDL, D_t = (1.4±0.5) x10^{-9} cm^2/s, is approximately an order of magnitude slower than that found in microemulsions or HDLs. The slower diffusion cannot be explained by the consideration of cholesterol alone since, cholesterol to phospholipid ratio in LDL is about the same as that found in VLDL. The slower diffusion compared to those found to other lipoproteins has been explained in terms of the structural features unique to LDL (Cushley *et al.*, 1987; Fenske. 1988b). At 45°C, however, the diffusion in LDL increased by approximately an order of magnitude (Table 24). The increase corresponded with the melt of the core such that the slower diffusion observed at 25°C was suggested to be due to the possible monolayer/core interactions since, at this temperature the core CEs are in the midst of their phase transition. An order of magnitude increase in diffusion has also been observed in DPPC vesicles at the gel to liquid crystalline state of the lipids (Cullis,

1976). Furthermore, the diffusion essentially remained unchanged either above or below the gel to liquid crystalline phase transition (Cullis, 1976). At 40°C, there is a marginal incease in phospholipid diffusion in VLDL (D_t = (1.2±0.2) x10^{-8} cm²/s,) suggesting that both the phospholipids and core triglycerides are in their liquid crystalline state. Furthermore, the effect of monolayer/core interactions on phospholipid diffusion in VLDL are expected to be equivalent at both study temperatures.

The residual ^{31}P chemical shift anisotropy, $\Delta\sigma$, of human serum lipoproteins, egg PC/TO microemulsion and phospholipid bilayer dispersions are presented in Table 24. From Table 24 it is seen that there is a dramatic increase in the $\Delta\sigma$ values from the egg PC/TO microemulsion (28 ppm) to VLDL and LDL (47 and 50 ppm, respectively) to HDL_2 (≃72 ppm) and finally to HDL_3 (≃146 ppm). Similar changes, though not as dramatic, are also obsevered in phospholipid bilayer structures (Table 24).

In the case of phospholipid multilamellar dispersions, $\Delta\sigma$ values are known to vary according to the type of phospholipid head groups, the gel-to-liquid crystalline phase transition and the degree of hydration of the phospholipid molecules (Seelig, 1978). Other factors which may also cause the $\Delta\sigma$ values to change are the surface curvature and the lipid-protein interactions. All of these factors may then reflect the differences in the conformation and/or the order of the phosphate segment in the head groups.

In the case of DPPC in excess water, Griffin *et al* (1978) have shown that, at -10°C, the $\Delta\sigma$ value decreases from 69 to 47 ppm at 48°C. The decrease in the $\Delta\sigma$ value has been explained in terms of the rapid reorientation about the long phospholipid axis which is parallel to the

bilayer normal, and segmental motions especially about the C(2)-C(3) bond of the glycerol backbone (Seelig and Gally, 1976). Similar motional models have also been used to explain the temperature dependence of the axially symmetric spectra of multilamellar dispersions of DPPE, DPPC and DPPS. In addition to the rapid reorientation, and a wobble about the bilayer normal, other models consider motions about the P-O(11) and C(1)-C(2) bonds to predict the lineshapes of many experimentally observed spectra (Kohler and Klein, 1977; Thayer and Kohler, 1981).

The headgroup conformation of the phosphate segment in the phospholipid bilayers has been examined by ^{31}P NMR, X-ray, and neutron diffraction studies. The ^{31}P NMR studies with orientated multibilayers of DPPC.H_2O have shown that the PO_4^{2-} is tilted with its O(3)-P-O(4) plane (where O(3) and O(4) refer to the nonesterified oxygen atoms) at approximately 47±5° with respect to the bilayer plane and the choline moiety is extended parallel to the bilayer surface (Griffin *et al.*, 1978). Further support for a tilted headgroup conformation and an extended choline moiety comes from the X-ray analysis of single crystals of PC (Pearson and Pascher, 1979) and neutron diffraction studies of fully hydrated DPPC bilayers (Buldt *et al.*, 1978; 1979).

A theoretical study by Thayer and Kohler (1981) has shown that $\Delta\sigma$ values can be altered drastically in PE multilamellar dispersions with the rotation about the C(1)-O(2) bond. Rotation about this bond cause the head group conformations to change with respect to the bilayer plane such that the resulting spectra have lineshapes that commonly observed in bilayers: hexagonal II phase or isotropic phase. For instance, at a torsional angle, ϕ = -116.9°, an axially symmetric spectrum is observed with $\Delta\sigma$ = -47 ppm,

at ϕ = -100.3° a narrow lineshape is observed reminiscient of lipids in an isotropic phase and at ϕ = -93.4° a typical hexagonal II phase spectra is observed $\Delta\sigma$ = 18.1 ppm.

The $\Delta\sigma$ value of VLDL = 47±1 ppm, from viscosity dependence, and 46±0.5 ppm, from field dependence, are in excellent agreement with those found in multilamellar phospholipid dispersions in their liquid crystalline state (45±5 ppm; Seelig, 1978). Hence, we propose similar motional behaviour of VLDL phospholipids as found in the phospholipid multilamellar dispersions. Furthermore, since the tilted headgroup conformation of the DPPC bilayer is consistant with $\Delta\sigma$ = 47 ppm, a similar tilted head group conformation is predicted for VLDL phospholipids. Further support for the tilted head group conformation in VLDL comes from the ^{31}P NMR studies of LDL, a metabolic product of VLDL, with $\Delta\sigma$ = 50 ppm. A $^{31}P\{^{1}H\}$nuclear Overhauser effect (NOE) study has shown that the positively charged N-methyl moiety is located near the negatively charged phosphate of the neighbouring phospholipid, indicating that the head group is tilted and the choline moiety is extended parallel to the lipoprotein surface plane (Yeagle *et al.*, 1977).

The change in headgroup conformation was assessed by employing the axially symmetric shielding tensors and Euler angles of PE (Thayer and Kohler, 1981) and principal components of DPPC (σ_{11} = -87, σ = -25 and σ = 119) (Kohler and Klein, 1977). Our results show that there is a progressive change in the headgroup conformation from roughly parallel to the monolayer surface in VLDL to approximately perpendicular to the monolayer surface in HDL_2 and HDL_3. However, as indicated by Thayer and Kohler other more complicated motional models could equally predict similar $\Delta\sigma$ values for different headgroup conformations that caution must be excercised when

using ^{31}P NMR data to predict the headgroup conformation.

A progressive change in $\Delta\sigma$ value from microemulsions to VLDL and finally to HDLs may be explained by considering the compositional differences between the monolayer surfaces. The surface monolayer of egg PC/TO microemulsions is composed of egg PC whereas that of VLDL also contains SPM, cholesterol and apoproteins, whose presence may influence the headgroup conformation. In the case of smaller HDL particles high curvature may also be of importantance since, it may force the phospholipid headgroups to adopt different conformations in relation to those found in phospholipid bilayers.

The effect of SPM and cholesterol on headgroup conformation are expected to be small. The ratio of SPM and cholesterol to phospholipids in VLDL is 0.14 and 0.27, respectively, and in LDL is 0.40 and 0.27, respectively, and yet, both particles exhibit essentially similar $\Delta\sigma$ values. The respective ratios in HDLs are small (0.15 and 0.12) and yet the $\Delta\sigma$ are large. Addition of SPM, up to 50 mol %, to 1-palmitoyl-2-oleoyl-*sn*-glycero-3-phosphocholine dispersions, deuterated at the α and β position of the choline moiety, had very little effect on the ^{2}H quadrupolar splittings suggesting that SPM had essentially no influence on the choline headgroup (Scherer and Seelig, 1987). The effects of cholesterol have been analysed by ^{2}H and ^{31}P NMR. Studies with multilamellar dispersions of $^{+}NCH_2CD_2$-DPPC with and without cholesterol (50 mole%), showed very little change in either the $\Delta\sigma$ value or in the ^{2}H quadrupolar splitting (Brown and Seelig, 1978). With $^{+}NCD_2CH_2$-DPPC, the quadrupolar splitting was reduced by $\simeq$2 times while the $\Delta\sigma$ value remained unaffected. The reduction in quadrupolar splitting was explained by

considering the change in the torsional angle about the C_α-C_β linkage (Brown and Seelig, 1978). Other studies utilizing $^{31}P\{^1H\}$ NOE have also failed to demonstrate the influence of cholesterol on PC headgroups in multilamellar dispersions (Yeagle *et al.*, 1975; 1977).

The change of headgroup conformation could result from the lipid-protein interactions. The weight-% of protein increases as the lipoprotein size decreases (see Table 1). Furthermore, the type and % composition of apoproteins also varies in each class of lipoprotein. The three common apoproteins in VLDL are apo-B, apo-E and apo-Cs and together they represent ≃10% of the particle by weight. Apoproteins are surface bound (Shen *et al.*, 1978) and since most of them possess charged amino acid side-chains it is possible that they may electrostatic interact with polar groups of lipids. An increase of ≃20 ppm from the protein free microemulsions to VLDL certainly suggests that lipid-protein interactions are influencing the headgroup conformations at the VLDL surface. Such interactions, if present, appear more likely in smaller HDLs where the protein/phospholipid ratio is high. A space filling model study has proposed that the polar faces of apoproteins (apo-Cl and apo-CII, apoproteins of VLDL) would allow electrostatic interactions with the zwitterionic phospholipids (Segrest *et al.*, 1974). Unfortunately, such electrostatic interactions have not been substantiated experimentally. Both ^{31}P and ^2H NMR studies of specifically deuterated phospholipid head groups in the biological and reconstituted membrane systems containing either intrinsic or extrinsic membrane proteins have shown negligible effects of proteins on the $\Delta\sigma$ and quadrupolar splitting values (Sixl *et al.*, 1984; Dempsey *et al.*, 1986; Ryba *et al.*, 1986; Seelig *et al.*, 1986; Watts, 1987). The ^2H NMR studies have shown that the quadrupolar splittings of the

head group and the fatty acyl chains broaden slightly compared to multilamellar dispersions having no proteins. Although the origins of such effects are not well understood. ^{2}H relaxation time measurements suggest that proteins tend to slow down the overall reorientation rate of phospholipid molecules but do not appear to involve in large-scale conformational changes (Watts, 1987). Unlike integral and peripheral proteins, apoproteins have amphipathic helical regions and as a result permit lipid-protein interactions (Segrest *et al.*, 1974).

The dynamics of phospholipid molecules across the surface monolayer of lipoproteins, as measured by ^{31}P NMR, varies for each class in spite of the fact that they all share a common underlying structure. Each lipoprotein class varies with respect to D_t and $\Delta\sigma$. VLDL displays slower diffusion and marginally higher $\Delta\sigma$ values than those found in egg PC/TO microemulsions, models of VLDL. These differences have been explained in terms of lipid-lipid and lipid-protein interactions.

CHAPTER VI

ORGANIZATION OF CHOLESTERYL ESTERS IN MEMBRANES

Selectively deuterated cholesterols and cholesteryl palmitates in multilamellar dispersions of DPPC at 45°C

RESULTS

Both cholesterol and cholesteryl esters are widely distributed lipids in biological membrane and lipoprotein systems. A number of studies have looked at the effects of these constituents on the membrane organization, and in general have focused attention on the phospholipid hydrocarbon chains rather than sterol moiety. In our study we have investigated the orientational order of the cholesterol moiety of several selectively deuterated cholesteryl palmitates in multilamellar dispersions of dipalmitoylphosphatidylcholine (DPPC), and compared the results with the orientational order of cholesterol under similar conditions.

The ^2H NMR spectra of 7.6 mol% [3-$^2H_1$]cholesterol in multilamellar dispersions of DPPC bilayers at 45.0±0.5°C, above the gel to liquid crystalline phase transition of the phospholipid, is shown in Figure 51A. The spectrum has a quadrupolar splitting $\Delta\nu_Q$ of 40.5 kHz. The central peak is due to the residual deuterium in water. The [3-$^2H_1$]cholesterol quadrupolar splitting is slightly smaller than in egg PC bilayers at an equimolar ratio (Taylor *et al.*, 1981).

The powder spectrum of 8.0 mol% [2,2,4,4,6-$^2H_5$]cholesterol in multilamellar dispersions of DPPC at 45.0±0.5°C is shown in Figure 52A. The

Figure 51: ^2H NMR spectra of 7.6 mol% [3-$^2H_1$]cholesterol and 4.5 mol% [3-$^2H_1$]cholesteryl palmitate in DPPC multilamellar dispersions at 45°C. The Fourier transforms spectra were obtained from 4K data sets. Spectral width = 200 kHz; plot width = 100 kHz; number of scans = 720,000 (A), 2,040,000 (B); line broadening = 100 Hz in both.

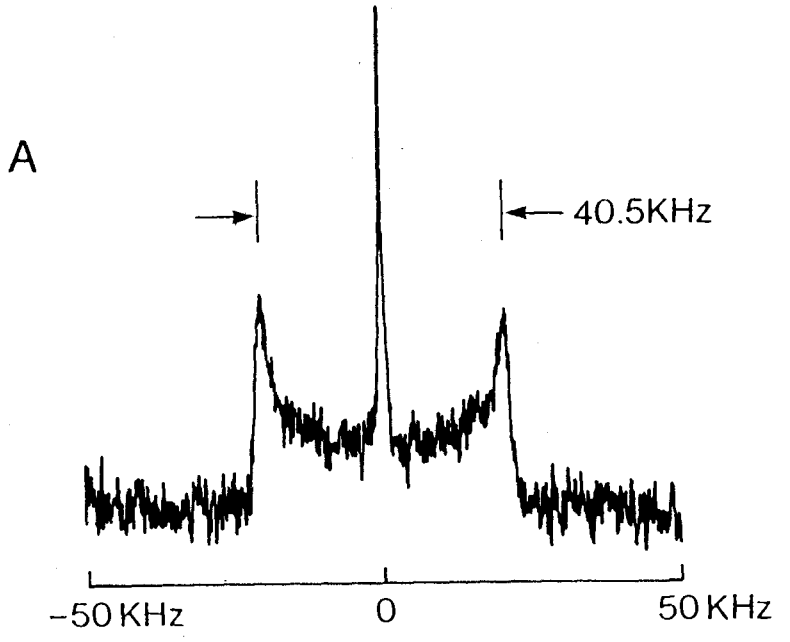
A
40.5KHz
-50 KHz
0
50 KHz

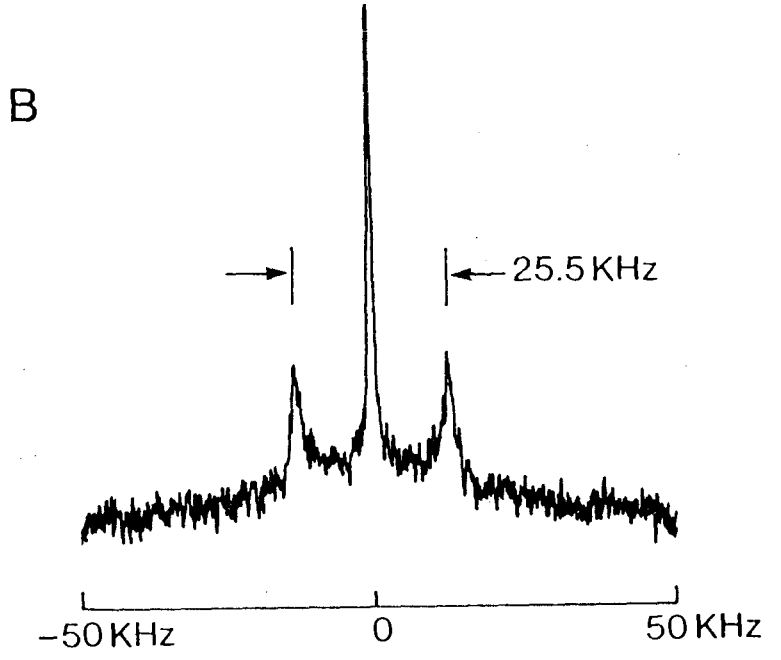
B
25.5 KHz
-50 KHz
0
50 KHz

spectral peaks, including axial and equitorial positions were assigned accroding to the calculations described below. The assignments corresponds to that of Taylor *et al.*, 1981, and Dufourc *et al.*, 1984. The quadrupolar splittings are listed in Table 25.

The ^2H NMR spectra of ≃4.5 mol% [3-$^2H_1$]cholesteryl palmitate and ≃4.8 mol% [2,2,4,4,6-$^2H_5$]cholesteryl palmitate in multilamellar dispersions of DPPC at 45.0±0.5°C are shown in Figures 51B and 52B, respectively. The quadrupolar splittings of the esters are considerably smaller in value (except those of the 6-position) than those of the unesterified cholesterol. The quadrupolar splittings are listed in Table 25. The splittings of the deuterons at the 6-position were estimated from the width of the central component and, to indicate the uncertainty, are entered as a range of values.

The ^2H NMR spectra of 7.6 mol % [7,7-$^2H_2$]cholesterol and ≃4.5 mol % [7,7-$^2H_2$]cholesteryl palmitate [1] in DPPC multilamellar dispersions are shown in Figure 53A and 53B, respectively. There are two splittings for the cholesteryl ester, indicating that the two C-^2H bonds are inequivalent. The values of the quadrupolar splittings found in Figure 53 are listed in Table 25.

---

[1] The bilayers are saturated in cholesteryl ester. In a previous study, the preparation of multilamellar dispersions of DPPC with ≃5 mol % cholesteryl palmitate added, only ≃0.5mol % is incorporated into the bilayer at 50°C (Gorrissen *et al.*, 1981) and we assume this to be the saturating level

Figure 52: ^2H NMR spectra of 8.0 mol% [2,2,4,4,6-$^2H_5$]cholesterol (A) and 4.8 mol% [2,2,4,4,6-$^2H_5$]cholesteryl palmitate in DPPC multilamellar dispersions at 45°C. The Fourier transforms spectra were obtained from 4K data sets. Spectral width = 200 kHz; plot width = 100 kHz; number of scans = 200,000 (A), 1,100,000 (B); line broadening = 100 Hz (A), 200 Hz (B).

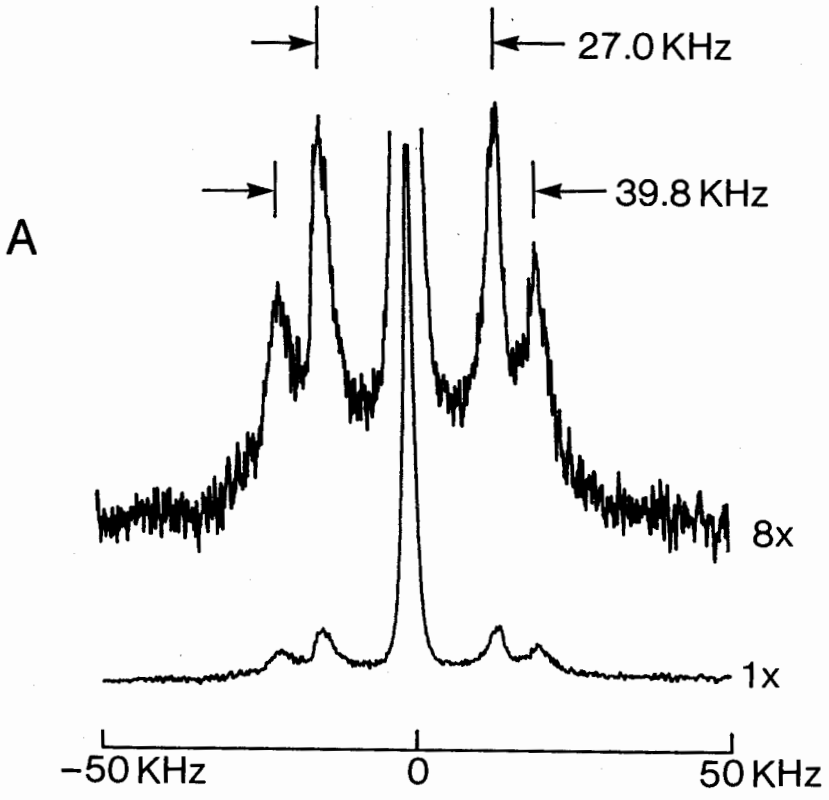
A
27.0 KHz
39.8 KHz
8x
1x
−50 KHz
0
50 KHz

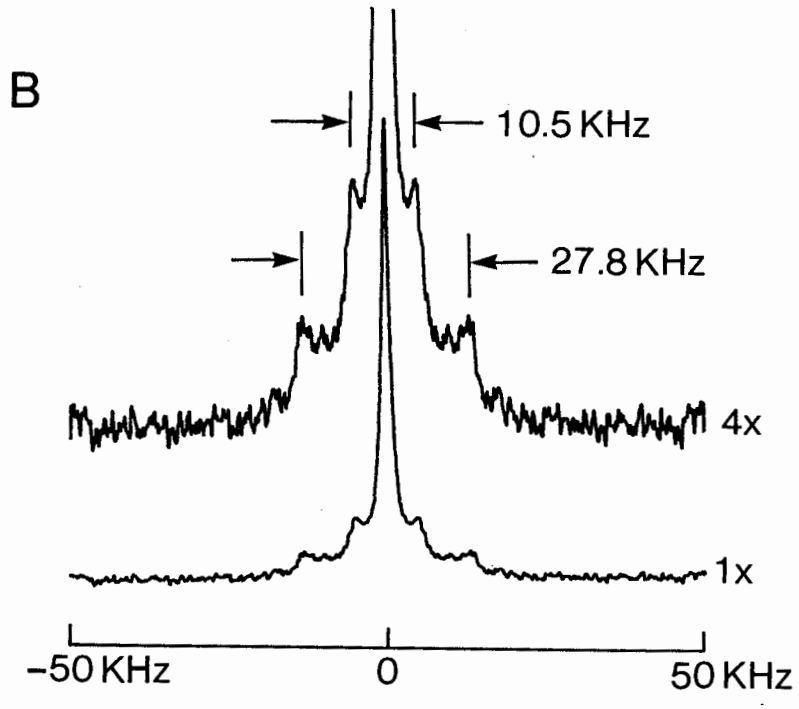
B
10.5 KHz
27.8 KHz
4x
1x
−50 KHz
0
50 KHz

Figure 53: ^2H NMR spectra of 7.6 mol% [7,7-$^2H_2$]cholesterol (A) and 4.5 mol% [7,7-$^2H_1$]cholesteryl palmitate (B) in DPPC multilamellar dispersions at 45°C. The Fourier transforms spectra were obtained from 4K data sets. Spectral width = 200 kHz; plot width = 100 kHz; number of scans = 1,200,000 (A), 1,500,000 (B); line broadening = 300 Hz in both.

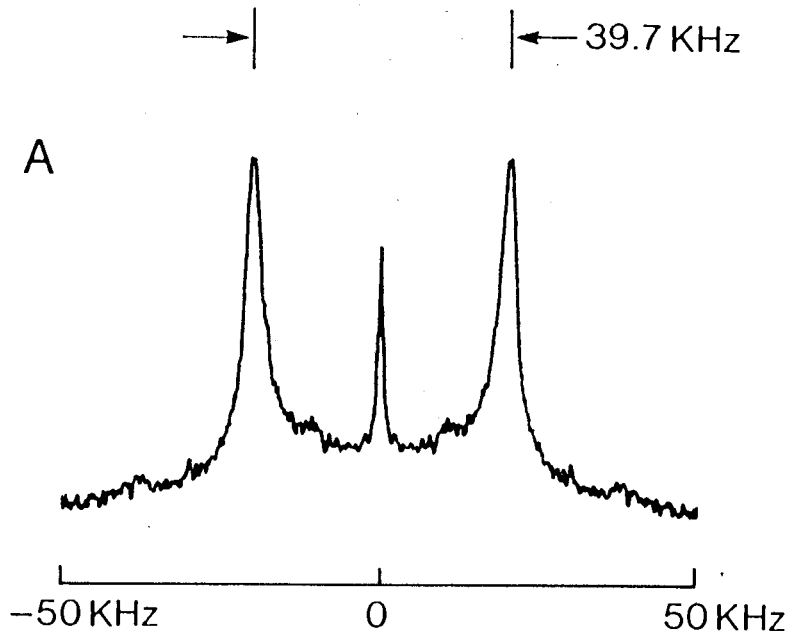
39.7 KHz
A
−50 KHz
0
50 KHz

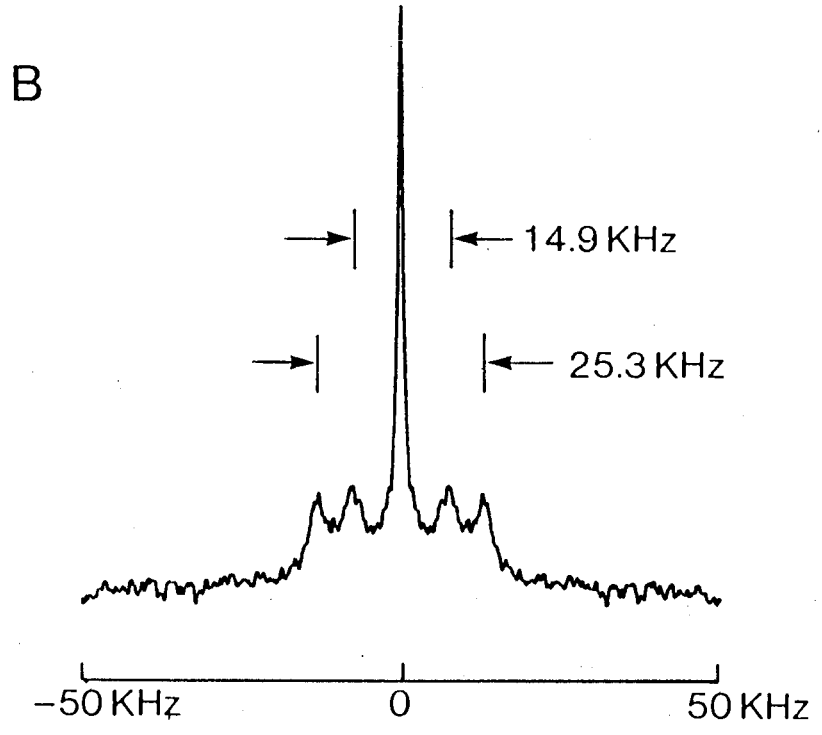
B
14.9 KHz
25.3 KHz
−50 KHz
0
50 KHz

Table 25: Quadrupolar splittings of selectively deuterated cholesterol and cholesteryl palmitate in multilamellar dispersions of DPPC at 45.0±0.5°C (kHz).

Labelled carbon position	Cholesterol	Cholesteryl palmitate
$[3\text{-}^2H_1]_{ax}$	40.5±2.1	25.5±1.2
$[2,4\text{-}^2H_2]_{ax}$	39.8±1.7	27.8±0.7
$[2,4\text{-}^2H_2]_{eq}$	27.0±2.0	10.5±0.5
$[6\text{-}^2H_1]$	0.5-1.8	0.5-2.4
$[7\text{-}^2H_1]_{eq}$	39.7±1.9	25.3±1.9
$[7\text{-}^2H_1]_{ax}$	39.7±1.9	14.9±1.6

DISCUSSION

The quadrupolar splitting of a C-^{2}H bond attached to the fused rings of cholesterol or cholesteryl palmitate is determined by the average orientation of this bond with respect to the axis of rotational diffusion and by the fluctuations in time of this axis, the 'wobbling' of the steroid skeleton, with respect to the director of the mesophase (cf. Theory). In other words, the quadrupolar splitting has contributions from the ordering (S_a) and the orientation (S_γ'). A change in quadrupolar splitting may therefore be due to a change in the extent of angular fluctuations undergone by the reporter molecule (ordering or disordering) and/or to a modification of the position of the rotational diffusion axis of the rigid unit bearing the C-^{2}H bond. From Table 25 it is observed that

the quadrupolar splittings of deuterated cholesteryl palmitate are smaller in all cases, except at the [6-$^2H_1$] position where it is equal, compared to those of cholesterol in the same model membrane at the same temperature. If this were due only to a decrease in S_a, all the cholesteryl palmitate $\Delta\nu_Q$ values would have a constant ratio with respect to cholesterol. From the data shown in Table 25 it is observed that the relative magnitude of quadrupolar splitting changes from cholesterol to cholesteryl palmitate. For instance, the ratio of $\Delta\nu_Q$'s for $[3\text{-}^2H_1]_{ax}$ position in cholesterol and cholesteryl palmitate is 1.59, whereas the ratio for the $[2,4\text{-}^2H_2]_{eq}$ and $[2,4\text{-}^2H_2]_{ax}$ positions are 2.57 and 1.43, respectively. In the cases of C7-position only one quadrupolar splitting is observed for cholesterol and two for cholesteryl palmitate. This later effect could arise from two different configurations of cholesteryl palmitate in membrane which are in slow exchange on the ^2H NMR timescale. If this was the case, then similar situations would be observed for other positions, especially in experiments with [3-$^2H_1$]-labelled molecules. This was not detacted in our data. The more likely explanation of these observations is that the axis of rotational diffusion occupies different positions in the fused ring systems of cholesterol and cholesteryl palmitate, in DPPC membrane. Similar observations have been reported for β-cholesterol and α-cholesterol in dimyristoylphosphatidylcholine (DMPC) by Dufourc *et al.*, 1984.

The procedure employed to quantitate the axis of rotational diffusion follows the description of Dufourc (1984). The calculations reported in this section were performed by Dr. E. J. Dufourc, present address. Centre de Recherche Paul Pascal, Domaine Universitaire, 33405 Talence Cedex, France. A brief outline of the method and the resulting calculations used for β-cholesterol and cholesteryl palmitate will be presented.

The coorinate system, $\zeta(x,y,z)$, attached to the fused ring system is that of Dufourc *et al.*, 1984; *i.e*, $\zeta(x, y, z)$ is defined as a Cartesian axis system such that the x-axis is colinear with the C_3-axial bond and z-axis lies in the HO-C_3-H plane. The atomic coordinates of both carbon and hydrogen atoms and, hence, the directional cosines of C-^{2}H bonds in ζ system, have been extracted from the fractional atomic coordinates of cholesteryl laurate (Sawzik and Craven. 1980).

The axis of the fused rings of cholesterol and cholesteryl palmitate, $\vec{n}$, about which rotational averaging takes place is defined in the axis system ζ as $\vec{n}$ = (cosγsinβ, sinγ sinβ, cosβ). From the well-known property of the scalar product of two vectors, the angle $\gamma'_{i,n}$ that an individual $C\text{-}^2\vec{H}_i$ bond vector makes with $\vec{n}$ is defined as:

$$\|\overrightarrow{C\text{-}^2H_i}\|\|\vec{n}\|\cos\ \gamma'_{i,n} = \overrightarrow{C\text{-}^2H_i}\ .\ \vec{n}$$

where $\|\overrightarrow{C\text{-}^2H_i}\|$ represents the magnitude of the vector $\overrightarrow{C\text{-}^2H_i}$. Since the directional cosines of each C-^{2}H bond are known, one sees that for given values of β and γ one can obtain $(3\cos^2\gamma'_{i,n} - 1)/2$ terms which can be compared with the experimental terms, $S_{\gamma'} = (3\cos^2\gamma'_{i,n} - 1)/2$. The method of comparison has been described elsewhere (Dufourc *et al.*, 1983, Appendix B). The position of the axis of motional averaging for the rigid steroid moiety is then sought by varying the angles β and γ. Once the correct orientation of $\vec{n}$ has been defined with respect to ζ by certain value of β and γ, $S_{\gamma'}$ is known for a given C-^{2}H bond and S_a can thus be obtained from equation 11. It is worthwhile mentioning that this approach assumes that the angular fluctuations of the axis of rotational diffusion of the fused ring system possess axial symmetry. When there was ambiguity in the assignment of a quadrupolar splitting to a given C-^{2}H bond, *e.g.* $C_{24}\text{-}_{ax}$ and $C_{24}\text{-}_{eq}$ or

C_7-$_{ax}$ and C_7-$_{eq}$, all posible combinations of splittings and C-^{2}H directional cosines were considered during the calculation. The quadrupolar splitting at C_6, when added in the calculation, induced large uncertainties and was therefore dicarded. It is easily seen that, due to the closeness of the C_6-^{2}H bond to the magic angle, even small inaccuracies in the atomic coordinates of this bond will lead to important changes in the $(3\cos^2\gamma'_{i,n} - 1)/2$ function, hence the uncertainties. C-^{2}H bonds away from the magic angle must be preferentially used in such calculations. However, the orientation of the C_6-^{2}H bond near the magic angle with respect to the axis of rotational diffusion for cholesteryl palmitate indicates that the orientation of this axis must be close to, though different from, that of the corresponding axis for cholesterol. The results obtained are listed in Table 26, for comparison purposes we have also include the results of β-cholesterol in DMPC. Examination of Table 26 reveals that the orientation of the axis of rotational diffusion of $\simeq$8 mol % cholesterol in DPPC is identical to that found for 30 mol % cholesterol in DMPC (Dufourc *et al.*, 1984) at 45°C. The angle β and γ are identical within the experimental error, indicating that the orientation of cholesterol in a membrane system does not depend upon the nature of the membrane lipid. Kelusky *et al.*, (1983) observed that cholesterol has the same orientation in DMPC and human erythrocyte membranes. However, S_a decreases on comparing cholesterol in DMPC and cholesterol in DPPC at the same temperature. This agrees well with the earlier finding that the ordering of cholesterol-containing systems depends upon cholesterol concentration (Oldfield *et al.*, 1978).

The angle γ defining the orientation of the rotation axis of cholesteryl palmitate in the ζ axis frame differs markedly from that of cholesterol (Table 26). This situation is visualized by representing

Table 26: Ordering and Orientation of β-Cholesterol and Cholesteryl Palmitate in Model Membranes, at 45.0°C

	≃5 mol % cholesteryl palmitate[a] in DPPC	≃8 mol % cholesterol in DPPC	≃30 mol % cholesterol in DMPC[b]
S_{mol} ±0.03	0.47	0.63	0.75
β ±1°	20	22	22
γ ±3°	140.5	107.5	106.5
$\gamma'(\overrightarrow{C_3-^2H},\vec{n})$[c] ±2°	75	84	84
$\gamma'(\overrightarrow{C_3-O},\vec{n})$[d] ±2°	33	30	30

[a] See Footnote 1.

[b] From Dufourc *et al.*, 1984.

[c] Angle between the C_3-^2H bond and the rotational axis of the fused ring system.

[d] Angle between the C_3-O bond and the rotational axis of the fused ring system.

spatially the four rings of cholesterol palmitate in the rotational diffusion axis system, Figure 54. The PLUTO 78 drawing package of a TSS/IBM 370 computer was used for this purpose. Figure 54 shows average orientations of both fused ring systems undergoing fast reorientation around their principal axis of rotational diffusion, $\vec{n}$, which, for purposes of this Figure (S_{mol} = 1), coincides with the director which is in the plane of the paper. This representation does not account for the 'wobble' of the steroid moiety and can be considered as a 'snap-shot' picture of

Figure 54: PLUTO 78 spatial representation of the fused ring system of β-cholesterol and cholesteryl palmitate; the arrow, $\vec{n}$, which, for $S_{mol} = 1$, corresponds to the director and lies in the plane of the page. The symbol is the oxygen attached at C3 and deuterium nuclei of interest are plotted as small open circles. Molecules are drawn in the overall motional averaging axis system. Arbitary views, amoung the 2π equivalent views (by symmetry around $\vec{n}$), are shown for each of the molecules. The Figure does not account for the 'wobbling' of the steroid skeleton.

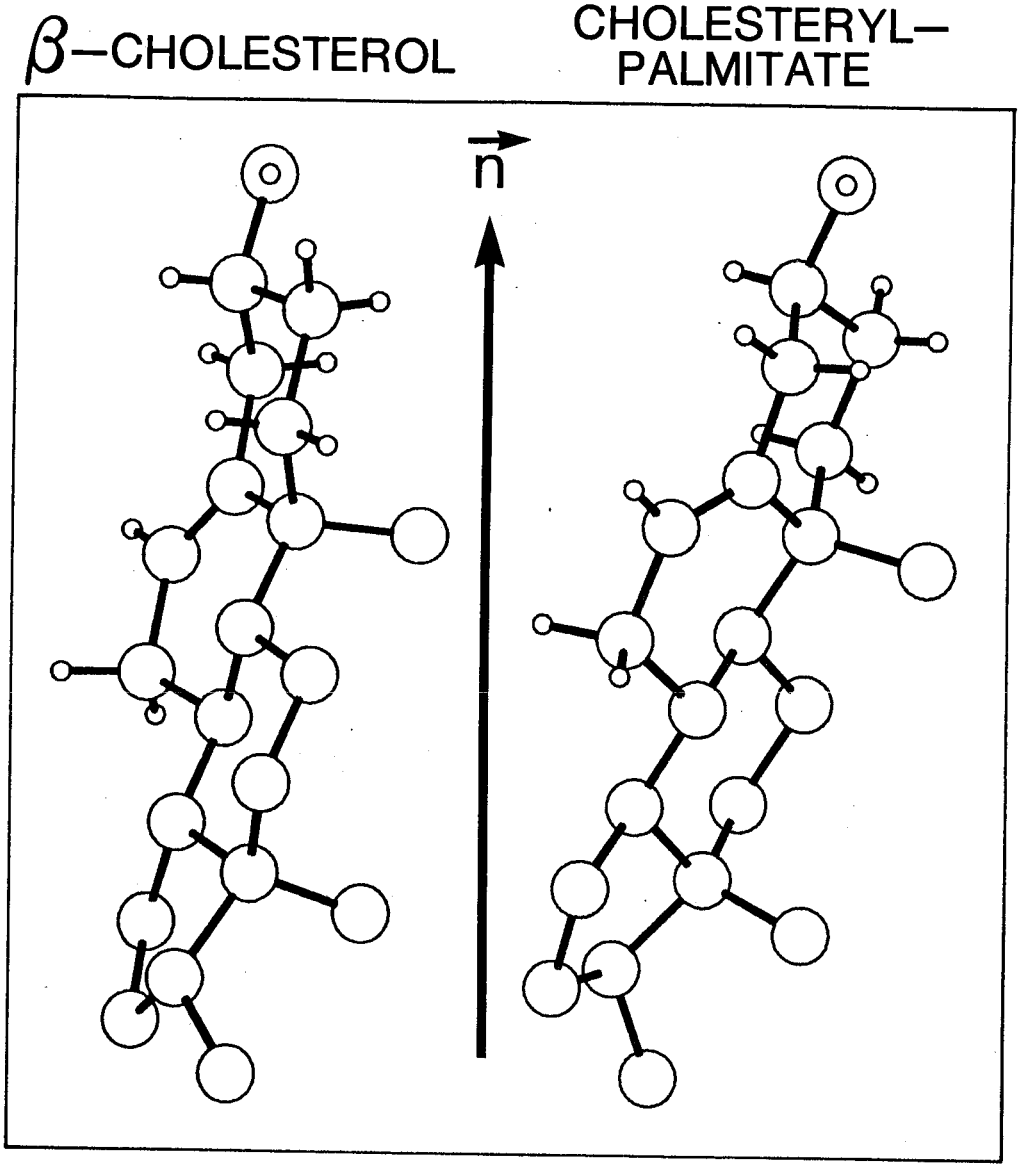
β–CHOLESTEROL
CHOLESTERYL–
PALMITATE
n

molecules when S_{mol} = 1. One must emphasize here that the viewing of molecules is arbitrary and that there exists 2π equivalent views, by symmetry around $\vec{n}$, of each fused ring system. One sees clearly that the steroid skeleton of cholesterol palmitate is markedly tilted away from the position of that of cholesterol. This reflects the presence of the palmitoyl chain attached to the oxygen at C3. The palmitoyl chain is known to fold back into the membrane (Gorrissen *et al.*, 1981) and therefore 'pulls' the rigid cholesteryl skeleton away from the average orientation found for cholesterol. S_a of cholesteryl palmitate in DPPC is smaller than that of cholesterol in DPPC, at the same temperature, indicating that the 'wobbling' of the former is greater than that of the latter.

CHAPTER VII

CONCLUSIONS

In the present study we have investigated the organization and dynamics of phospholipid acyl chains in the amphipathic monolayer of VLDL and egg PC/TO microemulsions, simple models of VLDL, by ^{2}H and ^{31}P NMR spectroscopy.

Selectively deuterated phospholipids, labelled at the *sn*-2 position, were incorporated into VLDL from vescicles using partially purified phosphatidylcholine transfer protein, isolated from bovine liver. This method gave high levels of phospholipid incorporation (3 mol % to 17 mol %) in relatively shorter incubation periods (1-1.5 hr). The effect of phospholipid incorporation on particle structure was analysed by wet chemistry, EM, QELS and ^{31}P NMR. The results from these studies demonstrated that high incorporation of deuterated lipid did not alter the chemical composition (Table 3) and size (Figure 10) of VLDL particles. Gel permeation chromatography (Figure 8) indicated that labelled phospholipids were intimately associated with VLDL and furthermore, no protein-free structures were produced during the incorporation of phospholipids. SDS-PAGE demonstrated that proteins in the crude transfer protein preparation did not associate with the VLDL particles following incubation. However, SDS-PAGE also showed that apo B-100 was cleaved into two smaller fragments (Figures 13 and 14). This appears to be due to some protease present in the crude transfer protein preparation. Protease inhibitors, PMSF and DIFP, were employed without any success (Figure 16). Biological testing of such particles revealed that stimulated synthesis of cholesteryl [^{3}H]oleate in the macrophages was similar for all the VLDL particles in

spite of the cleavage of apo B-100 (Figure 17).

The ^{2}H NMR linewidths for the deuterons on the acyl chain positions (C2-C16) remained essentially constant at ≃60 Hz at 25°C (Table 5). At the C16-position the ^{2}H NMR spectra revealed the superposition of resonances indicating the existance of two phospholipid domains of significantly different order (Figure 20; Table 6). The superposition of resonances for phospholipids labelled in the methylene position was demonstrated with [$^{2}H_{31}$]PC (Figure 21).

The method of exchanging phospholipids into VLDL resulted in the cleavage of apo B-100, we considered the possibility that this may alter the phospholipid acyl chain packing in the monolayer. Hence, an alternative approach to study the organization of phospholipid acyl chains in the amphipathic monolayer of VLDL involved the use of selectively deuterated palmitic acids. The effect of palmitic acid incorporation on VLDL size was investigated by EM, QELs and ^{31}P NMR. The results from these techniques demonstrated that VLDL size remains unaltered following the incorporation of palmitic acids. Gel permeation chromatography indicated that the label was intimately associated with VLDL and furthermore, no protein-free structures were formed during the incorporation procedure (Figure 24). SDS-PAGE demonstrated no cleavage of apo B-100 following the incorporation of palmitic acid (Figure 31).

The ^{2}H NMR spectra of C5,6- to C16-position reveal a superposition of resonances indicating the presence of two phospholipid domains in the surface of VLDL (Figure 27, 28 and 29; Table 9 and 10). The result of the C16-position palmitic acid is in excellent agreement with the corresponding position of phospholipid in VLDL. At 25°C, the order parameter of the low

order domain for palmitic acid (C4-C16-positions) is ≃ 0.015 and is in excellent agreement with the values obtained with the deuterated phospholipids (C2-C16-positions, S_{CD} = 0.014). In the high ordered domain, the S_{CD} value of palmitic acid (C11,12-positions) is 0.25 and decreased to 0.035 for the terminal methyl position (Table 14).

In an attempt to understand the occurance of two domains, the orientational order of phospholipid acyl chains in the amphipathic monolayer of model particles-microemulsions composed of egg PC/TO was measured using selectively deuterated phospholipids. Surprisingly, the ^2H NMR spectra also revealed the superposition of resonances, thereby indicating the presence of two phospholipid domains of different order in the surface monolayer of microemulsions (Figure 33 and 34). The order parameter of the low order domain in egg PC/TO microemulsions is ≃0.014 for C2-C11,12-positions (Table 16). This values is in excellent agreement with those found with selectively deuterated phospholipids and palmitic acid in VLDL (Tables 13 and 14). At 25°C, the order parameter of the high order domain in microemulsions detemined by C11,12-position is 0.17 (Table 16). This value is ≃32% less than the corresponding value in VLDL. The S_{CD} value of the C11,12-position in VLDL is in good agreement with those found in LDL (Treleaven, 1985) and HDLs (Parmar, 1985).

The low order domian suggest that in the monolayer of VLDL (Tables 13 and 14) and microemulsion (Table 16) a significant proportion of the phospholipid acyl chains are in an essentially isotropic environment. In VLDL the domain of low order comprises between ≃10% and ≃20% of the phospholipid molecules. Posible reasons, other than lipid-proteins interactions, have been considered to explain the origin of the low order

on pages 181-183.

The high order domain in the monolayer of VLDL (Tables 13 and 14) and microemulsion (Table 16) suggests that large porprotion of phospholipid acyl chains are in regions where there is high order. At 25°C, the S_{CD} value in VLDL is higher than the corresponding value in egg PC/TO microemulsions or multilamellar liposomes (Stockton *et al.*, 1976). The high orientational order in VLDL has been explained by considering the structural elements cholesterol, sphingomyelin, and apoproteins present in VLDL monolayer and possible monolayer/core interactions. These possibilities have been discussed on pages 184-189.

Spin-lattice relaxation times measured with selectively deuterated phospholipid in VLDL are constant at the plateau region and increase at the terminal region indicating that there are increased motions towards the terminal end of the acyl chain.

The lateral diffusion coefficient, D_t, of phospholipids in VLDL and egg PC/TO microemulsions was measured from the viscosity dependence of ^{31}P NMR linewidths as described by Cullis (1976). VLDL was subfractioned in order to remove larger sized partices. Wet chemistry of such particles revealed no variation of chemical composition from native VLDL particles and EM (Figure 40) demonstrated a narrow size distribution. Egg PC/TO microemulsions were prepared as described by Tajima *et al*, (1983) and examined for vesicle contamination using Mn^{2+}, Eu^{3+} and Pr^{3+} (Figures 47 and 48). From the choline N-methyl proton resonance the microemulsion prepararion was demonstrated to be less than 10% contaminated by vesicles.

At 25°C, D_t value of (9.1±1.0) X 10^{-9} cm^2/s and (2.5±0.4) X 10^{-8} cm^2/s was obtained for VLDL and egg PC/TO microemulsions, respectively. The slower diffusion in VLDL compared to microemulsions is explained by considering the presence of cholesterol in the monolayer of VLDL. At 40°C, there is a marginal increase in diffusion rate in VLDL compared to that found at 25°C suggesting that both phospholipids and triglycerides are in their liquid crystalline state. Furthermore, monolayer/core interactions have little effect on diffusion rate at 25°C and 40°C.

The ^{31}P residual chemical shift anisotropy ($\Delta\sigma$) measure from viscosity and frequency dependence of ^{31}P NMR line width of VLDL was 47±1 and 46.0±0.5, respectively, and are in excellent agreement with those observed in phospholipid bilayer, $\Delta\sigma$ = 45±5 ppm (Seelig, 1978). The $\Delta\sigma$ value of 28±1 ppm was measured for egg PC/TO microemulsions. The increase of $\Delta\sigma$ by ≃20 ppm from protein-free microemulsions to VLDL suggest that lipid-protein interactions may be responsible for altering the headgroup conformation and/or order in VLDL.

The orientation of the axis of motional averaging of cholesterol and cholesteryl palmitate in DPPC multilamellar liposomes at 45°C have been calculated from the quadrupolar splitting observed for deuterium labels at the 2-, 3-, 4, 6-, and 7-positions on the steroid moiety. The axis of motional averaging for cholesterol is 84±2° and for cholesteryl palmitate is 75±2° with respect to the C_3-^2H bond. The axis of motional averaging of cholesterol in DPPC is in excellent agreement with that found in DMPC (Duforc *et al.*, 1984). From the orientation of the steriod and the order parameter values calculated for the C-^2H bond, the molecular order parameter of the cholesterol and cholesteryl palmitate was ≃0.63 and ≃0.47,

respectively, demonstrating that the fluctuation of the steriod moiety from the axis of motional averaging is greater for cholesteryl palmitate than cholesterol in the membrane system.

CHAPTER VIII

REFERENCES

Abragam, A. (1961) *The Principles of Nuclear Magnetism,* pp. 424-427, Clarendon, Oxford.

Alexander, C. A., Hamilton, R. L., and Havel, R. J. (1976) *J. Cell. Biol.* 69, 241-263.

Ames, B. N. (1966) in *Methods in Enzymology,* Vol. 8, (Neufeld, E. F., and Ginsburg, V. editors) Academic Press, New York. pp. 115-118.

Assmann, G., Sokoloski, E. A., and Brewer, H. B., Jr. (1974) *Proc. Natl. Acad. Sci. USA* 71, 549-553.

Atkinson, D., and Small. D. M. (1986) *Ann. Rev. Biophys. Biophys. Chem.* 15, 403-456.

Barter, P. J., and Lally, J. I. (1979) *Metabolism* 28, 230-236.

Batzri, S., and Korn, E. D. (1973) *Biochim. Biophys. Acta* 751, 108-120.

Bennett-Clark, S., Atkinson, D., Hamilton, J. A., Forte, T., Russell, B., Feldman, E. B., and Small, D. M. (1982) *J. Lipid Res.*23, 28-41.

Birdsall, N. J. M., Feeney, J., Lee, A. G., Levine, Y. K., and Metcalfe, J. C. (1972) *J. C. S. Perkin II.* 1441-1445.

Bloom, M., and Smith, I. C. P. (1985) in *Progress in Protein-Lipid Interactions (Volume 1)* (Watts, A., and De Pont, J. J. H. H. M., eds) Elsevier Science Publishers, pp. 61-88.

Boggs, J. M. (1987) *Biochim. Biophys. Acta* 906, 353-404.

Bozzato, R. P., and Tinker, D. O. (1982) *Can. J. Biochem.* 60, 409-418.

Breckenridge, W. C. (1985) *Can. J. Biochem. Cell. Biol.* 63, 890-897.

Brown, M. F., Seelig, J., and Haberlen, U. (1979) *J. Chem. Phys.* 70, 5045-5053.

Brown, M. S., and Goldstein, J. L. (1983) *J. Clin. Invest.* 72, 743-747.

Brown, M. S., and Goldstein, J. L. (1984) *Sci. Am.* 251, 58-66.

Brown, M. S., Kovanen, P. T., and Goldstein, J. L. (1981) *Science* 212, 628-635.

Brown, M. F., and Seelig, J. (1979) *J. Chem. Phys.* 70, 5045-5053.

Brown, M. F. (1982) *J. Chem. Phys.* 77, 1576-1599.

Brown, M. F., Ribeiro, A. A., and Williams, G. D. (1983) *Proc. Natl. Acad. Sci. U.S.A.* 80, 4325-4329.

Brown, M. F. (1984) *J. Chem. Phys.* 80, 2808-2836.

Brown, M. F., and Williams, G. D. (1985) *J. Biochem. Biophys. Methods* 11, 71-81.

Buldt, G. and Wohlgemuth, R. (1981) *J. Membrane Biol.* 58, 81-100

Buldt, G., Gally, H. U., Seelig, A., Seelig, J., and Zacchai, G. (1978) *Nature* 271, 182-184.

Buldt, G., Gally, H. U., Seelig, J. and Zacchai, G. (1979) *J. Mol. Biol.* 134, 673-691.

Burnell, E. E., Cullis, P. R., and De Kruijff, B. (1980) *Biochim. Biophys. Acta* 603, 63-69.

Burnett, L. J., and Muller, B. H. (1971) *J. Chem. Phy.* 55, 5829-5831.

Bystrov, V. F., Dubrovina, N. I., Barsukov, L. I., and Bergelson, L. D. (1971) *Chem. Phys. Lipids* 6, 343-350.

Bystrov, V. F., Shapiro, Yu. E., Viktorov, A. V., Barsukov, L. I., and Bergelson, L. D. (1972) *FEBS Lett.* 25, 337- 338.

Castellino, F. J., Thomas, J. K., and Ploplis, V. A. (1977) *Biochem. Biophys. Res. commun.* 75, 857-862.

Chait, A., Hazzard, W. R., Albers, J. J., Kushwaha, R. P., and Brunzell, J. D. (1978) *Metab. Cli. Exp.* 27, 1055-1066.

Chen, S.-H., Yang, C. Y., and Chen, P.-F., Setzer, D., Tanimura, M., Li, W.-H., Gotto, A. M. Jr., and Chan, L. (1986) *J. Biol. Chem.* 261, 12918-12921.

Cryer, A., (1981) *Int. J. Biochem.* 13, 525-541.

Cullis, P. R. (1976) *FEBS Lett.* 70, 223-228.

Cullis, P. R. and de Kruijff, B. (1979) *Biochim. Biophys. Acta,* 559, 399-420

Cushley, R. J., Gorrissen, H., and Wassall, S. R. (1980) *Can. J. Chem.* 58, 2433-2441.

Cushley, R. J., Treleaven, W. D., Parmar, Y. I., Chana, R. S., and Fenske, D. B. (1987) *Biochem. Biophys. Res. Commun.* 146, 1139-1145

Davis, J. H. (1983) *Biochim. Biophys. Acta* 737,117-171.

Davis, J. H., Maraviglia, B., Weeks, G., and Godin, D. V. (1979) *Biochim. Biophys. Acta* 550, 362-366.

Deckelbaum, R. J., Tall, A. R., and Small, D. M. (1977) *J. Lipid Res.* 18, 164-168.

Deckelbaum, R. J., Eisenberg, S., Fainaru, M., Barenholz, Y., and Olivecrona, T. (1979) *J. Biol. Chem.* 254, 6079-6087.

DeLoof, H., Rossenue, M., Yang, C.-Y., Li, W.-H., Gotto, A. M. Jr., and Chan, L. (1987) *J. Lipid Res.* 28, 1455-1465.

Demel, R. A., Geurts Van Kessel, W. S. M., Zwaal, R. F. A., Roelofsen, B., and Van Deenen, L. L. M., (1975) *Biochim. Biophys. Acta* 406, 97-107.

Dempsey, C. E., Ryba, N. J. P., and Watts, A. (1986) *Biochemistry* 25, 2180-2187.

DiCorleto, P. E., Fakharzadeh, F. F., Searles, L. L and Zilversmit, D. B. (1977) *Biochim. Biophys. Acta* 468, 296-304.

Dolphin, P. J. (1985) *Can. J. Biochem. Cell. Biol.* 63, 850-869.

Dufourc, E. J., Smith, I. C. P., and Jarrell, H. C. (1983) *Chem. Phys. Lipids* 33, 153-177.

Dufourc, E. J., Parish, E. J., Chitrakorn, S., and Smith, I. C. P. (1984) *Biochemistry* 23, 6062-6071.

Eisenberg, S., and Schurr, D. (1976) *J Lipid Res.* 17, 578-587.

Eisenberg, S., and Olivecrona, T. (1979) *J. Lipid Res.* 20, 614-623.

Eisenberg, S. (1979) *Prog. Biochem. Pharmacol* 15, 139-165.

Eisenberg, S. (1980) *Ann. N. Y. Acad. Sci.* 348, 30-47

Ekman, S., Derksen, A., and Small, D. M. (1988) *Biochim. Biophys. Acta* 959, 343-348.

Fahey, P. F., Koppel, D. E., Barak, L. S., Wolf, D. E., Elson, E. L., and Webb, W. W. (1977) *Science* 195, 305-306.

Fainaru, M., Havel, R. J., and Imaizumi, K. (1977) *Biochem. Med.* 17, 347-355.

Fainaru, M., Mahley, R. W., Hamilton, R. L., and Innerarity, T. L. (1982) *J. Lipid Res.* 23, 702-714.

Fenske, D. B., Parmar, Y. I., Treleaven, W. D., Chana, R. S., and Cushley, R. J. (1988a) *Biochemistry* 27, 4491-4500.

Fenske, D. B. (1988b) *Ph.D. Thesis* Simon Fraser University.

Fielding, C. J., Shore, V. G., and Fielding, P. E. (1972) *Biochem. Biophys. Res. Commun.* 46, 1493-1498

Fielding, C. J. (1978) in *Disturbances in Lipid and Lipoprotein metabolism* (Dietschy, J. M., Gotto, A. M., Jr., and Ontko, J. A., eds) pp. 83-98. Amer. Physiological Society, Bethesda, Maryland.

Finer, E. G., Henry, R., Leslie, R. B., and Robertson, R. W. (1975) *Biochim. Biophys. Acta.* 380,320-337.

Forrest, B. J., and Cushley, R. J. (1977) *Atherosclerosis* 28, 309-318.

Glickman, R. M., Rogers, M., and Glickman, J. N. (1986) *Proc. Nat. Acad. Sci. USA* 83, 5296-5300.

Ginsburg, G. S., and Small, D. M. (1981) *Biochim. Biophys. Acta.* 664, 98-107.

Ginsburg, G. S., Walsh, M. T., Small, D. M., and Atkinson, D. (1984) *J. Biol. Chem.* 259, 6667-6673.

Goldstein, J. L., and Brown, M. S. (1977) *Annu. Rev. Biochem.* 46, 897-930.

Gorrissen, H., Mackay, A. L., Wassall, S. R., Valic, M. I., Tulloch, A. P., and Cushley, R. J. (1981) *Biochim. Biophys. Acta.* 644, 266-272.

Gorrissen, H., Tulloch, A. P., and Cushley, R. J. (1982) *Chem. Phys. Lipids* 31, 245-255.

Griffin, R. G. (1976) *J. Am. Chem. Soc,* 98, 851-853

Griffin, R. G., Powers, L., and Pershan, P. S. (1978) *Biochemistry* 17, 2718-2722.

Grover, A. K., and Cushley, R. J. (1979) *J. Labelled Comp. Radiopharm.* XVI, 307-313.

Grover, A. K., Forrest, B. J., Buchinski, R. K., and Cushley, R. J. (1979)

Biochim. Biophys. Acta. 550, 212-221.

Hale, J. E., and Schroeder, F. (1981) *J. Lipid Res.* 22, 838-851.

Hamilton, J. A., Talkowski, C., Childers, R. F., Williams, E., Allerhand, A., and Cordes, E. H. (1974) *J. Biol. Chem.* 249, 4872-4878.

Hamilton, J. A., Oppenheimer, N. J., Addleman, R., Clouse, A. O., Cordes, E. H., Steiner, P. M., and Glueck, C. J. (1976) *Science* 194, 1424-1427.

Hamilton, J. A., and Small, D. M. (1981) *Proc. Natl. Acad. Sci. U. S. A.* 78, 6878-6882.

Hamilton, J. A., and Small, D. M. (1982) *J. Biol. Chem.* 257, 7318-7321.

Hamilton, J. A., Small, D. M., and Parks, J. S., (1983) *J. Biol. Chem.* 258, 1172-1179.

Hamilton, J. A., and Morrisett, J. D., (1986) *Methods Enzymol* 128, 472-515.

Hamosh, M. and Hamosh, P. (1983) *Mol. Aspects Med.* 6, 199-289.

Hauser, H., Radloff, R. R., Sundell, S. and Pascher, I. (1988) *J. Am. Chem. Soc,* 110, 1054-1058

Havel, R. J. (1984) *J. Lipid Res.* 25, 1570-1576.

Herzfeld, J., Griffin, R. G. and Haberkorn, R. A. (1978) *Biochemistry,* 17, 2711- 2718

Higgins, J. A., and Hutson, J. L. (1984) *J. Lipid Res.* 25, 1295-1305.

Higgins, J. A. (1988) *FEBS Letts.* 232, 405-408.

Hoff, H. F., Heideman, C. L., Gaubatz, J. W., Scott, D. W., Titus, J. L., and Gotto, A. M., Jr., (1978) *Lab. Invest.* 38, 560-567.

Hoff, H. F. and Gaubatz, J. W. (1982) *Artherosclerosis* 42, 273-279.

Hopkins, G. L., and Barter, P. J., (1979) *Metabolism* 29, 546-550.

Hospattankar, A. V., Fairwell, T., Ronan, R., and Brewer, H. B., Jr. (1984) *J. Biol. Chem.* 259, 318-322.

Hui, D. Y., Innerarity, T. L., and Mahley, R. W. (1984) *J. Biol. Chem.* 259, 860-869.

Innerarity, T. L., Friedlander, E. J., Rall, S. C., Jr., Weisgraber, K. H., and Mahley, R. W. (1983) *J. Biol. Chem.* 258, 12341-12347.

Jackson, R. L., Sparrow, J. T., Baker, H. N., Morrisett, J. D., Taunton, O. D., and Gotto, A. M. Jr., (1974) *J. Biol. Chem.* 249, 5308-5313.

Jackson, R. L., Morrisett, J. D., Sparrow, J. T., Segrest, J. P., Pownall, H. J., Smith, L. C., Hoff, H. F., and Gotto, A. M. Jr. (1974) *J. Biol. Chem.* 249, 5314-5320.

Jackson, R. L., Wilson, D., and Glueck, C. J. (1979) *Biochim. Biophys. Acta.* 557, 79-85.

Jandacek, R. J., Webb, M. R., and Mattson, F. H. (1977) *J. Lipid Res.* 18, 203-210.

Janiak, M. J., Loomis, C. R., Shipley, G. G., and Small, D. M. (1974) *J. Mol. Biol.* 86, 325-339.

Jardetzky, O., and Roberts, G. C. K. (1981) in *NMR in Molecular Biology,* pp. 10-68, Academic Press, New York.

Johnson, J. D., Taskinen, M-R., Matsuoka, N., and Jackson, R. L. (1980) *J. Biol. Chem.* 255, 3466-3471.

Jonas, A., and Jung, R. W. (1975) *Biochem. Biophys. Res. Commun.* 66, 651-657.

Jonas, A. (1977) *Biochim. Biophys Acta* 486, 10-22.

Kamp, H. H., Wirtz, K. W. A., and van Deenen, L. L. M. (1973) *Biochim. Biophys. Acta* 318, 313-325.

Kane, J.P., Sata, T., Hamilton. R. L., and Havel, R. J. (1975) *J. Clin. Invest.* 56, 1622-1634.

Kane, J. P. (1983) *Annu. Rev. Physiol.* 45, 637-650.

Kaiser, E. T., and Kezdy, F. J. (1984) *Science* 223, 249-255.

Kang, S. Y., Gutowsky, H. S., Hsung, J. C., Jacobs, R., King, T. E., Rice, D., and Oldfield, E. (1979) *Biochemistry* 18, 3257-3267.

Kashyap, M. L., Hynd, B. A., and Robinson, K. (1980) *J. Lipid. Res.* 21, 491-495.

Kasper, A. M., and Helmkamp, G. M. Jr., (1981) *Biochemistry* 20, 146-151.

Katz, S. S., Small, D. M., Shipley, G. G., and Rogers, E. L. (1974) *Circulation* 50 (Suppl. 3), 6 (Abstr).

Katz, S. S., Shipley, G. G., and Small, D. M. (1976) *J. Clin. Invest.* 58, 200-211.

Klienman, Y. K., Krul, E. S., Burnes, M., Aronson, W., Pfleger, B., and Gustav, S. (1988) *J. Lipid. Res.* 29, 729-743.

Knott, T. J., Wallis, S. C., and Powell, L. M., Pease, R. J., Lusis, A. J., Blackhart, B., McCarthy, B. J., Mahley, R. W., Levy-Wilson, B., and Scott, J. (1986) *Nucleic Acid Res.* 14, 7501-7503.

Kohler, S. J., and Klein, M. P. (1976) *Biochemistry* 15, 967-973.

Kohler, S. J., and Klein, M. P. (1977) *Biochemistry* 16, 519-526.

Krishnaiah, K. V., and Wiegandt, H. (1974) *FEBS Letts* 40, 265-268.

Kroon, P. A., and Seidenberg, J. (1982) *Biochemistry* 21, 6483-6488.

Kuo, A.-L., and Wade, C. G. (1979) *Biochemistry* 18, 2300-2308.

Ladbrooke, B. D., Williams, R. M., and Chapman, D. (1968) *Biochim. Biophys. Acta* 150, 333-340.

Laemmli, U. K. (1970) *Nature* 227, 680-685.

Lang, P. D., and Insull, W,. Jr. (1970) *J. Clin. Invest.* 49, 1479-1488.

La Rosa, J. C., Levy, R. I., Herbert, P., Lux, S. E., and Fredrickson, D. S. (1970) *Biochem. Biophys. Res. Commun.* 41, 57-62.

Larsen, K. (1966) *Acta Chem. Scand.* 20, 2255-2260

Li, W.-H., Tanimura, M., Luo, C.-C., Datta, S., and Chan, L. (1988) *J. Lipid Res.* 29, 245-271.

Lowry, O. H., Rosebrough, N. J., Farr, A. L., and Randall, R. J. (1951) *J. Biol. Chem.* 193, 265-275.

Mackay, A. L., Burnell, E. E., Nichol, C. P., Weeks, G., Bloom, M., and Valic, M. I. (1978) *FEBS Lett.* 88, 97-100.

Mahley, R. W. (1979) in *Atherosclerosis Reviews* (eds. Paoletti, R., and Gotto, A. M., Jr., Vol 5, pp. 1, Raven Press. New York.

Mahley, R. W., and Innerarity, T. L., Weisgraber, K. H., and Oh, S. Y. (1979) *J. Cli. Invest.* 64, 743-750.

Mahley, R. W., and Innerarity, T. L., Brown, M. S., Ho, Y. K., and Goldstein, J. L. (1980) *J. Lipid Res.* 21, 970-980.

Mahley, R. W., and Innerarity, T. L. (1983) *Biochim. Biophys. Acta.* 737, 197-222.

Mahley, R. W., and Angelin, B. (1984) *Adv. Intern. Med.* 29, 385-396.

Mahley, R. W. (1985) *Circulation* 72, 943-948.

Mantsch, H. H., Saito, H., and Smith, I. C. P. (1977) in *Progress in Nuclear Magnetic Resonance Spectroscopy* (Emsley, J. W., Feeney, J., and Sutcliffe, L. H., eds.) Vol.11, pp. 212-272, Pergamon Press, London.

McLaughlin, A. C., Cullis, P. R., Berden, J. A., and Richards, R. E. (1975) *J. Mag. Reson.* 20, 146-165.

Miller, G. T., and Miller, N. E. (1975) *Lancet* 1, 16-19.

Miller, K. W., and Small, D. M. (1980) *Circulation* 62, 151a.

Miller, K. W., and Small, D. M. (1982) *J. Colloid. Interface Sci.* 89, 466-478.

Miller, K. W., and Small, D. M. (1983a) *Biochemistry* 22, 443-451.

Miller, K. W., and Small, D. M. (1983b) *J. Biol. Chem.* 258, 13772-13784.

Mims, M. P., Chari, M. V., and Morrisett, J. D. (1986) *Biochemistry* 25, 7494-7501.

Mjos, O. D., Faergeman, O., Hamilton, R. L., Havel, R. J., (1975) *J. Clin. Invest.* 56, 603-615.

Morrisett, J. D., David, J. S. K., Pownall, H. J., and Gotto, A. M. (1973) *Biochemistry*12, 1290-1299.

Morrisett, J. D., Segura, R., Taunton, O. D., Pownall, H. J., Jackson, R. L., and Gotto, A. M., Jr., (1975) *Biophys. J.* 15, 217a.

Morrisett, J. D., Pownall, H. J., Sparrow, J. T., Jackson, R. L., and Gotto, A. M. (1975) in *Lipids, Lipoproteins and Drugs* Eds, Kritchevsky, D., Paoletti, R., and Holmes, W. L. Plenum Press, New York. pp. 7.

Morrisett, J. D., Jackson, R. L., and Gotto, A. M. Jr., (1977a) *Biochim. Biophys. Acta.* 472, 93-133.

Morrisett, J. D., Pownall, H. J., Jackson, R. L., Segura, R., Gotto, A. M., and Taunton, O. D. (1977b) in *Polyunsaturated Fatty Acids Am. Oil Chem. Soc.* Monograph No. 4. eds, Holman, R. T., and Kunau, W. H. pp. 139-161, Am. Oil. Chem. Soc. Publishers, Champaign.

Oldfield, E., Gilmore, R., Glaser, M., Gutowsky, H. S., Hsung, J. C., Kang, S. Y., King, T. E., Meadows, M., and Rice, D. (1978) *Proc. Natl. Acad. Sci. U. S. A.* 75, 4657-4660.

Osterman, D., Mora, R., Kezdy, F. J., Kaiser, E. T., and Meredith, S. C. (1984) *J. Am. Chem. Soc.* 106, 6845-6847.

Pagnan, A., Havel, R. J., Kane, J. P., and Kotite, L. (1977) *J. Lipid Res.* 18, 613-622.

Parmar, Y. I., Gorrissen, H., Wassall, S. R., and Cushley, R. J. (1983) *J. Biol. Chem.* 258, 2000-2004.

Parmar, Y. I., Wassall, S. R., and Cushley, R. J. (1984) *J. Amer. Chem. Soc.* 106, 2434-2435.

Parmar, Y. I. (1985) *Ph.D. Thesis.* Simon Fraser University.

Pauls, K. P., Mackay, A. L., and Bloom, M. (1983) *Biochemistry* 22, 6101-6109.

Pearson, R. H., and Pascher, I. (1979) *Nature* 281, 499-501.

Petersen, N. O., and Chan, S. I. (1977) *Biochemistry* 16, 2657-2667.

Ponpipom, M. M., and Bugianesi, R. L. (1980) *J. Lipid Res.* 21, 136-139.

Pownall, H. J., Morrisett, J. D., Sparrow, J. T., and Gotto, A. M. (1974) *Biophys. Res. Commun.* 60, 779-786.

Pownall, H. J., Morrisett, J. D., and Gotto, A. M. Jr., (1977) *J. Lipid Res.* 18, 14-23.

Pownall, H. J., Jackson, R. L., Morrisett, J. D., and Gotto, A. M. Jr. (1979) in *The Biochemistry of Atherosclerosis* (Scanu, A. M., Wissler, R. W., and Getz, G. S. eds) pp. 123-143, Marcel Dekker, Inc.

Quin, M. T., Parthasarathy, S., and Steinberg, D. (1985) *Proc. Natl. Acad. Sci. USA* 82, 5949-5953.

Rall, S. C., Jr., Weisgraber, K. H., and Mahley, R. W. (1982) *J. Biol. Chem.* 257, 4171-4178.

Reman, F. C., Nieuwenhuizen, W., and Boonders, T. M. (1978) *Chem. Phys. Lipids* 21, 223-235.

Rice, D., and Oldfield, E. (1979) *Biochemistry* 18, 3272-3279.

Richter, H., Srey, C., Winter, K., and Furst, W. (1977) *Pharmazie* 32, 164.

Rubenstein, J. L. R., Smith, B. A., and McConnell, H. M. (1979) *Proc. Natl. Acad. Sci. U.S.A.* 76, 15-18.

Ryba, N. J. P., Dempsey, C. E., and Watts, A. (1986) *Biochemistry* 25, 4818-4825.

Scanu, A. M., and Hirz, R. (1968) *Nature* 218, 200-201.

Scanu, A. M., Pollard, H., and Reader, W. (1968) *J. Lipid Res.* 9, 342-349.

Scanu, A. M., and Kruski, A., (1975) in *International Encyclopedia of Pharmacology and Therapeutics*, Vol 1, Sec 24, pp. 21-28, (Masoro, E. ed), Plenum Press, New York.

Scanu, A. M., Edelstein, C., Shen, B. W. (1982) in *Lipid-Protein Interactions*, Vol 1, pp. 259-315, (Jost, P. C., and Griffith, O. H. eds), A Wiley-Interscience Publication.

Schaefer, E. J., Eisenberg, S., and Levy, R. I. (1978) *J. Lipid Res.* 19, 667-687.

Scherer, P. G., and Seelig, J. (1987) *EMBO Journal* 6, 2915-2922.

Schroeder, F., and Goh, E. H. (1979) *J. Biol. Chem.* 254, 2464-2470.

Schroeder, F., Goh, E. H., and Heimberg, M. (1979a) *FEBS Lett.* 97, 233-236.

Schroeder, F., Goh, E. H., and Heimberg, M. (1979b) *J. Biol. Chem.* 254, 2456-2463.

Seelig, J., and Niederberger, W. (1974) *Biochemistry* 13, 1585-1588.

Seelig, J., and Gally, H. U. (1976) *Biochemistry* 15, 5199-5204.

Seelig, J. (1977) *Q. Rev. Biophys.* 10, 353-418.

Seelig, J. (1978a) *Progr. Colloid and Polymer Sci.* 65, 172-179.

Seelig, J. (1978b) *Biochim. Biophys. Acta* 515, 105-140.

Seelig, J., and Seelig, A. (1980) *Q. Rev. Biophys.* 13, 19-61.

Seelig, J. (1982a) in *Physical Methods on Biological Membranes and Their Model Systems*, Vol 71, pp. 27-37, (Conti, F., Blumberg, W. E., de Gier, J., Pocchiari, F. eds), Plenum Press, New York.

Seelig, J., Seelig, A. and Tamm, L. (1982b) in *Lipid-Protein Interaction*,

Vol 2, pp. 127-148, (Jost, P. C. and Griffith, O. H. eds.), A Wiley-Interscience Publication, John Wiley and Sons, New York.

Seelig, J., MacDonald, P. M., and Scherer, P. G. (1987) *Biochemistry* 26, 7535-7541.

Segrest, J. P., Jackson, R. L., Morrisett, J. D., and Gotto, A. M., Jr. (1974) *FEBS Lett.* 38, 247-253.

Shapiro, Yu. E., Viktorov, A. V., Volkova, V. I., Barsukov, L. I., Bystrov, V. F., and Bergelson, L. D. (1975) *Chem. Phys. Lipids* 14, 227-232.

Sheetz, M. P., and Chan, S. J. (1972) *Biochemistry* 11, 4573-4581.

Shen, B. W., Scanu, A. M., and Kezdy, F. J. (1977) *Proc. Natl. Acad. Sci. U.S.A.* 74, 837-841.

Shulman, R. S., Herbert, P. N., Wehrly, K., and Fredrickson, D. S. (1975) *J. Biol. Chem.* 250, 182-190.

Singer, S. J. and Nicholson, G. L. (1972) *Science*, 175, 720-731

Singleton, W. S., Gray, M. S., Brown, M. L., and White, J. L. (1965) *J. Am. Oil. Chem. Soc.* 42, 53-56.

Sixl, F., Brophy, P. J., Watts, A. (1984) *Biochemistry* 23, 2032-2039.

Sklar, L. A., Doody, M. C., Gotto, A. M., Jr., and Pownall, H. J. (1980) *Biochemistry* 19, 1294-1301.

Sklar, L. A., Craig, I. F., and Pownall, H. J. (1981) *J. Biol. Chem.* 256, 4286-4292.

Slichter, C. P., (1963) in *Principles of Magnetic Resonance*, pp. 160-176, Harper and Row, New York.

Small, D. M. (1970) *Fed. Proc.* 29, 1320-1326.

Small, D. M., Puppione, D. L., Phillipis, M. L., Atkinson, D., Hamilton, J. A., and Schumaker, D. N. (1980) *Circulation* 62, Suppl. III, 118-444.

Small, D. M. (1981) in *Membrane Molecules, Toxin and Cells*. pp. 11-34, (Block, K., Bolis, L., and Tosteson, D. C. eds) John Wright. PGS Inc.

Smith, R. J. M., and Green, C. (1974) *Biochem. J.* 137, 413-415.

Smith, I. C. P., Stockton, G. W., Tulloch, A. P., Polnaszek, C. F., and Johnson, K. G. (1977) *J. Colloid Interface Science* 58, 439-451.

Smith, I. C. P. (1984) in *Biomembranes, Dynamics and Biology.* pp. 81-110, (Burton, R. M. and Guerra, F. C. eds.) Plenum Press. New York. USA.

Soutar, A. K., Garner, C. W., Baker, N. H., Sparrow, J. T., Jackson, R. D., Gotto, A. M., and Smith, L. C. (1975) *Biochemistry* 14, 3057-3064.

Sparks, J. D., and Sparks, C. E. (1985) *Adv. Lipid Res.* 21, 1-45.

Stanley, C. R., Jr., Weisgraber, K. H., and Mahley, R. W. (1986) *Methods Enzymol.* 128, 273-287.

Stockton, G. W., Polnaszek, C. F., Tulloch, A. P., Hasan, F., and Smith, I. C. P. (1976) *Biochemistry* 15, 954-966.

Stockton, G. W., and Smith, I. C. P. (1976) *Chem. Phys. Lipids* 17, 251-263.

Stone, A. J. (1973) *Nucl. Instr. and Methods* 107, 285-291.

Tajima, S., Yokoyama, S., and Yamamoto, A. (1983) *J. Biol. Chem.* 258, 10073-10082.

Tall, A. R., and Small, D. M. (1980) *Adv. Lipid Res.* 17, 1-51.

Tall, A. R. (1986) *J. Lipid Res.* 27, 361-367.

Taylor, M. G., and Smith, I. C. P. (1980) *Biochim. Biophys. Acta* 599, 140-149.

Taylor, M. G., Akiyama, T., and Smith, I. C. P. (1981) *Chem. Phys. Lipids* 29, 327-339.

Taylor, M. G., Akiyama, T., Saito, H., and Smith, I. C. P. (1982) *Chem. Phys. Lipids* 31, 359-379.

Taylor, M. G., and Smith, I. C. P. (1983) *Biochim. Biophys. Acta.* 733, 256-263.

Thayer, A. M., and Kohler, S. J. (1981) *Biochemistry* 20, 6831-6834.

Thewalt, J. L., Wassall, S. R., Gorrissen, H., and Cushley, R. J. (1985) *Biochim. Biophys. Acta* 817, 355-365.

Thompson, G., and Siguurdson, G. (1974) *Circulation* 50, Suppl. 3, 272.

Treleaven, W. D., Wassall, S. R., and Cushley, R. J. (1983) *Chem. Phys. Lipids* 33, 223-231.

Treleaven, W. D. (1985) *Ph. D. Thesis* Simon Fraser University.

Treleaven, W. D., Parmar, Y. I., Gorrissen, H., and Cushley, R. J. (1986) *Biochim. Biophys. Acta.* 877, 198-210.

Valic, M. I., Gorrissen, H., Cushley, R. J., and Bloom, M. (1979) *Biochemistry* 18, 854-859.

Verger, R. M., Mieras, M. C. E., and De Haas, G. H. (1973) *J. Biol. Chem.* 248, 4023-4034.

Villalain, J., Ortiz, A., and Gomez-Fernandez, J. C. (1988) *Biochim. Biophys. Acta.* 941, 55-62.

Vold, R. L., and Waugh, J. S., Klein, M. P., and Phelps, D. E. (1968) *J. Chem. Phy.* 48, 3831-3832.

Wassall, S. R., Treleaven, W. D., Parmar, Y. I., and Cushley, R. J. (1982) *Biochem. Biophys. Res. Commun.* 107, 429-434.

Watts, A. (1987) *J. Bioenergetics, Biomembranes* 19, 625-653.

Wennerstrom, H., and Lindblom, G. A. (1977) *Q. Rev. Biophys.* 10, 67-96.

Wu, A.-L., and Windmueller, H. G. (1978) *J. Biol. Chem.* 253, 2525-2528.

Yeagle, P. L., Hutton, W. C., Huang, C., and Martin, R. B. (1975) *Proc. Natl. Acad. Sci. U. S. A.* 72, 3477-3481.

Yeagle, P. L., Hutton, W. C., Huana, C., and Martin, R. B. (1977) *Biochemistry* 16, 4344-4349.

Yeagle, P. L., Langdon, R. G., and Martin, R. B. (1977) *Biochemistry* 16, 3487-3491.

Zannis, V. I., Breslow, J. L., Utermann, G., Mahley, R. W., Weisgraber, K. H., Havel, R. J., Goldstein, J. L., Brown, M. S., Schonfeld, G., Hazzard, W. R., and Blum, C. (1982) *J. Lipid Res.* 23, 911-914.

Zilversmit, D. B. (1968) *J. Lipid Res.* 9, 180-186.

Zilversmit, D. B. (1984) *J. Lipid Res.* 25, 1563-1569.